Evaluating Properties of Dystrophin and Delivery Methods of rAAV Gene Therapy for Duchenne Muscular Dystrophy

Julian N Ramos

A dissertation

submitted in partial fulfillment of the

requirements for the degree of

Doctor of Philosophy

University of Washington

2014

Reading Committee:

Jeffrey S Chamberlain, Chair

Stephen D Hauschka

Michael Regnier

Program Authorized to Offer Degree:

Molecular and Cellular Biology

University of Washington

Abstract

Duchenne muscular dystrophy (DMD) is a recessive muscle wasting disease caused by a deleterious mutation in the gene encoding the dystrophin protein. Dystrophin is an integral component the dystrophin-glycoprotein complex (DGC) that stabilizes the sarcolemma and allows transmission of mechanical force in striated muscle. Recombinant adeno-associated viral (rAAV) vectors have shown promise as a method for delivering therapeutic genes to dystrophic muscles. Vectors expressing miniaturized, or micro-, dystrophin proteins have repeatedly demonstrated rescue of rodent dystrophic animal models as well as improvement in larger dystrophic animal models. However, current micro-dystrophin constructs do not restore full, wild type function to transduced skeletal muscles. To improve the functionality of micro-dystrophin, we designed novel constructs and evaluated rAAV vector-treated dystrophic mice expressing these micro-dystrophins. We observed an improvement in functionality in two novel micro-dystrophins when compared to a previously established construct serving as our standard. We also examined the consequences of ablating micro-dystrophin expression in a mouse model. After determining that adult skeletal muscle falls into a dystrophic condition by three months after ablation, we concluded that rAAV vector-mediated gene therapy for DMD may require persistent expression of micro-dystrophin for life. We expanded on a previously reported immunosuppressive regimen in order to allow readministration of rAAV vectors in both dystrophic and wild type mice. Additionally, rAAV vectors effectively transduced striated muscle tissues after repeated, systemic delivery into wild type mice at doses that would be therapeutic for neuromuscular diseases. In order to further understand the tropism and properties of AAV serotypes that exhibit a high degree of tropism for skeletal muscle, we compared their

transduction properties in mice and canine animal models. We found that AAV serotypes 6, 8, and 9 all poorly transduce myogenic satellite cells. We also determined that AAV8 transduces mouse and canine skeletal muscle at a lower efficiency than AAV serotypes 6 and 9. Yet, serotypes 6 and 9 exhibited similar transduction when administered into the jugular vein of canines at sub-saturating doses. These results expand on several aspects of rAAV-mediated gene therapy for DMD involving the a) design and functionality of the therapeutic construct, b) consequences of lost expression of micro-dystrophin, c) immune responses in relation to repeat transduction of rAAV vectors, and d) properties of AAV serotypes and methods of delivery.

Evaluating Properties of Dystrophin and Delivery Methods of rAAV Gene Therapy for Duchenne Muscular Dystrophy

Julian Nathan Ramos

Chair of the Supervisory Committee:
Professor Jeffrey S Chamberlain
Department of Neurology

TABLE OF CONTENTS

LIST OF FIGURES

Figure Number **Page**

LIST OF TABLES

Table Number **Page**

ACKNOWLEDGEMENTS

I thank Jeff Chamberlain for allowing me to be a member of a great laboratory and for all his advice, enthusiasm, and encouragement. It has been a pleasure to study and research a significant topic that touches the lives of many.

There are numerous other scientists that contributed to this work and served as extended mentors during my graduate education. James Allen and Eric Finn produced the AAV vectors used in this work. In addition, they mentored me through the basics of tissue culture, AAV virology, vector preparation, and offered great comments and feedback on my experiments.

Glen Banks and Rainer Ng mentored me through the fundamentals of muscle physiology and assessment of muscle performance. Maja Zavaljevski and Ladan Mozaffarian provided assistance with tissue harvesting and cryosectioning for mouse studies. Andrea Arnett and Patryk Konieczny contributed equally to the studies focusing on transduction of myogenic satellite cells with AAV vectors. John Hall, Guy Odom, and Joel Chamberlain also contributed to the satellite cell transduction studies. Kristy Boyle mentored me through the isolation of satellite cells. The floxed micro-dystrophin transgenic mouse line that I used was previously produced by Luke Judge (Chamberlain Lab, UW) and Carol Ware (Department of Comparative Medicine, UW). Jane Seto contributed equally to the canine studies. Guy Odom also contributed to the canine studies as well as provided great advice and feedback on my experiments. Michael Mason performed the hindlimb surgeries for the canine studies. I thank Denny Liggitt, along with the veterinarians and veterinary technicians in the UW Department of Comparative Medicine, for

their invaluable assistance during the canine studies. I thank John Angelo, Connie Chen, and Quynh Nguyen (Hauschka Lab, Department of Biochemistry, UW) for assisting with tissue harvesting for the canine studies. Stephen Hauschka provided the regulatory expression cassette, CK8. Zipora Yablonka-Reuveni (Department of Biological Structure, UW) provided the nestin-GFP transgenic mice. Additional assistance, reagents, and helpful discussion were also provided by Niclas Bengtsson, Darren Bisset, Rachel Faber, Dilip Garikipati, Bobbi Miller, Lindsey Muir, Aisha Mushtaq, Scott Simpler, Anastasiya Vorontsova, Jacqueline Wicki, Emily Wing, and Vivyan Woods.

I thank my sister Monique for convincing me to declare biochemistry as my undergraduate major. I also thank my sister Jeanine, my relatives and friends who have encouraged and supported me during my time as a professional student. Finally, I thank my parents Aida and Manny for their endless love, support, and interest in the path that I have chosen.

DEDICATION

In memory of Ampelia Martinez Ramos and Maria Socorro Velarde Yañez.

Chapter 1

Background and Introduction

The Dystrophin Gene and Protein

Deleterious mutations in the dystrophin gene lead to DMD

Muscular dystrophy encompasses over 40 forms of inherited disorders that are characterized by progressive weakening and wasting of muscle. Duchenne muscular dystrophy (DMD) and Becker muscular dystrophy (BMD) are the most common forms of muscular dystrophy, resulting from mutations in the largest human gene, dystrophin (Emery 2003). DMD is a recessive disease in which the dystrophin gene, located in the Xp21.2 region of the X chromosome, is aberrantly expressed, or not expressed at all (Davies, Pearson et al. 1983, Kunkel, Monaco et al. 1985, Ray, Belfall et al. 1985, Kunkel, Hejtmancik et al. 1986, Hoffman, Brown et al. 1987). DMD is more severe than BMD and has a faster progression, it affects approximately 1 in 3500 newborn males (Emery 2003). Afflicted patients suffer from progressive muscle impairment and predominately succumb to premature death due to either cardiac or respiratory failure.

The commonality of DMD arises from a combination of the fact that female carriers are usually asymptomatic and that approximately a third of cases arise from new or sporadic mutations *in utero* (Davie and Emery 1978). Unless there is a family history of DMD, DNA testing for a mutation in the dystrophin gene (DMD in humans, *Dmd* in mice) is typically not performed in fetal or neonatal screens (Darras, Blattner et al. 1988). DNA testing will ultimately result after a suspected patient exhibits hallmark characteristics (Darras and Jones 2000). The first symptoms will be noticeable at 2-4 years of age as the child exhibits difficulty developing at the same physical, and

sometimes cognitive, pace as his peers. Approximately 60-65% of mutations afflicting DMD and BMD are large deletions. The majority (~80%) of deletions are found non-randomly throughout middle exons that encode the rod domain. Most of the rest are found at the 5' portion of the gene (Forrest, Cross et al. 1987). This distribution is seen throughout all tested populations and ethnic groups. It is important to note that there is no clear correlation between the location/size of the deletion and the severity and progression of these two allelic disorders (Monaco, Bertelson et al. 1988). When DNA analysis is inconclusive, a muscle biopsy is generally the defining assay. Immunohistochemical staining will determine if any dystrophin is expressed and if it's properly localized at the sarcolemma, while western blot analysis will reveal the size of any dystrophin expressed (Darras and Jones 2000). It is generally accepted that an out-of-frame mutation will result in either no translation or translation of an unstable dystrophin polypeptide (Monaco, Bertelson et al. 1988, England, Nicholson et al. 1990). However, in-frame deletions within the rod domain (discussed later) can yield stable truncated dystrophins with partial functionality, resulting in the milder dystrophy of Becker patients. The milder phenotype observed in more than 90% of BMD cases is attributed to a deletion that doesn't disrupt the translational reading frame of dystrophin mRNA (Malhotra, Hart et al. 1988). One BMD patient with an in-frame deletion of exons 17-48 has captured much attention for remaining ambulatory into his 70s (England, Nicholson et al. 1990). This patient was a source of inspiration for engineering truncated dystrophins for gene therapy (discussed later in this chapter).

Function and protein interactions of dystrophin in muscle

A common denominator among muscular dystrophies is deficient binding and stabilization of proteins that are responsible for the structural integrity of the muscle cell membrane (or sarcolemma). Throughout the contraction-relaxation cycle of muscle, intracellular pressure & heat are built up and external disturbances are created. A muscle fiber must be able to withstand these influences while transmitting force. An intricate network of protein interactions, known as costameres, prevents the fiber from being destroyed by external/internal effects (Ervasti 2003, Ozawa 2004). An actin network situated below the sarcolemma works with cytoskeletal proteins to form an internal system. A surrounding basal lamina interacts with sarcolemma-associated proteins and offers external protection. To transmit force and provide a functional connection between these two systems, dystrophin mediates the link between the actin network and sarcolemma-associated proteins, collectively known as the dystrophin glycoprotein complex (DGC). Therefore, dystrophin plays a role in helping maintain both structural integrity and muscle performance.

The DGC is a transmembrane, multi-protein complex that assembles at the sarcolemma and mediates the mechanical link between dystrophin and the basal lamina (**Fig. 1.1**). The intracellular interaction with dystrophin begins with the transmembrane protein β-dystroglycan (β-DG) (Ishikawa-Sakurai, Yoshida et al. 2004), which extracellularly binds to α-dystroglycan (α-Dg) (Ozawa, Nishino et al. 2001). α-DG binds directly with laminin, a main component of the basal lamina (Ibraghimov-Beskrovnaya, Ervasti et al. 1992, Burkin and Kaufman 1999). Though a continuous mechanical link is made, the interactions among the dystroglycans and between β-DG and dystrophin are

weak. The presence of another group of transmembrane proteins, the sarcoglycans (SGs), reinforces the binding throughout the DGC (Sandona and Betto 2009).

The sarcoglycan complex consists of four subunits; α-, β-, δ-, and γ-SG. All SG members bind to β-DG, while α-, β-, δ-SG interact with α-DG (Sakamoto, Ono et al. 1997, Noguchi, Wakabayashi et al. 1999). As with the dystroglycans, the stability of the sarcoglycans is reinforced by interaction with other proteins. Sarcospan is a transmembrane protein that binds to α-, β-, and δ-SG (Crosbie, Heighway et al. 1997, Marshall and Crosbie-Watson 2013). The presence of sarcospan on the sarcolemma stabilizes the DGC (Peter, Marshall et al. 2008, Marshall, Chou et al. 2012). Additionally, the cytosolic protein α-dystrobrevin binds to the intracellular side of the SG complex as well as the carboxy-terminal (C-terminal) domain of dystrophin (Grady, Grange et al. 1999). The C-terminal domain is just one of four major domains of the dystrophin protein.

The full-length dystrophin isoform, found in neurons and all types of muscle, has four major domains that allow dystrophin to mediate the link between the cytoskeleton and the DGC (Koenig, Hoffman et al. 1987, Winder 1997). The amino-terminal (N-terminal) domain has three sub-domains that bind to F-actin (Hemmings, Kuhlman et al. 1992, Way, Pope et al. 1992, Fabbrizio, Bonet-Kerrache et al. 1993, Pavalko and Otey 1994). The rod domain is the largest and has 24 repeats that share homology with spectrin family proteins. Two hinges flank the rod domain, and two others are interspersed among the spectrin-like repeats (SRs). Collectively, the central rod provides flexibility and elasticity that are crucial for the mechanical function of dystrophin (Winder 1997).

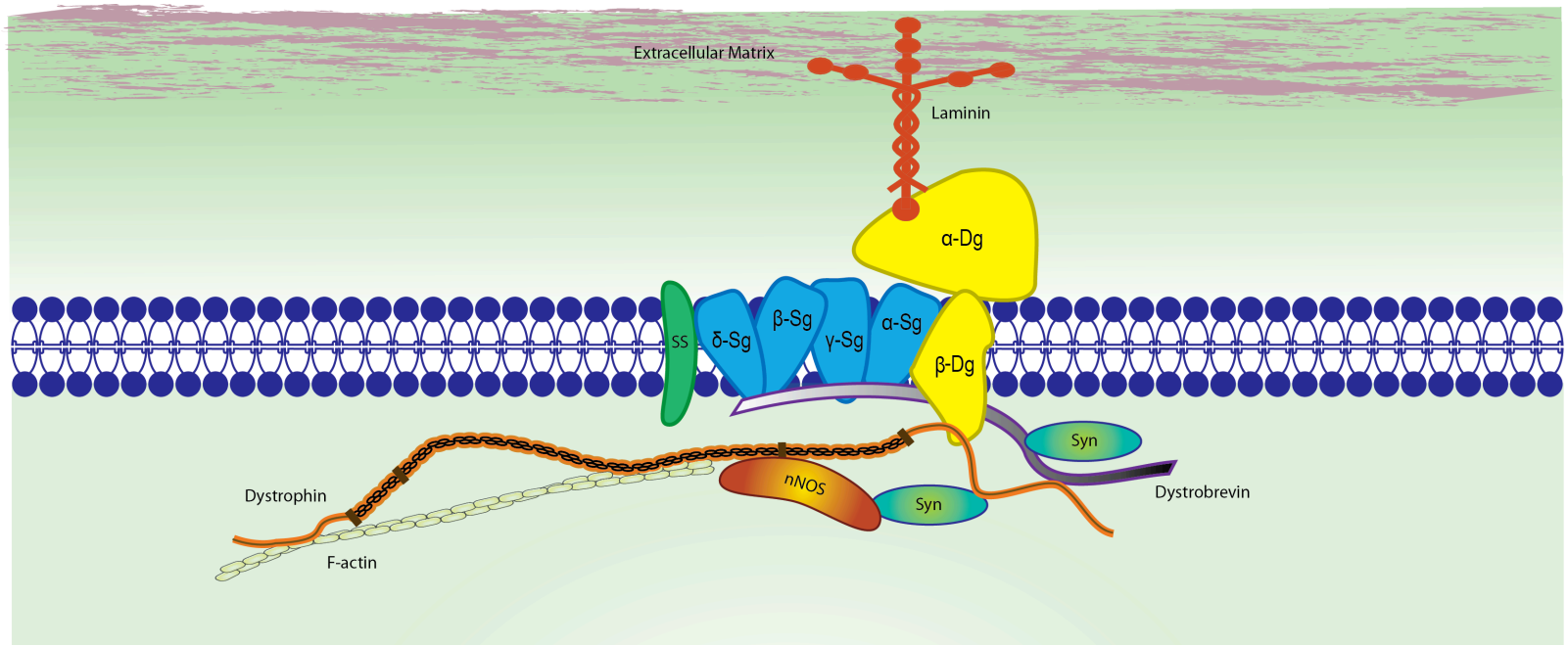

Figure 1.1 Model of dystrophin and the dystrophin glycoprotein complex (DGC) in skeletal muscle. Dystrophin provides a mechanical link between the intracellular cytoskeleton and the membrane-bound complex in order to stabilize the sarcolemma and transmit mechanical force. Dystrophin also serves as a scaffold for signaling proteins. This simplified illustration depicts some of the DGC components. Dg, dystroglycan; F-actin, filamentous γ-actin; nNOS, neuronal nitric oxide; Sg, sarcoglycan; synthase; Syn, syntrophin; SS, sarcospan.

The third major domain of dystrophin is the cysteine-rich (CR) domain that lies between the rod domain and the C-terminal domain. The CR domain contains binding motifs to β-DG (Blake, Weir et al. 2002, Ishikawa-Sakurai, Yoshida et al. 2004). However, binding between these two proteins also requires an additional motif that resides within the hinge region flanking the amino-terminus side of the CR domain (Ilsley, Sudol et al. 2002). The fourth major domain of dystrophin is the C-terminal domain, which binds DGC-members syntrophin and α-dystrobrevin (Grady, Grange et al. 1999). To provide a mechanical link between the intracellular cytoskeleton and the extracellular matrix, dystrophin must bind to multiple proteins. Yet, dystrophin's interactions described thus far are only a fraction of the known associations. Additional binding domains to other proteins have been reported.

Among the spectrin-like repeats of dystrophin are distinct binding domains that interact with multiple proteins, including F-actin (Rybakova, Amann et al. 1996) and the scaffolding protein dystrobrevin (Metzinger, Blake et al. 1997). Neuronal nitric oxide synthase (nNOS) also directly binds to spectrin-like repeats of dystrophin (Lai, Thomas et al. 2009, Lai, Zhao et al. 2013). In skeletal muscle, nNOS attenuates exercise-induced fatigue by mediating vasodilatation (Brenman, Chao et al. 1995, Lai, Thomas et al. 2009). Neuronal NOS can also associate with the DGC by binding to α1-syntrophin (Kameya, Miyagoe et al. 1999, Adams, Kramarcy et al. 2000, Adams, Tesch et al. 2008) which, in turn, binds to both dystrophin and dystrobrevin (Blake, Weir et al. 2002). Other studies have allocated the binding domains for other structural proteins within the rod domain including microtubules (Prins, Humston et al. 2009) and synemin (Bhosle, Michele et al. 2006). Apart from the previously mentioned interactions, keratin 19 and

plectin have been shown to interact with the N- and C-terminal regions of the dystrophin protein, respectively (Stone, O'Neill et al. 2005, Rezniczek, Konieczny et al. 2007). In its entirety, the DGC is a multifaceted complex that provides structural support for muscle function and a focal point for cellular signaling. As in the case of dystrophin, aberrations in a number of DGC members results in myopathies with varying degrees of severity and pathology.

Available treatments for DMD

Glucocorticoid steroids prednisone, prednisolone, and deflazacort are widely prescribed to DMD patients. Their exact mechanisms of action remain unclear but they have demonstrated modest reduction in inflammation and delayed loss of independent ambulation (Moxley, Ashwal et al. 2005, Biggar, Harris et al. 2006, Manzur, Kuntzer et al. 2008). Most patients succumb to fatal complications of the diaphragm muscle or heart due to a combination of muscle weakness and encroachment of adipose and fibrotic tissue. Several drugs originally designed to reduce blood pressure have shown promise in attenuating fibrosis and improving cardiac function (see below).

A system involving aldosterone, a mineralocorticoid family member that controls water and electrolyte levels, coordinates with the enzymes renin and angiotensinogen to regulate blood pressure in vertebrates. In this regulatory system, angiotensinogen is converted to angiotensin I by renin and subsequently converted to angiotensin II by angiotensin-converting enzyme (ACE). Angiotensin II stimulates vasoconstriction, aldosterone secretion as well as transforming growth factor beta (TGFβ) production. TGFβ is a multipurpose signaling protein that significantly contributes to skeletal muscle

fibrosis (Mann, Perdiguero et al. 2011, Lieber and Ward 2013). Long-term administration of the ACE inhibitor perindopril to DMD patients showed a reduced mortality rate when administered at a younger age (Duboc, Meune et al. 2007). A regimen of the ACE inhibitor lisinopril and the aldosterone antagonist spironolactone reduced fibrosis and necrosis in murine dystrophic striated muscle (Rafael-Fortney, Chimanji et al. 2011). Additionally, the benefits of these drugs were improved when treating these dystrophic mice even earlier. Similarly, a DMD patient study showed that the pharmacological benefits of perindopril increased when administered at earlier ages (Duboc, Meune et al. 2007). The angiotension II receptor blocker losartan also reduced fibrosis in murine dystrophic muscle (Cohn, van Erp et al. 2007). A clinical trial revealed lisinopril and losartan to result in equal improvement in cardiac function in DMD patients (Allen, Flanigan et al. 2013).

Despite the availability of these agents, no combination of drugs has been shown to halt the progression of the DMD pathology. There is also evidence of impeding effects between glucocorticoids and ACE inhibitors in dystrophic mice, where the anti-fibrotic effect of ACE inhibitors was reduced in striated muscle (Janssen, Murray et al. 2014) or the cardiomyopathy was accelerated (Bauer, Straub et al. 2009). It remains unclear which combination of drugs will provide the maximum benefit to cardiac and skeletal muscle and at what age and dose to administer the drugs to patients. Nevertheless, pharmacological treatment will be used in conjugation with palliative care that focuses on maintaining mobility and, in later stages of the disease, providing respiratory support (Bushby, Finkel et al. 2010). The state of the art for DMD therapy is management of the disease that results in, at best, a slowing of its inevitable progression. To definitively halt

or reverse the DMD pathology, the underlying molecular basis must be addressed: the failure to express a functional dystrophin protein.

Animal Models for DMD

The first mouse model for DMD, the *mdx* mouse, arose from a spontaneous dystrophin mutation first observed in 1984 (Bulfield, Siller et al. 1984). An additional five dystrophin-mutated strains were created by mutagenesis and designated accordingly from mdx^{2cv} to mdx^{5cv} (Chapman, Miller et al. 1989). In addition, *mdx52* strain was created by gene targeting to delete exon 52 of the dystrophin gene (Araki, Nakamura et al. 1997). Each strain has a different mutation in the DMD gene, where only the mdx^{3cv} mutation disrupts all isoforms of dystrophin (Sicinski, Geng et al. 1989, Cox, Phelps et al. 1993, Im, Phelps et al. 1996, Araki, Nakamura et al. 1997). Similarly to human patients, *mdx* skeletal muscle fibers are easily damaged and the muscle undergoes continuous cycles of necrosis, degeneration and regeneration. For the *mdx* mouse, the acute onset of pathology is observed around three weeks of age (Carnwath and Shotton 1987, Coulton, Morgan et al. 1988). However, the lifespan of the *mdx* mouse is only slightly shortened (Chamberlain, Metzger et al. 2007) in high contrast to DMD patients who succumb to premature death typically in their second or third decade of life (Emery 2003). The *mdx* mouse strains also display a relatively mild phenotype compared with patients. While this allows a homozygous mouse strain to be bred fairly easily, it also reflects several aspects of the *mdx* mouse physiology that contribute to a milder phenotype. Fibrosis and encroachment of adipose tissue in most skeletal muscles is not as pervasive in the *mdx* mouse as it is in patients (Sicinski, Geng et al. 1989, Chamberlain, Metzger et al. 2007). Exceptions to this model are in the diaphragm and intercostal muscles that assist with respiratory functions (Stedman, Sweeney et al. 1991). In addition, the telomeres of laboratory mouse strains are more than twice as long as

humans', giving murine myogenic precursor cells a higher proliferative capacity. Consequently, murine satellite cells are not depleted as fast by continuous cycles of degeneration and regeneration (Sacco, Mourkioti et al. 2010). Despite criticisms of the utility of the mouse model stemming from these discrepancies, the *mdx* mouse serves as a good biochemical model for the lack of dystrophin, displaying loss of DGC assembly in muscles, reduced muscle performance, and a clear histopathological muscular dystrophy.

Crossing various *mdx* mouse strains to other gene knockout lines has led to more severely affected DMD mouse models, including the *mdx*/*utrn*$^{-/-}$ mouse model that carries mutations in both dystrophin and utrophin genes (Deconinck, Rafael et al. 1997). Utrophin is a modular protein that shares a high degree of homology and function with dystrophin. Utrophin expression is upregulated in both human and mouse DMD muscles (Miura and Jasmin 2006). This upregulated expression of utrophin has been suggested to be one reason for the relatively mild phenotype of the mouse model (Roma, Munell et al. 2004); hence, the double knockout.

Several larger animal models for DMD have been identified, which in general display a phenotype more closely resembling the human disorder. Feline and canine models of DMD have been available for more than 16 years. The deleterious enlargement of the tongue and esophagus in the feline model drastically shortens its lifespan and has prevented it from being broadly used as a DMD model (Gaschen, Hoffman et al. 1992). However, multiple colonies of the muscular dystrophy dog (*cxmd*) have been created (Cooper, Winand et al. 1988). Severe symptoms commonly appear at six weeks of age in the *cxmd* dog, but unlike the *mdx* mouse, the degree of severity and time of progression are quite variable (Kornegay, Bogan et al. 2012). For example, some neonatal dystrophic

canines die from respiratory complications (Ambrosio, Valadares et al. 2008). Compounded by the increased cost of maintaining a larger species, the *cxmd* model can be problematic in breeding a sufficient number of dogs for research studies. However, use of the *cxmd* model has gained much emphasis with its more clinically similar pathology (Kornegay, Bogan et al. 2012). No dystrophic model currently exists in nonhuman primates, but continual studies in these animals are addressing systemic rAAV delivery and immune response challenges (Rodino-Klapac, Montgomery et al. 2010, Tarantal and Lee 2010, Toromanoff, Adjali et al. 2010, Gao, Bish et al. 2011).

Gene Therapies for DMD

Gene therapy is a field of experimental strategies that use DNA, or RNA, as the agent that treats or prevents disease. Strategies include inactivating the mutated gene responsible for the disease, modifying expression of the mutated gene, replacing the mutated gene with a functional copy, or introducing a new gene to treat the disease. DMD is an X-linked recessive form of muscular dystrophy that affects males, who have only one copy of the dystrophin gene. Inactivating expression of a mutated dystrophin gene will not treat or prevent DMD because a patient would still lack expression of a functional dystrophin. However, gene therapy research on DMD has shown great promise using other strategies. Here we discuss experimental approaches designed to modify expression of the mutated dystrophin gene, replace it with a functional copy, or introduce new genes to treat DMD.

Modulating dystrophin mutations

One approach to a gene therapy for DMD would be to restore dystrophin expression by modifying the way a muscle cell responds to expression of a mutant dystrophin gene. Two strategies are currently in clinical trials that attempt to either alter pre-mRNA splicing (to skip a mutant exon) or to suppress the recognition of premature stop codons. The antibiotic gentamicin, as well as the synthetic derivative PTC124, can cause the transcriptional machinery to read through premature stop codons (Barton-Davis, Cordier et al. 1999, Wagner, Hamed et al. 2001, Welch, Barton et al. 2007). Administration of this drug allowed functional dystrophin to be expressed in *mdx* mice where the mutation was a nonsense mutation. Unfortunately, this drug was shown to be

less efficient in human clinical trials (Dunant, Walter et al. 2003, Politano, Nigro et al. 2003). Expression of dystrophin from the endogenous gene can also be rescued by utilizing anti-sense oligonucleotides (AONs) in an exon-skipping strategy that circumvents mutations that disrupt the normal mRNA open reading frame, allowing a truncated dystrophin to be expressed (Takeshima, Nishio et al. 1995). This form of therapy has gone through several generations of refinement with improving results *in vitro* and *in vivo* (Takeshima, Wada et al. 2001, van Deutekom, Bremmer-Bout et al. 2001). Various chemical modifications to the backbone of AONs increase their stability and, in turn, the lasting effect from a given dose of AONs (Chamberlain and Chamberlain 2010). Exon-skipping strategies have expanded towards skipping multiple exons (Aartsma-Rus, Janson et al. 2004, Aoki, Yokota et al. 2012) and can be applied to deletion, splice site and duplication mutations (Greer, Lochmuller et al. 2014). Although modified transcripts have been detectable for several weeks *in vivo* after AON administration, the efficiency of this strategy diminishes as the number of AONs administered increases. Further studies may improve the biological distribution of AONs and premature stop codon drugs, yet this class of therapeutics will most likely require continuous treatment.

Gene replacement

Gene replacement therapies for DMD are conceptually simple since the disorder is inherited in a recessive X-linked manner where the dystrophin gene is aberrantly expressed, or not at all, in males (Davies, Pearson et al. 1983, Kunkel, Monaco et al. 1985, Ray, Belfall et al. 1985, Kunkel, Hejtmancik et al. 1986, Hoffman, Brown et al.

1987). Exogenous restoration of the dystrophin gene has been attempted by introducing a plasmid either by intramuscular or intravascular injection (Wolff, Malone et al. 1990, Jiao, Williams et al. 1992, Zhang, Ludtke et al. 2004). However, plasmids beyond several Kb show decreasing transduction efficiency when injected nakedly or with cofactors (Jiao, Williams et al. 1992). The full-length coding DNA (cDNA) is ~13.9 Kb (Koenig, Monaco et al. 1988), and the plasmid would also require an appropriate promoter and polyadenylation sequence. Not to begrudge an exogenous route of gene therapy, this method can be quite efficacious when using a suitable vehicle for delivery. Viral-vector mediated gene therapy has demonstrated such efficacy for gene delivery.

Adeno-associated virus: A vehicle for gene therapy

Adeno-associated virus (AAV) is a member of the parvovirus family and was originally discovered as a contaminant in adenovirus preparations(Atchison, Casto et al. 1965). The wild type virus has a single-stranded DNA genome of 4.7 Kb. The wild-type genome of AAV encodes Rep and Cap genes for replication and capsid proteins, respectively, yet this parvovirus is unable to fully replicate without the assistance of a helper viruses (e.g. adenovirus or herpes virus). The Rep and Cap genes are dispensable for transduction while the inverted terminal repeats (ITRs), ~150 bp in size, that flank the viral genome are required for genome replication and packaging into the capsid (McLaughlin, Collis et al. 1988). Thus, inserting a therapeutic gene of interest, along with promoter and polyadenylation sequences between the ITRs, and encapsulating this recombinant genome can turn the AAV genome into a vector. The caveat of the recombinant AAV (rAAV) vector genome is that the packaging constraints of the capsid

limit its size to ~5 Kb (Dong, Nakai et al. 2010, Wu, Yang et al. 2010). This is less than half the size of the dystrophin coding DNA. Yet numerous studies have successfully used rAAV vectors to deliver genes encoding truncated dystrophin isoforms to striated muscles (discussed later in this chapter).

Three different proteins (VP1, VP2, and VP3) assemble in a 1:1:10 ratio, respectively, into a non-enveloped icosahedral capsid of approximately 20-25 nm in size (Ivanovska, Wuite et al. 2007, Horowitz, Rahman et al. 2013). The lack of any known pathogenicity and the inability to replicate without the assistance of a replication-competent helper virus (e.g. herpesvirus or adenovirus) are attractive safety features for AAV-mediated gene therapy. Use of AAV as a gene therapy tool is promising due to its ability to transduce a wide array of tissues while eliciting a lower immune response than many previously tested vectors such as those derived from adenovirus (Chirmule, Propert et al. 1999, DelloRusso, Scott et al. 2002, Gilbert, Dudley et al. 2003). Additionally, AAV has a very low frequency of integration into the host genome (Nakai, Montini et al. 2003, Inagaki, Lewis et al. 2007), reducing concerns related to insertional mutagenesis; a problem that arose in early clinical trials using retroviral vectors (Muir and Chamberlain 2009). Attempts to modify the AAV capsid through sequence modifications including generating chimeric capsids from multiple serotypes have not significantly expanded the packaging capacity of the single-stranded DNA genome (Wu, Asokan et al. 2006). Yet, these permutations and serotype comparison studies have led to comprehensive analyses of many aspects of AAV vector use, including elicitation of immune responses (Rogers, Martino et al. 2011, Wang, Tapscott et al. 2011), tissue tropism, and kinetics of transduction *in vivo* (Zincarelli, Soltys et al. 2008, Zincarelli, Soltys et al. 2010).

Twelve primate AAV capsid sequences have been characterized thus far, with vectors from each serotype displaying a varying degree of tropism for different tissues (Asokan, Schaffer et al. 2012). Currently there is no consensus on the best serotype for targeting striated muscle, the primary tissue needing correction in gene therapy for the muscular dystrophies. Recombinant AAV serotypes 6, 8, and 9 have demonstrated widespread transduction of striated muscles in mouse (Wang, Zhu et al. 2005, Gregorevic, Allen et al. 2006, Pacak, Mah et al. 2006), canine (Yue, Ghosh et al. 2008, Gregorevic, Schultz et al. 2009, Kornegay, Li et al. 2010, Pan, Yue et al. 2013), and non-human primate models (Rodino-Klapac, Montgomery et al. 2010, Gao, Bish et al. 2011). Conflicting claims of the best serotype for striated muscle can be attributed to the route of rAAV vector administration and a lack of understanding of the basic biology of AAV serotypes, as well as poorly designed experiments. The biology of each serotype is partly defined by the cellular receptor and co-receptors required for transduction. AAV6 requires binding to α2,3/α2,6 N-linked sialic acid and heparan sulfate proteoglycans and can also use the epidermal growth factor receptor as a co-receptor (Wu, Miller et al. 2006, Ng, Govindasamy et al. 2010, Weller, Amornphimoltham et al. 2010, Arnett, Beutler et al. 2013). AAV9 requires N-linked galactose attached to sialic acid and binds to the 37/67-kDa laminin receptor for transduction (Akache, Grimm et al. 2006, Shen, Bryant et al. 2011). The primary receptor for AAV8 remains unknown but it also binds to the 37/67-kDa laminin receptor (Nam, Lane et al. 2007, Shen, Bryant et al. 2011). Intramuscular injections of multiple AAV serotypes can be used to compare transduction properties, but intravascular injections may lead to different, and more clinically

translatable, results. For example, the basic biology of an AAV serotype influences the rate of extravasation after intravenous delivery. AAV9 displays a prolonged persistence in the circulatory system compared to serotypes 6 and 8 (Zincarelli, Soltys et al. 2008, Kotchey, Adachi et al. 2011). Receptors and extravasation rates are just two aspects that help define an AAV serotype. Differences among serotypes are also observed with intracellular processing (Wu, Asokan et al. 2006, Schultz and Chamberlain 2008). Further AAV serotype comparison studies should focus not only on the end result of striated muscle transduction but also increase our understanding of this powerful tool for clinical applications.

Production of rAAV serotypes is scalable and with sufficient resources can meet the demands of pre-clinical and clinical studies (Blankinship, Gregorevic et al. 2006, Wright, Wellman et al. 2010). Recombinant AAV cannot replicate without assistance of a helper virus or a helper plasmid, which acts as a surrogate replication-competent virus. Generating rAAV requires use of a cell culture system (such as human embryonic kidney 293 cells) to provide the biological machinery for virus production. These cultures are transfected with two plasmids. One plasmid contains the vector genome with the transgene to be packaged into AAV capsids. The second plasmid encodes open reading frames (orf) of the *rep* and *cap* genes of AAV and encodes adenovirus genes that allow expression of the AAV orf during AAV vector production. Initial helper plasmid studies required three adenovirus genes, E2A, E4orf6, and VA RNA, for AAV vector production (Matsushita, Elliger et al. 1998, Xiao, Li et al. 1998). Further refinement of this system revealed that only one adenovirus gene, E4orf6, is necessary for AAV vector production (Allen, Halbert et al. 2000). Methods for purifying the virus from cell culture depend on

the serotype and purification requirements. AAV6 is one of several serotypes that bind to heparin sulfate (Asokan, Schaffer et al. 2012), which allows it to be purified by affinity chromatography for large-scale production. Other serotypes that lack heparin binding (e.g. serotypes 8 and 9) must be purified by other methods such as cesium chloride gradient centrifugation and ion exchange chromatography.

Functional, truncated dystrophin isoforms can rescue dystrophic muscle

In the case of the milder disorder Becker muscular dystrophy, deletion mutations in the dystrophin gene can result in the expression of truncated, yet partially functional, dystrophin (Koenig, Beggs et al. 1989, Beggs, Hoffman et al. 1991, Goldberg, Hausmanowa-Petrusewicz et al. 1998). This observation led to the idea of using truncated dystrophins for therapeutic use, which has already enabled body-wide amelioration of the dystrophic phenotype in *mdx* mice *via* rAAV vector-mediated gene transfer (Blankinship, Gregorevic et al. 2006). The limited rAAV vector carrying capacity of ~5 Kb requires the use of a truncated dystrophin, or micro-dystrophin (μDys), that conserves crucial functional domains yet is small enough to be packaged into an AAV capsid. This need to convert ~13.9 Kb of coding DNA down to approximately 4 Kb (due to the need for regulatory sequences in the expression cassette) has spurred the study of dystrophin structure and function and led to the design of a number of "micro-dystrophin" proteins. Their functional optimization requires not only specific goals for improvement of transduced muscles, but also a sufficiently sensitive testing system.

Several labs have explored the functionality of micro-dystrophins containing in-frame deletions within the dystrophin coding sequence. They have also demonstrated that

engineered constructs can be small enough to be packaged within the rAAV capsid while maintaining crucial functional domains. A functional connection between the cytoskeletal actin filaments and the integral membrane protein β-dystroglycan is an essential feature of any construct for both the stability of the protein and to provide mechanical function and enable assembly of the DGC (Cox, Sunada et al. 1994, Greenberg, Sunada et al. 1994, Harper, Hauser et al. 2002, Gardner, Kearney et al. 2006). Truncation of the N-terminal actin-binding domain severely disrupts the stability and function of dystrophin (Corrado, Rafael et al. 1996, Warner, DelloRusso et al. 2002, Banks, Gregorevic et al. 2007). However, the C-terminal domain has been found to be nonessential in properly localizing the majority of the DGC. Analysis of the correlation between deletions and phenotypic severity of BMD patients revealed that deletion of the entire C-terminal region results in a mild phenotype (McCabe, Towbin et al. 1989). Transgenic *mdx* mice expressing a C-terminal truncated dystrophin displayed no obvious impairment of DGC assembly, muscle morphology or muscle mechanics (Dunckley, Love et al. 1992, Grady, Grange et al. 1999, Crawford, Faulkner et al. 2000). However, further truncation within the dystroglycan-binding domain completely ablated stable assembly of the DGC (Koenig, Beggs et al. 1989, Beggs, Hoffman et al. 1991, Corrado, Rafael et al. 1996). Therefore, the amino-terminal and dystroglycan-binding domains are necessary for the generation of a functional dystrophin.

Analysis of various in-frame deletions in the rod domain revealed a high degree of functionality and stability even when the deletions removed several SRs and internal hinges (Harper, Hauser et al. 2002). These studies suggested that, secondarily to the C-terminal domain, the central rod might be the most tolerant region for deletions.

However, there is a correlation between the number of SRs and the degree of functionality in skeletal muscle. Constructs with less than four SRs exhibit minimal functionality, at best, while those with four or more exhibit varying degrees of functionality (Wang, Li et al. 2000, Harper, Hauser et al. 2002). Transgenic *mdx* mouse lines expressing dystrophins with eight SRs (mini-dystrophins) displayed an intact DGC and their muscles developed specific forces at near wild-type levels (Harper, Hauser et al. 2002). With a multitude of protein-binding domains spanning across the entire protein, designing optimal micro-dystrophins must find a balance between conserving the critical functional domains, recruiting associated proteins, and maintaining the structural stability of these miniaturized proteins.

Is AAV-mediated dystrophin replacement restricted to using a single vector?

As previously mentioned, the packaging capacity of rAAV vectors is approximately 5.0 Kb. This space must incorporate a promoter, polyadenylation signal, and a transgene between the ITRs of the recombinant AAV genome. In order to generate dystrophin transgenes larger than 5.0 Kb, several studies have delivered multiple rAAV vector genomes that were designed to become single episomal transgene *in vivo* by homologous recombination (Odom, Gregorevic et al. 2011, Koo, Popplewell et al. 2014, Lostal, Kodippili et al. 2014). This was first demonstrated using two rAAV vectors that overlapped ~370 nucleotides and recombined to generate an expression cassette of 7.3 Kb encoding a "mini-dystrophin" (Odom, Gregorevic et al. 2011). Intravascular delivery of both rAAV/mini-dystrophin recombination vectors in *mdx*^{4cv} mice resulted in widespread expression of the entire protein and improved skeletal muscle morphology

and strength. The same study also compared this novel two-rAAV vector treatment with a previously established method of treating *mdx*^{4cv} mice with micro-dystrophin construct encoded within a single rAAV vector (Gregorevic, Blankinship et al. 2004, Gregorevic, Allen et al. 2006). Despite lower expression levels, mini-dystrophin expressing-muscles performed better than micro-dystrophin, suggesting higher functionality with the larger construct. Other groups expanded on this multi-rAAV vector approach by using three vectors to transfer the full-length cDNA of dystrophin into skeletal muscle (Koo, Popplewell et al. 2014, Lostal, Kodippili et al. 2014). However, the efficiency of this triple recombination event was drastically lower compared to the dual recombination approach for mini-dystrophin (Odom, Gregorevic et al. 2011).

These studies showed that transfected cells can generate transgenes that are larger than what can be delivered by a single rAAV vector, and they suggest that expression of some larger dystrophins might be more efficacious than delivery of a single micro-dystrophin gene. However, this approach is limited by at least two important variables. First, the multiple vector genomes being delivered to muscle cells form concatemers in multiple ways (head to head, head to tail, etc), and several of these combinations would be expected to encode proteins with aberrant and possible undesirable sequences. Secondly, since the homolgous recombination event that forms the larger dystrophins presumably occurs in the nucleus, it can only occur if each component of the vector system is present in the same nuclei. The ITRs amongst the multiple vectors can be altered to help properly align the various concatemers, yet the efficiency dramatically decreases with each additional vector necessary to generate a final transgene product. Consequently, rAAV vector-mediated replacement for large genes such as dystrophin is

not yet technically feasible for large-scale delivery unless a truncated "mini" gene can be delivered using a single vector.

Using rAAV vectors for DMD gene therapy

The daunting task of generating enough vector for systemically delivering a therapeutic gene to striated muscle has been compensated for, in part, by the ability to scale up rAAV production on an industrial scale. A critical threshold concentration of vector particles is needed to achieve extravasation of the vector for systemic delivery via the vasculature. Making enough vector to achieve these levels in large animals has benefited from the improved production methods. However, if sub-optimal levels of vector enter muscle cells, several modifications of the vector genome can enhance gene expression. One study enhanced expression of a rAAV vector by codon-optimizing a previously established micro-dystrophin (Harper, Hauser et al. 2002, Foster, Sharp et al. 2008). Systemically injecting this codon-optimized vector into *mdx* mice resulted in high expression and improved muscle function. However, no direct comparison of expression was made between the codon-optimized and non-codon-optimized micro-dystrophin constructs. Future studies, along with a current one in our laboratory, will make such a comparison and determine if lower numbers of codon-optimized rAAV/micro-dystrophin vectors can rescue dystrophic animal models.

It is important to recognize that improvement of micro-dystrophin design is an on-going story in DMD research and creating novel junctions in the rod domain (generated during the miniaturization process) may have adverse effects on protein structure/function or immunogenicity that are not obvious. One instance is the creation of

the ΔR4-23/ΔCT construct ("hinge 2 micro-dystrophin") (Harper, Hauser et al. 2002). Both transgenic mice and *mdx*^{4cv} mice treated with rAAV vectors expressing this construct showed improved morphology at near wild type levels (Harper, Hauser et al. 2002, Banks, Judge et al. 2010). However, these initial assays were examining cross sections from the middle of the mouse muscles. Electron microscopy analysis at the myotendinous junctions of these mice revealed that this particular micro-dystrophin was causing an abnormal formation of ringbinden, where a subset of muscle myofibrils reorient themselves orthogonally to the rest of the muscle and encircle the muscle (Banks, Combs et al. 2008, Banks, Judge et al. 2010). Though this was found to reduce susceptibility to contraction-induced injury, the ringbinden was also obstructing muscle growth. An amino acid sequence comparison between the two hinges residing within the rod domain revealed a polyproline region in hinge 2, but not in hinge 3. Since polyprolines form a rigid α-helix (Rath, Davidson et al. 2005) and because hinge 2 isn't adjacent to spectrin-like repeat 24 in wild type dystrophin (Winder, Gibson et al. 1995), it was suspected that the polyproline was disrupting the normal confirmation of the rod domain. Two modified micro-dystrophin constructs were delivered to *mdx*^{4cv} mice by rAAV vectors. One construct replaced the internal hinge 2 with hinge 3 while the other had the polyproline region deleted from the "hinge 2 micro-dystrophin". Expression of both constructs did not result in ringbinden formation (Banks, Judge et al. 2010). This is an additional concern that must be addressed in proposed therapeutic constructs.

Apart from the design of micro-dystrophins, the choice and production method of a rAAV serotype, the amount of vector genomes to be delivered, which mouse model to

use, the use of specific methods of delivery, the precise time of evaluation of treated mice, and the assays used to monitor function are all important parameters that must be clearly defined by an individual research group, if the not the entire scientific community, in order to create a rubric for successful design, testing and evaluation of the effectiveness of future constructs. It is expected that deviations from an established rubric will occur as improvements in one or more parameters are made, yet it must be recognized that even one variable can lead to dramatically different results and add ambiguity to the field. One additional parameter that heavily influences the outcome of assessing micro-dystrophins is the age of the animal at treatment and evaluation. For example, treating *mdx* mice before or after the onset of the dystrophic phenotype with rAAV-micro-dystrophin vectors results in different morphological outcome as shown with the degree of degeneration/regeneration (centrally nucleated fibers) (Wang, Li et al. 2000, Gregorevic, Allen et al. 2006, Banks, Judge et al. 2010).

Obstacles for rAAV Gene Therapy

Bodywide delivery approaches

Since Duchenne muscular dystrophy primarily affects the heart and all skeletal muscles, the goal of gene replacement therapies is transducing all striated muscle in the body by a route of administration that is least likely to elicit an immune response and is clinically translatable. Systemic delivery of rAAV6/micro-dystrophins into neonatal or adult *mdx* mice *via* intravenous injection has been effective in achieving body-wide transduction (Gregorevic, Blankinship et al. 2004). Similarly, intra-arterial infusion via the femoral artery has also resulted in widespread expression in skeletal muscles in mice (Fougerousse, Bartoli et al. 2007). Systemic delivery into canine models, however, has proved to be a greater challenge due to the larger size of the animal, the need for higher quantities of vector, and heightened sensitivity to viral vectors that can result in diminutive transgene expression and an immune reaction against viral vectors or transgenic proteins (Wang, Tapscott et al. 2011). Thus far, a single bolus of rAAV vectors has only led to widespread transduction when delivered to neonatal canine pups (Yue, Ghosh et al. 2008, Kornegay, Li et al. 2010, Pan, Yue et al. 2013). These findings indicate that unless a DMD patient is diagnosed at a very young age, body-wide treatment will require multiple routes of rAAV vector administration. For older animals, transduction in canines and non-human primates has been achieved by targeting specific muscles or group of muscles for rAAV vector delivery. Tested methods include isolated limb perfusion (Gregorevic, Schultz et al. 2009, Rodino-Klapac, Montgomery et al. 2010) and transendocardial injections (Bish, Sleeper et al. 2008, Gao, Bish et al. 2011). However, rAAV vector delivery by intramuscular injection may not be feasible for a

dystrophic heart or for the diaphragm. Targeting a limb muscle using a safe and efficient method of transduction may be achieved by repeatedly passing a bolus of rAAV vector through the region using an extracorporeal circuit to maintain tissue homeostasis (Bieber, Halldorson et al. 2013). Targeting the heart and diaphragm in contrast may require direct vector infusion into catheters upstream of these muscle groups (Gregorevic, Schultz et al. 2009, Pan, Yue et al. 2013). Delivering rAAV vectors to striated muscle throughout the body of larger animal models remains an important aspect of future development for DMD gene therapy.

Immune responses to AAV capsid and transgene

Professional antigen presenting cells (APCs) typically mediate the immune responses to a viral infection. The context of which virus type, route of infection, viral load, and signaling responses from innate responses will influence how a naïve T cell lymphocyte responds to the infection. This response leads to differentiation into an effector T cell, one of several subsets with a distinct role. Functions of these effector T cell subsets are varied; both promoting and suppressing inflammation, assisting with $CD8^+$ T cell and B cell responses, and antiviral roles (Swain, McKinstry et al. 2012). Although effector T cells canonically direct a humoral immune response to viruses, B cells can also influence naïve and effector T cells through antigen presentation or their signaling stimuli. B cells can carry out this task either alone or in conjunction with other surrounding stimuli (Lund and Randall 2010, Swain, McKinstry et al. 2012). A multitude of preclinical and clinical studies is revealing the various immunological scenarios that face rAAV-mediated gene therapy.

The innate immune system has several sets of pathogen recognition receptors (PRRs). The complement system is a set of inactivated enzymes that circulate in the blood or serve as cell receptors awaiting activation by foreign antigens. AAV serotypes 1, 2, and 8 were found to bind complement and their receptors, allowing vector uptake by macrophages and result in innate signaling response and eventual humoral response (Zaiss, Cotter et al. 2008). Another set of PRRs is the Toll-like receptors (TLRs), which reside at the membrane or in endosomes. The endosomal TLR9 recognizes unmethylated cytosine guanine dinucleotide motifs that are prevalent in DNA originating from viruses or bacteria, but not in mammalian DNA. Current good manufacturing practices in rAAV viral generation uses vector plasmids grown from bacterial cultures (Wright, Wellman et al. 2010), leaving an inherit risk of using unmethylated rAAV vectors.

Unmethylated CpG rAAV vector genomes have been recognized by TLR9 in conventional (bone marrow-derived) dendritic cells (cDCs) and plasmacytoid dendritic cells (pDCs), neutrophils, macrophages, and natural killer cells (Zhu, Huang et al. 2009, Martino, Suzuki et al. 2011). TLR9 activation signaling is mediated through adaptor protein myeloid differentiation primary response 88, or MyD88, and leads to type I interferon (IFN-α/β) production. Although many cell types can produce these antiviral proteins, pDCs are a major source of IFN-α/β (Siegal 1999, Coccia, Severa et al. 2004). The pDCs' increased responsiveness to TRL9-MyD88 signaling over cDCs (Zhu, Huang et al. 2009) reinforces their active role in AAV immunity. This interferon response activates naïve $CD8^+$ T cells for cross-priming, where extracellular antigens are presented to them. However, pDCs cannot present exogenous antigens to $CD8^+$ T cells but can present endogenous antigens (Salio, Palmowski et al. 2004). The ability of AAV to

transfect pDCs (Zhang, Chirmule et al. 2000, Zhu, Huang et al. 2009) can cause CpG-activation and enable them to prime functional $CD8^+$ T cells, resulting in a cytotoxic lymphocyte (CTL) response. AAV capsid and transgene-specific responses by effector $CD8^+$ cells has been reported in multiple animal models and in humans (Zhang, Chirmule et al. 2000, Vandenberghe, Wang et al. 2006, Pien, Basner-Tschakarjan et al. 2009, Mendell, Campbell et al. 2010, Mendell, Rodino-Klapac et al. 2010, Li, Lasaro et al. 2011, Li, Tuyishime et al. 2011, Mays and Wilson 2011, Rogers, Martino et al. 2011, Wang, Tapscott et al. 2011). Removing most CpG motifs in the vector genome between the inverted terminal repeats (ITRs) reduced $CD8^+$ T cell response and production of INF-γ (Faust, Bell et al. 2013). However, CpGs were not removed from the ITRs, and it remains unknown if this removal will affect vector genome packaging and transduction.

Canonical generation of an effector $CD8^+$ T cell involves a helper $CD4^+$ T cell to activate, or license, the antigen presented to it by a third party APC. This process relies on co-stimulatory molecules expressed by the interacting cells, including CD40 and CD40 ligand (CD40L) (Lund and Randall 2010, Swain, McKinstry et al. 2012). Dendritic cells transduced with AAV2 were unable to produce a CTL response when adoptively transferred into CD40L null mice (Zhang, Chirmule et al. 2000). $CD8^+$ T cell responses to AAV serotypes 8 and rh32.33 were attenuated when $CD4^+$ T cells were ablated (Mays, Vandenberghe et al. 2009). Yet, initial responses of these two T cell populations to AAV, and viruses in general, are bidirectional and are further influenced by preceding stimuli from the innate immunity. $CD8^+$ T cell priming can occur without $CD4^+$ T cell help or CD40/CD40L interaction and instead rely on direct stimulation from DCs with type I interferons (Le Bon, Etchart et al. 2003). IFN-α/β, along with interleukin-12, activates

$CD8^+$ T cells to produce interferon gamma (IFN-γ) (Cousens, Peterson et al. 1999, Zhu, Huang et al. 2009). IFN-γ is one of the signature cytokines that drives naïve $CD4^+$ T cells to become effector T helper type 1 (T_H1) cells, which are characterized by IFN-γ production (Mosmann, Cherwinski et al. 1986). This creates a feed-forward mechanism to further commit other naïve $CD4^+$ T cells towards the T_H1 subset. T_H1 cells create a pro-inflammatory response, activate macrophages, and influences what type of neutralizing antibodies B cells produce (Lund and Randall 2010, Swain, McKinstry et al. 2012).

During viral infection, the spleen and lymph nodes develop sites called germinal centers where B cells can mature, switch immunoglobulin (Ig) isotype production, and become Ig-secreting plasma cells (Dorner and Radbruch 2007). Activated B cells secrete IgM as an initial reaction to infection that is independent of T cell influence. During the course of infection, T helper (T_H) cells travel to the spleen and lymph nodes to aid in germinal center formation. Within these specialized structures, T_H cells interact with B cells and influence their maturation and Ig class switching. Anti-viral antibody responses in mice are predominately IgG2a and are characteristic of a T_H1 cell-driven humoral response (Coutelier, van der Logt et al. 1987). B cells producing IgG1 neutralizing antibodies are characteristic of a T_H2 cell response (Mosmann, Cherwinski et al. 1986). Murine neutralizing antibody responses to several AAV serotypes, including 1 and 2, are predominately IgG2 class when administered intramuscularly or intravenously (Chirmule, Xiao et al. 2000, Xiao, Chirmule et al. 2000, Sudres, Cire et al. 2012). However, humans intramuscularly administered AAV serotypes 1 or 2 had a prevalent IgG1 antibody response, although IgG2 as well as T cell-independent IgG3 antibodies

also increased (Mingozzi, Meulenberg et al. 2009, Murphy, Li et al. 2009). The range in neutralizing antibody isotypes against AAV in both animal models and humans indicates that multiple T_H cell subsets provide help to B cells. Intravascular administration is the most clinically feasible route of administration. Since the lymphoid system and circulatory system are intertwined, an immune response to both the rAAV capsid and vector seems unavoidable unless precautions are taken to modulate the immune system.

As described, an immune response can be elicited against the viral vehicle and the genome encoding the transgene. There is also evidence that the dystrophin protein (full-length or micro-dystrophin) can be recognized as a novel antigen. This has been reported by a variety of experimental strategies including cell therapy transplantation studies (Huard, Roy et al. 1992, Ohtsuka, Udaka et al. 1998), adenovirus vector (Gilchrist, Ontell et al. 2002), and rAAV vector delivery (Mendell, Campbell et al. 2010). Dystrophin immunity in the rAAV vector human clinical (Mendell, Campbell et al. 2010) remains unclear, but the possibility of having an immune response to an engineered micro-dystrophin with novel splice junctions remains an obstacle. Cryptic epitopes arising from alternative reading frames in the rAAV vector can also serve as antigens. Codon-optimization of rAAV rector can remove alternative reading frames (Li, Goudy et al. 2009). Further studies will need to determine if dystrophin immunogenicity can be averted. A current approach is to avoid antigen presentation to immune cells by restricting exogenous expression to target tissues.

Reducing off-target expression of vectors

Initial dystrophin replacement studies using viral vectors used strong, non-cell specific expression cassettes derived from promoter and enhancer elements of viruses including Rouse sarcoma virus and cytomegalovirus (Wang, Li et al. 2000, Harper, Hauser et al. 2002, Sakamoto, Yuasa et al. 2002). To address concerns of off-target exogenous expression, muscle-specific promoters and enhancers have been utilized in gene therapy experiments for muscular dystrophies. The endogenous promoter for muscle cytoskeletal protein desmin has been used in rAAV vectors (Childers, Joubert et al. 2014), yet its size makes it impractical for dystrophin replacement. Regulatory elements from the muscle creatine kinase (MCK) gene have been studied to ascertain the minimal elements required for high expression that is almost exclusively restricted to skeletal and cardiac muscle. MCK-derived regulatory cassettes have exhibited striated muscle-specific expression after delivery by adenovirus and multiple rAAV serotypes (Donoviel, Shield et al. 1996, Hauser, Robinson et al. 2000, Gregorevic, Blankinship et al. 2004, Salva, Himeda et al. 2007). Hybrid promoters combining enhancer and promoter elements of the α-myosin heavy chain and MCK genes display similar expression patterns and have undergone several generations of refinement (Salva, Himeda et al. 2007, Sun, Young et al. 2008). The synthetic promoter "C5-12" also exhibited muscle-specific expression in both AAV and lentiviral vectors (Liu, Mingozzi et al. 2004, Richard, Douillard-Guilloux et al. 2008). Reducing off-target expression with tissue-specific regulatory elements is feasible. However, the pressure to incorporate larger micro-dystrophin constructs has led to the use of smaller regulatory cassettes that may be muscle specific but have differences in expression among muscle fiber types. Both

endogenous MCK and MCK-derived promoters have different expression levels among different muscle fiber types (Tai, Smith et al. 2012). The activity of the MCK-derived promoter is reportedly highest in Type IIb fibers and lowest in Type I fibers. Similarly to muscles that undergo prolonged inactivity (Scott, Stevens et al. 2001), DMD patients experience a transition of fast to slow muscle fiber type (Baloh and Cancilla 1972). These findings highlight the importance of balancing tissue-restricted expression while overcoming variances among cell types within the target tissue(s).

If rAAV-mediated gene therapy is to become safe for clinical application, the three-way interaction between serotype, target tissue(s), and the immune system must be understood to avoid rejection of the transgene. The potential of using this form of therapy repeatedly for a single patient requires not only tolerance to the transgene but prevention, or attenuation, of humoral immune response in order to avoid detrimental consequences.

The novel work in the following chapters expands on several aspects of rAAV-mediated gene therapy for DMD. Studies in Chapter 2 focus on methods to improve the functionality of rAAV/micro-dystrophin vectors by creating a rubric for testing novel constructs in dystrophic mice. While rescuing dystrophic mouse models with rAAV vectors has been repeatedly demonstrated, no one has addressed the possibility that these vectors may be lost through maintenance of skeletal muscle. Experiments in Chapter 3 were designed to determine the consequence of ablating expression of micro-dystrophin in *mdx*^{4cv} mice. Our results suggest that mature skeletal muscle cannot tolerate loss of micro-dystrophin expression. The rapid onset of dystrophic pathophysiology in these ablation studies reinforced the notion that rAAV-mediated gene therapy may require repeat administration of vectors. Additional studies in Chapter 3 demonstrated the ability

to attenuate a cell-mediated response after repeat administration of rAAV vectors using transient immunosuppression. We were able to treat skeletal muscle of *mdx*^{4cv} mice more than once by repeat administration of rAAV/micro-dystrophin vectors. As a third arm of experiments, Chapter 4 examines the tropism of AAV serotypes for myogenic stem cell transduction. Lastly, Chapter 5 describes a series of mouse and canine studies that compare transduction efficiencies among several AAV serotypes exhibiting a high tropism for muscle. Additionally, we examined alterations in rAAV vector formulation for potential effects in transduction. An improved understanding of dystrophin and its sub-domains as well as rAAV transduction can add valuable information for treating genetic diseases of striated muscle, like Duchenne muscular dystrophy. Providing further insight is the primary focus of the research presented in the following chapters.

Notes to Chapter

Portions of the following publications were reproduced or modified for this chapter:

Arnett AL, Ramos JN, Chamberlain JS (2012) Gene Therapy of Skeletal Muscle Disorders Using Viral Vectors. In: Hill JA, Olson EN, editors. Muscle Fundamental Biology and Mechanisms of Disease. 1 ed: Academic Press. pp. 1045-1051.

Ng R, Banks GB, Hall JK, Muir LA, Ramos JN, et al. (2012) Animal models of muscular dystrophy. Prog Mol Biol Transl Sci 105: 83-111.

Seto JT, Ramos JN, Muir L, Chamberlain JS, Odom GL (2012) Gene replacement therapies for duchenne muscular dystrophy using adeno-associated viral vectors. Curr Gene Ther 12: 139-151.

Chapter 2

Increased Functionality of Micro-Dystrophins by Altering Size and Rod Domain Composition

Introduction

Duchenne muscular dystrophy (DMD) is a recessive muscle wasting disease afflicting approximately 1 in 3500 males. DMD patients carry a mutation in the *dystrophin* gene, resulting in aberrant or absent expression of the dystrophin protein. Patients experience progressive wasting of skeletal muscles and progressive cardiac dysfunction, leading to loss of ambulation and premature death, primarily due to cardiac or respiratory failure. Current available treatments are only able to slow the pathology of this disease (Emery 2003). Gene therapy approaches for DMD have been effectively demonstrated in dystrophic animal models by either directly targeting a class of mutations, as with exon skipping, or replacing the mutated gene with viral-vector mediated delivery (Seto, Ramos et al. 2012, Benedetti, Hoshiya et al. 2013, Koo and Wood 2013). Recombinant adeno-associated viral (rAAV) vectors are a promising vehicle for gene therapy, being already tested in clinical trials for both DMD and limb-girdle muscular dystrophies (Mendell, Campbell et al. 2010, Mendell, Rodino-Klapac et al. 2010, Herson, Hentati et al. 2012). Several serotypes of AAV demonstrate a high degree of tropism for striated muscles (Seto, Ramos et al. 2012).

Pre-clinical studies designing and testing newer generations of therapeutic constructs for DMD are confined by the approximately 5.0 kb size of a single-stranded rAAV vector genome (Dong, Nakai et al. 2010, Wu, Yang et al. 2010). Packaging the entire 13.9 kb cDNA of the muscle-specific isoform of dystrophin into a single rAAV

capsid cannot be achieved, and thus requires use of miniaturized, synthetic versions of the cDNA. Although *in vivo* recombination of two and three rAAV vector genomes has been demonstrated to deliver a mini- or full-length dystrophin coding sequence, (Odom, Gregorevic et al. 2011, Koo, Popplewell et al. 2014, Lostal, Kodippili et al. 2014) the efficiency of delivering multiple vectors for reconstituting full-length dystrophin is suboptimal and increases the overall dose of viral capsid proteins needed for delivering vectors. However, highly beneficial rAAV-mediated gene therapy has been achieved using rationally-designed miniature versions of the dystrophin cDNA based in part on mRNA expressed in mild Becker muscular dystrophy patients carrying in-frame deletions of the gene (Koenig, Beggs et al. 1989, England, Nicholson et al. 1990, Beggs, Hoffman et al. 1991, Goldberg, Hausmanowa-Petrusewicz et al. 1998). Studies in transgenic and vector treated dystrophic mice expressing various dystrophin truncations have identified several elements of the *dystrophin* gene that are required for a highly functional micro-dystrophin (Harper, Hauser et al. 2002).

The full-length striated muscle isoform of dystrophin has an integral role in transmitting contractile force through the sarcolemma and out to the extracellular matrix. In addition to maintaining the mechanical link between the intracellular cytoskeleton and the membrane bound dystrophin glycoprotein complex (DGC), dystrophin is also a scaffold for signaling proteins (Campbell and Kahl 1989, Winder 1997, Ozawa 2004). The amino-terminal domain of dystrophin binds to F-actin filaments of the intracellular cytoskeleton (Hemmings, Kuhlman et al. 1992, Way, Pope et al. 1992, Fabbrizio, Bonet-Kerrache et al. 1993, Pavalko and Otey 1994). The middle, rod domain is the largest and is composed of 24 spectrin-like repeats (SRs) that are flanked and interspersed with four

hinge sub-domains. The rod domain gives dystrophin the necessary elasticity for maintaining the integrity of the sarcolemma during muscle contractility (Winder 1997). Various SRs provide unique regions that serve as additional binding sites for the intracellular cytoskeleton, the sarcolemma as well as members of the DGC (Rybakova, Amann et al. 1996, Metzinger, Blake et al. 1997, Warner, DelloRusso et al. 2002, Lai, Thomas et al. 2009). In particular, the cysteine-rich domain and the adjacent hinge 4 region form the β-dystroglycan binding domain (DgBD),(Blake, Weir et al. 2002, Ishikawa-Sakurai, Yoshida et al. 2004) while the carboxy-terminal domain is a scaffold for additional DGC components (Abmayr S 2006).

Functional micro-dystrophins (μDys) improve the dystrophic pathology in striated muscle by protecting the sarcolemma from contraction-induced injury and increasing the capacity to generate specific force. These parameters are achieved by binding to F-actin filaments and β-dystroglycan through the amino-terminal domain and the DgBD (Cox, Sunada et al. 1994, Greenberg, Sunada et al. 1994, Corrado, Rafael et al. 1996, Rafael, Cox et al. 1996, Harper, Hauser et al. 2002, Warner, DelloRusso et al. 2002, Gardner, Kearney et al. 2006). Prior studies indicate these two critical domains must be connected by at least four SRs from the central rod domain, but there are numerous ways in which miniaturized dystrophins containing at least 4 SRs can be constructed. Selection of specific SRs in μDys design can restore additional DGC components to the sarcolemma. Neuronal nitric oxide synthase (nNOS) is an important signaling protein required for vasodilation in response to muscle contractile activity (Brenman, Chao et al. 1995, Stamler and Meissner 2001, Torelli, Brown et al. 2004, Kobayashi, Rader et al. 2008), and proper association of nNOS with the DGC requires the presence of SRs 16 and 17

(Lai, Thomas et al. 2009, Lai, Zhao et al. 2013). Sequences within spectrin-like repeats 20-24 as well as Hinge 4 are needed for proper association of dystrophin with microtubules, which is important for maintaining the intracellular architecture and torque production in skeletal muscle (Prins, Humston et al. 2009, Belanto, Mader et al. 2014). Nonetheless, the carboxy-terminal and most of the SR domains have been found dispensable without severely compromising the health of striated muscles (McCabe, Towbin et al. 1989, Dunckley, Love et al. 1992, Crawford, Faulkner et al. 2000).

Several of the best micro-dystrophins tested to date are able to protect muscles from contraction-induced injury and restore some, but not all, the specific force generating capacity to dystrophic mouse and canine models for DMD (Wang, Tapscott et al. 2011, Seto, Ramos et al. 2012). Other micro-dystrophins carrying different combinations of SRs and hinges function less well in dystrophic muscles, and the reasons for differences in functionality are not always clear. However, they likely relate to effects on micro-dystrophin elasticity, folding, stability and the ability to assemble sub-portions of the DGC without steric hindrance. The variable degrees of effectiveness of micro-dystrophins tested to date suggest that additional clones with improved function might be designed (Banks, Judge et al. 2010, Koo, Malerba et al. 2011). Indeed, since current systemic delivery methods for AAV vectors are not yet able to restore normal levels of dystrophin proteins to muscles of large animal models for DMD, therapeutic interventions with AAV would benefit from the use of the most functional micro-dystrophins available.

In this study, we designed several new versions of μDys clones with a focus on increasing functional activity while allowing more complete restoration of the DGC.

These new clones were directly compared with our previously characterized ΔH2-R23+H3/ΔCT clone (μDysH3), which is highly functional in striated muscles of *mdx* mice (Banks, Judge et al. 2010). The design of these constructs focused on the central rod domain in efforts to improve the contractility of muscles expressing the constructs and to restore nNOS localization to the DGC (Lai, Thomas et al. 2009, Lai, Zhao et al. 2013). We also tested the ability to deliver larger constructs carrying 4, 5 or 6 SRs. To allow stable packaging of these larger μDys clones we incorporated a small regulatory cassette (RC) modified from the muscle creatine kinase gene. This CK8 RC displays strong, muscle-restricted expression yet is less than 500 bps in size (Martari, Sagazio et al. 2009, Goncalves, Janssen et al. 2011). Our findings show that μDys clones with increased function and size can be developed and delivered to striated muscles using rAAV vectors.

Results

Design of novel micro-dystrophin clones

Most micro-dystrophins (μDys) tested to date have contained between 4 and 5 spectrin-like repeat (SR) domains, the presence or absence of an internal hinge domain, as well as the N-terminal actin-binding domain (N-ABD) and the dystroglycan binding domain (DgBD) (Banks, Judge et al. 2010, Duan 2011). However, since there are thousands of alternatives for the design of μDys clones from the 24 SRs and multiple hinge regions in the full-length dystrophin, we designed seven new clones to test several logical variations on the rod domain structure. Each of the new clones retained coding sequences for the N-ABD and the DgBD, but incorporated novel combinations of SR and hinge domains, with a goal of generating μDys clones with improved functional properties that could be delivered and expressed from an AAV vector.

Our previous studies showed that the choice of hinge domains within a μDys clone could significantly impact the function of the protein (Banks, Judge et al. 2010). Thus, we asked whether alternative and shorter hinges could be substituted for Hinge 3, which was used in our previous best μDys clone, μDysH3. Since other studies have also shown that including SRs 16-17 can improve the function of μDys by recruiting nNOS to the DGC, we also tested these SRs in the context of various hinge domains. We also sought to minimize creation of novel junctions where domains not normally adjacent to one another in the full-length protein are brought together. Finally, we asked whether the inclusion of either 5 or 6 SRs would improve μDys function in the context of the newer hinge and nNOS localization domains being tested. The structure of the novel μDys clones, in comparison to the previously tested μDysH3 and the full-length protein are illustrated in **Figure 2.1a**.

Two regions in dystrophin were tested for their ability to substitute for hinge 3. The hinge regions of the rod domain are proline rich and lack alpha-helical signature motifs that compose the triple-helical coiled-coil of a spectrin-like repeat (Winder, Gibson et al. 1995). Interestingly, SR23 contains a proline-rich linker between alpha-helices *b* and *c*. We sought to determine if this sequence (with alpha-helix *c* of R23) could be used as a hinge domain either by itself (μDys1), adjoining R16-17 (μDys2) or together with H3 (μDys4). One additional construct replaced hinge 3 with the entire SR23 (μDys5; **Fig. 2.1a**). We also tested a second hinge-like region composed of a 20 amino acid insertion previously noted to be located between SRs 15 and 16 (μDys6) (Winder, Gibson et al. 1995).

Additional constructs were designed to test various combinations of the SR domains in the context of these hinges. Previous results have suggested that the context of SR domains is important for their function, so we also tested whether a hybrid SR, composed of the first half of SR20 and the final half of SR24 would improve function (μDys3). This hybrid SR thus merges the portion of SR20 normally adjacent to Hinge 3 with the portion of SR24 that merges into Hinge 4 (**Fig. 2.1a**). Similar considerations influenced the design of the μDys6 construct noted above, where the novel hinge located between SR15-16 was used in its normal context adjacent to the nNOS location region in SR16-17. This latter construct was also compared directly with a similar construct but which used Hinge 3 instead of the short hinge-like region from between SR15-16 (**Fig. 2.1b**). Note that μDys clones 5-7 also incorporated either 5 or 6 SR domains, potentially increasing the overall function of the protein (Harper, Hauser et al. 2002).

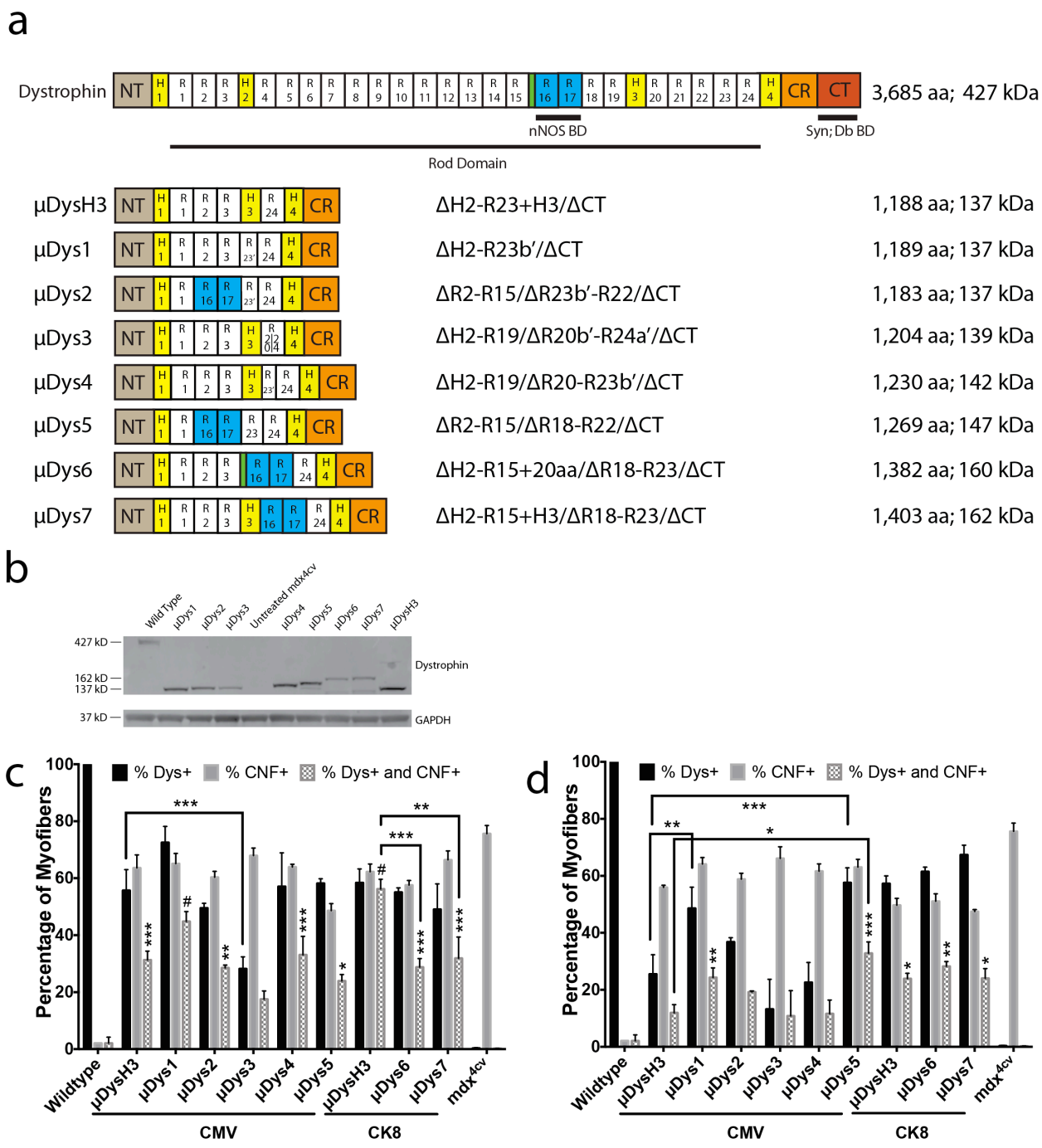

Figure 2.1 Initial screening of novel μDys constructs. Schematic of truncated dystrophin constructs used in this study (**a**). NT, amino terminal domain; H, hinge; R, spectrin-like repeat; nNOS BD, neuronal nitric oxide synthase binding domain; CR, cysteine-rich domain; CT, carboxyl terminal domain; Syn, syntrophin binding domain; Db BD, dystrobrevin binding domain. Green, unlabeled region marks 20-amino acids between R15 and R16. aa, amino acid; kDa, kilodalton. Dystrophic *mdx*^{4cv} mice were injected with 5x10^{10} vector genomes (vg) of AAV/CMV-μDys into one tibialis anterior

(TA) muscle while the contralateral served as an internal, untreated control. Expression of all tested constructs was verified at 4 weeks after treatment by Western analysis of TA muscle lysates, along with wild type and untreated *mdx*^{4cv} controls. Glyceraldehyde-3-phosphate dehydrogenase (GAPDH) served as internal loading control (**b**). Myofibers from TA cross sections were quantified for dystrophin expression and central nucleation at 4 or 12 (**c,d**) weeks post-treatment (N=3-5 per cohort for each time point, mean ± S.E.M.). μDysH3 served as a comparative gauge of performance. μDys6 and μDys7 were too large to be cloned into AAV-expression vectors using the ubiquitous cytomegalovirus (CMV) promoter. Consequentially, the CMV promoter was replaced with myogenic-specific CK8 promoter to allow efficient packaging and *in vivo* evaluation, which also required μDysH3 to be re-evaluated with this regulatory expression cassette. (**c,d**) Characters denote significance from wild type mice. *P<0.05, **P<0.01, ***P<0.001, #P<0.0001.

Functionality of partial spectrin-like repeats is dependent on the rod domain composition

An initial functional screen of the novel μDys clones 1-7 was made in comparison to the previously characterized μDysH3 by generating rAAV6 vectors regulated by the highly active CMV promoter. A dose of $5x10^{10}$ vector genomes (vg) was intramuscularly injected into one tibialis anterior of 5-6 week old dystrophic *mdx*^{4cv} male mice (Chapman, Miller et al. 1989), with the contralateral muscle serving as an internal negative control (N=4-5 mice per construct). Dystrophin expression and central nucleation, a hallmark of degeneration/regeneration, was measured at 4 weeks and 12 weeks post-injection (**Figs. 2.1c,d**) to determine how well each construct was expressed and able to prevent myofiber necrosis. All constructs generated μDys proteins of the predicted sizes, as shown by Western analysis (**Fig. 2.1b**). At this age and vector dose per injected TA muscle, all treated *mdx*^{4cv} cohorts had significantly fewer dystrophin positive (Dys+) myofibers compared to wild type C57BL/6 mice ($P<0.001$), yet differences of functionality were observed among the micro-dystrophins. Constructs μDys3 and μDys4 performed notably less well than μDysH3, having a reduction in dystrophin-positive myofibers between 4 and 12 weeks. Constructs μDys-1, 2, and 5 exhibited more dystrophin positive myofibers than μDysH3 by 12 weeks post-injection (**Fig. 2.1d**). An initial screen of μDys6 and μDys7 was made against μDysH3 driven by the CK8 promoter. Both the new constructs generated comparable levels of transduced (Dys+) and centrally nucleated (CNF+) myofibers by 12 weeks post-injection relative to μDysH3 (**Fig. 2.1d**). Myofibers exhibiting both dystrophin expression and central nucleation were quantified at both time points (**Figs. 2.1c,d**). Levels of Dys+ and CNF+ myofibers decreased from 4 to 12 weeks post-injection in the treated cohorts, yet remained higher than wild type. Whether this

was the result of poor functionality or sub-optimal dose of a micro-dystrophin construct remained uncertain with the initial screen alone, prompting a systemic administration for further evaluation.

Novel μDys constructs attenuate pathology in respiratory and hind limb skeletal muscles

The μDys-1, 2, 3, 4, 5, and μDysH3 vectors were re-cloned to replace the CMV with the smaller and muscle-specific CK8 promoter, enabling a direct comparison with the larger six SR-containing constructs (μDys6, 7). For systemic treatment, a bolus of 10^{13} vg was delivered to 14-day old *mdx*^{4cv} male mice via retro-orbital injection. Treated mice were assessed at either 3 or 6 months post-injection, along with age matched untreated and wild type controls. We designed this experiment to monitor expression of the μDys constructs and assess the relative extent to which they can halt dystrophic pathophysiology. Persistence of μDys expression was measured by immunofluorescence staining of gastrocnemius and diaphragm muscle cryosections. The recruitment of DGC members β-dystroglycan and nNOS (for applicable constructs) to the sarcolemma was also verified (**Fig. 2.2**).

At three months post-injection, all treated groups had greater than 60% expression of dystrophin at the sarcolemma in both the gastrocnemius and diaphragm myofibers. The percentage of dystrophin-positive myofibers that were centrally-nucleated was not significantly different from wild type controls (**Figs. 2.3a,c**). At this time point μDys2 was observed to be expressed at significantly lower levels compared with μDys5 in the gastrocnemius and the diaphragm (**Figs. 2.3a,c**). The μDys2-treated mice also had significantly fewer transduced

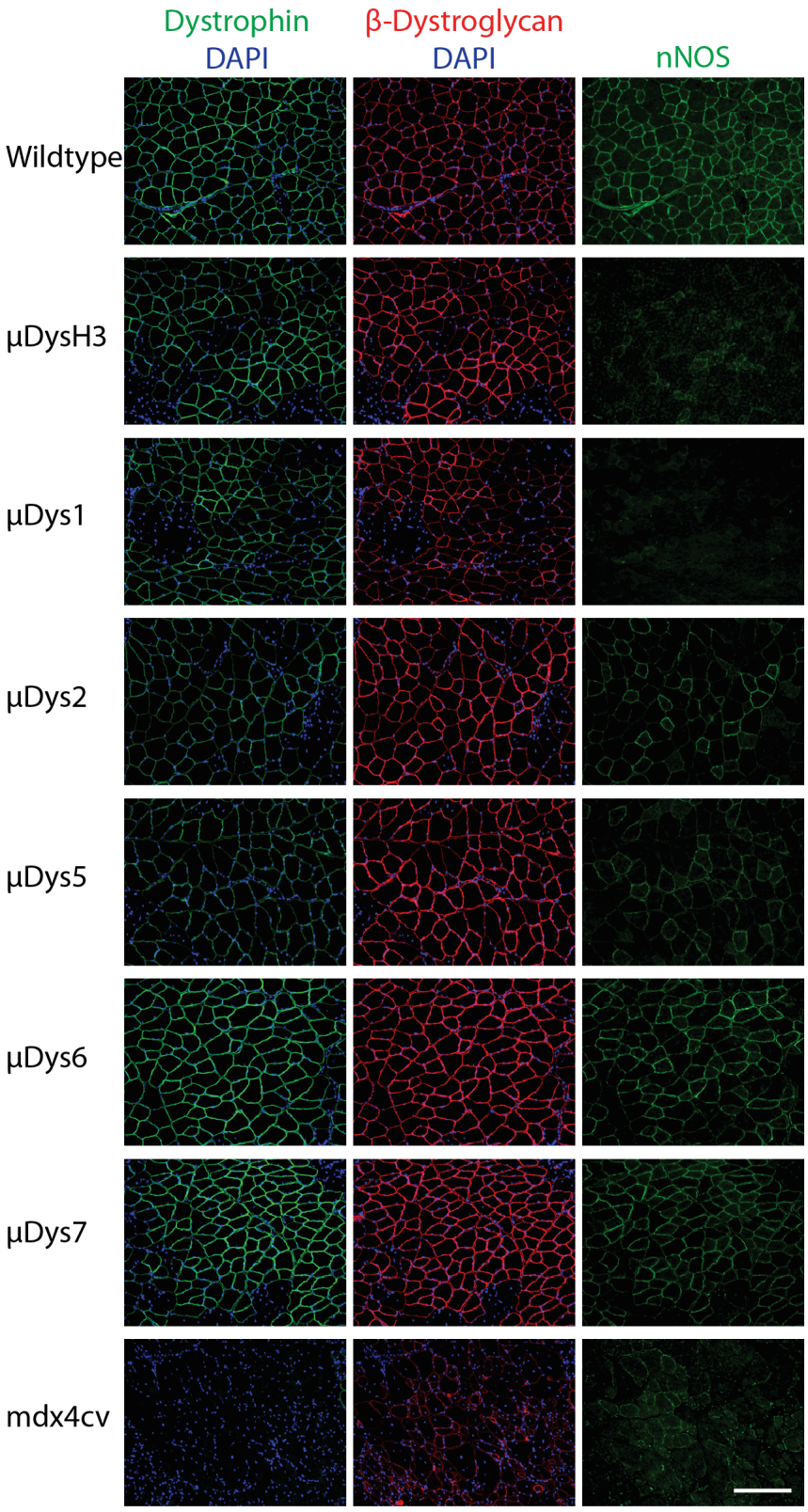

Figure 2.2 Recruitment of DGC members is dependent on binding domains within μDys constructs. Dystrophic *mdx*^{4cv} mice were injected retro-orbitally with 10^{13} vg of AAV6/CK8-μDys at 14 days of age. Three and six months post-treatment, skeletal muscles were immunostained for dystrophin glycoprotein complex members. Shown here are representative gastrocnemius cross sections at six months post-treatment. Dystrophin (green) and DAPI-stained nuclei (blue) are in left column, β-dystroglycan (red) and DAPI in middle column, and neuronal nitric oxide synthase (pseudo-colored green) in right column. Each row depicts representative results from cohorts of wild type, treated *mdx*^{4cv}, and untreated *mdx*^{4cv} mice. Scale bar, 200 μm.

myofibers in the diaphragm compared to μDys1, μDys 5, and μDysH3 injected animals (**Fig. 2.3c**). Conversely, μDys5 injected mice displayed significantly higher numbers of transduced myofibers in the gastrocnemius compared with all other treated groups (**Fig. 2.3a**). Morphological analysis of the same muscles demonstrated that all treated groups had significantly reduced percentages of centrally nucleated myofibers. In the diaphragm, there were no significant differences in the percentages of centrally nucleated myofibers between wild type and treated groups. However, μDys2 and μDysH3 injected mice displayed significantly higher levels of central nucleation (19% and 20%, respectively; $P<0.001$) than wild type (0%) in the gastrocnemius.

The absence of a functional dystrophin impairs assembly of the DGC. This results in a loss of mechanical force transmission as well as increased susceptibility to contraction-induced injury (Emery 2003, Ozawa 2004). Expression of rAAV-μDys vectors has demonstrated an ability to increase specific force generation and resistance to contraction-induced injury in dystrophic animal models (Seto, Ramos et al. 2012). We sought to determine which novel μDys constructs could improve these metrics at three months post-injection (**Figs. 2.3c,d**).

Gastrocnemius muscles and diaphragm muscle strips were prepared for *in situ* and *in vitro* measurement of mechanical properties, respectively. The specific force generation in the gastrocnemius muscle increased in all treated groups compared to untreated dystrophic controls (**Fig. 2.3b**). Only μDys1 and μDys2 injected mice displayed increased specific force in diaphragm muscle strips (156 kN/m^2 and 110 kN/m^2, respectively compared to 98 kN/m^2 in untreated mice) (**Fig. 2.3f**). Additionally, expression of all the novel μDys constructs increased resistance to contraction-induced

injury, yet there were no significant differences in comparison to each other (data not shown). The dystrophic pathology appeared halted by three months post-injection, yet the physiological performance wasn't significantly improved. Based on this single time point, it was unclear if the results fully reflected the functionality of the various μDys constructs, or if longer time points were needed for a more complete analysis.

Long-term expression exposes functional discrepancies of μ*Dys constructs*

By six months post-treatment, most treated groups exhibited reduced expression of dystrophin and a concomitant increase in the percentage of myofibers displaying central nucleation, albeit to varying degrees, compared to analysis at three months post-treatment. However, the percentage of myofibers exhibiting both dystrophin expression and central nucleation was not significantly different from wild type controls (**Figs. 2.4a,c**). The μDys1, -5, -6, -7 and –H3 injected mice displayed ≥60% dystrophin positive myofibers in the gastrocnemius and ≥74% in the diaphragm at 6 months. Transduction levels of μDys2 decreased approximately 2-fold in the gastrocnemius over the course of three months (from 63% to 31% positive myofibers), and decreased 20% in the diaphragm, making its performance the worst of the constructs tested ($P<0.001$; **Figs. 2.4a,c**). The degree of degeneration/regeneration had increased in both muscles for all treated cohorts, with the exception of two tested constructs. Central nucleation for μDys3 remained at 3% in the diaphragm, and μDysH3 decreased from 20% to 8% in the gastrocnemius (**Figs. 2.4a,c**).

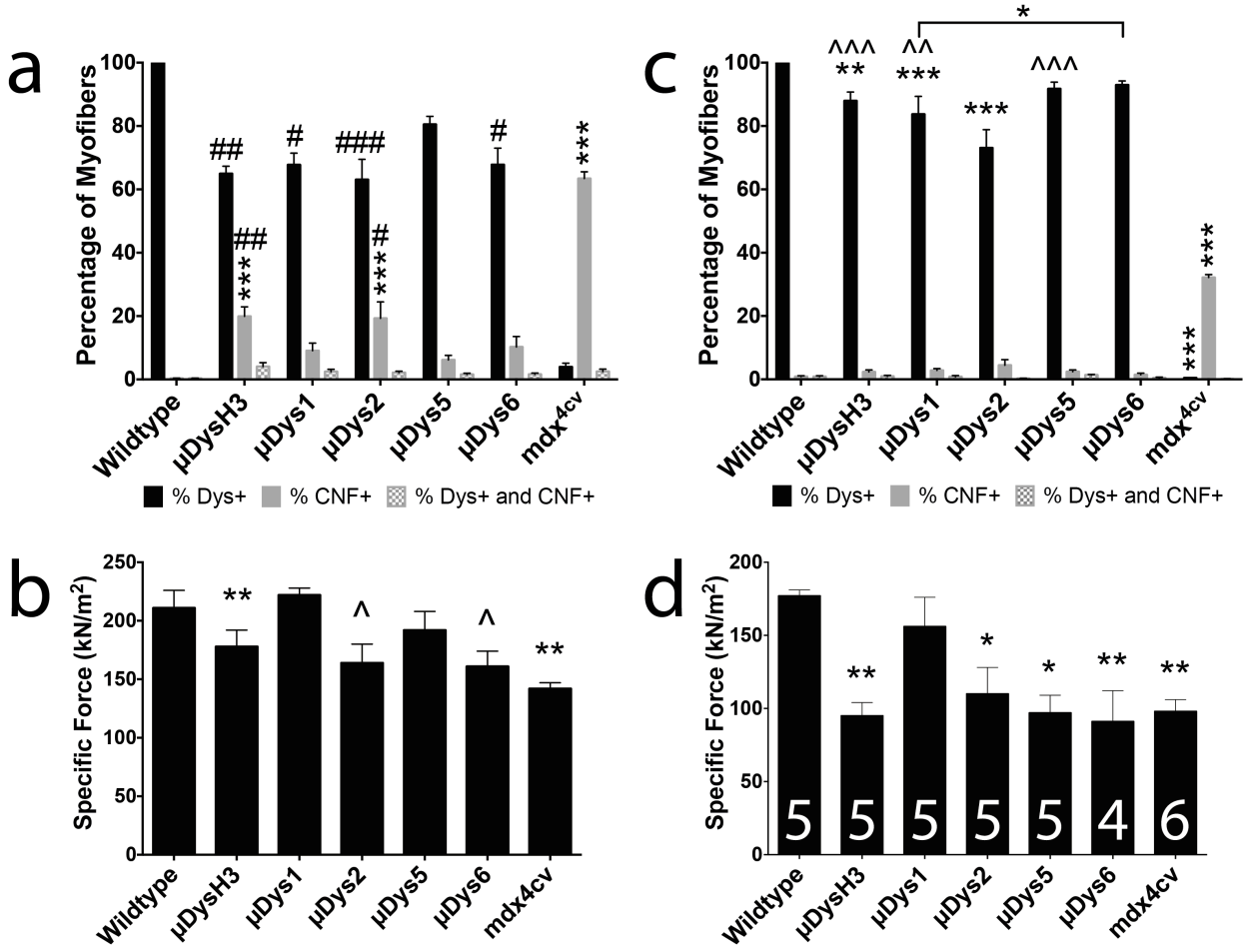

Figure 2.3 Evaluation of systemic treatment at 3 months post-treatment. Gastrocnemius (**a,b**) and diaphragm (**c,d**) muscles were evaluated to determine the performance of novel µDys constructs. Muscle cross sections were quantified for dystrophin expression and centrally nucleated myofibers. Levels of myofibers exhibiting dystrophin expression and/or exhibiting central nucleation are represented as percentages (**a,c**). Specific force generation was measured *in situ* for gastrocnemius (**b**) and *in vitro* for diaphragm strips (**d**). The n value for each cohort is listed in columns of (**d**). For non-bracketed characters, *P<0.05, **P<0.01, ***P<0.001 from wild type. ^P<0.05, ^^P<0.01, ^^^P<0.001 from µDys2-treated mice. #P<0.05, ##P<0.01, ###P<0.001 from µDys5-treated mice.

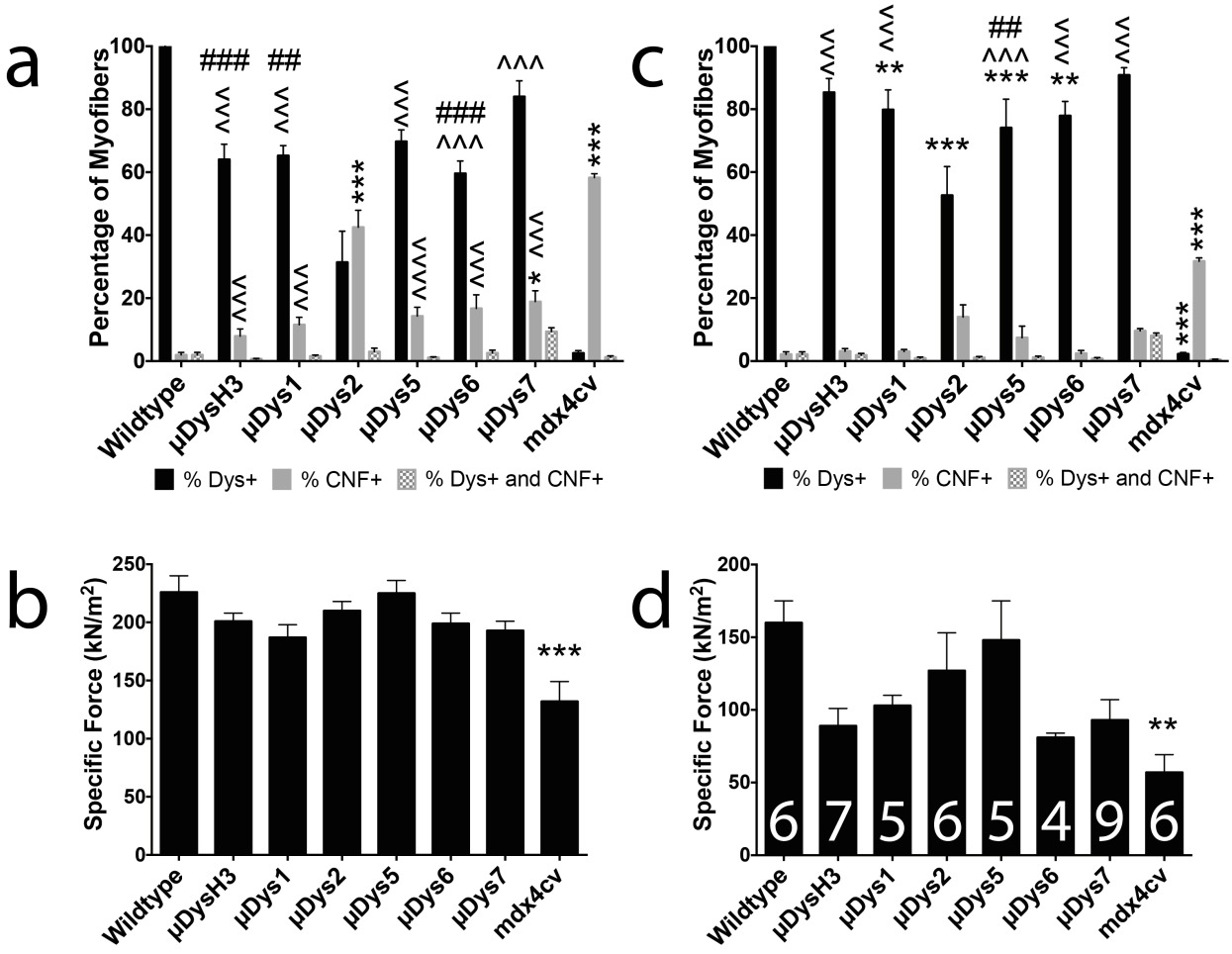

Figure 2.4 Evaluation of systemic treatment at 6 months post-treatment.
Gastrocnemius (**a,b**) and diaphragm (**c,d**) muscles were evaluated as described in **Figure 3**. The n value for each cohort is listed in columns of (**d**). *P<0.05, **P<0.01, ***P<0.001 from wild type. ^P<0.05, ^^P<0.01, ^^^P<0.001 from µDys2-treated mice. #P<0.05, ##P<0.01, ###P<0.001 from µDys7-treated mice.

Despite the morphological trend observed with the six-month post-treatment data, the specific force generation was still higher than in muscles from untreated controls. Injection of one construct, μDys5, led to force generation levels close to those in wild type mice in both the gastrocnemius (225 versus 226 kN/m^2; **Fig. 2.4b**) and the diaphragm (148 versus 160 kN/m^2; **Fig. 2.4d**). Based on previous studies with mini-dystrophins containing six to eight SRs, we had predicted that the μDys constructs containing six SRs would generate the most specific force as well as provide the greatest protection from contraction-induced injury (Harper, Hauser et al. 2002). However, specific force generation in the gastrocnemius muscles of μDys6 and μDys7-treated mice was significantly higher than untreated controls ($P<0.01$ and $P<0.0001$, respectively), but were not the highest (**Figs. 2.4b,d**). Instead, μDys5 injected mice displayed the highest levels of specific force generation. The larger constructs were also not necessarily the best at protecting from contraction-induced injury. For example, μDys6 injected mice had the largest force deficit while μDys7 provided the highest protection from contraction-induced injury in the gastrocnemius (**Fig. 2.5a**). However, resistance to contraction-induced injury in diaphragm muscle strips was the highest in mice expressing μDys6 and μDys7 as well as μDys5 and μDysH3 (**Fig. 2.5b**). The contrasting results among μDys6 and μDys7 between muscle groups and the significant difference in force deficits within the gastrocnemius ($P<0.0001$) suggest that the performance of a particular μDys construct may be influenced by the regulatory expression cassette and the muscle assessed (Harper, Hauser et al. 2002, Salva, Himeda et al. 2007). This point was also exemplified with μDys2-treatment, where the susceptibility to contraction-induced injury

was reduced in the gastrocnemius but unexpectedly exacerbated in the diaphragm, relative to untreated controls (**Fig. 2.5**).

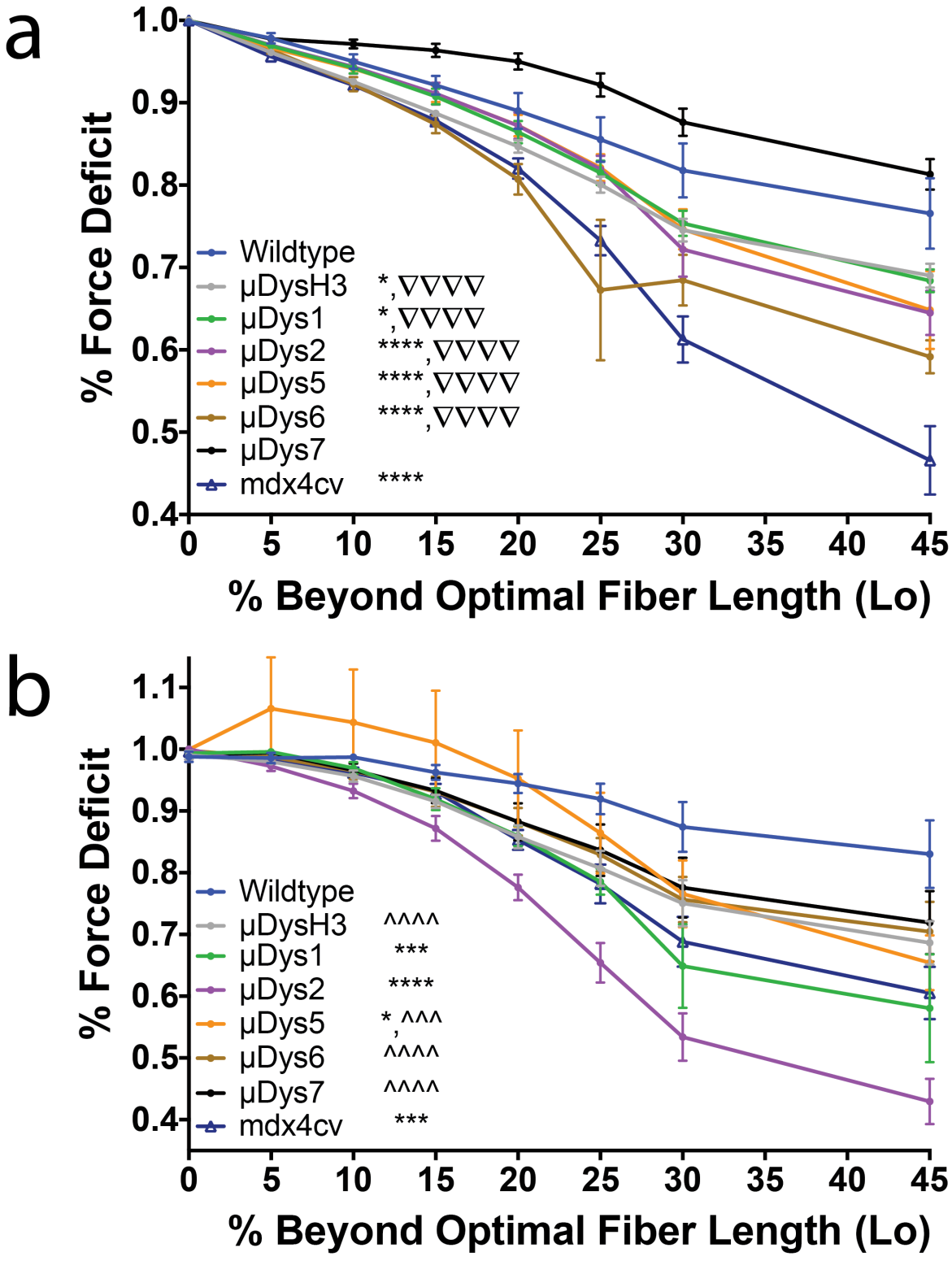

Figure 2.5 Extent of sarcolemmal protection from eccentric contraction in skeletal muscles. Systemically treated mice described in **Figures 2,4** were subjected to eccentric

contractions of increasing length. Gastrocnemius (**a**) and diaphragm strips (**b**) were measured for the maximum isometric force generated prior to an eccentric contraction. During stimulating contractions, muscles were lengthened at a defined distance beyond their optimum fiber lengths. Distances are reported as percentage beyond optimal fiber length (L_O). *P<0.05, ***P<0.001, ****P<0.0001 from wild type at 45% beyond L_O. ^^^P<0.001, ^^^^P<0.0001 from μDys2-treated mice at 45% beyond L_O. ∇∇∇∇P<0.0001 from μDys7-treated mice at 45% beyond L_O.

Discussion

Recombinant AAV-mediated gene therapy for Duchenne muscular dystrophy shows great potential as suggested by encouraging results in dystrophic animal model studies. However, the limited carrying capacity of rAAV vectors requires the truncation of the carboxy-terminal and rod domains of dystrophin to enable packaging. Animal studies indicate a positive correlation between the size of the rod domain and the functionality of dystrophin (Harper, Hauser et al. 2002). Although larger dystrophin constructs have been expressed through recombination of multiple rAAV vectors, the state of the art lacks the ability to ensure delivery of all moieties to each transduced cell (Odom, Gregorevic et al. 2011, Koo, Popplewell et al. 2014, Lostal, Kodippili et al. 2014). Apart from not being able to express a functional dystrophin, inadvertent competition with recombined dystrophin isoforms may result in a dominant negative affect as seen with expression of non-muscle specific isoforms (Judge, Haraguchiln et al. 2006). Therefore, we tested a novel series of micro-dystrophins with altered rod domain compositions that could be delivered by a single vector genome *in vivo*.

Our results demonstrate high functionality of some μDys when increasing the rod domain to five and even six entire spectrin-like repeats. Along with increased dystrophin-positive myofibers, an improvement in the specific-force generating capacity and resistance to contraction-induced injury was observed in muscles expressing several of the novel constructs at six months post-treatment. One construct with five SRs, μDys5, led to the highest measured specific force in both the gastrocnemius and diaphragm muscles of treated *mdx*^{4cv} mice. Also encouraging were the results with our largest tested construct with six SRs, μDys7. At six months post-treatment, μDys7-expressing muscles

displayed the highest resistance to contraction-induced injury. This coincides with previous studies demonstrating that truncated dystrophins with more spectrin-like repeats improve sarcolemma integrity (Harper, Hauser et al. 2002). Despite also having six SRs, μDys6 failed to perform as well as μDys7 in the gastrocnemius six months after treatment. The only difference between these two constructs was the middle of the rod domain, indicating that the 20-amino acid region between SRs 14 and 15 did not effectively function as a surrogate hinge.

Four of the novel constructs incorporated the nNOS localization domain, which has previously been shown to function in the contect of μDys expression by AAV-mediated gene delivery (Lai, Thomas et al. 2009, Lai, Zhao et al. 2013). Not only does sarcolemmal restoration of nNOS ameliorate exercise-induced fatigue (Torelli, Brown et al. 2004, Kobayashi, Rader et al. 2008), it also prevents ischemic damage (Thomas, Sander et al. 1998). The rod domain of most of our novel micro-dystrophin constructs incorporated SRs 16 and 17 in order to restore nNOS while allowing the size of the rod domain to increase, and each of these constructs displayed proper re-localization of nNOS to the sarcolemma of treated mice (**Fig. 2.2**).

Additionally, we assessed if expression of any of these novel constructs could result in ringbinden formation around myofibers. This unusual phenotype was observed in some muscles of mice expressing a previously described ΔR4-R23/ΔCT (μDysH2) construct (Banks, Combs et al. 2008, Banks, Judge et al. 2010). No ringbinden formation was observed with expression of any of the novel constructs in the gastrocnemius (**Fig 2.6**) nor any other skeletal muscles in systemically treated mice.

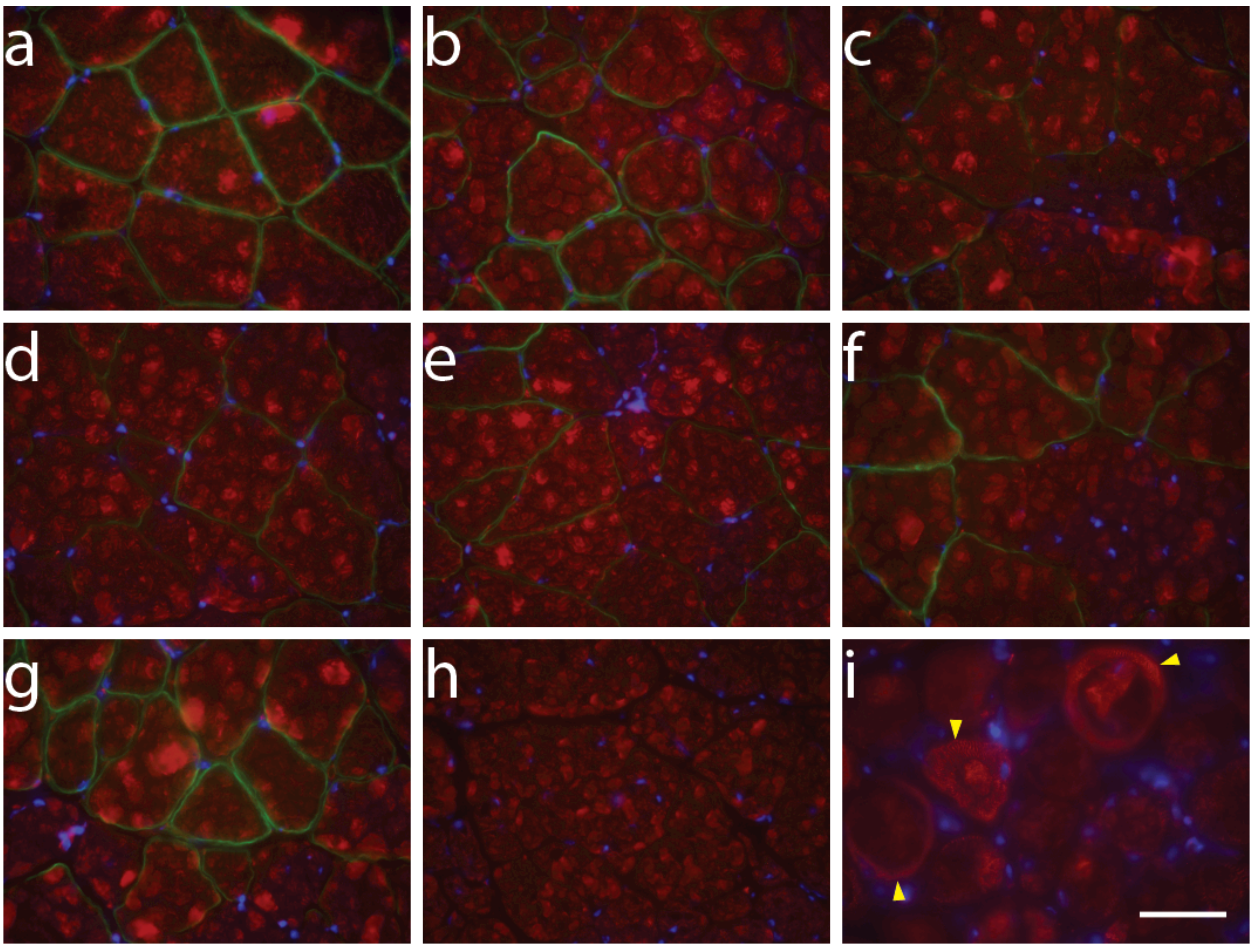

Figure 2.6 Systemically tested novel μDys constructs do not induce ringbinden phenotype in skeletal muscle. Dystrophic *mdx*^{4cv} mice were injected retro-orbitally with 10^{13} vg at 14 days of age. Six months post-treatment, cross sections of gastrocnemius muscles were immunostained for dystrophin (green), DAPI (blue) and α-sarcomeric actin (red). One representative section is shown from cohorts of wild type (**a**) and *mdx*^{4cv} treated with μDysH3 (**b**), μDys1 (**c**), μDys2 (**d**), μDys5 (**e**), μDys6 (**f**), μDys7 (**g**), or untreated *mdx*^{4cv} mice (**h**). Gastrocnemius from transgenic mice expressing ΔR4-R23/ΔCT (Harper, Hauser et al. 2002) on *mdx*^{4cv} background (**i**) was also immunostained as a positive control. Yellow arrowheads mark examples of ringbinden formation around myofibers. Scale bar, 50 μm.

Assessing treated mice at three and six months post-treatment allowed us to monitor the persistence and performance of the newer constructs *in vivo* and avoid premature functionality conclusions derived from analysis after only three months. Two constructs, μDys1 and μDys2, appeared to match or exceed our μDysH3 standard in certain metrics at three months post-treatment, yet showed poorer performance at the six-month time point. This finding emphazies that multiple time point analyses can discriminate between potential therapeutic constructs and help identify the most suitable one. With the immense number of variations that could be designed in a truncated dystrophin, full analyses of large numbers of constructs would require very large numbers of test animals. Perhaps incorporating transgenic biomarkers for degeneration/regeneration could reduce the number of animals required for powerful analyses (Maguire, Lim et al. 2013). This would also allow individual monitoring and greater insight into the functionality of μDys constructs prior to terminal procedures (e.g. functional analysis of multiple muscles).

Generating transgenic mice expressing all the constructs tested in this work would perhaps allow a more stringent characterization of these modified rod domain compositions. Our approach is arguably more translatable due to the fact that we also were determining how effective our standard and novel constructs were at halting the dystrophic pathogenesis in already affected animal. This approach also factors in the doses administered and the time of therapeutic intervention. Our study also incorporated the variable expression levels among myofiber types when using the myogenic-specific CK8 promoter. Previous myogenic-specific regulatory cassettes exhibited higher expression in fast, Type II myofibers, as identified by the expression of myosin heavy

chain isoforms (Tai, Smith et al. 2012). The CK8 promoter used in this study also displays similar differences in expression among myofiber types (Hauschka Lab, unpublished data). Our studies have identified two novel constructs, μDys5 and μDys7, that appear to function better than our previously best μDys, the μDysH3 construct. However, no single micro-dystrophin construct dominated in every test used or at all time points measured. This could be attributed to the experimental variability between animals (transcription/translation rates for individual sequences) and groups and the consideration that all treatments of dystrophic mice were either after or immediately prior to the onset of the degeneration and necrosis. Further studies will need to determine if one construct small enough to be packaged within a single rAAV vector genome will suffice for all examined muscle groups. Additionally, regulatory expression cassettes can also be refined for improved transduction of certain muscles groups such as heart and diaphragm. Our study suggests that micro-dystrophins may need to be engineered for particular muscles based on their composition and/or function.

Materials and Methods

Animal experiments

Male wild type and dystrophic *mdx*^{4cv} mice breed on C57BL/6 inbreed strain were used in this study. Animal experiments were performed in accordance with the Institutional Animal Care and Use Committee of the University of Washington. For initial screening, dystrophic *mdx*^{4cv} mice 5-6 weeks old were administered $5x10^{10}$ vector genomes of rAAV6 vector into the tibialis anterior muscle. Control mice were injected with Hank's balanced saline solution as a sham manipulation. In systemic analysis, 14-day old *mdx*^{4cv} males were administered 10^{13} vector genomes of rAAV6 vector intravenously via retro-orbital injection. Mice were sacrificed at either three or six months post-treatment for further evaluation.

Vector cloning and virus production

All micro-dystrophin transgenes were engineered using standard cloning techniques (Chamberlain 2004). Modified regions were subcloned into μDysHinge3 (ΔH2-R23/ΔCT, +H3) within the AAV vector genome backbone plasmid, pARAP4, using MfeI/XhoI or NheI/XhoI restriction sites flanking the majority of the central rod domain (Banks, Judge et al. 2010). The polyadenylation signal from the rabbit beta-globin gene was subcloned immediately after the μDys cDNA carboxy terminus. The CMV promoter composed of the cytomegalovirus immediate early promoter and enhancer drove expression of micro-dystrophin cDNA. The CK8 regulatory cassette (Goncalves, Janssen et al. 2011) was subcloned in SphI/SacII sites to replace the CMV promoter and drive expression of micro-dystrophin cDNA in myogenic cells.

Recombinant AAV6 vectors were made as previously described (Gregorevic, Allen et al. 2006). Briefly, expression constructs were co-transfected into HEK293 cells with pDGM6 packaging plasmid and later harvested and purified by a combination of filtration, heparin affinity chromatography, and ultracentrifugation. Viral preps were quantified by Southern and quantitative PCR analysis and always in comparison to other preps used in this study to ensure equal dosing in treating dystrophic mice.

Histological analysis

After physiological analysis, mice were sacrificed for necropsy. Muscles were embedded in Tissue-Tek OCT medium (Sakura Finetek USA, Torrance, CA) and frozen in liquid nitrogen-cooled isopentane. Transverse sections approximately 10 μm thick were used for immunofluorescence studies. Sections were blocked in 2% gelatin and 1% Tween-20 in KPBS. Sections were washed with 0.2% gelatin in potassium phosphate buffered saline (KPBS-G) and followed an incubation of primary antibodies diluted in 2% normal goat serum in KPBS-G. Sections were then rinsed in KPBS-G three times before incubation with secondary antibodies and DAPI (Sigma, St. Louis MO). After washing three more times in KPBS-G, slides were mounted in ProLong Gold antifade reagent (Life Technologies, Grand Island, NY). Primary antibodies included rabbit polyclonal N-terminal anti-dystrophin antibody (Harper, Hauser et al. 2002), mouse monoclonal anti-dystrophin (MANEX1011B clone 1C7, Developmental Studies Hybridoma Bank (DSHB) at the University of Iowa, Iowa City, IA) conjugated to Alexa-488 (Life Technologies), mouse anti-β-dystroglycan (MANDAG2 clone 7D11, DSHB) conjugated to DyLight-594 (Thermo Fisher Scientific, Rockford, IL), rat anti-α2-laminin

(clone 4H8-2, Sigma, St. Louis, MO), and rabbit anti-nNOS (Z-RNN3, Life Technologies). Secondary antibodies were goat anti-rabbit or anti-rat conjugated to Alexa-660 or Alexa-594, respectively (Life Technologies). Images were captured on an Olympus SZX16 dissection fluorescent microscope with DP software (Oympus, Center Valley, PA).

Immunoblotting

Tibialis anterior muscles of mice from initial screen were snap frozen in liquid nitrogen and then ground by dry ice-chilled mortar and pestle. Muscles were homogenized in kinase assay lysis buffer (1% Triton X-100, 50 mM Tris-HCl, pH 7.5, 150 mM NaCl, 1 mM EDTA supplemented with complete mini protease inhibitor cocktail tablet (Roche, Indianapolis, IN). Protein concentration of lysate was determined using the Coomassie Plus Bradford Assay (Pierce, Rockford, IL). 40 µg protein was suspended in NuPage LDS sample buffer (Life Technologies) supplemented with 100 mM dithiothreitol and loaded onto a NuPAGE 4-12% Bis-Tris polyacrylamide gel (Life Technologies). After running the gels and transferring samples onto Amersham Hybond-P polyvinylidene fluoride membrane (GE Healthcare Life Sciences, Piscataway, NJ), blots were blocked with 10% nonfat dry milk in PBS. Blots were then incubated with primary antibodies in 5% nonfat dry milk, 0.1% Tween-20 in PBS (PBST). After washing three times in PBST, secondary antibodies were incubated in 5% nonfat milk in PBST and followed by four washes in PBST. Primary antibodies included mouse anti-dystrophin (MANEX1011B clone 1C7, DSHB) and rabbit anti-glyceraldehyde 3-phosphate dehydrogenase (G9545, Sigma) as a loading control. Secondary antibodies

included donkey anti-rabbit or mouse (Jackson ImmunoResearch Labs, West Grove, PA). Blots were developed with Pierce ECL Plus western blotting substrate (Thermo Fisher Scientific) and scanned using a Storm 860 imaging system (GE Life Sciences).

Functional analyses of skeletal muscles

Muscles were assayed *in situ* (gastrocnemius) and *in vitro* (diaphragm) for force generation and susceptibility to contraction-induced injury as previously described with the noted modifications (Gregorevic, Plant et al. 2002, Banks, Combs et al. 2008). The maximum isometric force was determined at optimal muscle fiber length and then the muscle was subjected to a series of progressively increasing length changes under stimulation (Model 701C, Aurora Scientific). Maximum isometric tetanic force was measured by stimulating at 150 Hz and 180 Hz for the gastrocnemius and diaphragm, respectively. Eccentric contractions were performed at thirty-second intervals, each comprising stimulation at a fixed length to allow peak isometric force of either 150 ms (gastrocnemius) or 100 ms (diaphragm), followed by a continued 200 ms (gastrocnemius) or 300 ms (diaphragm) of stimulation during physical lengthening of the muscle. A series of length changes, or strains, of 0-45% of the optimum length was applied to potentiate overloading of the contractile properties and damage to the muscle architecture. The result from an eccentric contraction was measured in the peak isometric force generated just prior to the subsequent eccentric contraction.

Mice were anesthetized with 2,2,2-tribromethanol (Sigma) to be unresponsive to tactile stimuli and then prepped for *in situ* analysis of the gastrocnemius. The Achilles' tendon was exposed by incision at the ankle, sutured with 3-0 braided silk (Ethicon,

Cincinnati, OH), severed, and secured to the lever arm of a dual-mode force transducer-servomotor (Model 305B-LR, Aurora Scientific, Aurora, Ontario, CA). Mice were immobilized and secured to the apparatus by a stainless steel pin inserted through the knee, and by taping the hind paw to a customized Plexiglas platform. Gastrocnemius muscle was stimulated via two needle electrodes that were inserted through the skin on either side of the peroneal nerve in the region between the knee and hip. The servomotor's position was manipulated on three axis to help determine the optimal muscle fiber length. The servomotor was controlled by LabView software that also allowed data acquisition (National Instruments, Austin, TX).

For *in vitro* preparation of diaphragm, the anesthetized mouse was sacrificed after gastrocnemius analysis and the entire diaphragm muscle and surrounding ribcage was quickly excised to a dish containing oxygenated Tyrode solution (Lannergren, Bruton et al. 2000) containing (mM): NaCl 121, KCl 5, $CaCl_2$ 1.8, $MgCl_2$ 0.5, NaH_2PO_4 0.4, $NaHCO_3$ 24, glucose 5.5. Solution as bubbled by 5% CO_2-95% O_2 mixture (pH 7.3). A diaphragm strip composed of longitudinally arranged full-length muscle fibers, a portion of the central tendon, and a portion of rib bones and intercostal muscle on the distal end of the strip was isolated under a microscope. The muscle strip was tied with needle-lead braided surgical silk (6-0, P1; Ethicon) at the central tendon, sutured through the rib bone portion (5-0; Ethicon) and then secured to an *in situ* mouse apparatus with a temperature controlled, horizontal bath (Model 809A, Aurora Scientific). Apparatus bath was filled with bubbled Tryode solution described above and maintained at 25°C. Optimal fiber length was determined and isometric and eccentric contractile properties were assessed in a manner similar to gastrocnemius muscle analysis, with the conditions specified above

for the diaphragm muscle. Specific force of both muscle groups was determined by normalizing maximum isometric force to the mass of the gastrocnemius muscle or diaphragm strip, respectively. The following equation was used: specific force = maximum force × pennation × muscle length × 1.04 density/muscle weight (Burkholder, Fingado et al. 1994). Pennation is the angle at which bundles of skeletal muscle fibers orient themselves between the tendons of the muscle. For the gastrocnemius muscle, this angle was determined by a previous study (Banks, Judge et al. 2010). Diaphragm muscle strips were isolated in such a way that the myofibers would contract in a directly line between the semitendinosus junction to the myotendinous junction at the rib (Gregorevic, Plant et al. 2002). Pennation for the gastrocnemius and diaphragm equals 0.45 and 1, respectively.

Statistical analysis

All results are reported as mean ± standard error mean. Differences between cohorts were determined using one-way and two-way ANOVA with Tukey's *post hoc* multiple comparison test. All data analyses were performed with GraphPad PRISM 6 software (San Diego, CA).

Chapter 3

Evaluation of Micro-Dystrophin Ablation and Immunomodulation for Repeat Transduction with rAAV Vectors

Introduction

Recombinant adeno-associated virus (rAAV) vectors have been developed as a potential gene therapy approach for an array of genetic disorders, including Duchenne muscular dystrophy (DMD) (Seto, Ramos et al. 2012). DMD is an X-linked, recessive disease caused by a deleterious mutation in the *dystrophin* gene, which encodes a large structural and scaffold protein that's thought to maintain the integrity and function of striated muscle (Rahimov and Kunkel 2013, Constantin 2014). Males afflicted by this disease suffer an increasing loss in striated muscle strength and mass as well as ambulation, leading to a premature death (Emery 2003). Use of rAAV vectors to deliver truncated yet highly functional micro-dystrophin (μDys) transgenes has ameliorated pathological phenotypes and extended the lifespan in dystrophic animal models (Seto, Ramos et al. 2012). Testing of rAAV vectors in clinical trials has already begun for DMD and limb-girdle muscular dystrophies (Mendell, Campbell et al. 2010, Mendell, Rodino-Klapac et al. 2010, Herson, Hentati et al. 2012). Expression from vector-derived episomes remains detected up to 6 years after intramuscular injection in nonhuman primates (Rivera, Gao et al. 2005) and even a decade in a hemophilia B patient from a human clinical trial (Buchlis, Podsakoff et al. 2012). However, it remains unclear how long μDys-expressing vectors will persist in treated dystrophic muscles.

Skeletal muscle is a resilient tissue whose regenerative capacity predominately relies on myogenic stem cells, known as satellite cells (Yin, Price et al. 2013). While

skeletal muscle can recover from a substantial injury (e.g. contusion), episomal transgenes derived from rAAV vectors could be lost from dilution. This raises questions of how long would dystrophin protein persist after loss of its transgene and what consequences would its ablated expression have on skeletal muscle. Full-length dystrophin was shown to be present on the skeletal muscle membrane, or sarcolemma, for at least 6 months following transcriptional ablation (Ahmad, Brinson et al. 2000). Dystrophic murine studies examining another potential therapy for DMD gene therapy, known as exon-skipping, revealed that a dystrophin isoform lacking exon 23 had an estimated half-life in the range of 2-5 months, depending on the skeletal muscle examined (Wu, Lu et al. 2012, Verhaart, van Vliet-van den Dool et al. 2014). For rAAV-mediated gene therapy of DMD, the stability of μDys proteins expressed in skeletal muscle *in vivo* has not been reported. Regardless of the gene-therapy approach for DMD, all of them face the potential threshold where insufficient therapeutic transgene expression results in relapse of the disease pathology. If such is the case for rAAV vectors, repeated administration may be required. This feat may be far more difficult due to responses to the first treatment. Additionally, human populations exhibit a pre-existing humoral response to multiple AAV serotypes (Chirmule, Propert et al. 1999, Calcedo, Vandenberghe et al. 2009, Murphy, Li et al. 2009, Boutin, Monteilhet et al. 2010), which can further impede treatment. Despite the relatively lower immunogenicity compared to adenovirus (Zaiss, Liu et al. 2002), another non-integrating virus with tropism for skeletal muscle, evidence of innate and adaptive immune responses to AAV is accumulating.

AAV has been demonstrated to activate two mechanisms of innate immunity, eventually resulting in a humoral response. AAV serotypes 1, 2, and 8 were found to bind

complement and their receptors, allowing vector uptake by macrophages and result in innate signaling response and eventual humoral response (Zaiss, Cotter et al. 2008). Unmethylated CpG rAAV vector genomes have been recognized by TLR9/MyD88 pathway in conventional (bone marrow-derived) dendritic cells (cDCs) and plasmacytoid dendritic cells (pDCs), neutrophils, macrophages, and natural killer cells (Zhu, Huang et al. 2009, Martino, Suzuki et al. 2011). The ability of AAV to transfect pDCs (Zhang, Chirmule et al. 2000, Zhu, Huang et al. 2009) can cause CpG-activation and enable them to prime functional $CD8^+$ T cells, resulting in a cytotoxic lymphocyte (CTL) response. AAV capsid and transgene-specific CTL responses have been reported in multiple animal models and in humans (Zhang, Chirmule et al. 2000, Vandenberghe, Wang et al. 2006, Pien, Basner-Tschakarjan et al. 2009, Mendell, Campbell et al. 2010, Mendell, Rodino-Klapac et al. 2010, Li, Lasaro et al. 2011, Li, Tuyishime et al. 2011, Mays and Wilson 2011, Rogers, Martino et al. 2011, Wang, Tapscott et al. 2011). Removing most CpG motifs in the vector genome between the inverted terminal repeats (ITRs) reduced a CTL response (Faust, Bell et al. 2013). However, CpGs were not removed from the ITRs, leaving the potential effects on vector genome packaging and transduction to remain unknown. Murine neutralizing antibody responses to several AAV serotypes are predominately of the T-cell dependent IgG2 class (Chirmule, Xiao et al. 2000, Xiao, Chirmule et al. 2000, Sudres, Cire et al. 2012). However, humans administered AAV serotypes 1 or 2 had a prevalent T-cell dependent IgG1 antibody response, although IgG2 as well as T cell-independent IgG3 antibodies also increased (Mingozzi, Meulenberg et al. 2009, Murphy, Li et al. 2009). The range in neutralizing antibody isotypes against

AAV in both animal models and humans demonstrates that multiple T cell subsets provide help to B cells.

Primary exposure to immunocompetent animals and humans results in the generation of antibodies against the viral capsid, which reduces transduction efficacy upon readministration (Halbert, Standaert et al. 1997, Mingozzi, Maus et al. 2007, Petry, Brooks et al. 2008, Mays, Vandenberghe et al. 2009, Mingozzi, Meulenberg et al. 2009, Wang, Tapscott et al. 2011). This issue could be circumvented by use of alternate serotype(s) that exhibits tropism for the same target tissue(s) (Halbert, Rutledge et al. 2000, Riviere, Danos et al. 2006, Demaster, Luo et al. 2012). However, this approach for muscular dystrophy gene therapy limits the number of possible readministration events, as only a few serotypes share a comparably high degree of tropism and transduction efficiency for striated muscle (Zincarelli, Soltys et al. 2008, Zincarelli, Soltys et al. 2010). This finite number of serotype options could be further reduced if a patient already exhibits neutralizing antibodies to any of these AAV capsids (Chirmule, Propert et al. 1999, Calcedo, Vandenberghe et al. 2009, Boutin, Monteilhet et al. 2010). An alternative method would be to attenuate, or altogether prevent, a serotype-specific response during the initial exposure through transient immunosuppression. This has been successfully applied in multiple mouse studies targeting different tissues with rAAV vectors (Halbert, Standaert et al. 1998, Manning, Zhou et al. 1998, Lorain, Gross et al. 2008, McIntosh, Cochrane et al. 2012).

The $CD4^+$ T cell population has various roles with APCs, other lymphocytes, and even independently in response to viruses, which make them an ideal target for antibody blockade (Swain, McKinstry et al. 2012). Clinical application of depleting T cells is

undesirable for two foreseeable reasons. Depletion of this population would result in prolonged immunosuppression, raising risk of infection. Secondly, it has been recently revealed that a subset of regulatory T cells migrates to injured skeletal muscle to monitor inflammation and promote regeneration (Burzyn, Kuswanto et al. 2013). For rAAV-mediated gene therapy of striated muscle, non-depleting antibodies is preferable. Multiple cell receptors of T and B cells have been successfully targeted for immunomodulation in both mice and nonhuman primates using non-depleting antibodies (Qin, Cobbold et al. 1989, Qin, Wise et al. 1990, Qin, Cobbold et al. 1993, Halbert, Standaert et al. 1998, Manning, Zhou et al. 1998, Honey, Cobbold et al. 1999, Kenyon, Chatzipetrou et al. 1999, Kirk, Burkly et al. 1999, Graca, Honey et al. 2000, Lorain, Gross et al. 2008, McIntosh, Cochrane et al. 2012).

Transient immunosuppression with a combination of calcineurin inhibitor cyclosporine and a non-depleting anti-CD4 (NDCD4) antibody was previously shown to significantly diminish the humoral response to AAV serotype 8 after the initial intravascular injection and allow systemic readministration in mice (McIntosh, Cochrane et al. 2012). Yet the doses of rAAV vectors tolerated for intravascular delivery were on the log order of 10^{12} vector genomes per kilogram of body mass (vg/kg). Such a dose would be sub-optimal for gene therapy for muscular dystrophy, especially for deep muscle tissue that cannot be efficiently transduced by intramuscular injections. Multiple reports indicate that intravenous doses of rAAV vectors need to be on the order of 10^{14} vg/kg in order to achieve near saturating transduction of multiple muscle groups (Gregorevic, Allen et al. 2006, Yue, Ghosh et al. 2008, Kornegay, Li et al. 2010, Pan, Yue et al. 2013).

In this study, we first addressed how adult skeletal muscle would tolerate the ablated expression of a micro-dystrophin (μDys) transgene. Ablating μDys in adult skeletal muscle was detrimental, resulting in the onset of dystrophic pathology. Given the nature of these results, we tested the combination of cyclosporine and NDCD4 antibody to allow readministration of AAV6 by both intramuscular and intravascular routes. After validating this regimen with reporter vectors in wild type mice, dystrophic *mdx*^{4cv} mice were given two separate challenges of AAV6 delivering two different μDys constructs. Additionally, we tested systemic readministration of AAV serotypes 6 or 9 at doses deemed therapeutic for muscular dystrophy. Although serotypes 6 and 9 are phylogenetically distinct (Schmidt, Govindasamy et al. 2008, Vandenberghe, Breous et al. 2009), we also inquired if primary exposure to AAV6 at a high intravascular dose would lead to the development of neutralizing antibodies (nAbs) that could cross-react to AAV9. Our results prompted us to expand on this immunosuppressive regimen to determine if multiple systemic challenges of AAV6 could be achieved by concurrent transient immunosuppression with preceding challenges.

Results

Stability of micro-dystrophin in vitro and in vivo

Persistent expression of rAAV/μDys-expressing vectors has been repeatedly demonstrated in dystrophic animals models (Seto, Ramos et al. 2012), but consequences of ablated expression remain unclear. We employed the Cre-LoxP system in mice in order to ablate a floxed transgene encoding a previously reported micro-dystrophin construct, ΔR4-R23/ΔCT (Harper, Hauser et al. 2002). Transgenic mice expressing a floxed $\mu Dys^{\Delta R4\text{-}R23/\Delta CT}$ (flμDys) under the direction of the human skeletal actin (HSA) promoter were bred on the dystrophic *mdx*^{4cv} strain (Chapman, Miller et al. 1989). Resulting flμDys/*mdx*^{4cv} mice were further crossed with a line expressing a tamoxifen-inducible Cre fusion protein ($CreER^T$) (Hayashi and McMahon 2002). Our initial focus was to determine the stability of the flμDys protein, both *in vitro* and *in vivo*. Primary myoblasts were isolated from hindlimb skeletal muscles of flμDys/ $CreER^T$/*mdx*^{4cv} mice and cultured under myogenic differentiation conditions in order to activate the HSA promoter. Cultures were treated with metabolically active 4-hydroxytamoxifen (4-OHT) or vehicle alone and assessed for the percentage of myogenic cells expressing dystrophin (**Fig. 3.1a**). A significant decrease in dystrophin-expressing cells was observed by 7 days after the end of the 4-OHT treatments, suggesting the half-life of flμDys protein is within 7 to 10 days in both mononucleated and multinucleated cells. To confirm the findings in these results, we utilized flμDys/*mdx*^{4cv} mice and rAAV6/CMV-Cre vectors encoding a nuclear localization signal (NLS) to ablate the flμDys transgene. These components lead to genetic ablation without the need for tamoxifen, shifting temporal control of the system to the time of vector administration. One EDL muscle of the flμDys/*mdx*^{4cv} mouse

was injected with 10^{10} vector genomes (vg) of AAV6/CMV-CreNLS while the contralateral EDL muscle received a sham injection. A time-course Western blot analysis revealed flμDys expression was reduced to approximately 50% by 5 days after injection (**Figs. 3.1b,c**). Assessing the force generation capacity of EDL muscles revealed a decrease in muscles injected with AAV6/CMV-Cre-NLS that at 3 weeks but was recovering to untreated levels by 5 weeks post-injection (**Fig. 3.2**). Use of rAAV vectors allowed consistent, widespread knockdown of the flμDys transgene within a single muscle. Since rAAV vectors cannot efficiently transduce satellite cells (see Chapter 4), we proceeded to use flμDys/ $CreER^T/mdx^{4cv}$ mice to address our second question concerning the long-term consequences of μDys ablation.

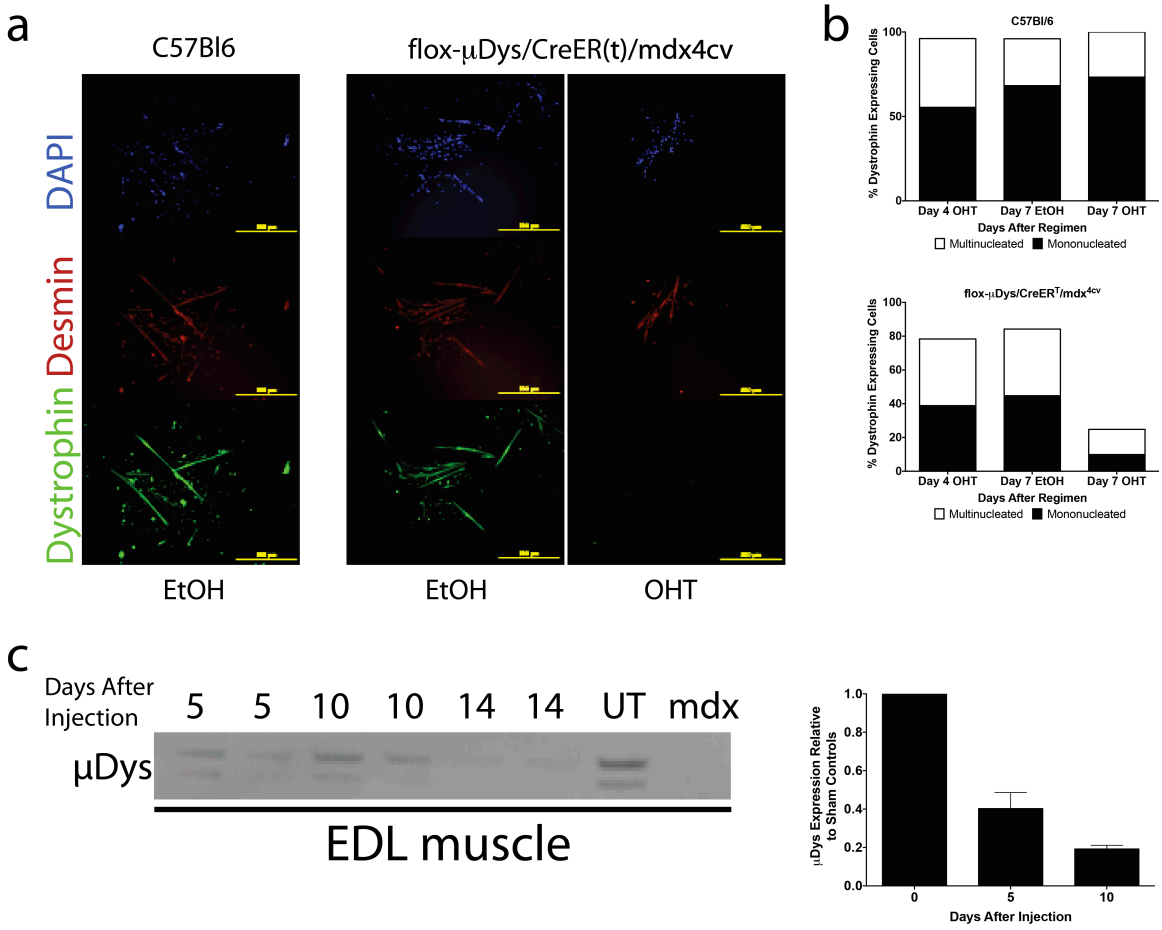

Figure 3.1 Stability of micro-dystrophin. (**a**) Primary myoblasts were isolated from wild type and flox-µDys/CreER^{T}/*mdx*^{4cv} mice. Myogenic differentiation program was induced while cultures were concurrently exposed to a three-day regimen of metabolically active 4-hydroxy tamoxifen (OHT) or vehicle alone (EtOH). Cultures were stained by immunohistochemistry for myogenic proteins desmin (red) and dystrophin (green) at specified time points. Scale bar, 200 µm. (**b**) Myogenic (desmin positive) cells were quantified for dystrophin expression in both mononucleated and multinucleated cells types. N = 3 per group (**c**) 10^{10} vector genomes (vg) of rAAV6/CMV-CreNLS were injected into extensor digitorum longus (EDL) muscle of flox-µDys/*mdx*^{4cv} mice while contralateral EDL received a sham injection. At specified time points, whole muscle lysates were immunoblotted for µDys expression. Expression levels were quantified by densitometry and are reported as relative fractions compared to untreated flox-µDys/*mdx*^{4cv} EDL lysates.

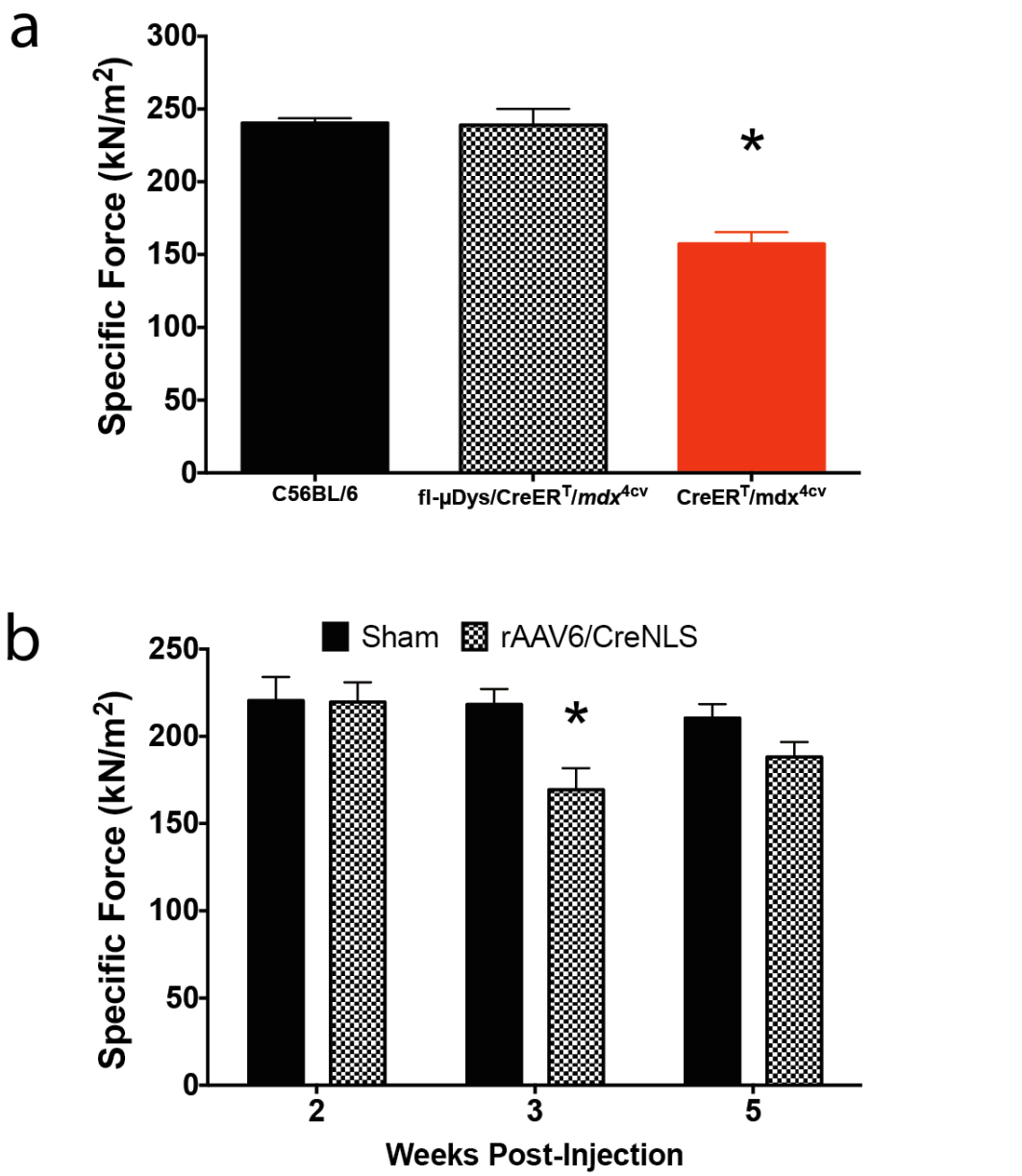

Figure 3.2 Transient knockdown of floxed micro-dystrophin expression. (**a**) Extensor digitorum longus (EDL) muscles from C57BL/6 wild type controls, floxed-µDys/CreER^{T}/*mdx*^{4cv}, and CreER^{T}/*mdx*^{4cv} controls were measured *ex vivo* for specific force generation. N = 7-8 per group. Mean ± S.E.M. *P<0.01 versus C57BL/6 and floxed-µDys/ CreER^{T}/*mdx*^{4cv}, one-way ANOVA with Tukey post test. (**b**) Floxed-µDys/*mdx*^{4cv} mice were injected with 10^{10} vg of rAAV6/CMV-CreNLS in one EDL while the contralateral received a sham (saline) injection. Specific force generation was assessed at 2, 3, and 5 weeks post-injection. N = 3-5 per group, per time point. Mean ± S.E.M. *P<0.05 versus sham-injected, two-way ANOVA with Sidak's multiple comparison test.

Mature skeletal muscle cannot sustain flμDys ablation

In both human DMD patients and murine dystrophic models, the pathology becomes acute and intensifies during post-natal growth (Coulton, Curtin et al. 1988, Coulton, Morgan et al. 1988, Emery 2003, Ng, Banks et al. 2012). To avoid results that could be skewed by accelerated growth in myofiber mass and length, CreER^{TM}/flμDys/*mdx*^{4cv} mice were administered a tamoxifen regimen between 9 and 10 months of age. Three months after finishing the regimen, skeletal muscles were examined. Morphological analysis revealed that tamoxifen-treated mice had reduced, patchy expression of flμDys (**Fig. 3.3a**). Treated mice also exhibited reduced myofiber cross-sectional area, increased centrally nucleated myofibers, and increased fibrosis within the muscle tissue. In multiple examined muscles, the degree of these dystrophic parameters was equivalent, or near equivalent, to CreER^{TM}/*mdx*^{4cv} controls (**Fig. 3.3**). Biochemical analysis showed a decrease in flμDys expression and a concurrent increase in utrophin, an endogenous homologue of dystrophin, in treated skeletal muscles (**Fig. 3.3b**). Utrophin upregulation is compensatory mechanism in DMD pathology that attempts to stabilize the sarcolemma in the absence of a functional dystrophin (Emery 2003). Knockdown of dystrophin expression correlated with reduced copy numbers of flμDys compared to untreated mice (**Fig. 3.3f**), which have 7±2 copies/host genome as determined by quantitative PCR analysis. These results indicate that lost expression of μDys constructs of a similar modular design results in muscular dystrophy within three months time. DMD patients previously treated by rAAV vectors expressing μDys may require readministration if they suffer a critical loss of therapeutic transgenes in treated tissue(s). As discussed, several immunomodulation strategies have been employed for

repeated AAV delivery. We proceeded to expand on the combination of cyclosporine and non-depleting anti-CD4 antibody, previously shown to achieve intravenous readministration (McIntosh, Cochrane et al. 2012).

AAV and reporter transgene tolerance observed with intramuscular administration

We explored readministration of rAAV vectors in the context of two separate methods of delivery, intramuscular and intravascular injections. A sensitive reporter was sought to compare transduction efficiencies between readministered cohorts and age-matched controls. Previous studies revealed that various AAV-delivered reporter transgenes elicit cellular toxicity at therapeutic doses for muscular dystrophy applications (Winbanks, Beyer et al. 2012, Wallace, Moreo et al. 2013). To circumvent this issue, the firefly luciferase transgene was cloned into a rAAV vector. For, intramuscular administrations, we injected one tibialis anterior (TA) muscle of C57BL/6 mice with $5x10^{10}$ vector genomes (vg) of rAAV6/CMV-luciferase during a transient immunosuppression regimen with cyclosporine (CsA) and NDCD4 antibody (**Fig. 3.4a**). The immunosuppression regimen slowed the growth rate of mice in the beginning of the regimen, but had no overall negative effect by the end of the regimen (**Figs. 3.5a,b**). Four weeks after the first challenge, the contralateral TA muscle was injected with the same dose of rAAV/CMV-luciferase packaged in serotype 6 or 9. Two weeks following the second challenge, TA muscles receiving the second challenge exhibited similar transduction efficiencies as age-matched control mice that had received only one challenge of rAAV/CMV-luciferase (**Fig. 3.4b**). Histological observation of muscles receiving the second challenge of rAAV/CMV-luciferase revealed no overt immune

response compared to controls receiving only a single challenge of rAAV6/CMV-luciferase (**Fig. 3.4c**). This suggests that firefly luciferase transgene expression unlikely induces cellular toxicity in skeletal muscle and that transient immunosuppression allows tolerated readministration of AAV serotypes 6 and 9.

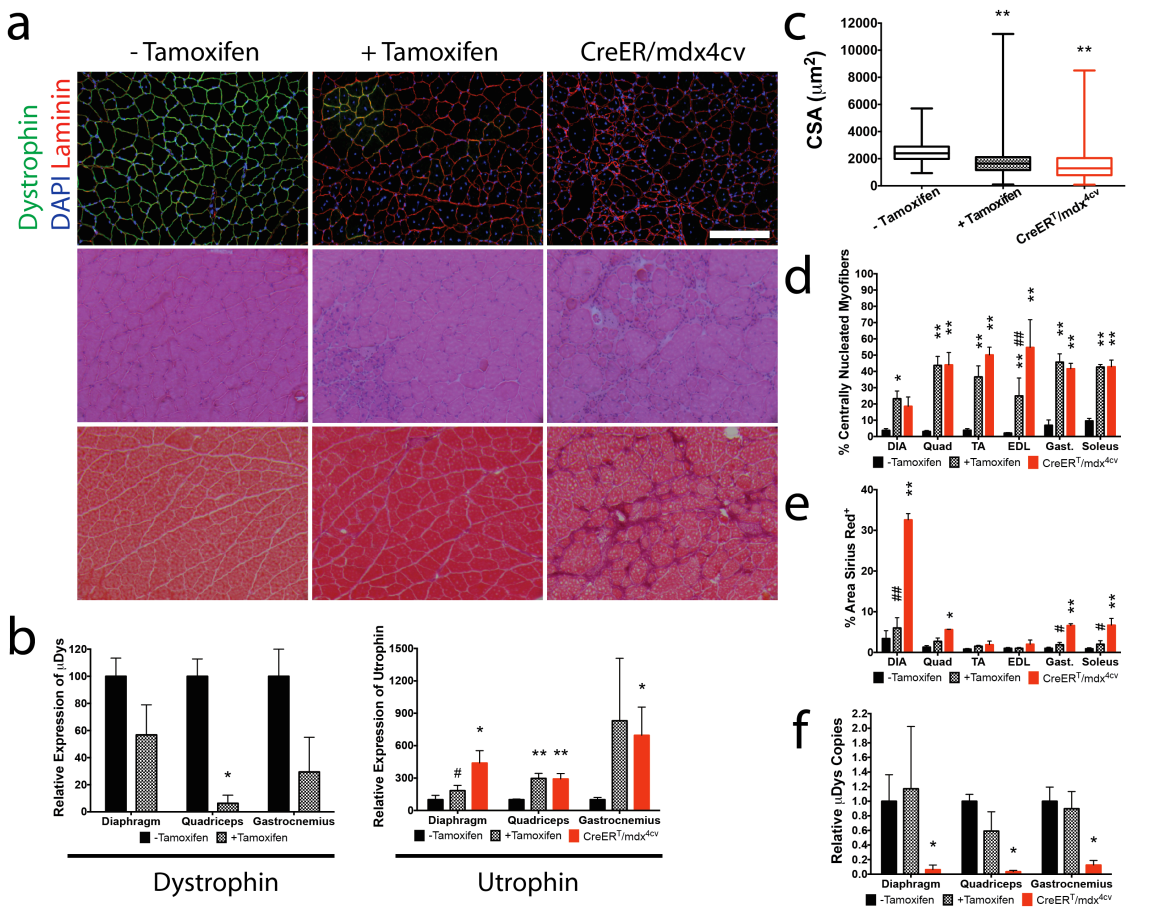

Figure 3.3 Consequences of dystrophin ablation. Flox-µDys/CreER^{T}/*mdx*^{4cv} mice were given a tamoxifen regimen and assessed three months afterwards. (**a**) Representative sections of gastrocnemius muscles were examined by immunofluorescence (top row), hematoxylin and eosin (middle row), and Sirius red staining (bottom row). Scale bar, 200 µm. (**b**) Immunoblots of selected muscles were examined for µDys and utrophin levels, in comparison to untreated and CreER^{T}/*mdx*^{4cv} controls. N = 7-8 per group. Mean ± S.E.M. *P<0.05, **P<0.001 versus untreated; #P<0.05 versus CreER^{T}/*mdx*^{4cv}; Student t-test (µDys) or two-way ANOVA with Tukey post test (utrophin). (**c**) Box –and-whisker plots of myofiber cross sectional area (CSA) of gastrocnemius muscles. **P<0.01 versus untreated, one-way ANOVA with Mann-Whitney test. Percentage of centrally nucleated myofibers (**d**) and area positive for Sirius Red staining (**e**) in selected skeletal muscles. N = 7-8 per group. Mean ± S.E.M. *P<0.05, **P<0.001 versus untreated; #P<0.05, ##P<0.05 verus CreER^{T}/*mdx*^{4cv}; two-way ANOVA with Tukey post test. (**f**) Copy numbers of flox-µDys gene in treated mice was measured in comparison to untreated and CreER^{T}/*mdx*^{4cv} controls by quantitative PCR analysis. N = 3-6 per group. Mean ± S.E.M. *P<0.01 versus untreated, multiple t tests with Holm-Sidak multiple comparison test.

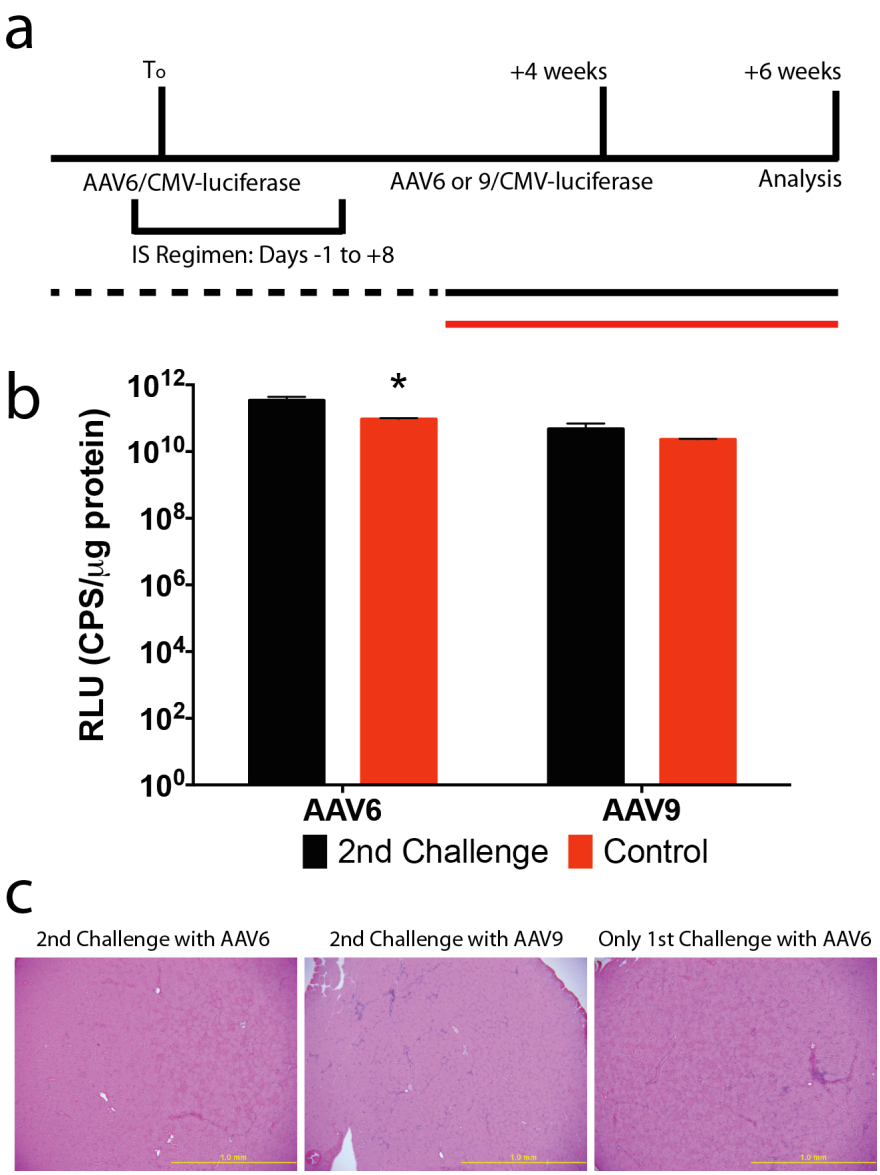

Figure 3.4 AAV tolerance observed with intramuscular injection. (**a**) Experimental design. T_0, Day of first viral challenge; AAV, adeno-associated virus; IS Regimen, immunosuppression regimen; TA, tibialis anterior muscle. Under immunosuppression, mice were injected with $5x10^{10}$ vg of AAV6/CMV-luciferase into one TA. Four weeks after T_0, contralateral leg was injected with $5x10^{10}$ vg of rAAV-CMV-luciferase vector packaged in serotype 6 or 9. End point was six weeks after T_0. Distal halves of muscles were generated into lysates for reporter activity (**b**). Black bars define groups given a specified serotype as second challenge. Grey bars define age-matched control groups with same serotype. N = 3 per group. Mean ± S.E.M. *P<0.01, multiple t test with Holm-Sidak multiple comparison test. (**c**) Cross sections from proximal halves of muscles were stained with hematoxylin and eosin. Scale bar, 1.0 mm.

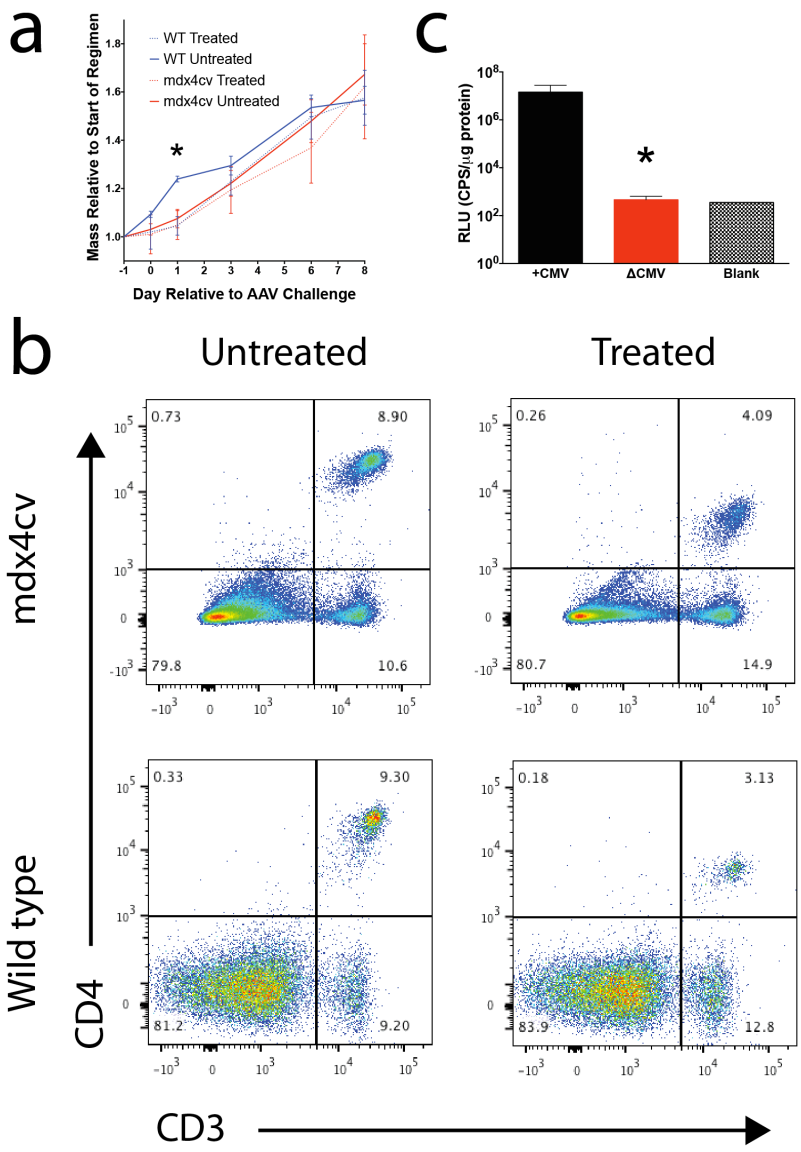

Figure 3.5 Effects of transient immunosuppressive regimen. (**a**) Body masses of both wild type (blue) and *mdx*^{4cv} (red) males were measured during the course of the regimen. Growth rate of treated (dotted line) animals was compared to untreated controls (solid line). Mean ± S.E.M. N ≥ 6 per group. *P<0.01. (**b**) Validating non-depleting effect of anti-mouse CD4 antibody by collecting peripheral blood mononuclear cells and staining for lymphocyte markers CD3 (Alexa 594) and CD4 (APC). Representative results from treated and untreated (N = 3) mice are shown for each strain. Note the decrease of CD4-postitive cells due to down modulation with non-depleting antibody while the CD3-postitive cell levels are essentially unchanged. (**c**) Expression of luciferase vector is dependent on the presence of a promoter. Luciferase activity in cultures transfected with vectors either with (+CMV) or without (ΔCMV) a promoter was compared to untransfected control. Mean ± S.E.M. N = 3 per group. *P<0.01, (**a**) multiple t tests using Hold-Sidak method, (**b**) Student t test.

Re-treatment of dystrophic muscle with multiple micro-dystrophin constructs

Efficient skeletal muscle transduction with rAAV vectors has been repeatedly demonstrated in dystrophic animal models (Wang, Tapscott et al. 2011, Seto, Ramos et al. 2012). The nature of AAV vector genomes makes this form of gene therapy susceptible to loss through muscle turnover or repair from acute (e.g. contusion) injury. We used notexin venom as a model of acute injury to determine if dystrophic muscle, previously treated with a micro-dystrophin (μDys) vector, could be retreated with another μDys vector (**Fig. 3.6a**). These constructs were packaged in AAV6 and were expressed by the myogenic CK8 promoter (Goncalves, Janssen et al. 2011). The TA muscles of dystrophic *mdx*^{4cv} mice were injected with 10^{11} vg of rAAV6/CK8-μDysH3 (ΔH2-R23+H3/ΔCT (Banks, Judge et al. 2010)) with or without immunosuppression. Four weeks after treatment, one of the TA muscles were injected with notexin in order to cause a large degree of ablation of the original μDysH3 construct. Two weeks following injury, the same TA muscle was injected with 10^{11} vg of a different μDys construct (ΔR2-R15/ΔR18-R22/ΔCT; see Chapter 2) that contains the neuronal nitric oxide synthase (nNOS) binding domain (Lai, Thomas et al. 2009). This allowed us to ascertain the degree of transduction and immune tolerance to the second challenge (**Figs. 3.6b,c; 7**).

TA cross sections were quantified for necrotic myofibers, alternatively activated macrophages, and collagen composition (**Fig. 7**). Necrotic myofibers was highest in *mdx*^{4cv} muscles that received both AAV6 challenges as well as the notexin injury without any immunosuppression; higher than *mdx*^{4cv} muscles receiving no AAV6 or acute injury (6% versus 2%, respectively). Yet all three morphological assays revealed no significant differences amongst the various muscle manipulations. Morphological analysis at the 19-

week time point may have been too late to observe the immune response of a second AAV6 challenge and be masked by the dystrophic pathology of the *mdx*^{4cv} strain.

Regardless of immunosuppression, administration of μDysH3-expressing rAAV vectors reduced the amount of centrally nucleated myofibers, an indicator of degeneration and regeneration (**Figs. 3.6b,c**). Notexin injury reduced expression of μDysH3, as determined by myofibers expressing dystrophin but not nNOS at the sarcolemma. Greater than 50% of myofibers expressed ΔR2-R15/ΔR18-R22/ΔCT μDys expression (nNOS^{+} myofibers) in mice that were immunosuppressed during the first administration of AAV6 as well as in mice that only received AAV6 after notexin injury. The degree of expression from this second transgene was significantly higher than mice that were readministered AAV6 without immunosuppression ($P<0.01$; **Fig. 3.6c**). These results suggest that this immunosuppression scheme allows dystrophic mice to tolerate doses of 10^{11} vg of rAAV6 vectors by intramuscular injection.

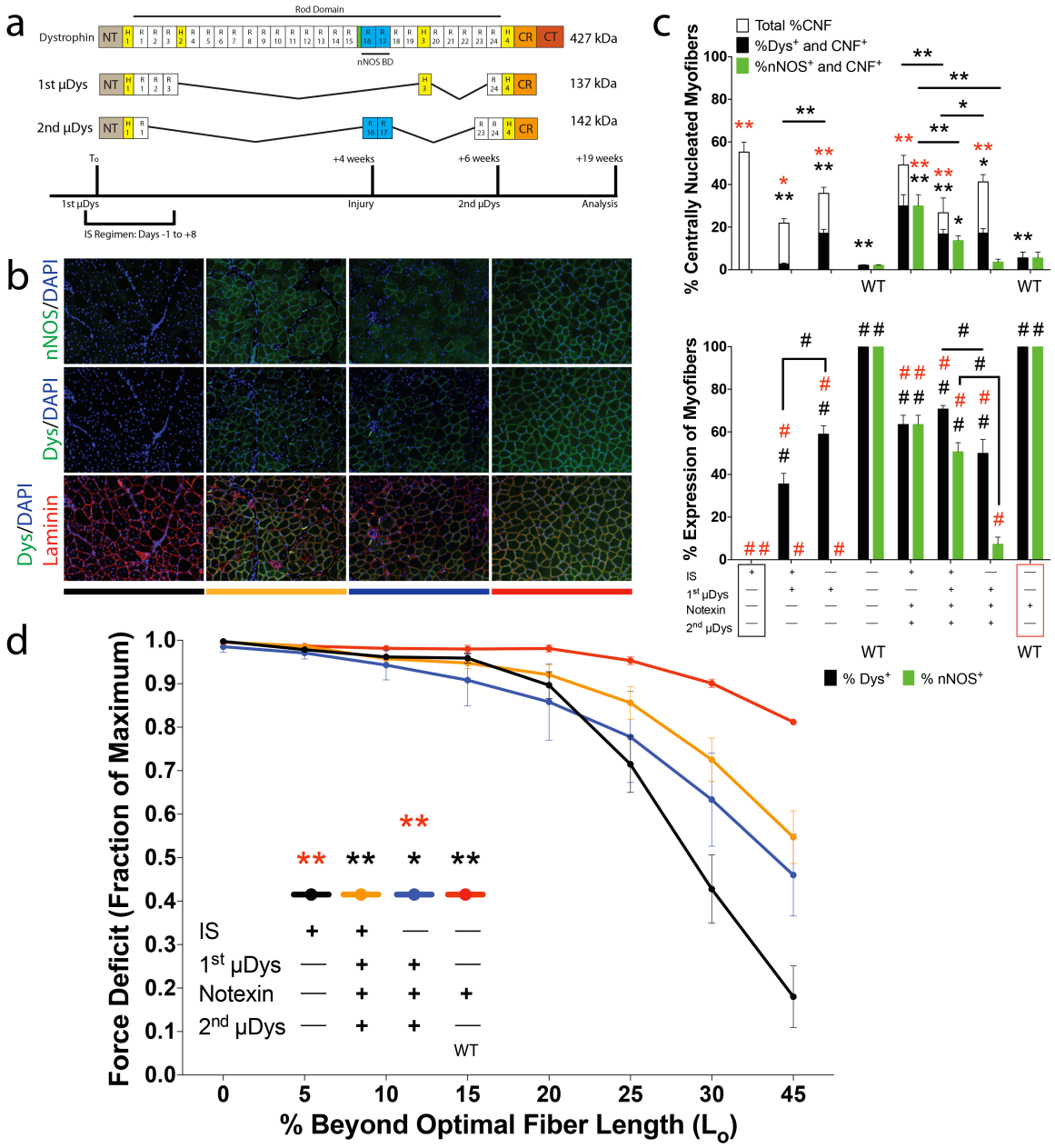

Figure 3.6 Treating dystrophic skeletal muscles with multiple micro-dystrophin constructs. (**a**) Experimental design. NT, amino terminal domain; H, hinge; R, spectrin-like repeat; nNOS BD, neuronal nitric oxide synthase binding domain; CR, cysteine-rich domain; CT, carboxyl terminal domain; µDys, micro-dystrophin; IS, immunosuppression; T_0, day of first treatment. Green, unlabeled region marks 20-amino acids between R15 and R16. Dystrophic *mdx*^{4cv} mice were divided into two cohorts; one receiving immunosuppression and the other not. At T_0, tibialis anterior muscles of *mdx*^{4cv} mice were injected with either 10^{11} vg of the 1st AAV6/CK8-µDys or sham. Four weeks after T_0, one TA of each mouse was injected with notexin. Six weeks after T_0, the previously injured TA was then injected with 10^{11} vg of the 2nd AAV6/CK8-µDys. Mice were assessed three months after the 2nd µDys treatment. Age-matched wild type (WT)

mice received sham injections and notexin only. (**b**) Representative TA cross sections from conditions defined by matching colored labels in (**d**). (**c**) Top: percentage of centrally nucleated myofibers and breakdown of those also expressing dystrophin (black bars) or nNOS (green bars) *P<0.05, **P<0.01. Bottom: percentage of myofibers expressing dystrophin (black bars) and nNOS (green bars) #P<0.01. (**d**) *In situ* assessment of TA muscles in resisting contraction-induced injury. *P<0.05, **P<0.01. Mean± S.E.M. N = 5-7 per condition. Black and red characters denote significant differences from groups whose conditions are outlined by black and red boxes, respectively. Two-way ANOVA with Tukey post test.

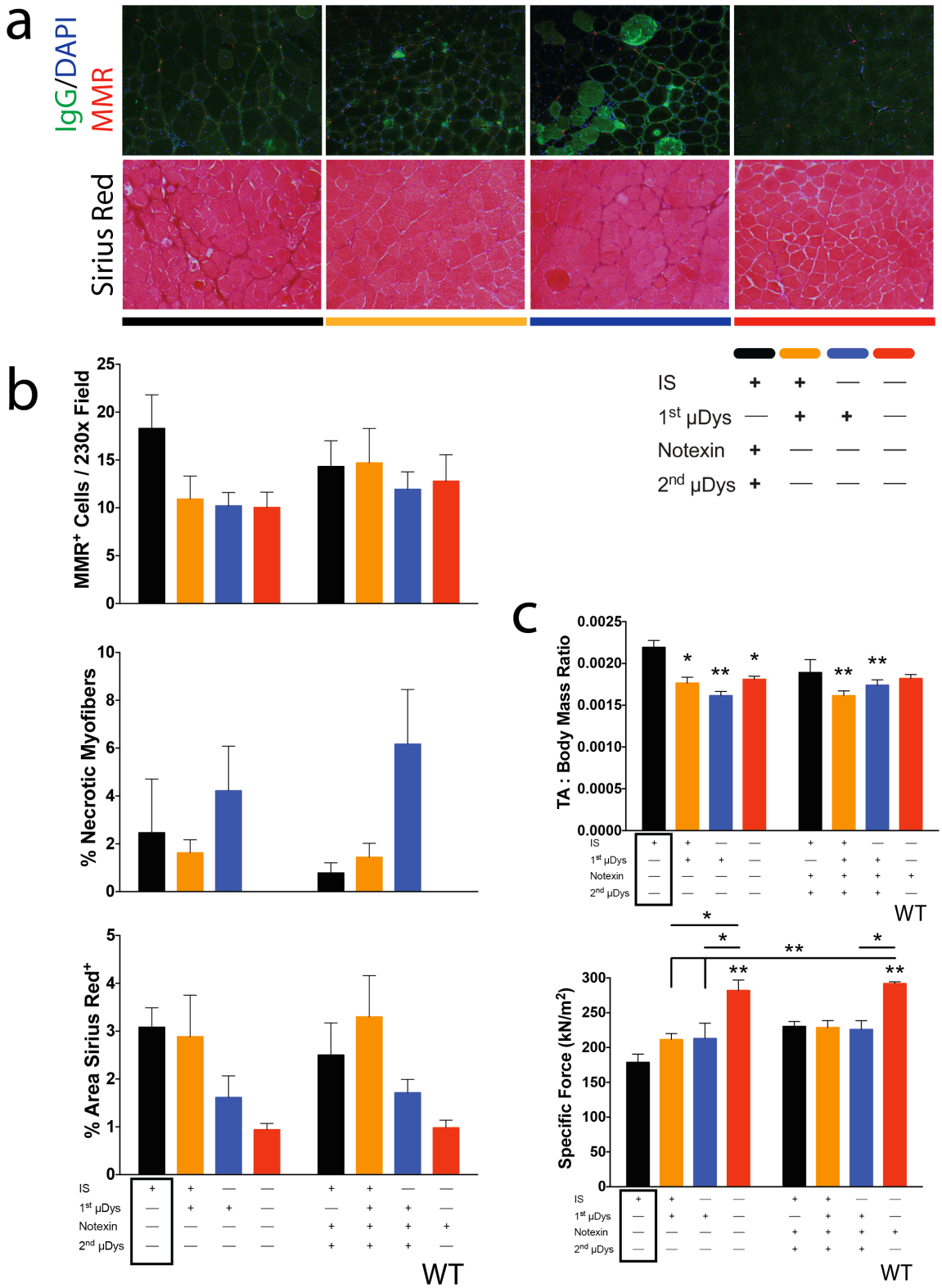

Figure 3.7 Assessment of tibialis anterior muscles after rAAV6 readministration. (**a,b**) At the endpoint of the experiment described in **Figure 3.6**, tibialis anterior (TA)

muscles were examined for presence of alternatively activated macrophages, necrotic myofibers, and collagen composition. Representative TA cross sections from conditions defined by key underneath the panel. IS, immunosuppression; WT, wild type. Histological staining: (top row) maacrophage mannose receptor (MMR, red) IgG (green), DAPI; (bottom row) Sirius red staining for collagen. (**c**) Physical properties of TA muscles measured; TA to body mass ratios (top) and specific force generation (bottom). Mean ± S.E.M. N = 5-7 per condition, as defined under graphs. *P<0.05, **P<0.01. Characters lacking brackets denote significant differences from conditions outlined by black box. Two-way ANOVA with Tukey post test.

Effective transduction with systemic readministration is serotype-dependent

To evaluate the potential response to the AAV capsid independently of the transgene, the CMV promoter was removed from the luciferase expression vector and packaged into AAV for the initial (1°) challenge. The second (2°) challenge contained the CMV promoter, allowing vector expression. Expression of the promoter-less rAAV vector was negligible as the measured activity was at or below background level (**Fig. 3.2b**). Under immunosuppression, C57BL/6 mice were challenged with a bolus of $1.5x10^{12}$ vg of rAAV6/ΔCMV-luciferase via retro-orbital injection. Four weeks after the first challenge, mice were again challenged with another retro-orbital injection of $1.5x10^{12}$ vg of rAAV/CMV-luciferase packaged in serotype 6 or 9. No mice exhibited any signs of illness or abnormal behavior and were housed for an additional four weeks before reaching the end point. Luciferase activity was measured in select muscle groups as well as the liver (**Fig. 3.8**). Initial exposure to AAV serotype 6 did not inhibit transduction of rAAV/CMV-luciferase when delivered by serotypes 6 or 9 upon the second challenge (**Fig. 3.8a**). We then asked if such efficacy could similarly be achieved using rAAV9/ΔCMV-luciferase as the initial exposure.

Mice systemically administered $1.5x10^{12}$ vg rAAV9/ΔCMV-luciferase were given a second challenge of rAAV/CMV-luciferase either in serotype 6 or 9 (**Fig. 3.8c**). Luciferase activity in 1°-AAV9/2°-AAV6 mice was similar to 1°-AAV6/2°-AAV6 mice and to mice that received only one challenge, rAAV6/CMV-luciferase (AAV6). However, the reporter activity level was greatly diminished in livers of 1°-AAV9/2°-AAV6 mice compared to AAV6 and 1°-AAV6/2°-AAV6 mice. Systemic gene transfer was dramatically inhibited upon readministration with rAAV9/CMV-luciferase (**Fig.**

3.8c). It has been repeatedly reported that capsid antigen presentation can lead to $CD8^+$ T cell activation and memory, leading to clearance of cells transduced by AAV as well as prevention of further transduction upon readministration (Vandenberghe, Wang et al. 2006, Pien, Basner-Tschakarjan et al. 2009, Li, Tuyishime et al. 2011). However, histological staining did not reveal any overt immune response or myofiber regeneration to the second challenge of AAV in any examined tissue (**Fig. 3.9**), suggesting that the absence of reporter activity could instead be attributed to neutralizing antibodies.

Sera of mice readministered with AAV serotypes 6 or 9 were collected at the end point and measured for the prevalence of neutralizing antibodies against the capsid of both serotypes to also determine the degree of cross-reactivity, if any. Sera was diluted and incubated with rAAV/CMV-human placental alkaline phosphatase (hPLAP) reporter vectors packaged in AAV serotype 6 or 9 and then added to HT1080 cultures. Two days after transduction, cultures were fix, stained, and quantified for colony forming units (**Figs. 8b,d**). Mice were not under immunosuppression during the second systemic challenge of AAV, which correlated to the robust antibody response to AAV6 and AAV9 from the second challenges, as expected. However, we observed neutralizing antibodies against AAV6 in the sera of all cohorts that were under immunosuppression when challenged with this serotype, including 1°-AAV6-only mice. A previous study was able to attenuate a humoral response against rAAV vectors using the combination of CsA and NDCD4 (McIntosh, Cochrane et al. 2012). In our hands, the same immunosuppressive reagents did not lead to the same results. This could be attributed to the difference in the serotype and vector doses used by McIntosh and colleagues and in our study.

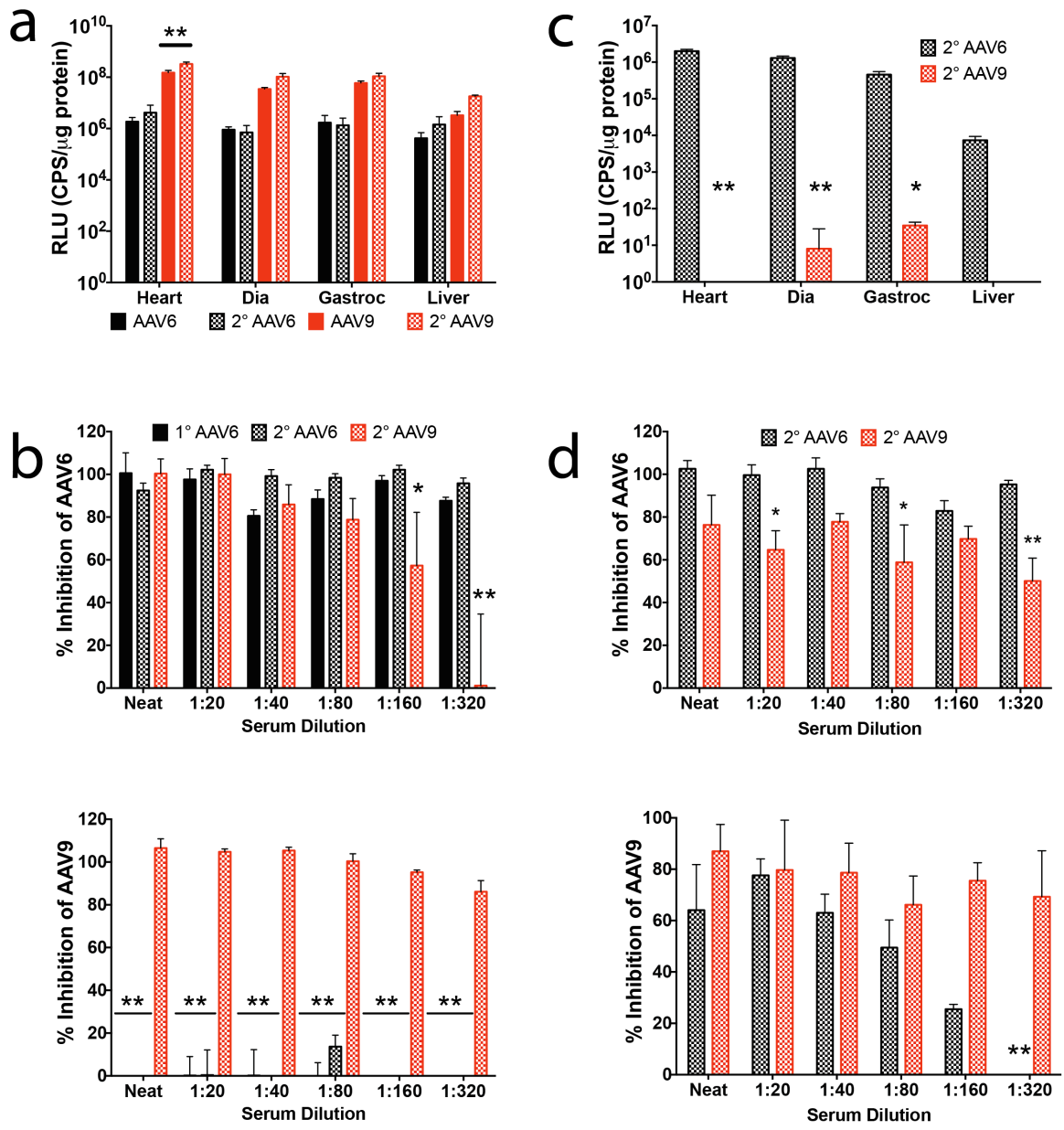

Figure 3.8 Effective transduction with systemic readministration. Under immunosuppression as described in **Figure 3.4**, mice were challenged with $1.5x10^{12}$ vg of non-expressing vector AAV6/ΔCMV-luciferase (**a,b**) or AAV9/ΔCMV-luciferase (**c,d**). Four weeks after challenge, mice were administered $1.5x10^{12}$ vg of expressing vector CMV-luciferase that was packaged in either AAV serotype 6 or 9. Four weeks after second AAV challenge, luciferase activity was measured in selected tissue lysates (**a,c**). Mice receiving a second challenge of AAV (2°) are also denoted by serotype. Age-matched controls that didn't receive immunosuppression and were only administered the expressing vector are denoted by serotype (AAV6 or AAV9). Luciferase activity in age-matched control mice receiving only the rAAV/ΔCMV-luciferase vectors was measured at or below background level and thus activity of the other cohorts was normalized to this group. (**b,d**) Sera were collected from mice that were administered transient

immunosuppression. Mice included those that were challenged only once (1°) or twice (2°). (**b**) Sera from mice challenged with AAV6 during transient immunosuppression. (**d**) Sera from mice challenged with AAV9 during transient immunosuppression. Sera were assayed for neutralizing antibodies against AAV serotypes 6 and 9. Heat inactivated serum, neat or at indicated dilution, was mixed with rAAV/CMV-hPLAP and incubated prior to addition to cell cultures. After transduction, cultures were fixed, stained, and quantified for colony forming units. Results are presented as percentage of transduction inhibition, relative to control cultures that were transduced with AAV/CMV-hPLAP without any exposure to serum. Values reported as mean ± S.E.M. N = 3 for all groups. *P<0.05, **P<0.01. (**a,c)** Multiple t tests using Sidak's multiple comparison test. (**b**) Two-way ANOVA with Dunnett's multiple comparison test. (**d**) Two-way ANOVA with Holm-Sidak multiple comparison test.

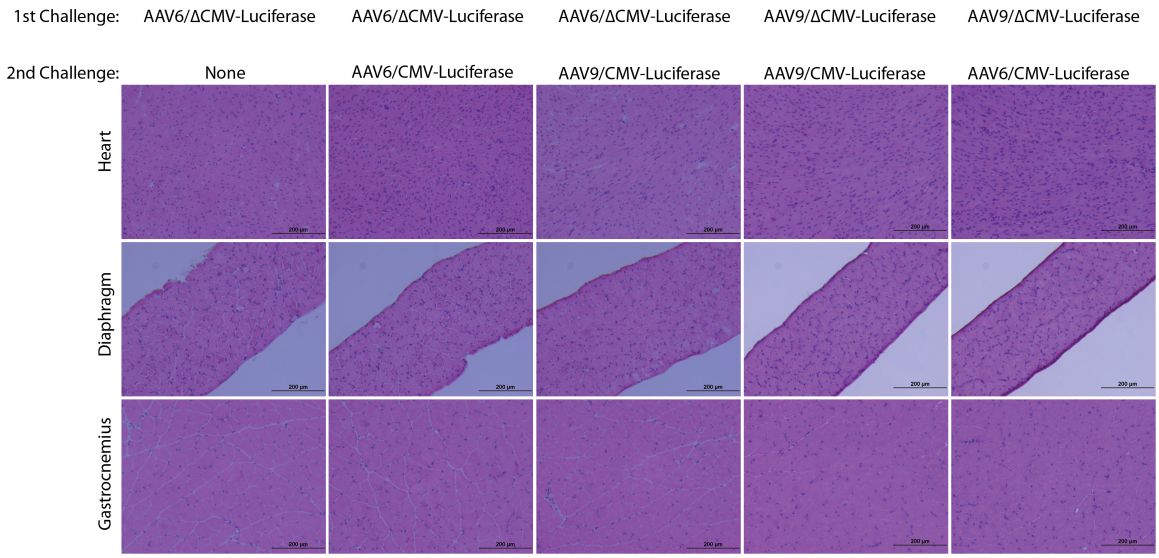

Figure 3.9 Absence of overt immune response to AAV after systemic readministration. Hematoxylin and eosin staining of heart (top row), diaphragm (middle row), and gastrocnemius (bottom row) cross sections from mice described in **Figure 3.8**. Scale bar, 200 μm.

Previous success with CsA and NDCD4 antibody was with 10^{12} vg/kg packaged in AAV8 (McIntosh, Cochrane et al. 2012). The mean dose of AAV6 or AAV9 that we delivered for initial challenge was $1.94x10^{14} \pm 1.45x10^{13}$ vg/kg. One possible explanation for the extensive reduction in transduction is that our implemented doses of immunosuppressive drugs were too low to prevent the generation of AAV-specific antibodies. The shift in AAV6 antibody specificity in the sera of cohorts exposed to serotype 9 (≤50% transduction inhibition at 1:320 serum dilutions) suggests a change in the B cell repertoire. Sera from cohorts exposed to AAV6, whether once or twice, inhibited transduction of HT1080 cultures by at least 80% in all tested serum dilutions. Yet the pronounced antibody response in 1°-AAV6/ΔCMV-luciferase mice did not lead to premature death nor decreased transduction after the second challenge of AAV6. Cumulatively, this suggests that the immunosuppression regimen was able to prevent clearance of transduced cells, but failed to attenuate neutralizing antibody responses to multiple AAV serotypes. A previous report showed that intravenous immunoglobulins neutralizing AAV could be overcome if the bolus included empty capsids, or capsids lacking a rAAV vector (Mingozzi, Anguela et al. 2013). Thus far, our systemic readministration studies with rAAV/luciferase vector used viral preparations that had only capsids with vector genomes (full capsids). This led us to ask if AAV6 could efficiently transduce striated muscle if intravenously delivered under immunosuppression with the addition of empty capsids.

Widespread transduction with multiple, high doses of rAAV6 vectors

Initial experiments with rAAV vectors (**Figs. 4,8**) consisted only of capsids with packaged rAAV genomes, or full capsids, in order to reduce the total capsid protein load in each challenge (see Materials and Methods in this chapter). Recombinant AAV vectors prepared with this method have high transduction efficiency (Ayuso, Mingozzi et al. 2010). However, removal of empty capsids reduces transduction efficiency in naïve mice (see Chapter 5) and leaves a full-capsid prep without any sacrificial protein to bind to neutralizing proteins in the serum (Mingozzi, Anguela et al. 2013). Therefore, all rAAV6 vectors used for triple intravenous administration were prepared to incorporate both empty and full capsids at ratio of approximately 3:1 (see Materials and Methods in Chapter 5) (Gregorevic, Allen et al. 2006). Incorporating empty capids to viral preparations may overcome existing neuralizing antibodies in subsequent administrations, but secondary exposure to antigen can lead to accelerated memory B cell activation and expansion of clones (McHeyzer-Williams, Okitsu et al. 2012, Swain, McKinstry et al. 2012). The response to the second challenge could be robust enough to inhibit transduction of the third challenge. To achieve a balance of maximum transduction and attenuating a humoral immune response to the AAV6 capsid, doses of CsA and NDCD4 antibody was kept the same but the regimen was adjusted for more frequent administration; days -1, 0, +1, +2, +3, +6, +7, and +8 relative to the first and second AAV6 challenges.

We sought to determine if C57BL/6 mice could tolerate three intravenous doses of AAV6 at 10^{13} vg per dose. This allowed a therapeutically relevant dose throughout the

experiment (**Table 3.1**). To determine transduction of each challenge, all three vectors actively expressed their own reporter gene. First and second challenges consisted of the CMV promoter driving the expression of fluorescent proteins mKalama (Ai, Shaner et al. 2007) and mCherry, respectively. The third vector expressed hPLAP driven by the CK8 promoter. Doses of rAAV6 vectors were delivered at 4-week intervals and were $>3.5x10^{14}$ vg/kg in both triple-administered (3xAAV) and age-matched control mice injected with only rAAV6/CK8-hPLAP (1xAAV; **Table 3.1**). Four weeks after administration with rAAV6/CK8-hPLAP, mice were assessed. Expression of all three reporters was evident in multiple muscles (**Fig. 10**). Activity of hPLAP reporter was measured in striated muscle groups to determine the efficacy of triple systemic transduction (**Fig. 10e**). Diaphragm, quadriceps, and soleus muscles had reduced hPLAP activity, but no tissues examined had significantly different activity compared to age-matched control mice receiving only the hPLAP reporter vector. No overt immune response or tissue damage was observed in muscles that exhibited lower transduction, as assessed by histological staining and quantification of collagen deposition (**Figs. 10a-d,f**). Cumulative data suggests that lower transduction in certain muscles may have resulted in neutralization of AAV6 capsids, as oppose to immune-mediated clearance of transduced cells.

Table 3.1 Dosage of rAAV6 vectors in C57BL/6 male mice. Mice were intravenously administered 10^{13} vector genomes (vg) by retro-orbital injection. One group (Triple Administration) received three boluses of rAAV6 vectors at 3, 7, and 11 weeks of age. Triple Administration mice were under transient immunosuppression during the first two vector administrations. A control group (Single Administration) received only one vector at 11 weeks of age without any immunosuppression. Masses of animals were recorded prior to injection. Dosage is reported as vector genomes per kilogram of body mass (vg/kg). N = 3 per group.

Single Administration			
Number	**Reporter Gene**	**Average vg/kg**	**S.E.M.**
1	hPLAP	3.60E+14	3.28E+12
Triple Administration			
Number	**Reporter Gene**	**Average vg/kg**	**S.E.M.**
1	mKalama	1.16E+15	1.44E+14
2	mCherry	4.76E+14	4.16E+12
3	hPLAP	3.93E+14	8.30E+12

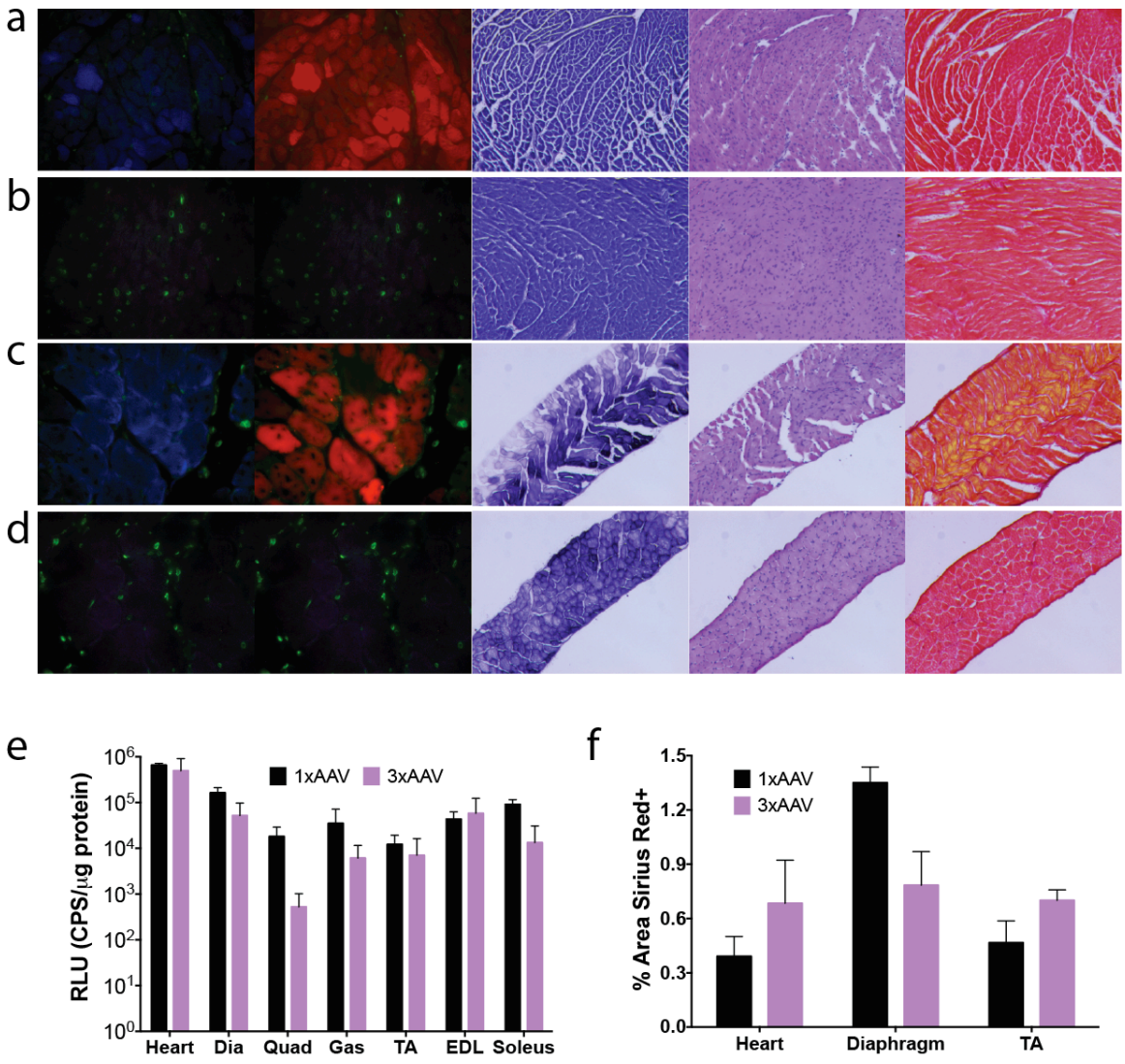

Figure 3.10 Triple systemic administration of rAAV6 vectors at high doses. Three boluses of 10^{13} rAAV6 vector genomes were intravenously injected in wild type mice. The first two were administered during transient immunosuppression. Each bolus delivered reporter genes mKalama, mCherry, and hPLAP, in that order, four weeks apart. Four weeks after administering hPLAP reporter vector, selected muscles were examined for extent of transduction. Cross sections of heart (**a,b**) and diaphram (**c,d**) were assessed for reporter expression and histology. Columns are representative images of (left to right): mKalama (blue) with LaminA/C (green), mCherry (red) with LaminA/C, hPLAP, hematoxylin and eosin, Sirius red. Rows are representative images from mice administered three AAV boluses (3xAAV; **a,c**) or age-matched controls only administered with hPLAP vector (1xAAV; **b,d**). (**e**) Lysates of selected muscles were measured for hPLAP activity. (**f**) Selected muscle cross sections were quantified for area positive for Sirius red staining. Mean ± S.E.M. N = 3 per group. Multiple t tests with Holm-Sidak multiple comparison test.

Discussion

This study addressed the maintenance of adult skeletal muscle after a widespread, temporally controlled loss of micro-dystrophin (μDys) expression. Such constructs are employed in rAAV-mediated gene replacement strategies for Duchenne muscular dystrophy, but the stability of these constructs has not been fully characterized. The half-life of flμDys employed in this work was estimated at approximately 5 to 7 days (**Fig. 3.1**), only a fraction of the near full-length isoforms produced by exon-skipping strategies (Wu, Lu et al. 2012, Verhaart, van Vliet-van den Dool et al. 2014). Unfortunately, ablating μDys expression resulted in a rapid onset of muscular dystrophy (**Fig. 3.3**). The use of tamoxifen-inducible Cre-loxP system resulted in a high degree of ablation but was unable to lead to an flμDys-null model. Despite the long tamoxifen regimen, ablating all copies of the floxed gene may not have been as successful in myogenic precursor cells. Effects of long-term ablation of μDys expression could not be addressed in this study. However, our results reveal that adult skeletal muscle cannot sustain lost μDys expression despite upregulation of endogenous utrophin.

In this study we examined the ability to generate tolerance with repeated administration of AAV serotypes 6 and 9 for transducing murine striated muscle with multiple transgenes. The combination of cyclosporine (CsA) and non-depleting anti-CD4 (NDCD4) antibody was used to attenuate immunity to viral capsid protein. Initial experiments demonstrated tolerance of AAV6 capsid by intramuscular injection into wild type mice (**Fig. 3.4**). This concept was expanded to address a more clinically relevant question of whether or not dystrophic muscle could be treated multiple times with rAAV vectors encoding micro-dystrophin (μDys) transgenes. As a means to create rapid

transgene loss and a context to warrant readministration of rAAV/CK8- μDys, muscles of previously treated mdx^{4cv} mice were acutely injured with notexin. We show that a transient regimen of CsA and NDCD4 antibody allowed significantly higher transduction of the second μDys transgene compared to mice that didn't receive the regimen. Immunosuppression also allowed acutely injured muscles to have lower centrally nucleated myofibers and increased resistance to contraction-induced injury months after the second AAV challenge (**Fig. 3.6**). Although encouraging as a treatment for Duchenne muscular dystrophy, we did not assume the same degree of success directly translated to intravenously delivery of therapeutically relevant doses. Previous studies demonstrated that the humoral response is dependent on the dose of AAV and the route of delivery (Xiao, Chirmule et al. 2000, Petry, Brooks et al. 2008). Therefore, we utilized this transient regimen for systemic delivery of AAV serotypes 6 and 9.

Wild type mice were intravenously administered a non-expressing rAAV/ΔCMV-luciferase vector packaged in either AAV6 or AAV9. Four weeks after the initial challenge, rAAV/CMV-luciferase vectors packaged in serotype 6 or 9 were administered (**Fig. 3.8**). The initial challenge of serotype 6 didn't significantly reduce transduction of examined striated muscles with either serotype. However, initial challenge with serotype 9 significantly reduced transduction upon readministration of AAV9 but not with AAV6. Similarly, a previous report showed that secondary administration of rAAV6 vectors did not inhibit transduction to the same degree as secondary administration of rAAV2 vectors (Halbert, Rutledge et al. 2000). The generation of neutralizing antibodies against AAV6 and AAV9, despite being under immunosuppression during the initial administration, suggests inadequate CD4 blockade and/or a T cell-independent (TI) B cell response to

AAV. Inadequate CD4 blockade would presumably allow AAV-specific cytotoxic T cell activation, yet we observed no overt immune response in wild type mice by histological examination. Any clearance of transduced skeletal muscle would be observed at our time points by the presence of necrotic or regenerating myofibers with central nuclei. This begs the question of how rAAV6 was able to transduce multiple tissues upon the second challenge and rAAV9 was not.

Our findings from the neutralizing antibody assays (**Fig 3.8)** suggest that the initial administration of AAV serotypes 6 and 9 resulted in a humoral response despite being under immunosuppression. The second challenge with the same serotypes essentially became a recall antigen for memory B cells, which can respond, proliferate, and differentiate into high-affinity plasma cells an at enhanced rate compared to naïve B cells (McHeyzer-Williams, Okitsu et al. 2012). Yet the second administration of rAAV6 vectors led to successful transduction of the examined tissues, while rAAV9 readministration did not. Both serotypes were readministered intravascularly, suggesting that the extravasation process may differ between the two serotypes. Previous studies, including our own (see Chapter 5), have shown that rAAV9 vectors extravasate at slower rates compared to rAAV6 vectors after intravenous delivery (Zincarelli, Soltys et al. 2008, Kotchey, Adachi et al. 2011). The faster extravasation of rAAV6 vectors may have limited their exposure to neutralizing antibodies, allowing them to transduce more efficiently than rAAV9 vectors.

Another possible explanation for the differences in tolerance among serotypes 6 and 9 could be differences in cell-specific tropism. Mice transduced with rAAV9 vectors using a non-cell specific CMV promoter (**Fig. 3.8a**) exhibited higher luciferase activity in

the heart, diaphragm, and gastrocnemius muscles compared to mice transduced with rAAV6 vectors with the same promoter. Yet, when transduction efficiencies were compared using the muscle-specific CK8 promoter to drive expression of hPLAP, the differences in reporter activity between serotypes 6 and 9 was dramatically lower in the same muscles (**Fig. 3.11**). It is possible that the tropism repertoire of rAAV9 includes antigen-presenting cells (APCs) that can contribute to a virus-specific immune response. In an attempt to validate previous studies using CsA and NDCD4 antibodies, we found this regimen was unable to attenuate a humoral response to AAV capsids at doses that were 10 to 100-fold higher than previously tested (McIntosh, Cochrane et al. 2012). The possibility that the doses used in our study led to T cell-independent (TI) B cell response cannot be ruled out.

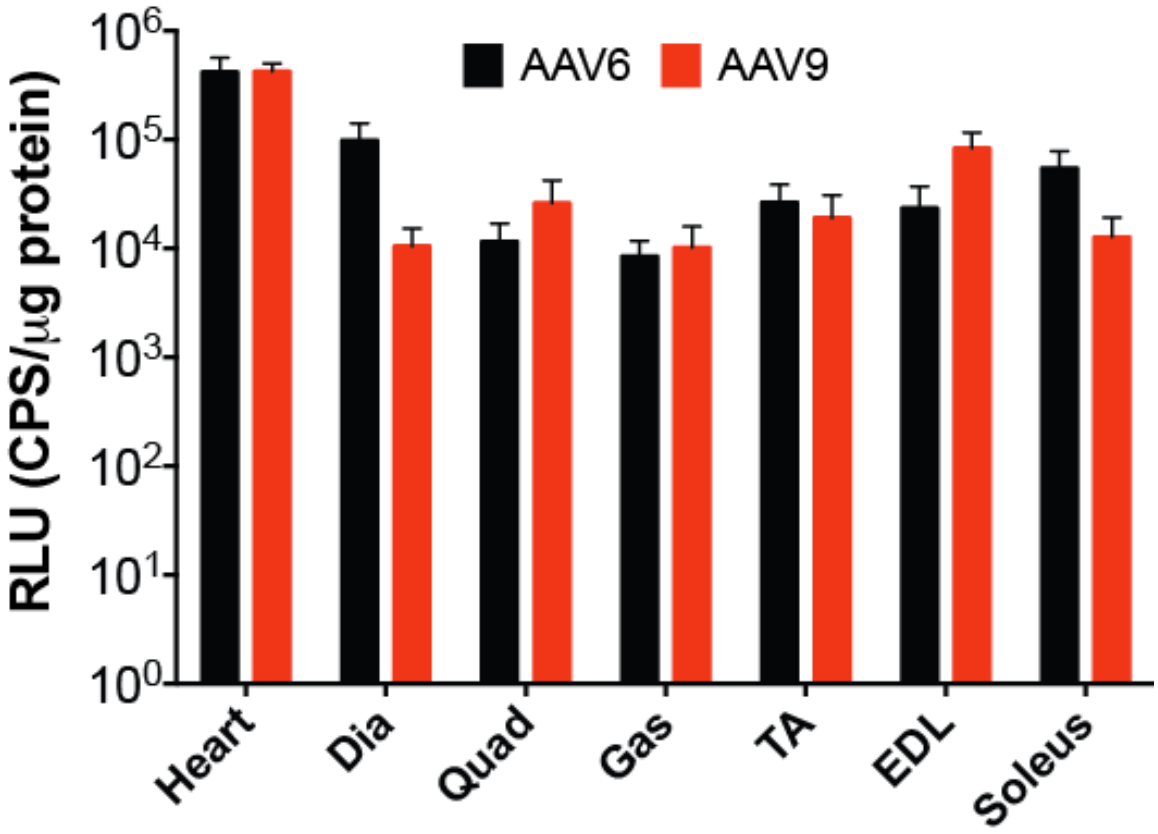

Figure 3.11 Tropism for striated muscle cells revealed by myogenic promoter. Wild type males 10-12 weeks of age were intravenously administered 10^{13} vg of AAV6/CK8-hPLAP and assessed four weeks later. Lysates from selected striated muscles were measured for hPLAP activity; heart, diaphragm (Dia), quadriceps (Quad), gastrocnemius (Gas), tibialis anterior (TA), extensor digitorum longus (EDL), and soleus. Mean ± S.E.M. N = 3 per group. One-way ANOVA with Tukey post test.

B cells can detect an antigen independently of T cells and become activated, yet they require interaction with T cells in order differentiate into a plasma cell and secrete antibodies (Tangye, Ma et al. 2013). CD40 is a surface receptor expressed on B cells, as well as APCs and $CD8^+$ T cells, that interacts with CD40 ligand (CD40L) expressed by $CD4^+$ T cells. CD40-CD40L interactions are required for proper Ig class switching and maturation of B cells (Kawabe, Naka et al. 1994, Xu, Foy et al. 1994) and for mediating CTL responses (Bennett, Carbone et al. 1998, Ridge, Di Rosa et al. 1998, Schoenberger, Toes et al. 1998). CD40L null mice fail to generate CTL and humoral immune responses to AAV (Chirmule, Xiao et al. 2000, Zhang, Chirmule et al. 2000). Use of a non-depleting anti-CD40 antibody enabled readministration of rAAV vectors by attenuating humoral immunity. This was achieved both with and without the use of non-depleting CDTLA4-Ig antibody (Halbert, Standaert et al. 1998, Lorain, Gross et al. 2008), another immunosuppressive agent that targets co-stimulatory molecules CD80 and CD86 which are also expressed on APCs and B cells (Swain, McKinstry et al. 2012). Successful attenuation of an immune response to rAAV vectors will likely require drugs, or antibodies, that disrupt multiple signaling processes among the immune cell populations.

As mentioned, human populations can exhibit pre-existing antibodies for AAV serotypes. Unless one introduces an AAV serotype to which a patient is naïve, blockading B-T cell and APC-T cell interactions with CD40 and CDTLA4-Ig antibodies won't overcome this transduction barrier. In this study, we demonstrated successful readministration of high doses of rAAV vectors with and without the inclusion of empty capsids. Though successful in this study, we acknowledge that this method of viral preparation may only exacerbate the humoral response to AAV and require the empty-to-

full capsid ratio to increase in subsequent administrations in order to overcome higher concentrations of neutralizing antibodies. Plasmapheresis has already been explored as a means to remove or dilute pre-existing neutralizing antibodies to AAV and increase transduction (Hurlbut, Ziegler et al. 2010, Monteilhet, Saheb et al. 2011, Chicoine, Montgomery et al. 2014). Other attempts to attenuate humoral immunity to AAV by depleting B cells have been reported (Sack, Merchant et al. 2012, Unzu, Hervas-Stubbs et al. 2012). However, recovery from B-cell ablation can take weeks or even months, depending on the dose, and may influence antibody responses against novel and recall antigens (Townsend, Monroe et al. 2010).

If rAAV-mediated gene therapy is to become safe for clinical application, the three-way interaction between serotype, target tissue(s), and the immune system must be understood to avoid rejection of the transgene. Significant loss of micro-dystrophin expression in skeletal muscle would require readministration of rAAV vectors. Our findings support the need for taking immunomodulating precautions for rAAV-mediated gene therapy. Though CTL-mediated response was avoided with a combination of cyclosporine and non-depleting CD4 antibody, a humoral to rAAV was not prevented at the high doses and intravenous route of delivery used in this study. We propose that this combination of immunomodulating drugs can be used in conjunction with other agents that disrupt humoral immune responses so that repeat administration of rAAV vectors can remain a viable therapeutic option for gene therapy.

Materials and Methods

Animal experiments

Animal experiments were performed in accordance with the Institutional Animal Care and Use Committee of the University of Washington. All mice in this study were males breed on C57BL/6 inbred background and housed in a specific pathogen free barrier facility. HSA-loxP-μDys$^{\Delta R24\text{-}R23/\Delta CT}$-loxP (flμDys) mice were created by Carol Ware (Institute for Stem Cell and Regenerative Medicine, University of Washington, Seattle, WA) by pronuclear injection. Three founder lines were established and crossed with dystrophic *mdx*^{4cv} on C57BL/6 background. Two of these lines, 5415 and 5419, were chosen for this study. C57BL/6J-CAGGCre-ER^{TM} (CreER^{TM}) mice (Jackson Laboratory) were crossed with *mdx*^{4cv}/C57BL/6 mice. Male hemizygote HSA- loxP-μDys$^{\Delta R24\text{-}R23/\Delta CT}$-loxP/CAGGCre-ER^{TM}/*mdx*^{4cv} mice were breed with female *mdx*^{4cv} mice.

At approximately 10-15 weeks of age, flμDys/*mdx*^{4cv} mice were intramuscularly injected into extensor digitorum longus for acute transgene ablation. At approximately 9 to 10 months of age CreER^{TM}/flμDys/*mdx*^{4cv} mice were administered 0.25 mg/kg tamoxifen diluted in corn oil (Sigma-Aldrich, St. Louis, MO) by intraperitoneal injection every 3-4 days for a total of 5 injections. Mice were 3 weeks of age at the start of immunosuppression regimen. Mice were anesthetized with isofluorane for all rAAV vector and notexin injections. For intramuscular administration of rAAV vectors, the extensor digitorum longus or tibialis anterior muscle was injected with a 10-μL or 30-μL bolus, respectively. Untreated control muscles received a sham injection of Hank's balanced saline solution. Systemic administration of rAAV vectors was performed by retro-orbital injection. For acute injury model, mice were given an intramuscular

injection of notexin (1μg/mL [Sigma-Aldrich, St. Louis, MO]). Immunosuppression regimen consisted of cyclosporine (CsA; Sandimmune injection, USP; Novartis Pharmaceuticals Corporation, East Hanover, NJ) at 25 μg/g body mass and YTS 177.9.6.1 monoclonal anti-mouse CD4 antibody at 50 μg/g body mass. For experiments delivering firefly luciferase rAAV vectors, CsA and CD4 antibody were administered on days -1, 0, +1, +3, +6, and +8 relative to day of rAAV administration. For experiments delivering mKalama, mCherry, and hPLAP rAAV vectors, CsA and CD4 antibody were administered on days -1, 0, +1, +2, +3, +6, +7, and +8 relative to day of rAAV administration. Body mass was recorded on days of immunosuppression administration and doses were accordingly adjusted.

Primary Myoblast Culturing and Analysis

Hind limb muscles of CreER^{TM}/flμDys/*mdx*^{4cv} mice (10-15 weeks of age) were dissected, cleaned, and minced in cold PBS, without $CaCl_2$. Type II collagenase and Dispase was added to minced muscle slurry to a final concentration of 446 U/mL and 1.2 U/mL, respectively (Worthington Biochemical, Lakewood, NJ), and incubated at 37°C. During 60-minute digestion, slurry was triturated every 15 minutes by pipetting. Digestion was quenched by 15% horse serum (HS), 1 mM $CaCl_2$ in F10 medium (Life Technologies, Grand Island, NY) and strained through 70-μm and 40-μm BD Falcon nylon cell strainers (BD Biosciences, San Jose, CA). Cell mixture was pelleted and resuspended in growth medium (15% HS, 1 mM $CaCl_2$, 1% penicillin/streptomycin in F10). Cell suspension was pre-plated in uncoated dishes twice, for 60 minutes each time, in order to remove non-myogenic cells and cellular debris. Final cell suspension was

quantified for viable cells (Trypan Blue, Sigma-Aldrich) and 0.67-gelatin coated plates were seeded at approximately $20x10^3$ cells/mL. Seeded cultures were supplemented with FGF-2 at final concentration of 5 ng/mL. Two days after seeding, growth medium was removed, cultures were rinsed in saline, and feed differentiation medium (1.5% HS, 1 mM $CaCl_2$, 1% penicillin/streptomycin in F10) supplemented with 2 μM (Z)-4-hydroxytamoxifen (4-OHT; Sigma-Aldrich). For the next two consecutive days, medium was exchanged with fresh differentiation media supplemented with 2 μM 4-OHT. Following the last day of 4-OHT treatment, medium was exchanged for differentiation medium. Cultures were fixed and stained at specified days after end of 4-OHT treatment.

For immunohistochemistry, an equal volume of 4% PFA/3% sucrose in PBS was added to culture with medium and incubated at room temperature for 10 minutes. After washing three times with PBS, cells were permeabilized with 0.5% TritonX-100 in PBS for 10 minutes. Cells were washed three times with PBS and blocked in solution of 1% BSA, 0.05% Tween-20 in PBS (PBS-B) for 30 min at room temperature. Primary antibodies were diluted in PBS-B and added to cells either at 2 hours at room temperature or overnight at 4°C. After washing with PBS, cells were incubated with secondary antibodies diluted in PBS-B for 1 hour at room temperature, protected from light. Cells were washed with PBS and incubated with 4',6-diamidino-2-phenylindole (DAPI) in PBS for 10 minutes. Cell were washed three times in PBS, once with distilled water, and mounted with ProLong Gold antifade reagent (Life Technologies). Primary antibodies used were mouse monoclonal anti-desmin (clone D33, Dako, Carpinteria, CA) and monoclonal anti-dystrophin (MANEX1011B clone 1C7, Developmental Studies Hybridoma Bank (DSHB) at the University of Iowa, Iowa City, IA) conjugated to Alexa-

488 (Life Technologies). Secondary antibodies used were goat anti-mouse IgG1 conjugated to Alexa-594 (Life Technologies).

Quantitative PCR Analysis

DNA extracts were generated from selected tissues using DNAeasy Blood & Tissue Kit (Qiagen, Valencia, CA). All real time PCR reactions were performed on an Applied Biosystems 7500 Real Time PCR System using TaqMan Universal PCR Master Mix (Life Technologies), custom primers (IDT), and custom probes (Eurofins Genomics, Hunstville, AL). The following primers and probe were used to quantify copies of floxed-μDys gene; 5'- GGTGACCACAAGGGAACAG -3', 5'-TCTTGAAGTTCCTGGAGTCTTTC -3', probe: 5'- 6FAM-TCCACCACCACCTCCCCAAAAG-BHQ1 -3'. The following primers and probe were used to quantify copies of endogenous murine LDLR gene; 5'-CGTGCTCCCAGGATGACTTC- 3', 5'- CTCCATCACACACAAACTGCG -3', probe: 5'-6FAM-ATGCCAGGATGGCAAGTGCATCTCC-TAMRA -3'. Samples were measured in triplicate and calculated as floxed-μDys gene number per diploid genome. Values were reported relative to untreated control transgenic mice.

Antibody production

YTS 177.9.6.1 hybridoma cell line (a kind gift from Steve Cobbold and Herman Waldmann, University of Oxford) was maintained at 37°C in an atmosphere of 5% CO_2 to generate monoclonal anti-mouse CD4 antibody. Cells were originally cultured in 5% fetal bovine serum, 1% penicillin/streptomycin in Iscoves modified Dulbeccos medium

(IMDM, Life Technologies). The cell line was then gradually adapted to 2 mM GlutaMAX, 1% penicillin/streptomycin in chemically defined (CD) hybridoma medium (Life Technologies). Corning polystyrene roller bottles (Fisher Scientific, Rockford, IL) were seeded at approximately $2x10^5$ cells/mL in 200-mL cultures for 8 days, rotating at 0.25 rpm. Upon harvesting, cultures were centrifuged twice, in order to remove the cell pellets. Supernatant was then filtered through Express PLUS 0.22-μm filters (Millipore, Billerica, MA). Antibody in the filtered supernatant was concentrated in Amicon Ultra-15 100K centrifugal filter devices (Millipore) and transferred into Slide-A-Lyzer dialysis cassette with 20K membrane molecular-weight cutoff (Thermo Scientific, Rockford, IL) for dialysis in Dulbeccos phosphate buffered saline (Life Technolgies). Dialyzed antibody solution was filtered in Express PES 0.22-μm filter (Millipore), aliquoted, and stored at -20°C until used. Antibody solution was checked for purity by running non-reduced samples on NuPAGE gel (Life Technologies) with rat myeloma IgG2a (Life Technologies) as positive control for molecular weight bands. Antibody concentration was determined using the Coomassie Plus Bradford Assay (Pierce, Rockford, IL).

Expression vectors

Recombinant AAV vectors expressing mCherry (Stratagene, Agilent Technologies, Santa Clara, CA), mKalama1 (Campbell (Ai, Shaner et al. 2007), Addgene plasmid 14892), and Firefly luciferase (kindly provided by Stephen Hauschka, University of Washington) were driven by cytomegalovirus (CMV) promoter. CMV promoter in neutralizing antibody assays and CK8 promoter (Goncalves, Janssen et al. 2011) in triple systemic administration experiments drove the expression of human placental alkaline

phosphatase (hPLAP) reporter. The CK8 promoter drove micro-dystrophin expression. HEK293D cells were transfected with pAAV-CMV-luciferase and pAAV-ΔCMV-luciferase plasmids using Lipofectamine LTX and PLUS reagent (Life Technologies) to confirm ablated expression in the absence of the promoter (see luminometry assay below).

Virus production

Viral preps with Firefly luciferase in AAV serotypes 6 and 9 were purified to only use capsids containing vector genomes. Briefly, expression constructs were co-transfected with pDGM6, pDGM8, or pDGM9 packaging plasmids for AAV serotypes 6 and 9, respectively, in HEK293D cells. Cultures were then harvested, microfluidized (Microfluidics, Newton, MA), and processed through 0.22-μm filter (Millipore). Clarified lysate was then subjected to polyethylene glycol precipitation in order to isolate AAV capsids (Ayuso, Mingozzi et al. 2010). Once resuspended, vector capsids were separated by ultracentrifugation in a cesium chloride gradient. A visible band of AAV capsids lacking vector genomes, or 'empty' capsids, were removed in order to isolate another, distinct band of AAV capsids with packaged vector genomes, or 'full' capsids that has a different density. The full capsids were dialyzed in HBSS. Recombinant AAV6 vectors involved in readministration of micro-dystrophin constructs and triple systemic administration experiments were made as previously described (Gregorevic, Allen et al. 2006) to include both 'empty' and 'full' capsids. Purification scheme included a HiTrap heparin affinity column with an Amersham AKTA10HPLC machine (GE Healthcare Life Sciences, Piscataway, NJ). All rAAV preps were quantified by Southern analysis.

Luminometry assays

For *in vivo* analysis, whole muscles of quadriceps, gastrocnemius, tibialis anterior, extensor digitorum longus, and soleus were used. Contralateral muscles were used for histological analysis, as described below. The aria of the heart and half of the costal region of the diaphragm were used for luminometry assays while the rest of these tissues were used for histology. Luminometry-dedicated tissues were snap-frozen in liquid nitrogen and ground using a dry ice-chilled mortar and pestle. For Firefly luciferase activity, lysates were obtained using Reporter Lysis Buffer (Promega, Madison, WI). Briefly, tissues were homogenized with pellet pestle and motor (Kimble-Kontes, Vineland, NJ) within an ice-chilled microcentrifuge tube. Homogenates were spun at 10,000xg for 10 minutes at 4°C and supernatants were transferred to new tubes and stored at -80°C until used. Firefly luciferase reporter activity was measured using Luciferase Assay System (Promega) according to manufacturer's instructions. For human placental alkaline phosphatase activity, lysates were obtained as described above with AP lysis buffer (0.5% NaDOC, 50 mM Tris pH 7.5, 150 mM NaCl, 1% Triton X-100, supplemented with complete protease inhibitor cocktail (cOmplete, Mini, Roche, Indianapolis, IN). The hPLAP activity was measured using Phospha-Light system (Applied Biosystems, Bedford, MA) according to manufacturer's instructions. Coomassie Plus Bradford Assay was used to determine protein concentration of samples. Bradford and luminometry assays were measured with a Victor^{3}V multilabel counter (PerkinElmer, Shelton, CT) using microplates. Values are reported as relative light units (RLU) defined as counts per second normalized to μg protein in the reaction.

Neutralizing antibody assays

AAV neutralizing antibody assays were performed as previously described (Halbert, Rutledge et al. 2000, Calcedo, Vandenberghe et al. 2009). Briefly, a mouse serum samples were isolated in BD Microtainer serum separator tubes (Fisher Scientific, Rockford, IL). Samples were then heat inactivated at 56°C for 30 minutes. Serum was added to 100 μL volumes of rAAV/CMV-hPLAP in serotype 6, 8 or 9 (full capsids only) to reach a final serum dilution (neat, 1:20, 1:40, 1:80, 1:160, or 1:320). Serum and virus solutions were incubated at 37°C for 1 hour and then added to HT1080 cells plated at 10^4 cells per well (12-well plates; Falcon, Fisher Scientific) the day prior. Two days following transduction, plates were fixed, stained for hPLAP expression (*FAST* BCIP/NBT substrate solution; Sigma, St. Louis, MO) overnight in the dark. Cells were washed three times in phosphate buffered saline (PBS) and quantified for colony forming units (CFUs).

Histology

For sacrificed mice involved in triple systemic AAV6 administration experiments, harvested tissues were fixed in ice cold 4% paraformaldehyde (PFA; Electron Microscopy Sciences [EMS], Hatfield, PA) for 2 hours at 4°C. After washing three times in cold PBS, tissues were placed in ice cold 30% sucrose in PBS and incubated overnight at 4°C. Tissues were then rinsed once in cold PBS, gently padded dry and embedded as described below. Histology-dedicated tissues of all sacrificed mice were embedded in Tissue-Tek OCT medium (Sakura Finetek USA, Torrance, CA) and frozen in isopentane

chilled by liquid nitrogen. Transverse sections approximately 10 μm thick were used. For hematoxylin and eosin (H&E) staining, sections were fixed for 5 minutes in methanol and stained according to standard H&E protocol. Sections were then dehydrated in ascending series of ethanol washes (70, 95, 100%), xylene, and mounted with permount (EMS). For Sirius red staining, sections were fixed in 4% PFA for 10 minutes. After washing in PBS, sections were stained in 0.1% Sirius red in saturated picric acid (EMS) for 1 hour. Sections were washed twice in acidified distilled water (0.5% acetic acid- glacial) and then dehydrated and mounted as described above. For hPLAP staining, sections were fixed in ice cold 4% PFA, washed three times in cold PBS, and incubated at 65°C for 90 minutes in pre-warmed PBS. Sections were then washed in AP buffer (0.1 M Tris-HCl pH 9.5, 0.1 M NaCl, 0.01 M $MgCl_2$) for 10 minutes and then incubated with *FAST* BCIP/NBT substrate solution (Sigma) for 20 minutes at room temperature in the dark. After rinsing three times in room temperature PBS, sections were dehydrated and mounted as described above.

For immunofluorescence studies, sections were blocked and stained as previously described (see Methods section of Chapter 2). Primary antibodies used were mouse anti-dystrophin (MANEX1011B) conjugated to Alex-488, rat anti-α2-laminin (clone 4H8-2, Sigma, St. Louis, MO), rabbit anti-nNOS (Z-RNN3, Life Technologies), rat anti-mouse F4/80 (Ab Serotec, Raleigh, NC), and rabbit anti-mouse mannose receptor (Abcam, Cambridge, MA). Secondary antibodies were goat anti-rabbit conjugated to Alex-488 or -594, chicken anti-rat conjugated to Alexa-660, goat anti-rat conjugated to Alexa-594, and Goat anti-mouse IgG2a conjugated to Alexa488 (Life Technologies). Nuclei were stained with DAPI and mounted with ProLong Gold antifade reagent (Life Technologies).

Images were captured using an Olympus SZX16 dissection fluorescent microscope with DP software (Oympus, Center Valley, PA) or a Nikon Eclipse E1000 fluorescent microscope (Melville, NY) with QImaging camera and QCapture software (Surrey, British Columbia, CA). Sirius red staining was quantified using Image J analysis software (National Institute of Health, Bethesda, MD).

Peripheral blood mononuclear cell analysis

Under isoflurane-induced anesthesia, peripheral blood mononuclear cells (PBMCs) were collected from mice via retro-orbital bleeds into BD Microtainer lithium heparin tubes (Fisher Scientific). Four volumes of cold erythrocyte lysis buffer (155 mM NH_4Cl, 10 mM $KHCO_3$, 0.1 mM EDTA) was added to blood and incubated on ice for 10 minutes. PBMCs were washed once in lysis buffer and then twice in PBS. Cells were stained with rat anti-mouse CD4-APC (clone RM4-4, BioLegend, San Diego, CA), CD8-Alex488 (clone 5H10-1, BD Biosciences), and Armenian hamster anti-mouse CD3 (clone 145-2C11, BioLegend) in 2% FBS, 0.09% NaN_3 diluted in PBS. Clone RM4-4 was used because it the epitope of this antibody doesn't overlap with clone YTS 177.9.6.1(Vignali and Vignali 1999). Cells were rinsed twice in PBS and stained with Goat anti-Armenian Hamster conjugated to Alexa594 (Jackson ImmunoResearch Labs, West Grove, PA). After rinsing in PBS and resuspending in 0.09% NaN_3 in PBS, PBMCs were analyzed on a FACSCanto RUO system (BD Biosciences) with FlowJo software (TreeStar, Ashland, OR).

Physiological analysis

Tibialis anterior muscles were assessed as previously described (Gregorevic, Allen et al. 2006). Briefly, anesthetized mouse was prepped for *in situ* analysis of muscle performance by immobilizing the knee to a heated (37°C) platform of a custom built Plexiglas apparatus. Sutures knotted to the distal, severed tendon were used to secure distal end to the lever arm of a dual-mode force transducer-servomotor (Model 305B-LR, Aurora Scientific, Aurora, Ontario, CA). After placing platinum-tipped electrodes into the leg above and knee, flanking the peroneal nerve, the tibialis anterior was stimulated by pulses and manipulated on three axes to find the optimal fiber length. Once this was determined, the muscle was stimulated to produce a maximum isometric tetanic force. Eccentric contractions were performed at thirty-second intervals in an ascending series of length changes, or stains, of 0-45% of the optimum myofiber length. Specific force was determined by normalizing maximum isometric force to the mass of the tibialis anterior muscle. Force deficit was calculated as the decrease of isometric force preceding a given eccentric contraction from the maximum isometric force observed throughout the protocol. Extensor digitorum longus (EDL) muscles were assessed as previously described. Briefly, EDL muscle was sutured on distal and proximal tendons within an anesthetized mouse prior to severing excess tendons. Excised muscle was quickly moved to a bath of Tyrode solution (Lannergren, Bruton et al. 2000) (containing (mM): NaCl 121, KCl 5, $CaCl_2$ 1.8, $MgCl_2$ 0.5, NaH_2PO_4 0.4, $NaHCO_3$ 24, glucose 5.5) within an *in vitro* physiology rig (Model 809A, Aurora Scientific). Solution was saturated with 5% CO_2/95% O_2 gaseous mixture and maintained at 25°C. Tendons were secured to sever

motor described above and to a submerged hook in the bath. Optimal length and maximal isometric force was ascertained in a similar fashion as the tibialis anterior muscle.

Statistical analysis

All data analyses were performed with GraphPad PRISM 6 software (San Diego, CA).

Chapter 4

Adeno-associated Viral Vectors do not Efficiently Target Muscle Satellite Cells

Introduction

Adeno-associated virus (AAV) is a small, single-stranded DNA parvovirus that has featured prominently in the field of gene therapy. Recombinant AAV (rAAV) is a promising therapeutic candidate for use in gene replacement strategies due to encouraging results in numerous animal models of genetic disease and in human clinical trials. Unlike the wild type virus, recombinant AAV vectors lack the viral genes that promote integration, and thus persist almost entirely in episomal form within transduced tissues (Duan, Sharma et al. 1998, Schnepp, Jensen et al. 2005, Smith 2008). This feature of rAAV biology contributes to the safety profile of the vector by reducing the risk of deleterious integration near oncogenes and in germ cells (Nakai, Yant et al. 2001, McCarty, Young et al. 2004, Inagaki, Lewis et al. 2007, Inagaki, Piao et al. 2008).

Numerous primate serotypes and over 100 AAV variants have been isolated, many of which exhibit unique patterns of tissue tropism and transduction (Schultz and Chamberlain 2008). The transduction profile of several of these vectors has been extensively compared in multiple studies, and a high degree of tropic variability has been observed between serotypes. For example, rAAV8 and rAAV9 have been shown to achieve high levels of hepatocyte transduction (Gao, Alvira et al. 2002, Nakai, Fuess et al. 2005, Inagaki, Fuess et al. 2006), whereas rAAV1 and rAAV5 perform effectively within the central nervous system (Alisky, Hughes et al. 2000, Davidson, Stein et al. 2000, Wang, Wang et al. 2003, Burger, Gorbatyuk et al. 2004). In striated muscle, high transduction levels have been attained using rAAV1, 6, 7, 8, and 9 (Chao, Liu et al. 2000,

Blankinship, Gregorevic et al. 2004, Gregorevic, Blankinship et al. 2004, Wang, Zhu et al. 2005, Inagaki, Fuess et al. 2006, Pacak, Mah et al. 2006, Zincarelli, Soltys et al. , Zincarelli, Soltys et al.). In particular, rAAV6 is strongly tropic for striated muscle and has demonstrated the highest efficiency of cardiac transduction amongst rAAV serotypes 1-9 (Blankinship, Gregorevic et al. 2004, Gregorevic, Blankinship et al. 2004, Zincarelli, Soltys et al. , Zincarelli, Soltys et al.). Thus, rAAV6 is a candidate for treatment of a large number of genetic disorders related to skeletal and cardiac muscle.

The muscular dystrophies comprise a heterogeneous group of genetic disorders affecting striated muscle. The most common of the dystrophies is Duchenne muscular dystrophy (DMD), a lethal X-linked recessive disorder affecting approximately 1 in every 3,500 live male births (Emery 2003). DMD is characterized by progressive and debilitating wasting of striated muscle, culminating in cardiac and respiratory failure by the third decade of life. At this time, no curative treatment exists, and high-dose corticosteroids remain the primary component of the majority of established treatment regimens (Chamberlain and Rando 2006). DMD is caused by mutations in the gene encoding for dystrophin. The full-length isoform of dystrophin is a structural protein that localizes to the sarcolemma of myofibers and serves to stabilize the muscle membrane during periods of mechanical stress (Emery 2003). In the absence of dystrophin, muscles are highly susceptible to contraction-induced injury and are repeatedly damaged during normal use (Brooks and Faulkner 1988, Cox, Phelps et al. 1993, Petrof, Shrager et al. 1993, Campbell 1995). This leads to a chronic cycle of necrosis and regeneration that ultimately results in widespread fibrosis and deposition of adipose tissue.

The successful use of rAAV to treat DMD depends on efficient transduction of muscle tissue in a pro-inflammatory, dystrophic environment. Histologically, dystrophic muscles are characterized by a chronic inflammatory cell infiltrate and a heterogeneous combination of myofibers at various stages of degeneration and regeneration (Emery 2003). Activated and proliferating muscle progenitor cells can be observed in response to a high degree of dystrophic turnover. While it has been clearly demonstrated that rAAV6 can transduce mature myofibers *in vivo* (Blankinship, Gregorevic et al. 2004, Gregorevic, Blankinship et al. 2004, Zincarelli, Soltys et al. 2008), the transduction efficiency of muscle precursor cells (MPCs) and immature myotubes has not been characterized. Recombinant AAV vectors exhibit a very low rate of integration (Schultz and Chamberlain 2008), suggesting that transduction of MPCs may only extend AAV-mediated transduction by one additional round of degeneration/regeneration. Nevertheless, the capacity to target MPCs is an important aspect to consider in the development of any gene replacement strategy for the muscular dystrophies, as transduced MPCs could potentially serve to replenish myofibers that are lost during normal fiber turnover and extend AAV-mediated DMD gene therapy.

In the following studies, we evaluated the capacity of rAAV6 to transduce both MPCs and myofibers in wild type C57BL/6 and dystrophic *mdx*^{4cv} (*mdx*) mice. The *mdx* mouse demonstrates many of the pathological features of DMD and serves as a well-established genetic model for this disease (Banks and Chamberlain 2008). Our results demonstrate that rAAV6 does not effectively transduce muscle satellite cells, but preferentially transduces differentiated myofibers, both *in vitro* and *in vivo.*

Results

rAAV6 transduces myotubes more efficiently than myoblasts in culture.

The MM14 cell line is an immortalized mouse myoblast line that has been extensively utilized to study skeletal muscle myogenesis (Olwin and Rapraeger 1992, Templeton and Hauschka 1992, Hannon, Kudla et al. 1996, Fedorov, Jones et al. 1998, Jones, Fedorov et al. 2001, Motamed, Blake et al. 2003). When grown in appropriate culture conditions, including serum and FGF-2 supplementation, MM14 myoblasts proliferate and remain in a mononuclear state. Serum depletion and withdrawal of FGF-2 induces withdrawal from the cell cycle and terminal differentiation into myocytes and myotubes within a few days of induction (Chamberlain, Jaynes et al. 1985, Clegg, Linkhart et al. 1987, Olwin and Rapraeger 1992, Templeton and Hauschka 1992).

We independently evaluated rAAV6 transduction of myoblasts and myotubes *in vitro* utilizing an alkaline phosphatase (AP) reporter (**Fig. 4.1**). Serum and FGF-2 were withdrawn from proliferating myoblasts and rAAV6-CMV-AP ($3x10^9$ vector genomes per well in 1 ml of media) was added to the culture media. Cells were harvested 3 days post-transduction, and reporter expression and vector genomes (vg) were quantified via a chemiluminescence assay (**Fig. 4.1a**) and by quantitative PCR (**Fig. 4.1b**], respectively. An additional cohort of myoblasts was incubated with vector for a shorter duration of time (1 hr), at which point the media was exchanged and maintained until the 3 day endpoint. Interestingly, shortened exposure to vector was not associated with a statistically significant decrease in transduction, suggesting that the majority of transduction-competent vector particles are taken up by the cells within the first hour in culture. This is consistent with previous reports demonstrating rapid uptake of rAAV

particles in cultured fibroblasts (Bantel-Schaal, Hub et al. 2002, Bantel-Schaal, Braspenning-Wesch et al. 2009).

A similar transduction protocol was evaluated in maturing myotubes. Differentiation was induced via withdrawal of serum and FGF-2, and cells were transduced at either 5 or 10 days post-induction. As described above, cells were harvested for analysis 3 days post-transduction. We observed a significant increase in transduction of differentiating MM14 myotubes in comparison to myoblasts. In contrast, there was no significant difference in transduction between cultures transduced at 5 days versus 10 days post-differentiation. This implies that modulation of transduction efficiency occurs early in the differentiation process, prior to 5 days post-induction.

Vector-mediated reporter expression is diminished under conditions of myoblast proliferation and turnover.

rAAV vectors integrate only at very low frequencies (McCarty, Young et al. 2004, Inagaki, Lewis et al. 2007, Inagaki, Piao et al. 2008), and thus, vector-mediated transgene expression is predicted to diminish over time under conditions of ongoing cellular proliferation and turnover. We modeled this condition via serial dilution and passaging of transduced myogenic C2C12 cells (Yaffe and Saxel 1977). Cells were transduced with rAAV6-CMV-*lac*Z at an MOI of 100. This MOI was sufficient to induce visually detectable levels of β-Galactosidase (βGal) expression in nearly all cells, whereas an MOI of 50 resulted in approximately 60% of cells staining positively for βGal (data not shown). Transduced cells were passaged and diluted 1:10 every 2 days (90% of the population was discarded with each passage) (**Fig. 4.2**). Prior to each passage, a

subset of wells was stained for βGal expression, and the total number of positive cells was quantified. We observed an approximately 90% decrease in the total number of positive cells following a single cycle of proliferation and dilution. This loss was less dramatic at subsequent passages, but the total number of positive cells continued to decline. After four passages, only a few cells stained positively for βGal expression. These results confirm that rAAV6-mediated transgene expression from non-integrated vector genomes is negatively impacted by cellular turnover in cultured myoblasts. It is possible that the remaining βGal expression was from integration into these few cells. This could have been determined by further passages of the transduced cell culture, allowing cells with integrated transgenes to increase in number.

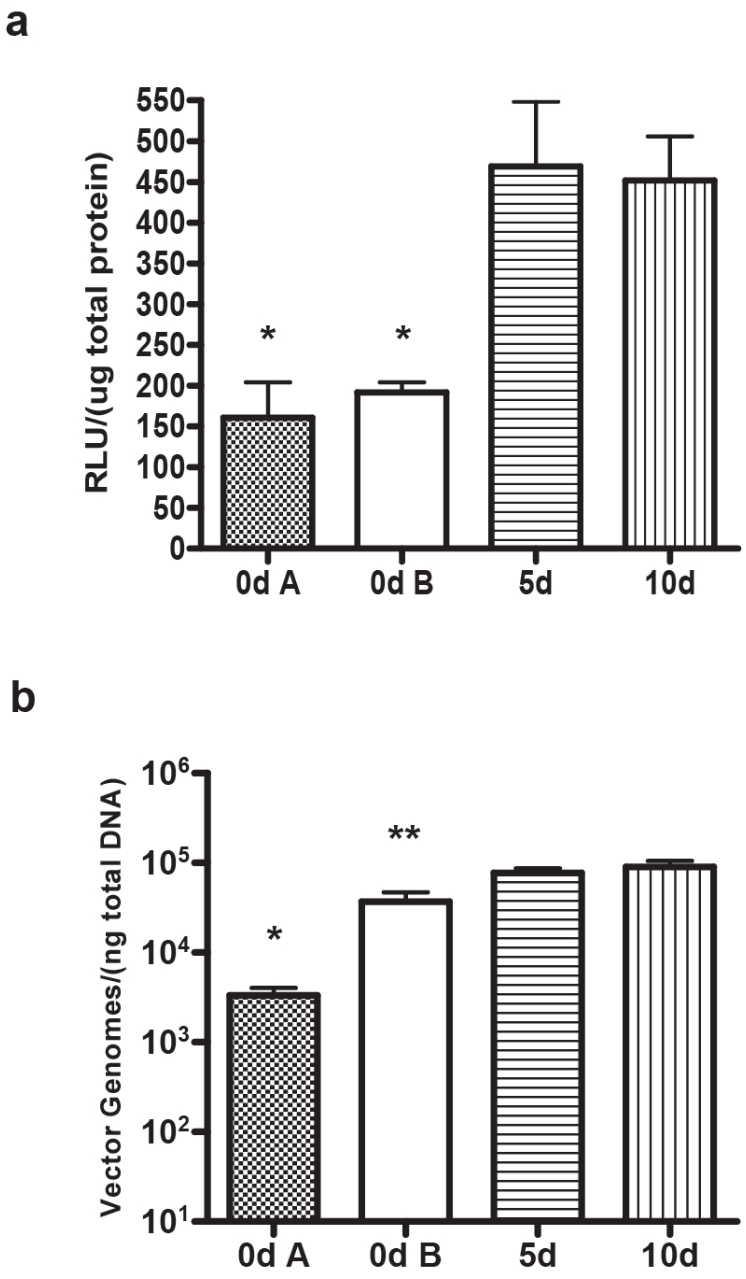

Figure 4.1 rAAV6 transduction of myotubes is more efficient than myoblast transduction *in vitro*. MM14 myoblasts or myotubes were transduced with rAAV6-CMV-AP, and both AP expression **(a)** and vector genome number **(b)** were quantified. Myoblasts were incubated with vector for either 1 hr *(0d A)* or 3 days *(0d B)* subsequent to withdrawal of FGF-2 and serum to halt proliferation. Shortened exposure to vector did not result in a statistically significant decrease in transduction. Myofibers were transduced at either 5 days *(5d)* or 10 days *(10d)* post-differentiation. Myofiber transduction at either timepoint was significantly increased compared to myoblasts. * indicates significantly different compared to 5d and 10d cohorts. ** indicates significantly different in comparison to 10d cohort only. $P<0.05$, one-way ANOVA with Tukey post-test analysis.

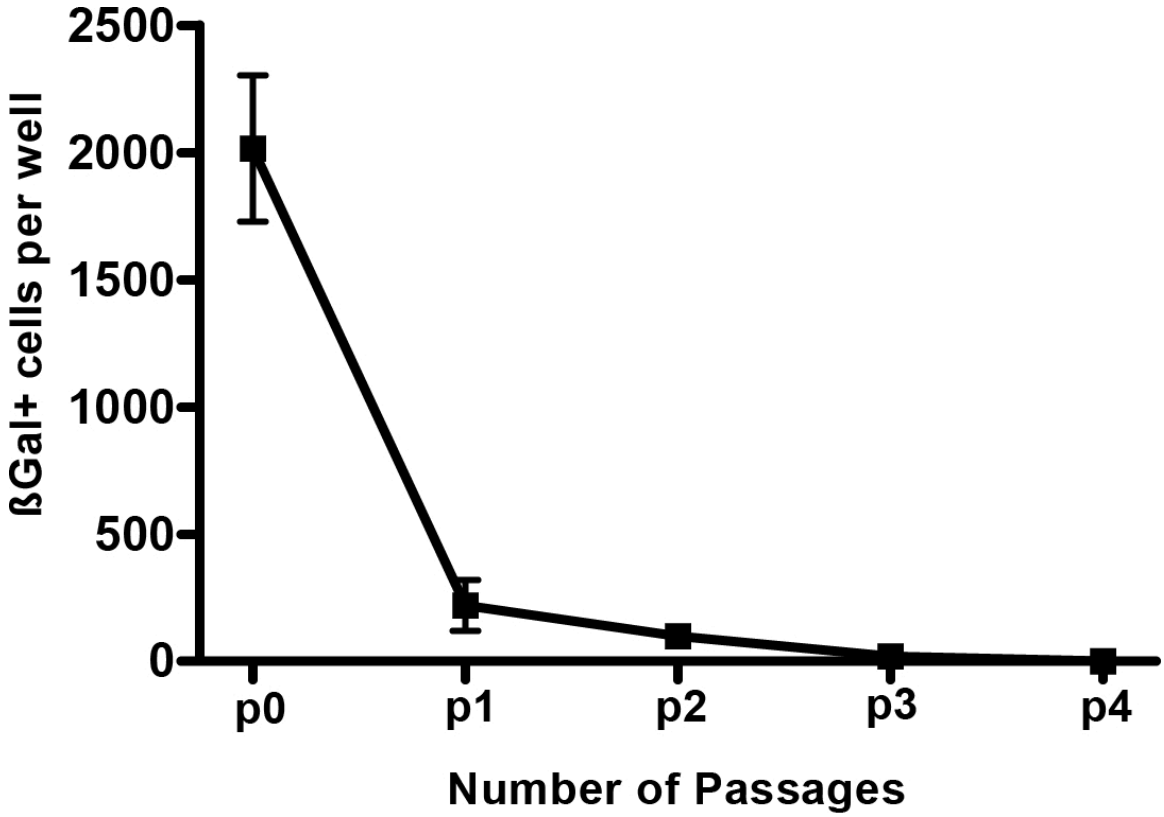

Figure 4.2 Vector-mediated reporter expression is diminished under conditions of high myoblast proliferation and turnover. C2C12 myoblasts were transduced with rAAV6-CMV-βGal at an MOI of 100. Cells were serially passaged every 2 days and diluted 1:10 with each passage. 90% of the population was discarded with each passage. At each passage, a cohort of wells (n=2) was stained for βGal expression and the number of positive cells was quantified. Myoblasts gradually lost reporter expression over multiple cycles of dilution and proliferation. After 4 passages, the number of positive cells was reduced to approximately 2 per well.

rAAV6 transduction of single-fiber cultures reveals a marked preference for multinucleated muscle cells and mature myofibers.

To investigate transduction of MPCs and myofibers, we isolated single, intact myofibers from both *wt* and *mdx* mouse muscles (**Fig. 4.3**). Fibers were cultured to stimulate proliferation and differentiation of resident satellite cells on the isolated fibers, and cultures were maintained briefly in proliferation media prior to induction of differentiation, as previously described (Huard, Feero et al. 1996, Shefer and Yablonka-Reuveni 2005). Single myofibers cultured in this manner produce a mixed population of mononuclear activated satellite cells and myoblasts and multinucleated myotubes. Thus, single fiber cultures can be utilized to investigate the *in vitro* tropism of rAAV6 in a mixed population of MPCs and myofibers.

Fiber cultures were transduced with rAAV6-CMV-mCherry following either 7 or 9 days in culture and fixed for immunofluorescence staining 48 hours post-transduction. The total number of transduced muscle cells was quantified and subdivided into mononuclear and multinuclear components. Positivity was defined as co-expression of mCherry and the muscle-specific marker, desmin. Both transduction timepoints revealed a significant bias towards transduction of multinucleated muscle cells (**Fig. 4.3**). Similar trends were observed in both *mdx* and *wt* fiber cultures, indicating that transduction bias towards multinucleated muscle cells is independent of dystrophin expression.

Transduction efficiency is reduced during the proliferative phase of skeletal muscle regeneration.

In skeletal muscle, the regenerative response to injury is characterized by an inflammatory response and satellite cell activation, followed by a rapid increase in myoblast proliferation (Brunelli and Rovere-Querini 2008, Villalta, Nguyen et al. 2009, Wallace and McNally 2009, Ten Broek, Grefte et al. , Tidball and Villalta). Within a few days post-injury, MPCs fuse to regenerate damaged myofibers, and normal muscle architecture is gradually restored during the process of fiber maturation. Thus, the early stages of muscle regeneration present an opportunity to evaluate rAAV6 transduction of skeletal muscle during a period of high myoblast proliferation and myofiber formation *in vivo*.

We employed a notexin (NTX)-induced injury model, which was previously shown to destroy the majority of muscle fibers and induce generation of fibers *de novo* in the extensor digitorus longus (EDL) muscle of the hindlimb (Lefaucheur and Sebille 1995, Plant, Colarossi et al. 2006) and evaluated the efficiency of muscle transduction following sequential, timed injections of rAAV6 at different stages post NTX treatment. (**Fig. 4.4**). Mice received an IM injection of NTX into EDL, followed by IM injection of rAAV6-CMV-AP (10^{10} vg) at either 2, 3, 4, or 5 days post-injury. Muscles were harvested at 2 wks post-injection of rAAV6 and stained for AP expression (**Fig. 4.4a**). In addition, vector genomes were quantified via QPCR (**Fig. 4.4b**). We observed a progressive increase in transduction efficiency as the interval between injury and AAV-injection increased. AAV injection two days post-injury resulted in minimal transduction

and a mosaic pattern of AP expression. In contrast, AAV injection four days post-injury resulted in an approximately 5-fold increase in transduction compared to the initial 2d timepoint, and a more even distribution of AP expression. This correlates with the timing of fusion of proliferating myoblasts and myofiber formation, which have been shown to occur 3-4 days post-injury (Sharp, Kornegay et al. 1993, Lefaucheur and Sebille 1995, Plant, Colarossi et al. 2006). Transduction increased approximately 9-fold when the interval between injury and rAAV6 injection was increased to 5 days. These data are consistent with our *in vitro* results indicating that myofibers are more efficiently targeted than myoblasts, and suggests that the rate of myoblast proliferation and myofiber formation may limit the efficiency of rAAV6 in regenerating muscle. Once the myofibers were formed, no significant change in the transduction efficiency was observed when compared to uninjured muscles, suggesting that the process of fiber maturation does not adversely affect transduction efficiency.

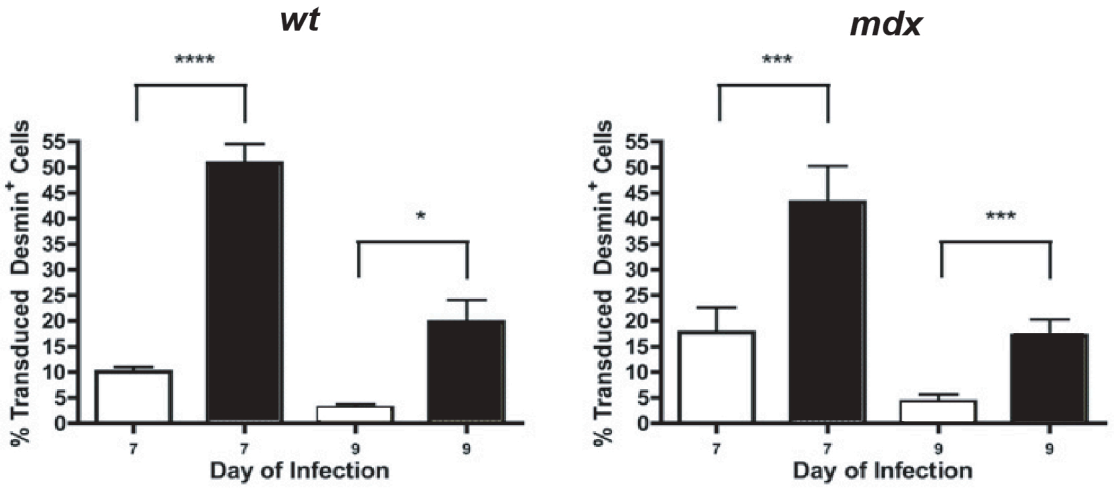

Figure 4.3 *In vitro* rAAV6-mediated transduction of single myofiber cultures reveals a marked preference for multinucleated muscle cells. Single myofibers from both *wt (left)* or *mdx (right)* mice were isolated and cultured to establish a mixed population of mononuclear muscle progenitor cells (white bars) and multinuclear myotubes (black bars). Cultures were transduced with rAAV6-mCherry on either day 7 or day 9. Cells were stained for desmin expression 2 days post-transduction, and the number of cells co-expressing both desmin and mCherry was quantified**.** Multinucleated muscle cells were preferentially targeted at both transduction timepoints. In cultures transduced on day 9, the total number of desmin-positive cells was reduced, but the proportion of myofiber transduction increased. * $p<0.05$ ***$p<0.01$ ****$p<0.001$, student t-test.

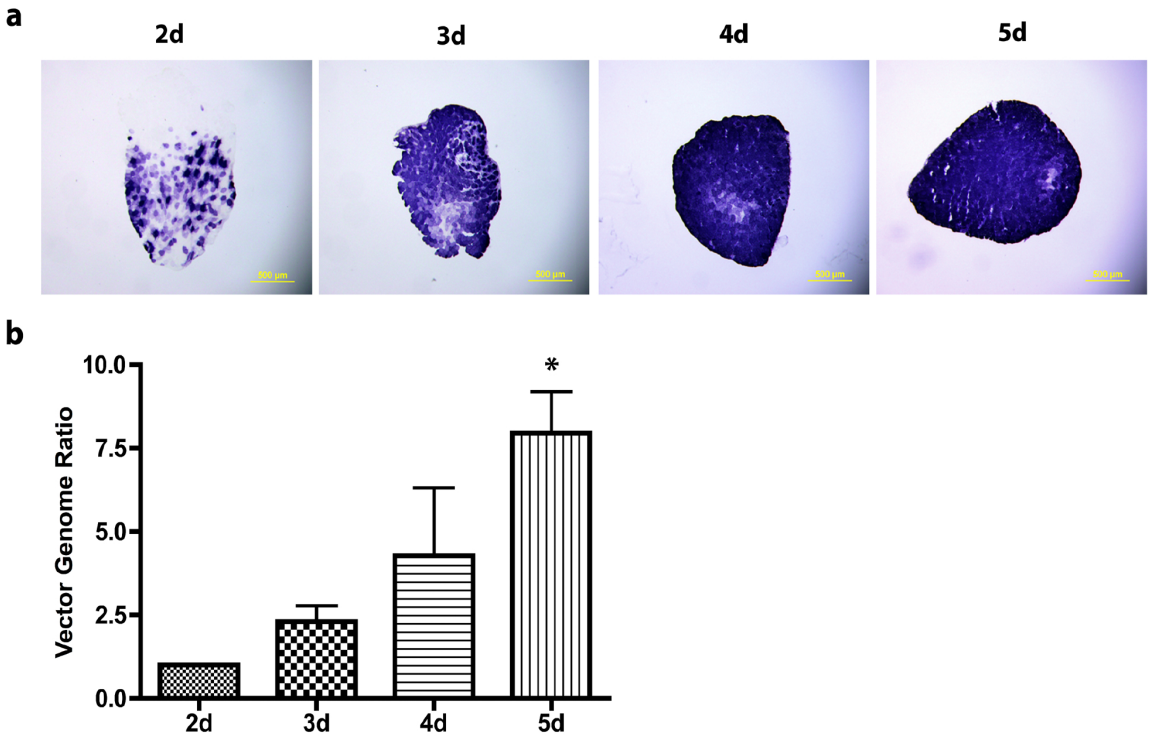

Figure 4.4 rAAV6 transduction efficiency is reduced during the early proliferative and inflammatory phase of muscle regeneration. Mice (N=3) received an IM injection of notexin in the EDL muscle, followed by rAAV6-CMV-AP injection at 2, 3, 4, or 5 days post-injury. Muscles were collected 2 wks following rAAV6 injection and evaluated for AP expression **(a)** and vector genomes **(b)**. We observed a trend towards increased transduction efficiency that correlated with an increase in the interval between injury and rAAV6 injection. Vector genome ratio is reported relative to copy number at the earliest injection timepoint (2 days). *P<0.05 versus vector genome ratio at 2 days.

rAAV6 does not effectively transduce satellite cells in vivo.

We employed three strategies to evaluate transduction of skeletal muscle satellite cells *in vivo*. Our initial experiment was performed using both wt and *mdx* nestin-eGFP mice. These latter mice express an eGFP reporter under control of the nestin promoter, which is active in quiescent satellite cells (Day, Shefer et al. 2007, Yablonka-Reuveni, Day et al. 2008). Thus, satellite cells in nestin-eGFP mice can be readily identified by fluorescence microscopy. Mice received bilateral IM injections of rAAV6-CMV-mCherry (10^{10} vg) in the EDL muscle. Approximately 50 fibers were isolated from both *wt* and *mdx* muscles 4 wks post-injection and cultured as described above. Of these, approximately 80% were positive for mCherry. Co-expression of eGFP and mCherry was not observed in any satellite cell (e.g., **Fig. 4.5a**). This observation held true irrespective of whether the originating myofiber was positive or negative for mCherry expression. Instead, eGFP-positive/mCherry-negative satellite cells were observed to migrate from isolated fibers and initiate proliferation and differentiation (**Figs. 4.5b,c**). None of the derived mononuclear cells and myotubes became positive for mCherry expression, with the exception of myotubes that fused with the originally plated mCherry positive fiber (**Fig. 4.5c**, inset].

To expand our analysis to a larger population of satellite cells and other MPCs, we injected the tibialis anterior (TA) of *wt* mice with rAAV6-CMV-eGFP (10^{11} vg) and isolated MPCs and mononuclear cells from the entire muscle at 4 wks post-injection. Approximately $3x10^5$ mononuclear cells were isolated and sorted for GFP expression via FACS (**Fig. 4.6a**). Of these, approximately 13% were positive for eGFP expression (**Fig.**

4.6b). The entire eGFP-positive population was plated under myogenic differentiation conditions, and cultures were tracked for four days. A total of four myogenic colonies were identified within the sorted population, but all four of these colonies originated from contaminating eGFP-negative cells. In parallel, approximately $4x10^5$ cells were directly plated without sorting. The unsorted population of cells generated a large number of myogenic colonies, but none of these contained eGFP-positive cells.

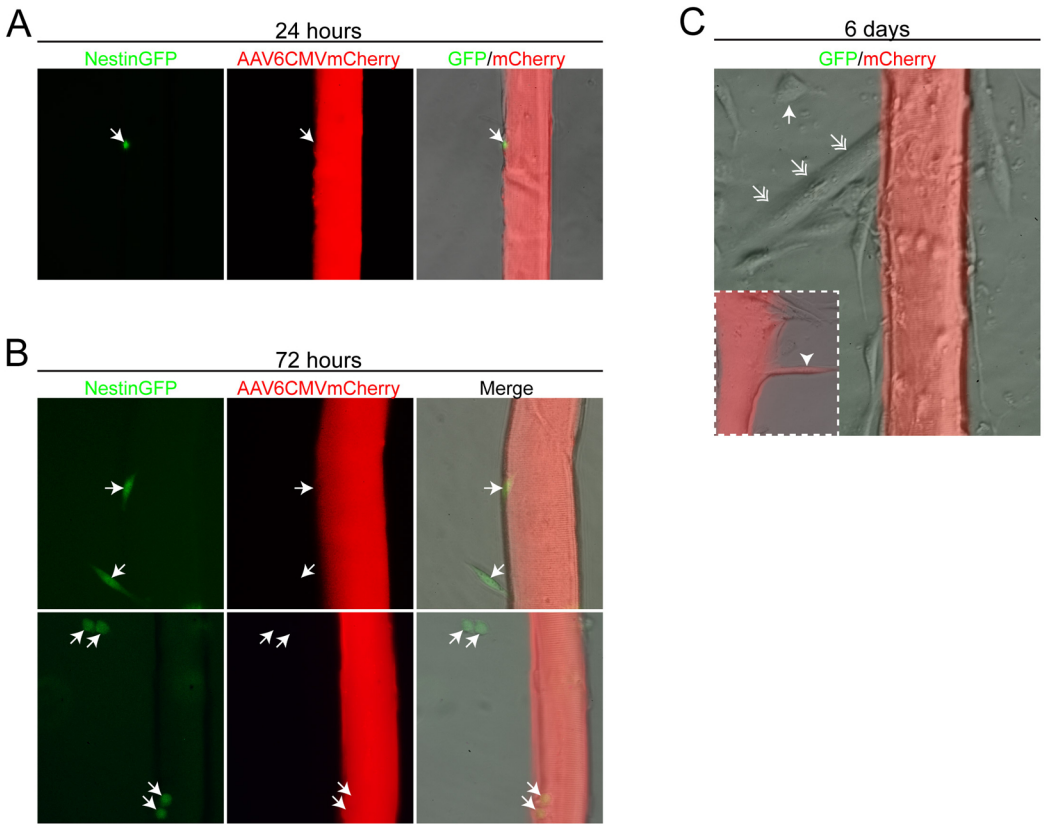

Figure 4.5 Single fiber cultures from nestin-GFP mice injected with rAAV6. Mice received an IM injection of rAAV6-CMV-mCherry in the EDL muscle. Fibers were isolated from injected muscles 4 wks post-transduction and cultured for up to 6 days. At 24 hours Nestin/eGFP-positive satellite cells could be visualized on myofibers, but no cells stained for both eGFP and mCherry (a). eGFP-positive, mCherry-negative satellite cells were tracked as they migrated from the parent fibers and established myogenic colonies **(b)**. Satellite cells remained negative for mCherry expression. By 6 days numerous myotubes had formed in the cultures from the proliferating and terminally differentiating myoblasts (c), but the only eGFP-positive myotubes observed were those that had fused with the original myofiber (c-inset).

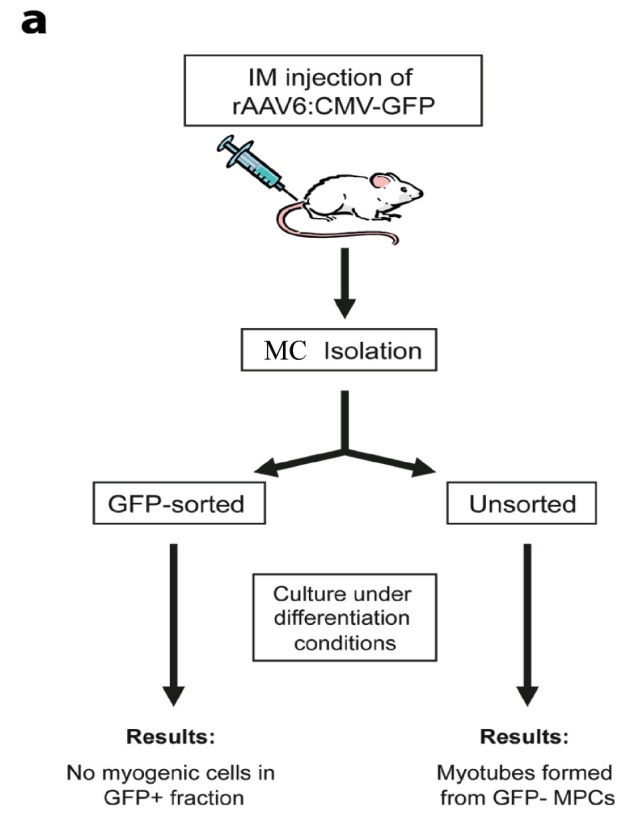

Figure 4.6 FACS analysis of myoblasts isolated from rAAV6-injected muscle. Mice received bilateral IM injections of rAAV6-CMV-GFP in the TA muscle. Myoblasts and other mononuclear cells were isolated and treated as indicated in the flowchart **(a)**. 13% of mononuclear cells were GFP-positive **(b)**, but no myogenic colonies were found to contain GFP-positive cells.

It is unclear if satellite cells and MPCs didn't express eGFP because they were not transduced after injection or if the episomal vector genome was lost through proliferation prior to differentiation in culture. To address this question, we sought to monitor vector transduction and quantify vector genomes directly in satellite cells. We examined cross-sections from rAAV6-injected *wt* and *mdx* muscles for rAAV transduction. As above, mice received bilateral IM injections of rAAV6-CMV-GFP (10^{11} vg) in the TA. Muscles were harvested 4 weeks post-injection and either used for satellite cell isolation or fixed, sectioned, and stained for Pax7 (Kuang, Gillespie et al. 2008, Yablonka-Reuveni, Day et al. 2008), which is expressed in quiescent satellite cells (**Fig. 4.7a**). Consistent with our previous results, no Pax7-positive cells were found to co-express eGFP in either wt (**Fig. 4.7a**) or *mdx* (not shown) muscles (in approximately 150 satellite cells per cohort). Taken together, these results reveal a lack of satellite cell transduction *in vivo* and indicate that rAAV6 preferentially targets myofibers in adult skeletal muscle.

To determine the presence of vector genomes in satellite cells *in vivo*, TA and EDL muscles of both *wt* and *mdx* mice were injected with rAAV6-CMV-mCherry. At 4 weeks post-injection, injected muscles were harvested and directly imaged for mCherry fluorescence prior to satellite cell isoloation by MACS (**Figs. 4.7b,c**) (Brack, Conboy et al. 2008). DNA extracted from isolated satellite cells as well as whole muscle was measured by quantitative PCR. No significant level of rAAV DNA was detected in satellite cells from either strain. However, vector genomes were detected in DNA extracted from whole injected EDL muscles (**Fig. 4.7c**). Together, these data indicated that rAAV vector genomes do not target satellite cells despite the widespread transduction apparent upon gross muscle dissection (**Fig. 4.7b**).

In addition to rAAV6, vectors from AAV8 and AAV9 have emerged as promising for muscle transduction (Wang, Zhu et al. 2005, Inagaki, Fuess et al. 2006, Zincarelli, Soltys et al. 2008). To examine whether vectors psueotyped with AAV8 or AAV9 capsids could target satellite cells we injected rAAV6, 8, or 9 vectors expressing CMV-eGFP into TA muscles of wild type mice. In other studies we have observed that rAAV6 gives higher levels of transduction when intramuscularly injected into mouse muscles (see Chapters 4 and 6). Also, since we already established that rAAV failed to transduce satellite cells, we injected approximately 40-fold higher levels of rAAV8 and rAAV9 than rAAV6. All three vector types efficiently transduced myofibers, as expected (**Fig. 4.8**). By co-staining with Pax7 and laminin we were able to identify satellite cells in each cohort. As before, we saw no Pax7-positive/eGFP-positive cells when using rAAV6 nor did we observe positive satellite cells with rAAV9 (**Fig. 4.8**). With rAAV8 we did observe rare Pax7-positive/eGFP-positive satellite cells, but they represented less then %5 of the observed satellite cells in the injected muscle. Interestingly, either due to injection site trauma or perhaps toxicity of eGFP expression, we observed areas of regenerating myofibers in rAAV6-injected muscles. In these regions we found rare Pax7-negative/eGFP-positive cells between the basal lamina and the sarcolemma, suggesting that they might be activated satellite cells.

Finally, since therapeutic approaches for muscular dystrophy using rAAV vectors will likely rely upon systemic delivery protocols to target muscles bodywide (Gregorevic, Blankinship et al. 2004) we asked whether systemically injected mice would allow for satellite cell targeting. For this study rAAV vectors expressing CMV-eGFP were retro-

orbitally injected into wild type mice. However, as with the intramuscular injections, no Pax7-positive/eGFP-positive satellite cells were observed (**Fig. 4.9**).

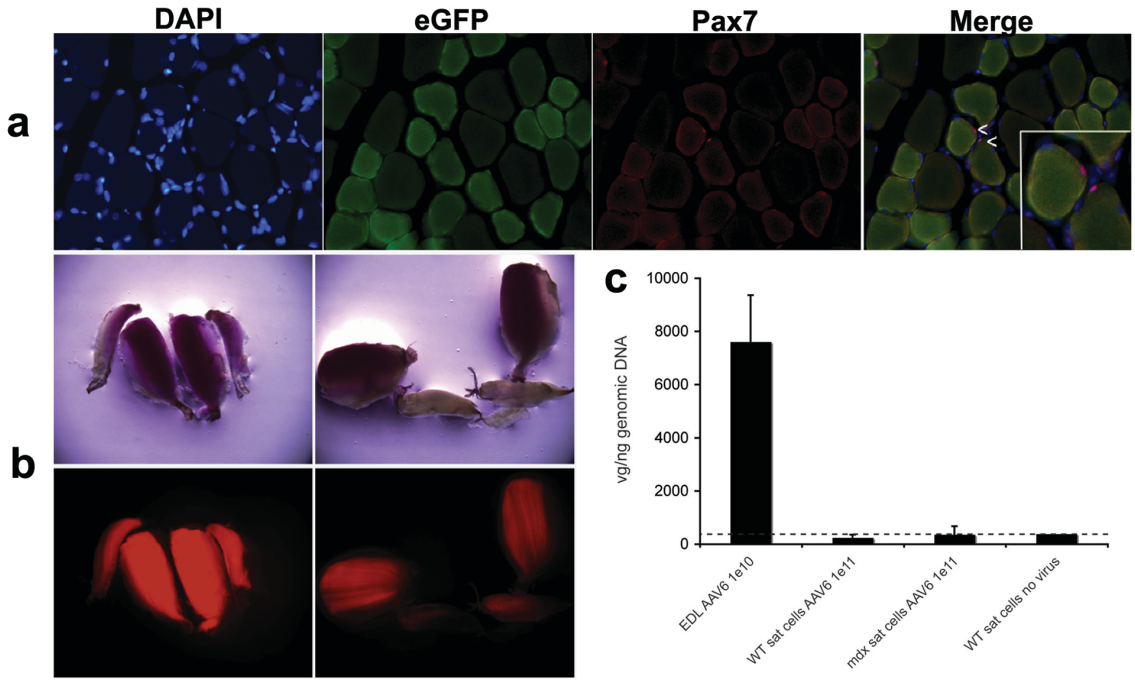

Figure 4.7 Analysis of satellite cell transduction in muscles injected with rAAV6. (**a**) Cross-sections of wild type muscles injected with rAAV6-CMV-eGFP. Injected muscles were collected 4 weeks post-injection and stained for Pax7 and DAPI, then visualized under a fluorescence microscope. eGFP expression was not observed in any Pax7-positive cells. (**b,c**) Both wild type and *mdx* mice were injected with rAAV6-CMV-mCherry into the TA (10^{11} vg) and EDL (10^{10} vg) muscles and harvested 4 weeks post-injection. The high level of transduction was evident upon harvesting the muscles (**b**) (images taken at 7x magnification). No vector genomes were detected among satellite cells isolated from TA muscles of either mouse strain. However, vector genomes were detected in DNA extracted from whole, injected EDL muscles (**c**).

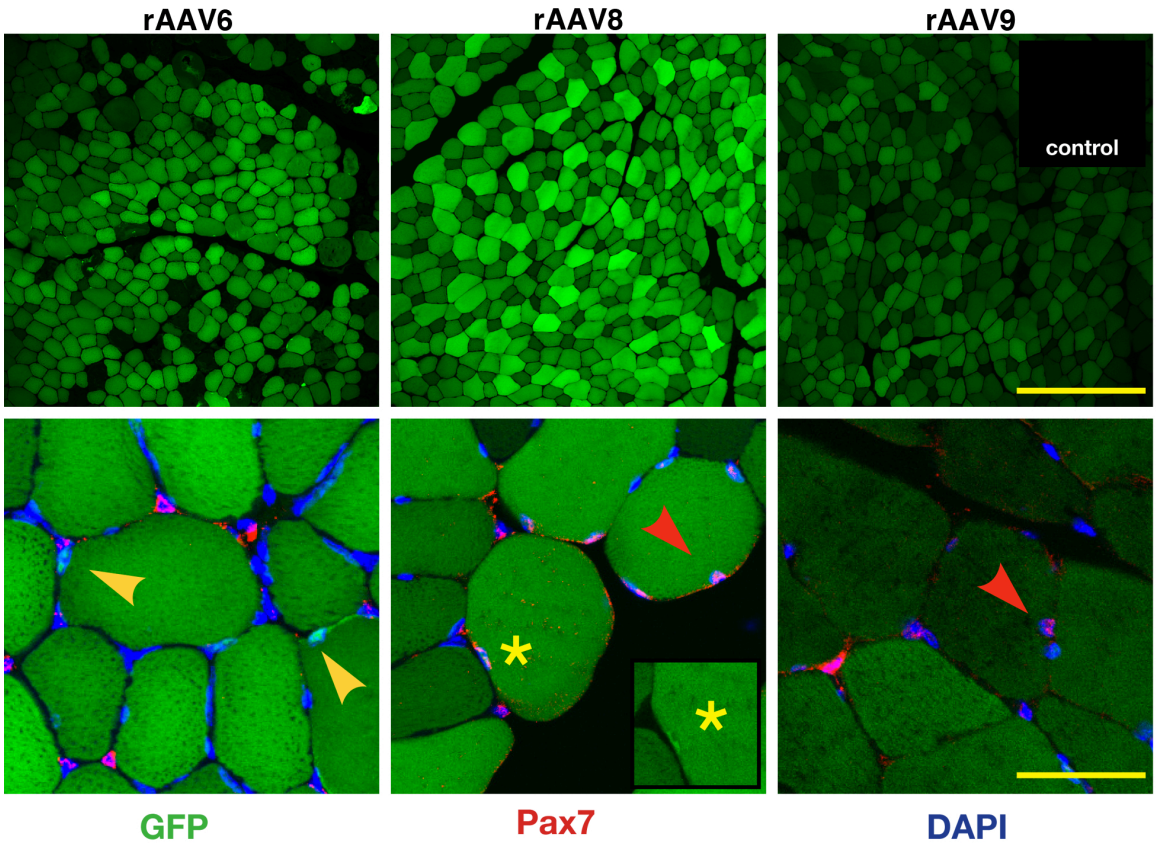

Figure 4.8 Comparison of rAAV6, 8 and 9 for satellite cell transduction. Eight-week-old C57Bl/6 mice were injected intramuscularly into the TA muscle with rAAV-CMV-eGFP vectors pseudotyped with either serotype 6 (left panels), 8 (middle panels) or 9 (right panels) capsids. After 2 weeks, muscles were harvested and cyrosections were imaged for eGFP (top panels). The inset shows background eGFP fluorescence in uninjected muscles. Cyrosections were also stained with DAPI, and immunostained with antibodies against laminin (not shown) and Pax7. Vector doses were adjusted to generate similar levels of transduction (rAAV6: $5x10^{10}$ vg; rAAV8 and 9: $2x10^{12}$ vg; n = 4 muscle per serotype). As in the studies in Figure 6, no Pax7-positive/eGFP-positive cells were observed following rAAV6 injection. However, a few rare instances were observed of cells between the basal lamina and the sarcolemma that were Pax-negative/eGFP-positive (bottom left panel, arrowheads). As with rAAV6, no Pax7-positive/eGFP-positive cells were observed following rAAV9 injection (e.g., bottom right panel, arrowhead points to a Pax7-positive satellite cell). In contrast, following injection of rAAV8 several Pax7-positive/eGFP-positive cells were observed, but these represented less than 5% of the total Pax7-positive cells scored (bottom of middle panel, arrowhead; the positive satellite cell adjacent to the myofiber with the asterisk is shown in the insert minus the red [Pax7] fluorescence). Scale bars: 150 μm top; 30 μm bottom.

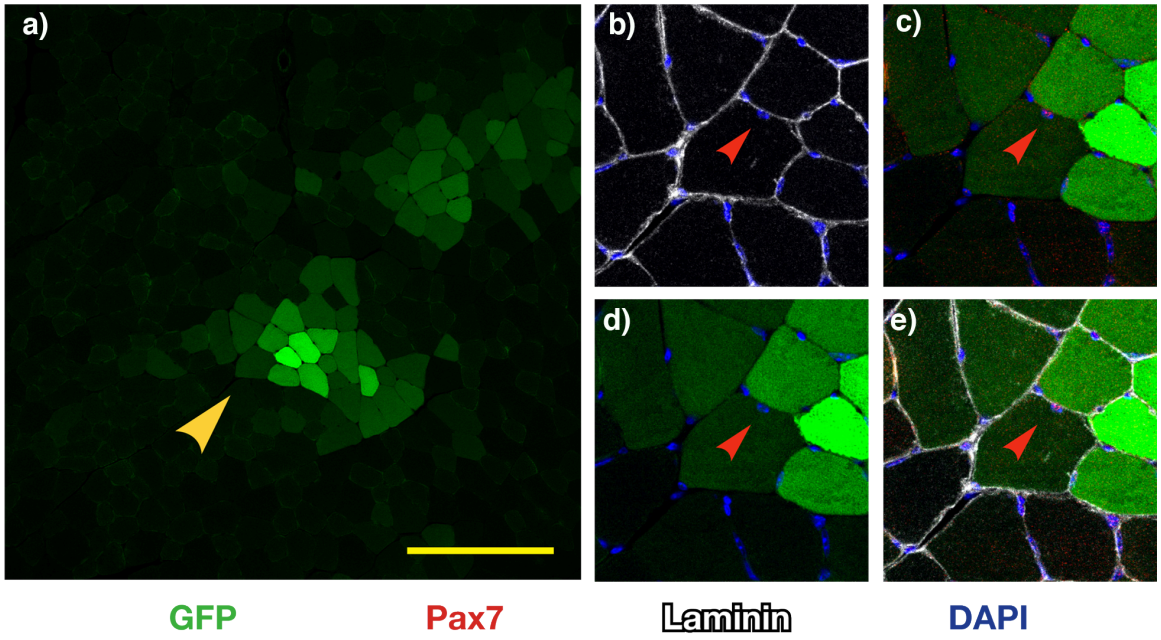

Figure 4.9 Analysis of satellite cell transduction following systemic injection of rAAV6. Four-week-old C57Bl/6 mice were retro-orbitally injected with $4x10^{12}$ vg of rAAV6-CMV-eGFP and analyzed 4 weeks later (n = 4 mice). **(a)** eGFP fluorescence in a cryosection of an isolated TA muscle showing transduced myofibers. **(b-e)** Cryosections were stained with DAPI to visualize nuclei, and immunostained with laminin and Pax7. An example of a Pax7-positive/eGFP-negative satellite cell is shown. Laminin and DAPI imaging **(b)**; Pax7, DAPI, and eGFP merged imaging **(c)**; GFP and DAPI imaging **(d)**; merge **(e)**. The arrowhead points to a Pax7-positive/eGFP-negative satellite cell. No Pax7-positive/eGFP-positive cells were observed. Scale bars: 150 μm.

Discussion

Dystrophic muscle is characterized by a chronic state of degenerative turnover. Cycles of degeneration and regeneration lead to a heterogeneous population of MPCs and regenerating myofibers in different stages of maturation. This diverse population represents a potential target for gene replacement strategies. rAAV6 is known to transduce skeletal muscle with high efficiency (Blankinship, Gregorevic et al. 2004, Gregorevic, Blankinship et al. 2004, Zincarelli, Soltys et al. 2008), but transduction of MPCs and developing myofibers is less well-characterized. As rAAV6 is a candidate for treatment of genetic disorders of muscle, it is important that we possess a thorough knowledge of its transduction profile in myogenic cells. Thus, we evaluated both *in vitro* and *in vivo* rAAV6-mediated transduction of satellite cells, myoblasts, and developing myotubes and myofibers.

Our results demonstrate that rAAV6 preferentially targets myofibers and transduces myoblasts with reduced efficiency. This trend was apparent in both MM14 cells (**Fig. 1**) and primary myogenic cultures (**Fig. 4.3**). In a mixed population of mononuclear MPCs and developing myotubes, we observed a significant bias towards transduction of multinucleated muscle cells (**Fig. 4.3**). Myoblast differentiation and myotube formation are complex processes governed by a number of transcriptional elements and regulatory factors (Ten Broek, Grefte et al.). Myoblasts undergo extensive remodeling and reorganization as they fuse to form myotubes, and differentiation is accompanied by significant changes in extracellular matrix (ECM) composition and expression of cell-surface receptors. While the mechanisms regulating enhanced myofiber transduction remain unclear, these changes have the potential to influence

tropism of rAAV6. We have previously demonstrated that heparin-binding capability in rAAV6 positively influences skeletal muscle transduction (Arnett, Beutler et al. 2013), indicating that heparin interactions could differentially impact transduction efficiencies.

We also evaluated rAAV6 transduction efficiency in regenerating muscle (**Fig. 4.4**). Though environmental factors *in vivo* are significantly more complex than *in vitro*, the results were generally consistent with our earlier findings. We observed a significant increase in transduction efficiency as the interval between notexin-injury and rAAV6-injection was increased. Notexin induces rapid necrosis of muscle fibers, but does not disrupt the basal lamina or promote satellite cell necrosis (Plant, Colarossi et al. 2006).

Reduced transduction efficiency and clearance of vector at earlier rAAV6-injection timepoints may be influenced by a number of factors. Within 3-4 days post-injury, myoblasts begin to fuse and initiate formation of new myofibers (Lefaucheur and Sebille 1995, Wallace and McNally 2009). Thus, the increase in transduction may simply reflect an increase in the percentage of available myofibers, which are more efficiently targeted by rAAV6. We did detect rare Pax7-negative cells under the basal lamina that had been transduced by rAAV6 vectors in some intramuscular injections studies, suggesting that activated satellite cells are able to be transduced *in vivo* following injury (**Fig. 4.8**). However, rapid proliferation of satellite cells and myoblasts during the initial injury response may reduce transduction efficiency. As shown in **Figure 4.2**, proliferation and turnover negatively impacts transgene expression. Thus, it is conceivable that a substantial number of myoblasts transduced within the first few days of the injury response lose transgene expression during proliferation. Additionally, the inflammatory response to injury may increase clearance of vector.

Together our results indicated that rAAV6 does not effectively transduce satellite cells *in vivo*. All of the detection methods employed failed to obtain any evidence of satellite cell transduction (**Figs. 4.5-4.9**). It is unclear why quiescent satellite cells are not targeted by rAAV6. Skeletal muscle satellite cells reside in a quiescent state beneath the basal lamina until activated in response to muscle injury. It is possible that either the quiescent state of satellite cells or intrinsic features of the satellite cell niche limit transduction.

Our survey of rAAV6-injected muscles was extensive, but the possibility exists that satellite cells were transduced at only a very low frequency, and were thus undetected by our methodologies. Nevertheless, a low level of satellite cell transduction is unlikely to be therapeutically relevant due to significant dilution and loss of vector genomes during the proliferative response. Since vector genomes remain primarily in an episomal state (Duan, Sharma et al. 1998, McCarty, Young et al. 2004), persistence of viral DNA and transgene expression is limited under conditions of high cellular turnover. Our analysis of reporter gene expression in rapidly proliferating C2C12 cells support this hypothesis (**Fig. 4.2**). In addition, loss of vector genomes and transgene expression has been demonstrated in a model of partial hepatectomy (Nakai, Yant et al. 2001). Nakai *et al.,* evaluated rAAV2 injection via portal vein, followed by partial hepatectomy. They observed a 92% reduction in vector genomes following liver regeneration. In contrast, transgene expression via a stably-integrated construct was unaffected by partial hepatectomy. Thus, as a non-integrating vector, the persistence of rAAV *in vivo* is limited during tissue regeneration.

Our results also do not rule out the possibility that rAAV vectors may enter satellite cells and possibly express transiently before being lost. Such loss of vector would need to occur rapidly, as we did not detect vector genomes in freshly isolated satellite cells harvested 4 weeks after injection (**Fig. 4.6**), nor did we detect significant numbers of Pax7-posititve satellite cells expressing vector-delivered transgene at 2 weeks post-injection (**Fig. 4.8**). If even low levels of transgene expression could be obtained for short interval then it genome editing strategies, such as Cas9/CRISPR or AAV-mediated homologous recombination, could be utilized to permanently modify the genome of muscle stem cells prior to vector loss(Chamberlain, Schwarze et al. 2004, Hsu, Lander et al. 2014).

These data have implications for the design of future therapies, as a failure to deliver therapeutic genes to muscle stem cells indicates that any subsequent cycle of myofiber degeneration and regeneration would result in a loss of AAV genomes. It is unknown what the half-life of a normal myofiber is in humans, but it seems reasonable to assume that such cells will display a low rate of turnover during normal activity. These results therefore suggest that re-administration of vector will likely be necessary to maintain persistent transgene expression in skeletal muscles of dystrophic patients. However, the use of therapeutically protective constructs and other treatment strategies that reduce the rate of myofiber turnover should effectively minimize the required frequency of vector re-administration. Moreover, these results emphasize a niche for integrating vectors and cell-based therapies, and predict significant benefit from a combined therapeutic approach.

Materials and Methods

Tissue culture.

MM14 cells and C2C12 cells were cultured as previously described (Lim and Hauschka 1984, Olwin and Hauschka 1988). Cells were maintained at 37ºC in an atmosphere of 5% CO_2. C2C12 cells were transduced with rAAV6-CMV-βGal and all timepoints were run in duplicate. MM14 cells were plated at $5x10^4$ cells per well on 12-well plates and transduced with rAAV6-CMV-AP ($3x10^9$ vg per well) either 0, 5, or 10 days following induction of differentiation. 12 wells were transduced per timepoint, and cells were harvested 3 days post-transduction for quantification of protein expression and vector genome copy number. 6 of the 12 wells were independently analyzed for AP expression. For vector genome quantification, lysates from wells were combined in sets of two, for a total of N=3 samples per timepoint. Experiments were performed in triplicate.

Primary myoblasts were isolated, sorted, and cultured as previously described (Li, Kimura et al. 2006, Kimura, Han et al. 2008). Briefly, TA muscles were digested in 0.2% collagenase II (Sigma-Aldrich, St. Louis, MO) and filtered through 70 μm and then 40 μm filters (BD, San Diego, CA). Mononuclear cells were cultured on gelatin-coated plates with F10C media (Invitrogen, Carlsbad, CA) in the absence of FGF-2, to promote differentiation and myotube formation. Cultures were maintained for 4 days and GFP-expressing cells were tracked.

EDL myofibers were isolated and cultured as described (Rosenblatt, Lunt et al. 1995, Shefer and Yablonka-Reuveni 2005). The first day of fiber plating was designated as Day 1. Three days after plating, cultures were switched to proliferation media for an

additional three days. On Day 7, cultures were switched to differentiation media. On the day that cultures were transduced, each well was administered 10^{11} vector genomes of AAV6-CMV-mCherry mixed into 50 μL of differentiation media. Vector was removed and media was exchanged for fresh media 16 hrs post-transduction. Fibers were fixed 48 hrs post-transduction, as described (Shefer and Yablonka-Reuveni 2005).

Animal experiments.

Animal studies were performed in accordance with the guidelines set forth by the University of Washington IACUC. All mice were bred on the C57Bl/6 background, in the University of Washington specific pathogen free barrier facility. For satellite cell transduction experiments, animals received bilateral IM injections of either rAAV6-CMV-mCherry (10^{10} vg per injection) or rAAV6-CMV-eGFP (10^{11} per injection) into the EDL or TA, respectively. rAAV6-CMV-mCherry was delivered to *mdx*:*Nestin-eGFP* (N=2) and *wt*:*Nestin-eGFP* (N=2) mice (Day, Shefer et al. 2007), and rAAV6-CMV-eGFP was delivered to *wt* (N=4) and *mdx* (N=2) mice. At 4 wks post-injection, mice were euthanized according to approved protocol, and muscles were harvested for single fiber cultures, primary myoblast cultures, or immunofluorescent staining. For *in vitro* transduction assays, fibers were collected from untreated *wt* (N=2) or *mdx* (N=2) EDL muscles, and an additional two *wt* mice were used as untreated controls for primary myoblast cultures.

For regeneration studies, *wt* mice (N=3 muscles per timepoint) were given a IM injection of NTX (1 μg/ml [Sigma-Aldrich, St. Louis, MO]). Animals were then administered a second injection of rAAV6-CMV-AP (10^{10} vg per injection) on days 2, 3,

4, or 5 post-injury. Both injections were performed under isofluorane-induced anesthesia. At 2 wks following rAAV6 injection, animals were euthanized according to approved protocol, and muscles were harvested for analysis.

Vector production.

rAAV6 vectors were generated as previously described, (Gregorevic, Blankinship et al. 2004). An Amersham AKTA10 HPLC machine (Amersham, Piscataway, NJ) was used for affinity purification on a HiTrap heparin column (Amersham). Southern analysis was utilized to determine the number of genome-containing particles in the vector preparation.

Luminomety assay.

MM14 cells were harvested in 0.05% trypsin, 0.53 mM EDTA (Invitrogen, Carlsbad, CA). Cells were pelleted at approximately 2,000 x *g* and the supernatant was discarded. Cells were re-suspended in tissue lysis buffer (0.5% Sodium Deoxycholate, 50 mM Tris, 150 mM NaCL, 1% Triton, 0.8% protease inhibitor cocktail [Sigma-Aldrich, St. Louis, MO]). Protein was quantified via spectrophotometric absorption using Bradford reagent (Peirce, Rockford, IL). The extract was then analyzed for alkaline phosphatase expression using a commercial luminometry kit (Applied Biosystems, Carlsbad, CA).

Vector genome quantification.

Muscles were snap frozen in liquid nitrogen and then pulverized with a mortal and pestle. Pulverized muscle tissue was resuspended in tissue lysis buffer (0.5% NaDOC, 50 mM Tris, 150 mM NaCL, 1% Triton, 0.8% protease inhibitor cocktail [Sigma-Aldrich, St. Louis, MO]). MM14 cell lysates were prepared as described above. DNA was isolated from cell and tissue lysates using a DNeasy blood and tissue kit (Qiagen, Valencia, CA) according the manufacturer's guidelines. Genome quantification was performed utilizing a SV40 polyadenylation site-specific probe and quantitative PCR, as described (Gregorevic, Blankinship et al. 2004).

β-Galactosidase staining.

Media was aspirated and cells were fixed in 2% formaldehyde and 0.8% gluteraldehyde in PBS for 10 min at room temperature. Wells were then washed in cold PBS and incubated in staining solution (5 mM K-ferricyanide, 5 mM K-ferrocyanide, 2 mM $MgCl_2$ and 4% Xgal in PBS) at 37ºC overnight.

Alkaline phosphatase staining.

Muscle tissue was embedded in Tissue-Tek OCT medium (Sakura Finetek USA, Torrance, CA), rapidly frozen, and sectioned transversely. Sections were fixed with ice cold 4% paraformaldehyde (PFA), washed in cold phosphate-buffered saline (PBS), placed in 65º C phosphate-buffered saline for 90 minutes, rinsed in room temperature PBS, and washed in alkaline phosphatase buffer (0.1 M Tris-HCl, 0.1 M NaCl, 0.01 M

$MgCl_2$) for 10 minutes. Excess liquid was removed from the sections, and Sigma *FAST* BCIP/NBT substrate solution (Sigma, St Louis, MO) was applied to each section for 30 minutes at room temperature. Slides were rinsed in PBS, dehydrated in 70% ethanol (EtOH) for 5 minutes, 2X (95% EtOH for 2 minutes), 2X (100% EtOH for 2 minutes), 2X (xylene for 3 minutes), and cover-slipped with Permount mounting media (Fisher Scientific, Fair Lawn, NJ). Images were captured using QIcam or Olympus digital cameras and processed using Qcapture Pro (Qimaging, British Columbia, Canada).

Immunofluorescence staining.

Single fiber cultures were fixed for immunofluorescent staining as previously described (Shefer and Yablonka-Reuveni 2005). Cultures were stained with mouse anti-desmin primary antibody (clone D33, at 1:100 dilution [Dako, Carpenteria, CA]) with goat anti-mouse Alexa Fluor 488 (Invitrogen, Carlsbad, CA) used as the secondary.

Muscles injected with rAAV6-CMV-GFP were excised and prepared for immunofluorescence staining as previously written (Day, Shefer et al. 2007). Briefly, muscles were fixed in 4% PFA and 1% sucrose for 2 hrs, and were then successively immersed in 5%, 10%, and 20% sucrose for 30 min at each concentration. Muscles were then placed in 30% sucrose at 4°C overnight and frozen in OCT for sectioning. For Pax7 staining, muscle cross-sections were incubated in citrate buffer (10 mM citric acid monohydrate, 0.05% Tween 20, pH 6) for 15 min at 100ºC, washed with room temperature PBS, permeabilized for 10 min with 0.25% Triton-X in PBS, and washed again with room temperature PBS. Sections were then stained with a M.O.M. kit (Vector Labs, Burlingame, CA) following the manufacturer's instructions, using anti-Pax7

(Abcam, San Francisco, CA), 1:100 for 1 hr, Alexa Fluor 594-streptavidin (Invitrogen, Carlsbad, CA) and DAPI, 1:1000 for 45 min. Images in Figures 5 and 6 were captured using Olympus or QIcam digital cameras, respectively. Images in Figures 7 and 8 were captured using a Leica TCS SPV II laser scanning confocal microscope (Leica-microsystems, Buffalo Grove, IL).

Notes to Chapter

This chapter has been accepted for publication by *Molecular Therapy - Methods and Clinical Development*:

Arnett A*, Konieczny P*, Ramos JN*, Hall J, Odom G, Yablonka-Reuveni Z, Chamberlain JR and Chamberlain JS: Adeno-associated viral (AAV) vectors do not efficiently target muscle satellite cells. *Molecular Therapy- Methods and Clinical Development* (in press).

*These authors contributed equally to the work.

Contributions to the work as follows:

AA*: Design and implementation of experiments, analysis, including MM14 and C212 cell cultures, notexin-injury, myoblasts cell sorting, and Pax7 immunohistochemistry. Writing of the manuscript, with feedback and suggestions from JNR, PK and JSC.

PK*: Design and implementation of experiments and analysis, including EDL fiber cultures, notexin-injury, and quantitative-PCR experiments.

JNR*: Design and implementation of experiments and analysis, including EDL fiber cultures and transduction assays, rAAV-CMV-mCherry reporter administrations, quantitative-PCR, and satellite cell isolation experiments.

JH: Confocal microscopy imaging and analysis.

GO: Plasmid preparation for rAAV-CMV-eGFP vector production.

ZYR: Input on experimental design and providing *nestin-GFP* transgenic mice.

JRC: rAAV-CMV-eGFP vector administration.

Chapter 5

Comparison of rAAV6 and rAAV9 Transduction via Jugular Vein Delivery to Young Canines

Introduction

Duchenne muscular dystrophy (DMD) is a lethal X-linked muscle disorder characterized by progressive skeletal muscle wasting and weakness (Moser 1984), and is caused by mutations in the *DMD* gene resulting in the loss of functional dystrophin protein in muscle. There is no cure for DMD; current interventions slow progression of the disease and during later stages provide cardio-pulmonary support (Gomez-Merino and Bach 2002). Cardiac involvement is present in about 90% of DMD and the milder Becker muscular dystrophy (BMD) patients, being the cause of death in about 20% of the DMD and 50% of the BMD patients (Bushby, Muntoni et al. 2003, Finsterer and Stollberger 2003). Therefore, targeted treatment of the heart and diaphragm by correcting the primary defect - the absence of dystrophin in muscle cells - is critical for DMD therapies. Efficient gene transfer using recombinant adeno-associated viruses (rAAV) has been reported extensively in small animal models of muscular dystrophy (Harper, Hauser et al. 2002, Gregorevic, Blankinship et al. 2004, Wang, Zhu et al. 2005, Gregorevic, Allen et al. 2006, Pacak, Mah et al. 2006), however, a major obstacle in the field of DMD research is the failure to translate therapeutic efficacy from mice to human patients.

Canines are an ideal model for efficacy and toxicity trials for developing therapies, as they are relatively outbred and have an immune system that is more similar to humans than rodents (Felsburg 2002). Furthermore, the dystrophin-deficient canine (*cxmd*) is the most commonly studied large mammalian model for DMD. Both young canines and humans present antigen in the context of a fully developed immune system,

and several studies suggest that immunosuppression is required to prevent activation of T cell-mediated immune response and maintain transgene expression in outbred animals (Wang, Allen et al. 2007, Gregorevic, Schultz et al. 2009, Wang, Storb et al. 2010). Loss of long term transgene expression due to activated immune responses against both the viral capsid proteins and/or transgene has been observed in wild-type canines, the *cxmd* model, and in DMD patients (Wang, Allen et al. 2007, Yuasa, Yoshimura et al. 2007, Ohshima, Shin et al. 2009, Mendell, Campbell et al. 2010, Flanigan, Campbell et al. 2013). Other studies have attempted to overcome this obstacle by treating neonatal dogs, which have a more naïve immune system (Kornegay, Li et al. 2010, Pan, Yue et al. 2013).

To further reduce the immune response to rAAV-mediated therapies while increasing efficiency of gene transfer, work is underway by several groups to determine the ideal serotype, regulatory cassette, method of vector purification, formulation, and route of administration that will result in long-term transduction of muscle. Due to their high tropism for striated muscles in mice, the majority of recent DMD gene therapy studies have been conducted using AAV serotypes 6, 8 and 9 (Zincarelli, Soltys et al. 2008). Various studies have examined the transduction efficiency of one or more of these serotypes in canine striated muscles, either by intramuscular injection (Wang, Allen et al. 2007, Wang, Kuhr et al. 2007, Wang, Storb et al. 2010, Koo, Okada et al. 2011), percutaneous transendocardial delivery to target the heart (Bish, Sleeper et al. 2008), isolated limb perfusion (Gregorevic, Schultz et al. 2009, Ohshima, Shin et al. 2009), intravascular injections through the jugular vein to target the heart and diaphragm (Yue, Ghosh et al. 2008, Gregorevic, Schultz et al. 2009, Kornegay, Li et al. 2010, Pan, Yue et

al. 2013) or the femoral artery or saphenous vein to target hindlimb muscles (Gregorevic, Schultz et al. 2009, Ohshima, Shin et al. 2009). While all serotypes have been reported to demonstrate effective transduction, only one study has performed a side-by-side comparison of the striated muscle transduction efficiency of rAAV6, rAAV8 and rAAV9 in the dog (Bish, Sleeper et al. 2008). In this study transendocardial injections were performed showing that rAAV6 vectors gave the highest levels of transduction.

Although studies using direct intramuscular injections provide valuable information of the tissue transduction efficiency of injected vectors and activation of local immune response, gene transfer is more limited compared to intravascular delivery, which provides a global picture of vector fate as it distributes throughout the body *via* the blood stream. One drawback of intravascular delivery is the significant uptake within organs such as the liver, the lymphatic system, or potential inhibition of the vector within blood by pre-existing neutralizing antibodies (NAb) or other serum proteins. Recent reports have indicated the presence of high titers of NAb's specific to AAV6 in canine and human sera (Rapti, Louis-Jeune et al. 2012, Shin, Yue et al. 2012). Furthermore, the serum factor galectin-3 binding protein, a natural ligand of macrophage secreted galectin-3 that plays a role in innate and adaptive immunity, has been shown to aggregate and inhibit rAAV6 transduction *in vitro* (Denard, Beley et al. 2012). These results contradict our previous finding of effective striated muscle transduction in the dog by jugular vein administration of rAAV6 (Gregorevic, Schultz et al. 2009). Therefore, we hypothesized that NAb titers in canine sera differ depending on the source of the dog population. Since recent findings in the mouse have shown that addition of empty capsid decoys in vector formulations can overcome pre-existing Nab and/or enhance transduction (Mingozzi,

Anguela et al. 2013) Schultz et al., submitted), we further hypothesized that the inclusion of empty capsids within our vector formulation could alter the transduction efficiency of rAAV in the canine.

In a side-by-side comparison of rAAV6, 8 and 9 we observed that transduction efficiencies were in the order rAAV6 > rAAV9 > rAAV8 in skeletal muscle cultures as well as in direct intramuscular and systemic injections in mouse and canine striated muscle. Additionally, the creatine kinase-based CK8 and CMV enhancer/promoter regulatory cassettes both functioned in canine cardiac, diaphragm, and leg muscles following jugular vein infusion, albeit with possibly lower overall expression from CK8 likely due to the lack of expression in non-muscle cells. We also demonstrated that naïve dogs obtained from Marshall Bioresources have low titers of NAb against rAAV6, and that successful gene transfer to the canine heart can be achieved with rAAV6 via jugular vein administration. Finally we demonstrated that while empty capsids may act as decoys to overcome preexisiting humoral immunity, the presence of empty capsids did not enhance the transduction efficiency of rAAV in canines.

Results

Expression cassettes and vectors for testing rAAV transduction

For these studies we developed a common expression cassette with which to compare vector transduction in myogenic cells both *in vitro* and *in vivo*. To enable histochemical visualization of transduction as well as quantitative measurements the human placental alkaline phosphatase (hPLAP) reporter gene was used (Alexander, Russell et al. 1994), with gene expression controlled by the synthetic 436-bp striated muscle-restricted regulatory cassette *CK8*. *CK8* was used in lieu of the more promiscuous CMV enhancer/promoter in the side-by-side rAAV serotype comparisons in order to avoid the complication of obtaining expression from non-striated muscle cells. *CK8* is primarily derived from the murine muscle creatine kinase (MCK) promoter/enhancer; it differs from the previously published *CK7* regulatory cassette in that additional non-conserved regions of both the MCK enhancer and promoter sequence have been omitted resulting in a highly active striated muscle regulatory cassette (Salva, Himeda et al. 2007, Goncalves, Janssen et al. 2011). Since rAAV2 has been shown to efficiently transduce monocyte/dendritic cell precursors (Liu, Santin et al. 2000), and dendritic cells are potent antigen presenting cells, the use of a muscle-specific regulatory cassette such as *CK8* should also minimize activation of immune effector cells and elimination of transgene expression when used *in vivo* (Cordier, Gao et al. 2001, Hartigan-O'Connor, Kirk et al. 2001).

The presence of empty capsids in vector formulations can influence transduction (Mingozzi, Anguela et al. 2013). Therefore, rAAV serotype comparisons were performed

using “fulls only” vector preparations (where we specifically removed capsids lacking vector genomes by isopycnic centrifugation) in addition to native preparations containing empty capsids (“fulls+empties”, or “f+e”). Quantification of the native rAAV6 (f+e) and rAAV9 (f+e) preps showed that empty capsids are 3 to 4-fold in excess of “fulls only” capsids (**Figure 5.1**). As additional precautions against differences between rAAV serotypes, vector purification and titering were performed in the same facility by the same personnel, and quantified in parallel by Southern analysis, quantitative PCR (for vector genome copy number) and by SDS-PAGE (for capsid levels) as described in methods.

Comparisons of rAAV6, rAAV8 and rAAV9 in cultured myotubes

Expression of the hPLAP transgene by rAAVs of each serotype (rAAV6-CK8-hPLAP, rAAV8-CK8-hPLAP and rAAV9-CK8-hPLAP) was first verified in C2C12 myogenic cell cultures (**Fig. 5.2a**). Of the three serotypes tested, rAAV6 was most efficient at transducing murine C2C12 myotubes: a dose of 10^{10} vector genomes (vg) of rAAV6 was sufficient to elicit widespread expression hPLAP in the cultures, while the same outcome required 10^{12} vg of rAAV8 and rAAV9. Interestingly, the presence of empty capsids enhanced rAAV6 transduction by ~10-fold, with widespread hPLAP expression at a dose of 10^{9} vg. This was contrary to expectations, as empty capsids have only been reported to enhance rAAV transduction through inhibition of NAb in serum *in vivo* (Mingozzi, Anguela et al. 2013). In contrast, the presence of empty capsids did not result in a noticeable difference in the transduction efficiency of AAV9-CK8-hPLAP in these myogenic cells.

a.

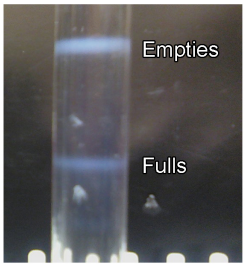

b.

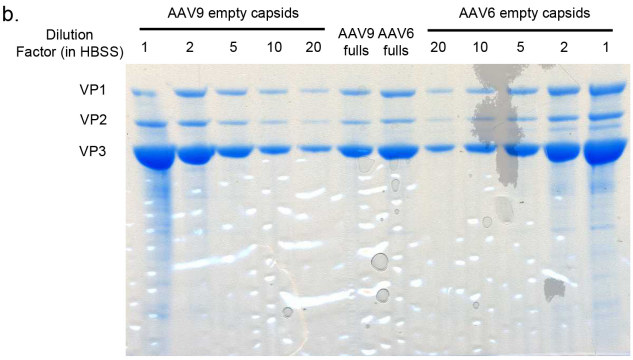

c.

	Dilution factor	Measurement	Area	Mean	255-mean	Minus blank	xDil. Factor
AAV9 empties	2	1	976	179.249	75.751	47.212	
	5	2	976	199.188	55.812	27.273	
	10	3	976	209.708	45.292	16.753	
	20	4	976	217.034	37.966	9.427	
	AAV9 Fulls	5	976	195.184	59.816	31.277	**3.8**
	AAV6 Fulls	6	976	177.526	77.474	48.935	**3.2**
AAV6 empties	20	7	976	213.499	41.501	12.962	
	10	8	976	202.731	52.269	23.73	
	5	9	976	189.055	65.945	37.406	
	2	10	976	167.495	87.505	58.966	
	1	11	976	151.984	103.016	74.477	
	Blank	12	976	226.461	28.539	0	

d.

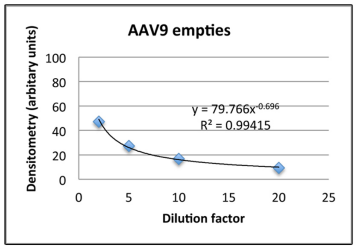

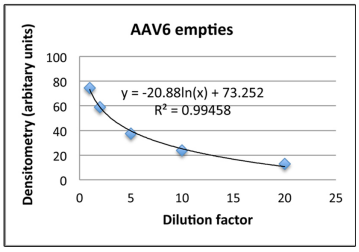

e.

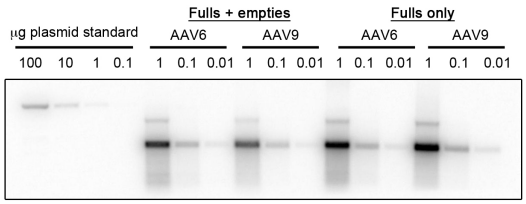

Figure 5.1 Preparation of fulls only (f) and fulls and empties (f+e) vector. (**a**) Genome containing vectors (fulls) were separated from empty capsids (empties) by high speed ultracentrifugation through a cesium chloride gradient over 72 hours. (**b**) Coomassie stained SDS-PAGE gel showing separation of rAAV6 and rAAV9 viral capsid proteins 1, 2 and 3 (VP1, VP2, VP3). Each lane was loaded with 2µl of material, either of fulls only vector (AAV9 fulls, AAV6 fulls) or empties that were serially diluted in HBSS at 1, 2, 5, 10 and 20-times dilution factor. (**c**) Densitometry of VP1 bands was performed using Image J software. (**d**) Standard curves for both AAV9 and AAV6 were generated using serial dilutions of purified empty capsids from each respective serotype, and used to determine the concentration of fulls only vectors relative to empty capsids. Results showed that fulls only preps were more dilute compared with empty capsids (AAV9 fulls - 3.8x; AAV6 fulls - 3.2x). Separated empty capsids were reconstituted with the fulls only preps in their native amounts to generate the fulls and empties (f+e) preps, indicating a 3.8-fold and 3.2-fold excess empty capsids in the AAV9 (f+e) and AAV6 (f+e) preps, respectively. (**e**) Southern blot was used to determine the vector genome titer for all rAAV6 and rAAV9 fulls and empties and fulls only preps. Serial dilutions (1µl, 0.1µl and 0.01µl) for each prep are shown. Plasmid DNA encoding the rAAV vector genome was used to generate the standard curve.

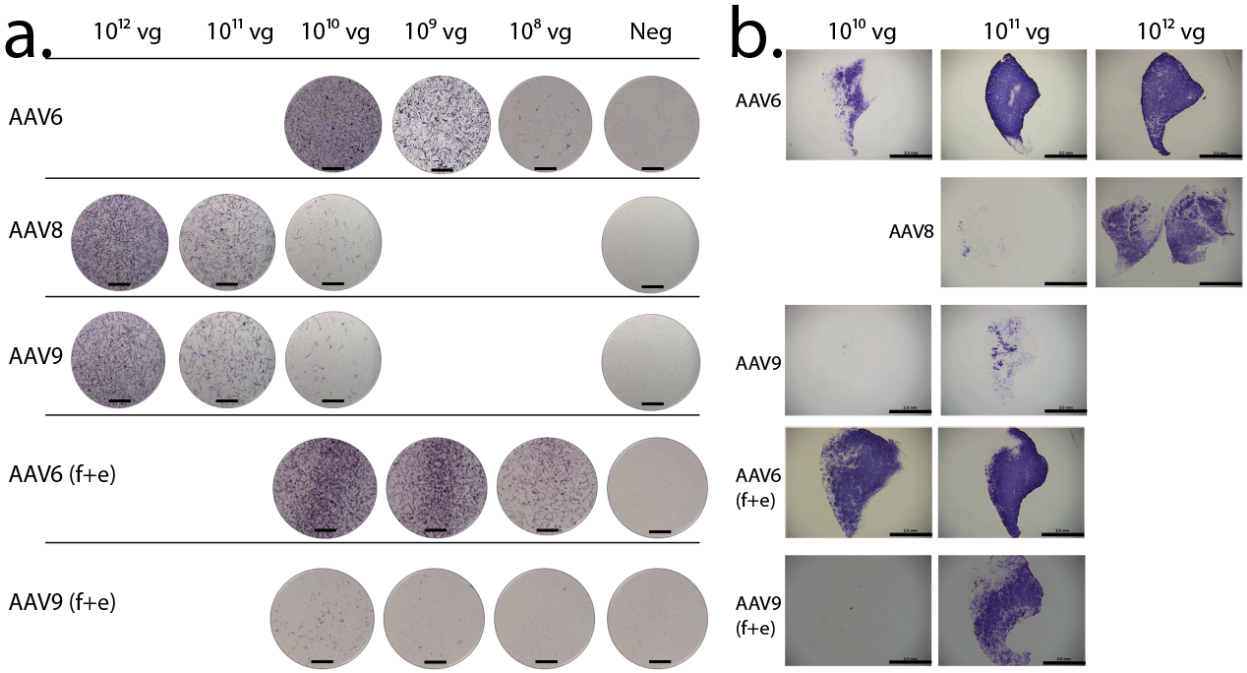

Figure 5.2 Comparisons of the transduction efficiency of rAAV6-CK8-hPLAP, rAAV8-CK8-hPLAP and rAAV9-CK8-hPLAP in C2C12 myotubes and in mice. (a) C2C12 myotubes were infected with serial dilutions of CK8-hPLAP reporter vector (10^8 vg to 10^{12}vg) and examined for hPLAP activity 3 days post differentiation. CK8-hPLAP reporter vector was also delivered to mice by (**b**) intramuscular injection into tibialis anterior muscles and examined two weeks post injection, where the bottom two rows represent the inclusion of empty capsids (f+e). Dose and capsid serotype that the vector was packaged in is indicated. Images are representative sections of 2-4 mice tested per condition. Scale bar, 2.0 mm.

Comparisons of rAAV6, rAAV8 and rAAV9 in mouse muscles

We further examined transgene expression of each serotype in wild-type C57BL/6 mice by intramuscular (IM) administration into the tibialis anterior (TA) (**Fig. 5.2b**). Based on histochemical hPLAP detection 14 days post-injection, rAAV6 exhibited higher transduction efficiency compared with rAAV8 and rAAV9. At a dose of 10^{11} vg, rAAV6 transduced nearly every myofiber within the TA muscle, while the same dose of rAAV8 and rAAV9 resulted in relatively poor transduction. Similar to results from myogenic cultures, the presence of empty capsids again enhanced transduction of rAAV6. Enhanced transduction was also observed with rAAV9 (f+e), although rAAV6 continued to show higher transduction relative to rAAV9.

The relative transduction efficiencies of rAAV6 and rAAV9 were also compared by intravenous delivery into C57BL/6 mice and examination of gene expression in the heart, diaphragm, quadriceps, TA, extensor digitorum longus (EDL), gastrocnemius and the soleus (**Fig. 5.3**). The level of transduction was not overtly different between the two serotypes when full-capsid preparations were administered. Virtually the entire heart was transduced at a rAAV6 dose of $5x10^{12}$ vg, while 10^{13} vg resulted in complete transduction of the heart as well as scattered hPLAP-positive fibers in the diaphragm and hindlimb muscles. Similarly, rAAV9 almost completely transduced the heart at a dose of 10^{13} vg. Consistent with direct IM delivery, the presence of empty capsids enhanced the transduction profile of both rAAV6 and rAAV9 (rAAV6 f+e, rAAV9 f+e; **Fig. 5.3**). Compared to full-capsid vectors alone, there was complete saturation of the heart and

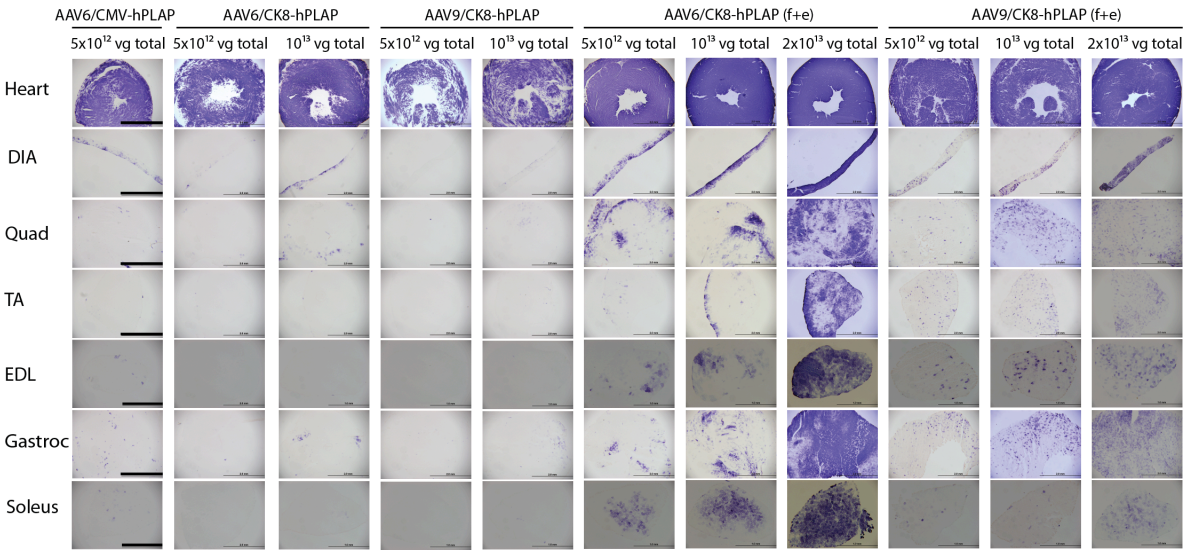

Figure 5.3 Comparisons of the transduction efficiency of rAAV serotypes, promoters, and vector formulations. C57BL/6 mice were administered specified amounts of vector genomes (vg) by retro-orbital injection and examined four weeks post injection. rAAV6 and rAAV9 were also compared with the inclusion of empty capsids (f+e). CMV, cytomegalovirus promoter; CK8, myogenic-specific promoter; DIA, diaphragm; Quad, quadriceps; TA, tibialis anterior; EDL, extensor digitorum longus; Gastroc, gastrocnemius. Images are representative sections of 2-4 mice tested per condition. Scale bar for images of heart, diaphragm, quadriceps, TA, gastrocnemius, 2.0 mm. Scale bar for images of EDL and soleus, 1.0 mm.

higher hPLAP expression, as indicated by histochemical staining, in the diaphragm and quadriceps for both serotypes at a dose of $5x10^{12}$ vg. Increasing dosage of both serotypes also increased hPLAP expression in other hindlimb muscles examined, but rAAV6 again showed greater transduction than rAAV9. At a dose of $2x10^{13}$ vg, rAAV6 resulted in widespread expression of hPLAP in all hindlimb muscles examined.

Comparison of rAAV6, rAAV8 and rAAV9 by intramuscular injection in the canine

We further compared the transduction efficiency of rAAV6, rAAV8 and rAAV9 by intramuscular injection into the canine gracilis muscle, a relatively large yet easily accessible skeletal muscle (Fig. 2), using vector formulations that lack empty capsids. Comparisons were only performed with fulls-only preparations because the presence of empty capsids may further exacerbate the immune response caused by the trauma from direct injections. For each vector, 10^{10} vg and 10^{11} vg were injected in triplicate. At both doses, rAAV8 injected tissues showed minimal hPLAP activity (**Fig. 5.4a**). At the high dose, only modest hPLAP activity was detected following injection of the rAAV9 vector, which was not sufficient to generate positive hPLAP staining on muscle sections (data not shown). In contrast, rAAV6 injected tissues showed markedly higher hPLAP activity relative to other serotypes at each dose tested (**Fig. 5.4b**).

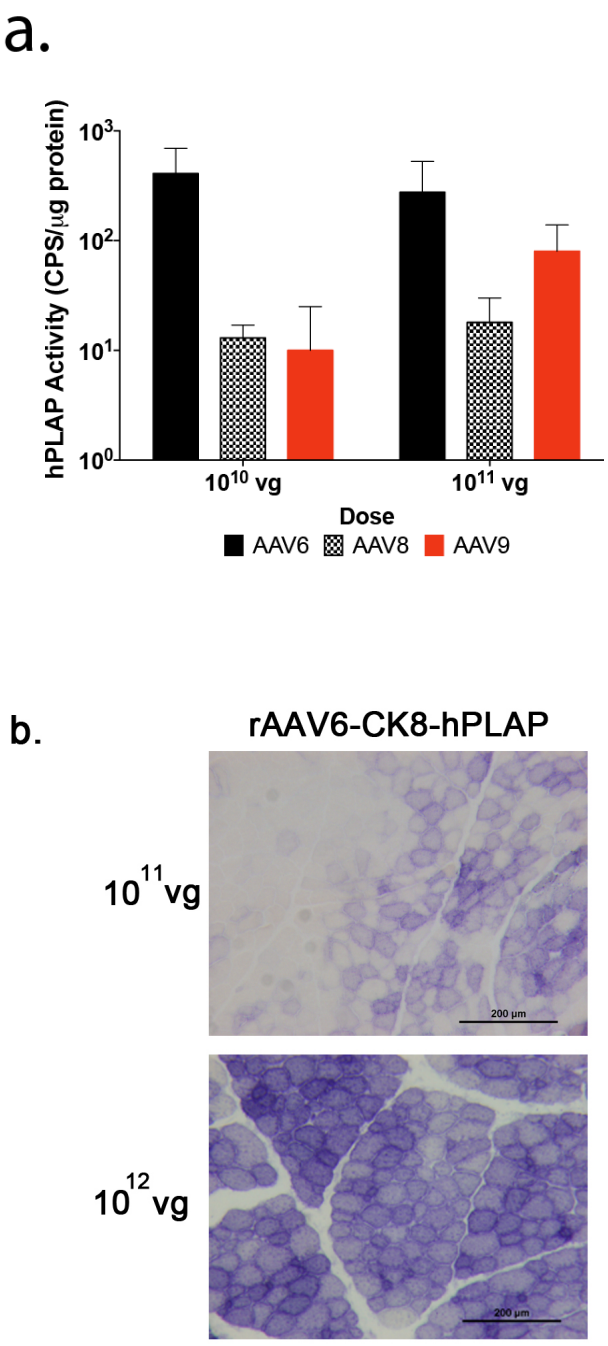

Figure 5.4 Intramuscular injection of rAAV6-CK8-hPLAP, rAAV8-CK8-hPLAP and rAAV9-CK8-hPLAP in canine skeletal muscle. Triplicates of low (10^{10} vg) and high (10^{11} vg) doses of each vector were injected into the gracilis muscle in a volume of 250 μl. Injections were spaced approximately 2 cm apart, and the site of injection marked by sutures. (**a**) Four weeks post-injection, muscles were harvested and examined for hPLAP activity. (**b**) rAAV6 showed the highest activity of the three serotypes at both doses, as confirmed by positive hPLAP staining. Scale bar, 200 μm.

Canine sera contain low titers of neutralizing activity against AAV6

Some previous studies have reported that canine sera contain high levels of neutralizing activity against rAAV6 vectors (Rapti, Louis-Jeune et al. 2012, Shin, Yue et al. 2012), although we have not observed such activity in our animals (Gregorevic, Schultz et al. 2009). We thus measured serum levels of neutralizing activity against rAAV6 in the dogs used in our study, as well as from 47 canine serum samples (pure bred beagles and mongrels) obtained from Marshall Bioresources (North Rose, New York). In addition, 4 serum samples from outbred golden retriever/beagle dogs bred at the Fred Hutchinson Cancer Research Center (FHCRC) and a pooled canine serum sample (Sigma) were examined. Since it has been reported that titers of neutralizing antibodies (NAb) against AAV6 decrease with age (Shin, Yue et al. 2012), sera from beagles and mongrel dogs of different ages were assessed (**Table 5.1**). Neutralizing titers for sera were determined by counting positive foci on HT1080 cells that were transduced with AAV vectors carrying *CMV* promoter driven human placental alkaline phosphatase reporter cassettes (rAAV6-CMV-hPLAP) after pre-incubation with canine serum. The titer dilution at which there was 50% or more inhibition compared to vector alone was reported as the neutralizing titer. (Halbert, Miller et al. 2006)

Almost all samples tested showed low or no neutralization against rAAV6 (<1:2). Only four samples showed slightly elevated titers (<1:32), and the pooled serum sample showed a titer of 1:16 (**Table 5.1**). As a positive control, serum samples were also collected 4 weeks post-injection from 6 of the dogs (from the group of naïve 10-12 week old dogs tested) that were infused via the jugular vein with known doses of rAAV6. Neutralizing antibodies were detected in all sera of rAAV6-infused canines. The

increases in NAb titer correlated with the vector dose (**Table 5.1**). Dogs #035 and #990 received $1.4x10^{13}$ vg/kg and $1.7x10^{13}$ of rAAV6-CMV-hPLAP, respectively, and showed a low NAb titer (1:20), while dogs #162 and #007 received $7x10^{13}$ vg/kg and showed much higher NAb titers (1:160). Dogs #861 and #864 demonstrated the highest titers (1:1024) after receiving $1.8x10^{14}$ vg/kg of rAAV6-CK8-hPLAP. In sum, our results revealed minimal to no detectable levels of pre-existing NAb against rAAV6 in naïve canine sera from beagles and mongrels acquired from Marshall Bioresources or canines bred in house at the FHCRC.

Table 5.1 Neutralizing antibody titers against rAAV6 in canine sera.

			Titer					
Breed	**Age**	**Total # examined**	**≤1:2**	**1:4**	**1:8**	**1:16**	**1:32**	**1:64**
Beagle	10-12 weeks	14	12	1			1	
	6 months	7	7					
	9 months	2	2					
	12 months	13	12		1			
Mongrel/Hound	8-10 weeks	3	2	1				
	6 months	3	3					
	12 months	5	5					
Golden retriever mix	?	4	4					
Pooled serum	n/a	1				1		

			Titer		
Beagle ID	**Injected rAAV6 vector dose (vg/kg)**	**Serum Examined**	**1:20**	**1:160**	**1:1024**
035	$1.4x10^{13}$	4 weeks post-injection	X		
990	$1.7x10^{13}$		X		
162	$7x10^{13}$			X	
007	$7x10^{13}$			X	
861	$1.8x10^{14}$				X
864	$1.8x10^{14}$				X

Myocardial transduction with rAAV6 in young canines via jugular vein administration

The ability of rAAV vectors to transduce cardiopulmonary tissues via jugular vein delivery was first examined using rAAV6-CMV-hPLAP in the young canines described above (#035, #990, #007 and #162), with dogs #007 and #162 receiving the high dose ~$7x10^{13}$ vg/kg, while dogs #035 and #990 received a 5x and 4x lower dose, respectively. These initial studies used vector preparations lacking empty capsids (**Table 5.2**). Canines were immunosuppressed with cyclosporine (15 mg/kg) and mycophenolate mofetil (5 mg/kg) for at least 10 days prior to vector infusion. Four weeks after infusion, canines were sacrificed and the heart, diaphragm and other organ tissues were harvested for assessment of hPLAP activity, histology and vector genomes.

Of the two high-dose (~$7x10^{13}$ vg/kg) dogs, only one (#007) demonstrated strong transduction in various areas of the heart and in the aortic arch (aorta; **Figs. 5.5**) with corresponding hPLAP expression in large groups of fibers in both the atria and ventricles (**Fig. 5.5e**). The other high-dose dog (#162) showed markedly lower hPLAP activity in the heart and aorta. One low dose dog, #990, which received 4-fold lower dose, showed approximately 8-fold lower hPLAP activity in the heart, with scattered fibers staining positive (data not shown). Canine #035, which received a 5-fold lower dose compared to #007, displayed ~45-fold lower hPLAP activity in the heart. These results suggest an exponential, rather than linear relationship between dosage and hPLAP activity. Only low levels of hPLAP activity were detected in the diaphragm of the canines. Vector genomes correlated well with hPLAP activity for most samples, with the exception of the heart and diaphragm from dog #035 and aortic arch from dog #162 (**Fig. 5.5b**). This discrepancy could be explained by sampling, as results are averaged from several samples in each

organ. This variation between samples is apparent (**Figs. 5.5c-e**) where analysis of discrete portions of the heart from dog #007 showed distinctly better correlations between vector genomes (**Fig. 5.5d**), hPLAP activity (**Fig. 5.5c**) and expression (**Fig. 5.5e**), reflective of the concentrated vector uptake and expression in the atria. There was variable hPLAP activity in all muscles and non-muscle tissues tested, with the duodenum and liver showing the highest hPLAP activity (**Fig. 5.6**). Such strong expression in non-muscle tissues may be due to the ubiquitous and robust expression of the CMV promoter, suggesting that the use of a striated muscle-restricted promoter would be important to reduce off-target, non-muscle transgene expression. In sum, myocardial transduction can be achieved by jugular vein delivery of rAAV6-CMV-hPLAP, however efficiency is strongly dependent on dosage.

Vector clearance rates and transduction comparisons in canine cardiac and skeletal muscles following jugular vein administration of rAAV6- and rAAV9-CK8-hPLAP

We next examined the transduction efficiency of rAAV6 and rAAV9 vectors in the absence of empty capsids (rAAV6 (f) - dog #861; rAAV9 (f) - dog #860) using the hPLAP transgene driven by the muscle specific CK8 regulatory cassette, following jugular vein injections of $1.8x10^{14}$ vg/kg (**Figs. 5.7, 5.8**). We also examined the effect of empty capsids on the transduction efficiency of the two serotypes (rAAV6 (f+e) – dog #864; rAAV9 (f+e) – dog #865) (**Figs. 5.7, 5.8**). Since rAAV8 vectors did not appear to perform as well as rAAV6 and 9 in the previous studies, we focused here on the latter vectors.

Table 5.2 Summary of canines used in these studies.

Animal ID	rAAV serotype	Promoter	Reporter gene	Dosage (vg/kg)	Capsids (fulls only vs. fulls + empties)
035	rAAV6	CMV	hPLAP	$1.4x10^{13}$	Fulls only
990	rAAV6	CMV	hPLAP	$1.7x10^{13}$	Fulls only
162	rAAV6	CMV	hPLAP	$7.0x10^{13}$	Fulls only
007	rAAV6	CMV	hPLAP	$6.9x10^{13}$	Fulls only
860	rAAV9	CK8	hPLAP	$1.8x10^{14}$	Fulls only
861	rAAV6	CK8	hPLAP	$1.8x10^{14}$	Fulls only
864	rAAV6	CK8	hPLAP	$1.8x10^{14}$	Fulls + empties
865	rAAV9	CK8	hPLAP	$1.8x10^{14}$	Fulls + empties

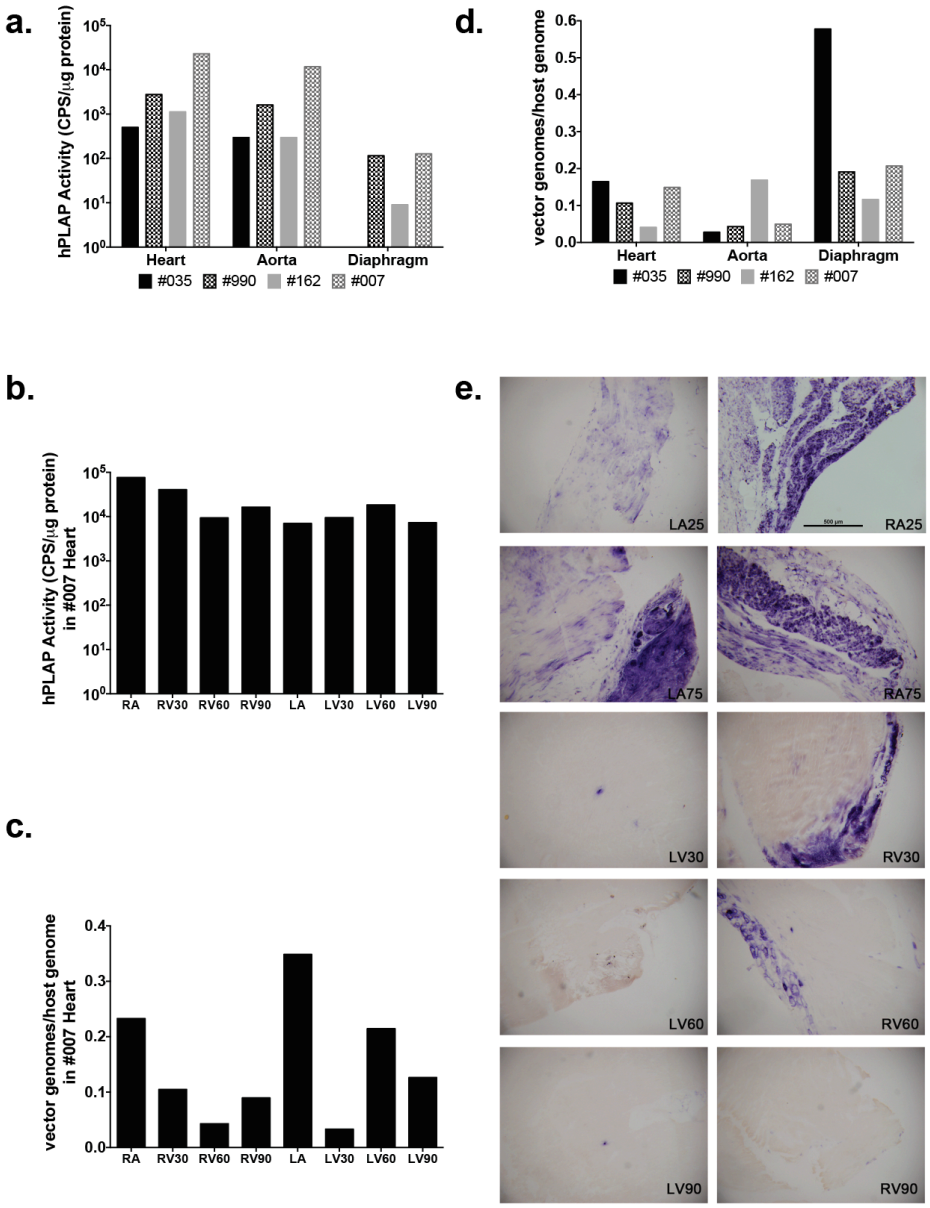

Fig 5.5. Intravascular administration of rAAV6-CMV-hPLAP via jugular vein administration. Dogs were injected with the following low and high doses of rAAV6-CMV-hPLAP: Low dose: #035: $4x10^{13}$ vg/kg, #990: $1.7x10^{13}$ vg/kg; High dose: #007: $6.9x10^{13}$ vg/kg, #162: $7.0x10^{13}$ vg/kg. Heart, aorta and diaphragm were harvested 4 weeks post-injection and examined for hPLAP expression by (**a**) activity assays and (**b**) vector genomes. Dog #007 showed the highest transgene expression throughout the heart, as confirmed by (**c**) hPLAP activity, (**d**) vector genomes, and (**e**) hPLAP staining. No staining was detected in the diaphragm (data not shown). Endogenous alkaline phosphatase was heat inactivated prior to assays and staining. RA = right atria, RA25 = proximal portion right aria, RA75 = distal portion right aria, RA RV30 = proximal portion right ventricle, RV60 = medial portion right ventricle, RV90 = distal portion right

ventricle, LA = left atria, LA25 = proximal portion left aria, LA75 = distal portion left atria, LV30 = proximal portion left ventricle, LV60 = medial portion left ventricle, LV90 = distal portion left ventricle. Scale bar, 500 μm. Results from activity and vector genome assays were measured in triplicate and are shown as means.

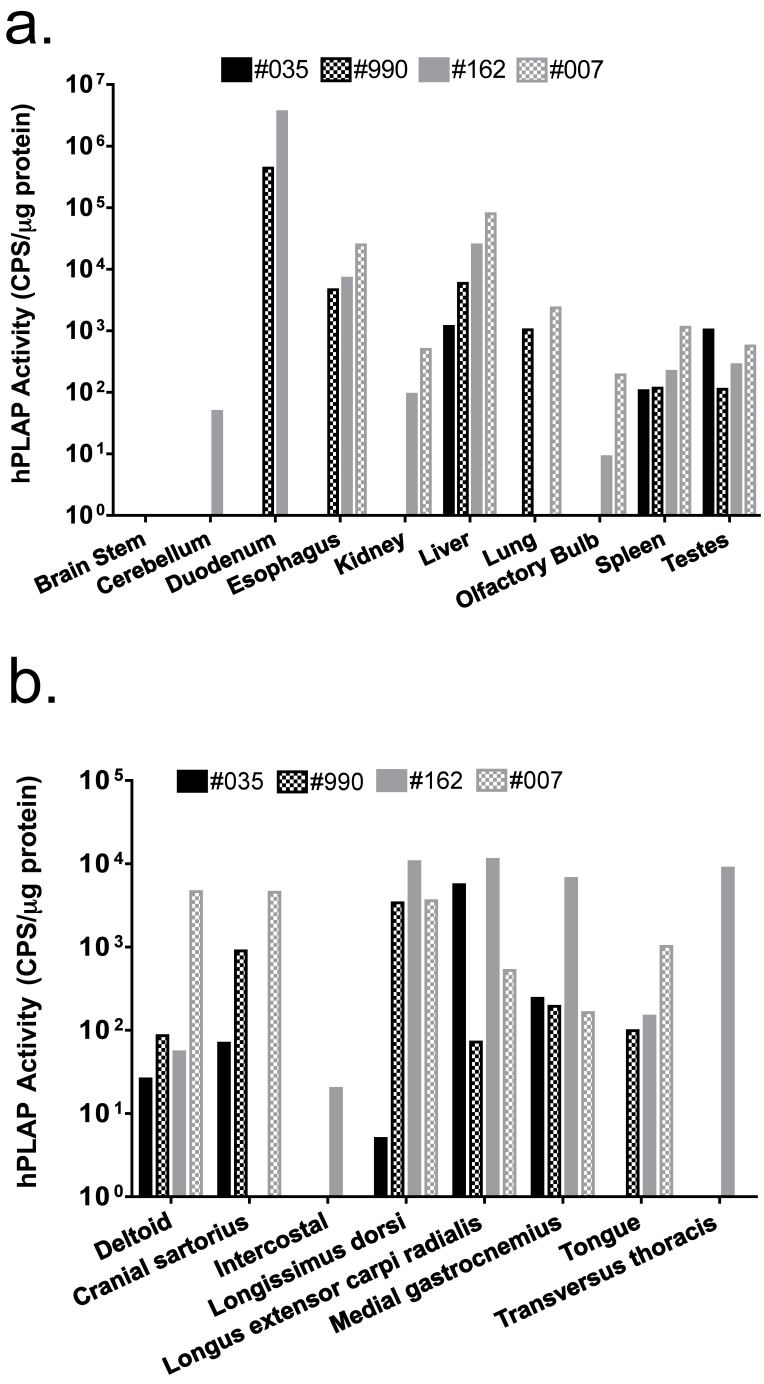

Figure 5.6 Canine biodistribution of rAAV6-CMV-hPLAP (fulls alone) via jugular vein administration. Lysates from selected non-muscle (**a**) and muscle (**b**) tissues were assessed for reporter activity. Highest hPLAP activity was observed in duodenum, followed by the liver and several skeletal muscles. Absent bars from select tissues indicate that reporter activity was at or below background level.

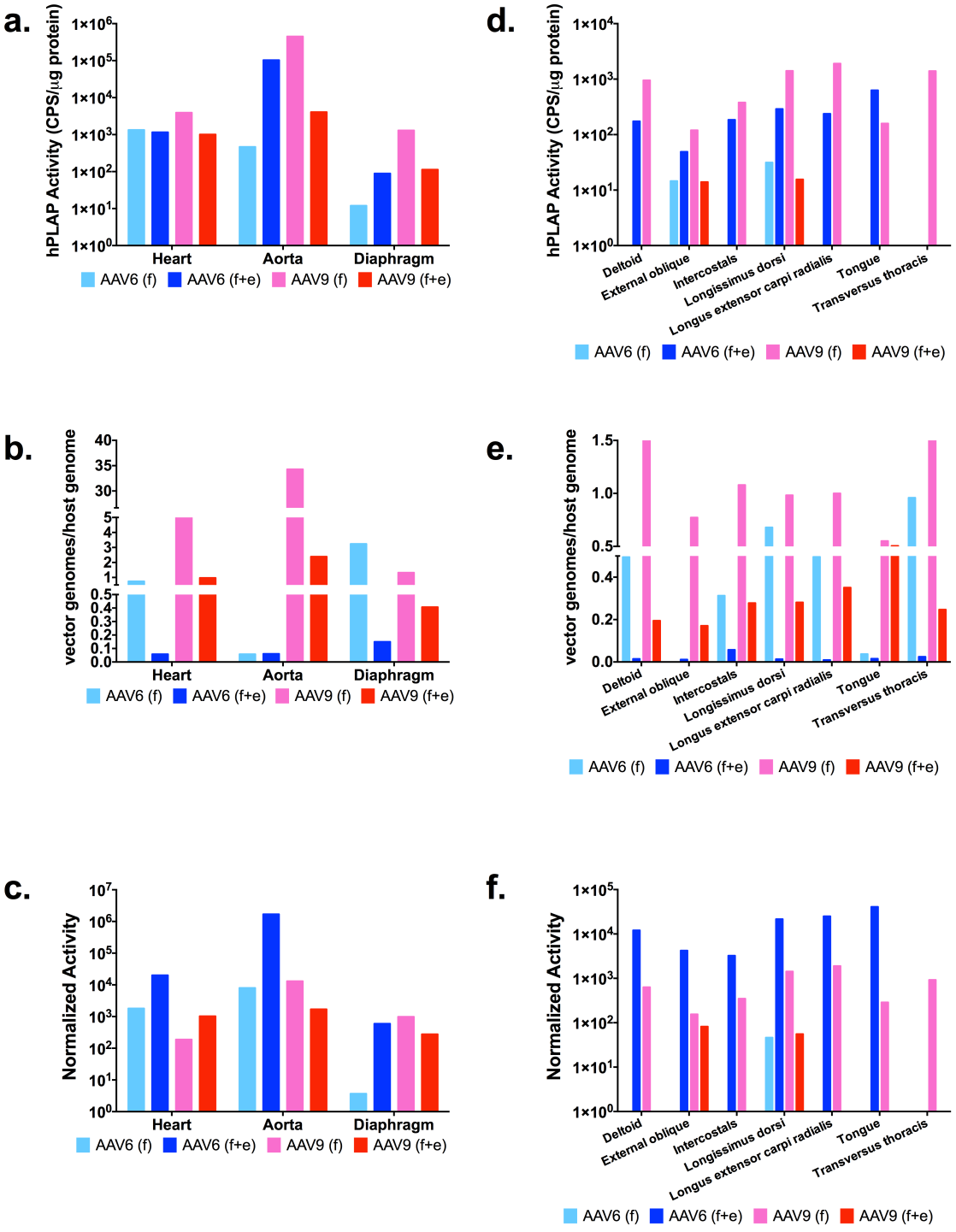

Figure 5.7 Comparison of rAAV6 and rAAV9-CK8-hPLAP in canine heart, skeletal muscle and organs by jugular vein administration. (**a**) hPLAP activity, and (**b**) vector genomes in the heart, aorta and diaphragm were examined in dogs injected with rAAV6- or rAAV9-CK8-hPLAP, with the inclusion of empty capsids (f+e) or without (f). (**c**)

Examination of normalized activity (hPLAP activity relative to genome copy number/host genome) in the heart, aorta and diaphragm showed that rAAV6 (f+e) is superior to rAAV9 in myocardial transduction efficiency. (**d**) hPLAP activity, and e) vector genomes of skeletal muscles (deltoid, external oblique, intercostals, longissimus dorsi, longus, extensor carpi radialis, tongue and tranversus thoracis) were also examined. Some muscle tissues demonstrated hPLAP activity that was below background levels (absent bars); however rAAV9 (f) again showed the highest hPLAP activity and vector genomes in all skeletal muscles examined, except the tongue. (f) Consistent with heart and aorta, normalizing for vector genomes showed that rAAV6 (f+e) was the most potent vector, followed by rAAV9 (f).

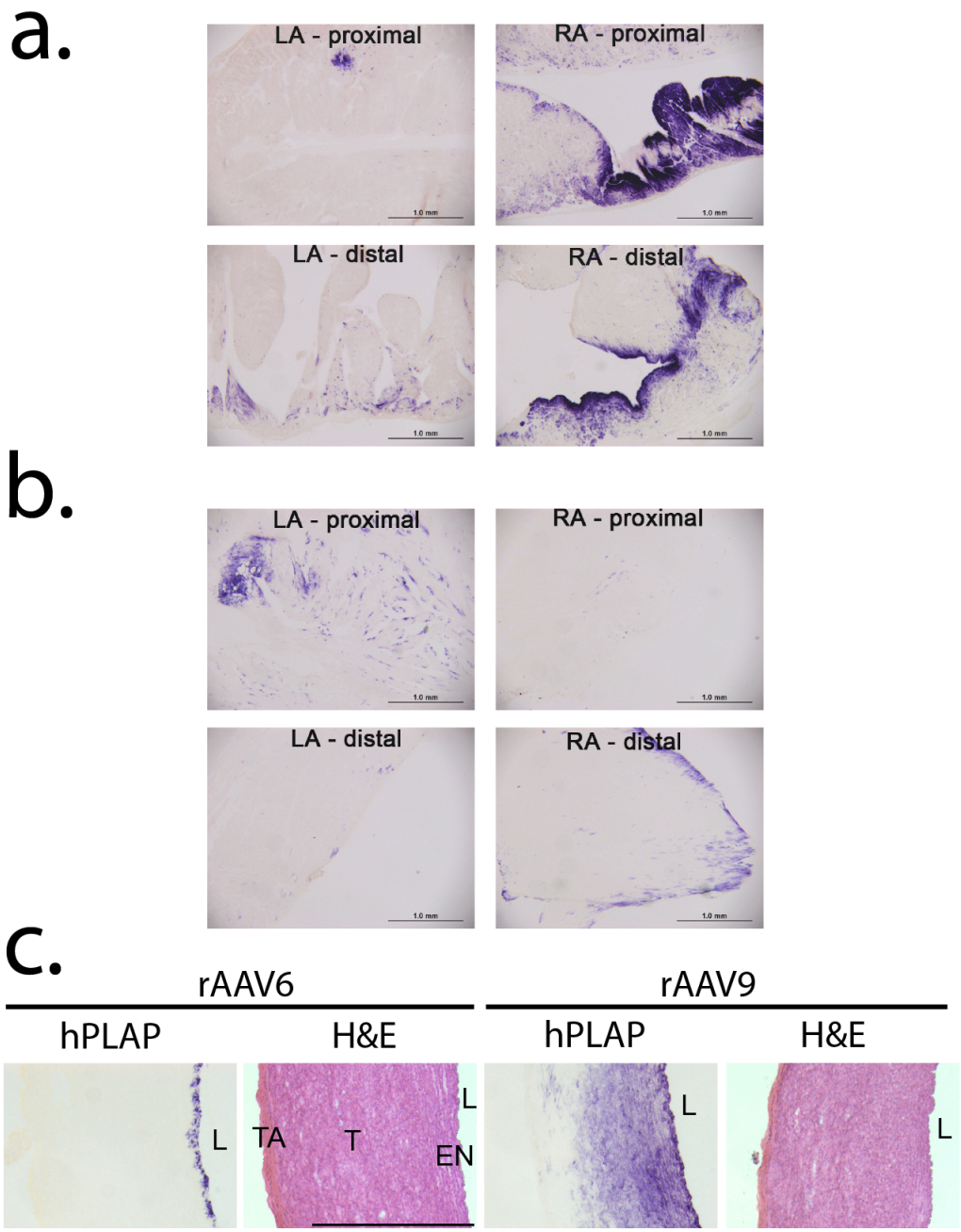

Figure 5.8 hPLAP staining in sections of canines infused with rAAV-CK8-hPLAP via jugular vein administration. Vectors packaged in AAV serotypes 6 or 9 were infused at a dose of $1.8x10^{14}$ vg/kg, at a flow rate of 4 ml/min. Transduction and morphology was examined 4 weeks post-infusion in various tissues by hPLAP histochemical and hematoxylin and eosin (H&E) staining, respectively. RA = right atria, LA = left atria. Activity was most prominent in the atria portions of the heart. (**a**) Heart cross sections of #861 infused with only full rAAV6 capsids. (**b**) Heart cross sections of #864 infused with both empty and full rAAV6 capsids. (**c**) Despite a lack of hPLAP

staining in the heart of rAAV9-CK8-hPLAP injected canines (data not shown), rAAV9 showed a broader zone of penetrance within the aorta vessel wall, with hPLAP expression present in the tunica media of the aorta in the rAAV9-injected dog, while staining was limited to the endothelium of the rAAV6-aorta. L = lumen, TA = tunica adventitia, TM = tunica media, EN = endothelium. Scale bar, 1.0 mm.

Since vector transduction efficiencies could be affected by the duration of circulating vectors in the blood, we compared circulating vector genome levels in blood samples obtained during the infusion procedure at 1, 5 and 10 minutes post-injection. Consistent with trends previously observed in mice (Zincarelli, Soltys et al. 2008, Kotchey, Adachi et al. 2011), rAAV6 was cleared from the bloodstream much more quickly than rAAV9; e.g., compared to 1-min levels 97% of rAAV6 vectors had been cleared by 5 min, whereas only 14% of rAAV9 had been cleared (**Table 5.3**).

At necropsy 4 weeks post-injection, hPLAP activity in the heart, aorta and diaphragm was highest with rAAV9 (f) (**Fig. 5.7a**). However, using vectors carrying empty capsids (f+e) rAAV6 performed as well as rAAV9 in these same tissues (**Fig. 5.7a**). Additionally, when vector genome copy number was taken into account (**Fig. 5.7b**), rAAV6 showed higher hPLAP activity per vector genome in the heart (Normalized Activity, as defined by hPLAP activity/(vector genome per host genome); **Fig. 5.7c**). At a qualitative level, these data suggest that rAAV6 and rAAV9 are both capable of myocardial transduction, and both serotypes also transduced the diaphragm and other skeletal muscles following jugular vein delivery. These studies also suggest that the presence of empty capsids is beneficial for rAAV6 transduction of heart and diaphragm muscle as well as the aorta (see below), but that empty capsids have no, or possibly negative effects on rAAV9 transduction (**Figs. 5.7a-c**). Interestingly, hPLAP staining was not detected in heart muscle sections of rAAV9-injected canines, despite moderate hPLAP activity in the heart extracts. While positive hPLAP staining was detected in some of the cardiac cryo-sections from the rAAV6-injected canines (**Fig. 5.8**), many sections exhibited little to no staining. Thus while rAAV6 and rAAV9 both transduced

cardiac muscle when administered via the jugular vein, many cardiac regions exhibited low transduction at relatively high doses of each serotype.

When used in conjunction with the CK8 regulatory cassette, only minimal hPLAP activity was detected in non-muscle tissues (data not shown), despite high vector genome levels in non-muscle tissues from rAAV6 (f+e) and rAAV9 (f+e) injected dogs (**Fig. 5.9**). This greatly contrasts with the high hPLAP activity found in the liver of dogs infused with rAAV6-CMV-hPLAP (**Fig. 5.6**), suggesting that the use of a muscle-specific promoter such as *CK8* provides an additional safety factor in gene therapy for a variety of muscular dystrophies by preventing non-muscle transgene expression. Interestingly, the CK8 regulatory cassette did exhibit substantial expression in the aorta when delivered via either rAAV6 or 9 (f+e) (**Fig. 5.8**). hPLAP activity in aorta cryosections indicated clear hPLAP staining of the endothelial cells on the luminal edge of the rAAV6-aorta, while hPLAP expression extended into the tunica media of the rAAV9-aorta, indicating that rAAV9 can also transduce vascular smooth muscle and that the CK8 promoter can support expression in these cells (**Fig. 5.8b**).

Table 5.3 Clearance of rAAV vector genomes from blood after infusion via jugular vein. Vector was infused at 4 ml per minute in a total volume of 4 ml at a dose of $1.8x10^{14}$ vg/kg. Blood was drawn at 1, 5 and 10 min intervals and assessed for serum vector concentration.

	Time	**vg/μl**	**% clearance (relative to concentration at 1 min)**
rAAV6	1 min	$3.4x10^{7}$	0
	5 min	$1.1x10^{6}$	96.8
	10 min	$4.8\ x10^{5}$	98.6
rAAV9	1 min	$5.8x10^{7}$	0
	5 min	$5.0x10^{7}$	13.8
	10 min	$4.4x10^{7}$	24.1

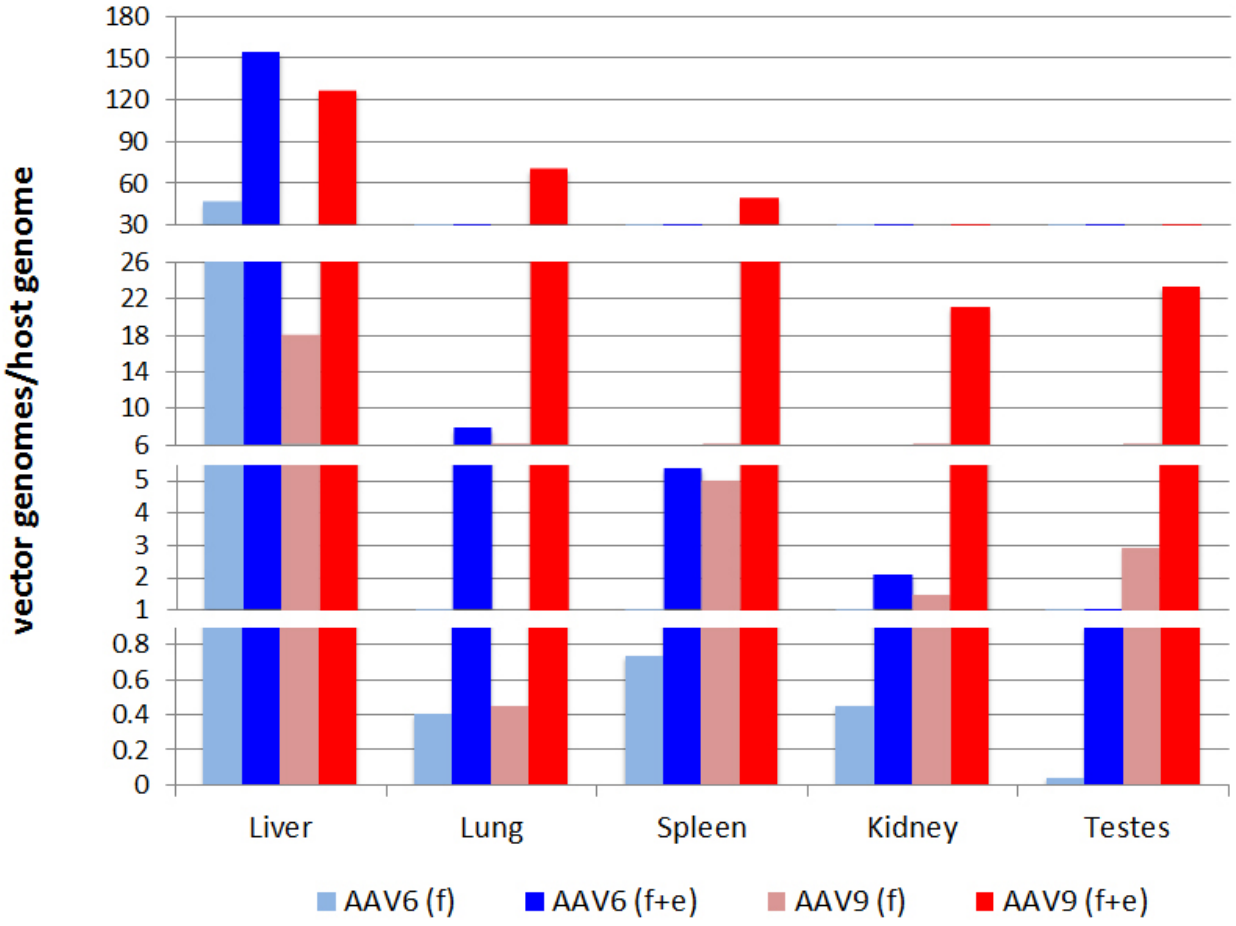

Figure 5.9 CK8 driven vector genomes in non-muscle tissues from rAAV6 (f), rAAV6 (f+e), rAAV9 (f) and rAAV9 (f+e) injected dogs. Liver, lung, spleen, kidney and testes from dogs infused with rAAV6 (f), rAAV6 (f+e), rAAV9 (f) and rAAV9 (f+e) vectors were examined for vector genomes 4 weeks post treatment. In all tissues, the presence of empty capsids enhanced transduction for both rAAV6 and rAAV9.

Discussion

In this study, young, immunosuppressed beagles were injected with AAV vectors via jugular vein catheterization. At sub-optimal doses (relative to studies in mice) both rAAV6 and rAAV9 vectors, in conjunction with either the CMV enhancer/promoter or the CK8 regulatory cassette provided successful gene delivery into canine heart muscles. Large areas of the heart, in particular the atria, stained positively for hPLAP in a single canine injected with rAAV6-CMV-hPLAP; and there was reduced staining in a canine that received rAAV6-CK8-hPLAP. Although the data was obtained from only single animals, the higher CMV-mediated hPLAP levels are consistent with comparisons between CMV and CK8 activities in mice following systemic delivery of AAV6 (unpublished data from Hauschka and Chamberlain Labs). However, since CMV expresses in all transduced cell types, an unknown portion of the detected CMV activity comes from non-muscle cells, such as the significant proportion of fibroblast cells present in cardiac tissue (Souders, Bowers et al. 2009).

Our results compared favorably to prior studies with rAAV8 and rAAV9, which used neonatal canines, in part because the relative immaturity of the neonatal immune system mounts a less robust immune response upon exposure to transgene and viral capsid proteins (Yue, Ghosh et al. 2008, Kornegay, Li et al. 2010, Pan, Yue et al. 2013). At close to equivalent doses, jugular vein administration of rAAV8-RSV-hPLAP at a dose of $1.35x10^{14}$ vg/kg conferred only minimal hPLAP expression in the heart 1.5 months post-injection (Pan, Yue et al. 2013), while low transduction in the heart was reported with rAAV9-RSV-hPLAP at $2\text{-}2.5x10^{14}$ vg/kg (Yue, Ghosh et al. 2008), and

with AAV9-CMV-mini-dystrophin at a dose of $1.5x10^{14}$ vg/kg in neonatal *cxmd* dogs (Kornegay, Li et al. 2010) after extended periods of incubation. In our study, the hearts from rAAV9-injected dogs similarly showed only scattered hPLAP-positive cells, whereas rAAV6 led to more widespread expression. However, we did observe comparable overall levels of hPLAP enzymatic activity in extracts from hearts injected with either rAAV6 or rAAV9, suggesting that the hPLAP activity in rAAV9-injected hearts may be concentrated in smaller focal areas. The lack of widespread hPLAP staining in rAAV9-injected hearts is remarkable, since AAV9 has enabled robust transgene expression in the hearts of mice and non-human primates (Inagaki, Fuess et al. 2006, Pacak, Mah et al. 2006, Zincarelli, Soltys et al. 2008). These results thus suggest that rAAV6 can transduce wider areas of canine hearts more efficiently than rAAV9 when delivered to young beagles at sub-optimal doses via the jugular vein.

Vector infusion via jugular vein administration also resulted in modest hPLAP activity in the diaphragm and limb muscles in injected canines (**Figs. 5.5, 5.7, 5.6**). Previous studies with rAAV8 and rAAV9 demonstrated transduction of these muscles at doses of $1x10^{14}$ vg/kg (Yue, Ghosh et al. 2008, Kornegay, Li et al. 2010, Pan, Yue et al. 2013), although this could be explained by the use of neonatal canines, which have a comparatively smaller circulatory system and blood volume, resulting in faster, less diluted vector delivery throughout the body. In our study, while only single dogs were compared, the overall hPLAP activity in limb muscles was highest in a dog that was infused with purified full AAV9 capsids, closely followed by a dog that was infused with rAAV6 full and empty capsids. This could be attributed, in part, to enhanced perfusion of rAAV9 (f), as evidenced by the consistently higher vector genomes per host genomes in

rAAV9 tissues. Longer persistence in the blood might also aid rAAV9 tissue penetrance (Kotchey, Adachi et al. 2011) (**Table 5.3**). Interestingly though, direct injections of rAAV6 and rAAV9 into canine gracillis muscles resulted in much higher transduction with rAAV6 (**Fig. 5.4**). Enhanced, widespread transduction of the body with AAV9 has also been shown in systemically injected mice (Zincarelli, Soltys et al. 2008). Our study thus suggests that despite poorer myocardial transduction, systemically delivered rAAV9 might transduce canine limb skeletal muscles more efficiently than rAAV6.

Enhanced perfusion may also allow rAAV9 to penetrate into the tunica media of the aorta resulting in transduction of the vascular smooth muscle. Efficient transduction of vascular smooth muscle has been demonstrated with rAAV9 in swine carotid, coronary and femoral arteries administered via balloon catheter inserted into the arteries (Pankajakshan, Makinde et al. 2012). However, results from a rat carotid model of restenosis suggested that transduction might be more efficient with rAAV2.5 (Lompre, Hadri et al. 2013). While we did not study AAV2.5, these *in vitro* data are in contrast to our *in vivo* canine vascular delivery comparisons of AAV6 and AAV9 in which AAV9 appeared superior to AAV6. To our knowledge this study represents the first report of clear differences in the capacity of these myogenic serotypes to penetrate the medial layer of an uninjured arterial vessel following intravenous delivery (Richter, Iwata et al. (2000), (Hadri, Bobe et al. 2010). AAV9 targeting of diseased vessels thus appears to have strong potential for vascular gene therapy approaches. The penetrance of rAAV vectors into blood vessels could be clinically relevant in rAAV-mediated gene therapy for DMD. Dystrophin is normally expressed in the tunica media of blood vessels, and its absence in the vessels of mdx mice and DMD patients is thought to contribute to the

deficiency of neuronal nitric oxide synthase (nNOS) mediated vasodilation during exercise, as well as to the dystrophic pathology due to vascular insufficiency (Sander, Chavoshan et al. 2000, Thomas, Shaul et al. 2003, Kobayashi, Rader et al. 2008, Lai, Thomas et al. 2009).

The relatively low levels of reporter gene expression observed in our studies may be partially due to the short post-injection time prior to carrying out the assays. While we have previously detected strong hPLAP expression in a beagle pup heart 3 weeks after jugular vein delivery of rAAV6 (Gregorevic, Schultz et al. 2009), other studies involving rAAV9 have allowed at least 16 weeks for transgene expression (Yue, Ghosh et al. 2008, Kornegay, Li et al. 2010). Biopsies taken from rAAV9 infused canines at 2, 3 and 6 weeks showed a distinct increase in hPLAP expression in various limb muscles, with every skeletal muscle evaluated showing hPLAP expression at 6 months, even at the lower dose tested ($1x10^{14}$ vg/kg; (Yue, Ghosh et al. 2008). Further studies in the canine model are required to determine the species-specific differences in time of onset and expression of transgenes delivered by rAAV6 and rAAV9. An increase in dose may also enhance striated muscle transduction for both serotypes. For example, jugular vein infusion of rAAV8 at a high dose of 9.06 $x10^{14}$ vg/kg dramatically increased striated muscle transduction (relative to a 5-7 fold lower dose) and resulted in homogeneous hPLAP expression in the heart after 2.5 months (Pan, Yue et al. 2013).

Our study also compared serotype differences in transduction efficiencies of rAAV6, 8 and 9 by direct intramuscular injection in the dog. Consistent with trends observed in the mouse, rAAV6 was the most efficient serotype for transducing skeletal muscle by direct intramuscular injections. Our data are also consistent with a previously

published study comparing the level of cardiac gene transfer of these serotypes via percutaneous tranendocardial delivery (Bish, Sleeper et al. 2011), which found that AAV6 is about 1 log more potent than AAV8 and AAV9 in canine heart. Similar results were also found in non-human primates (Gao, Bish et al. 2011), indicating that rAAV6 is also more efficient at transducing striated tissue than rAAV8 and rAAV9 in large animal models by direct injection.

In the present study, we have also independently examined the levels of pre-existing neutralizing activity against AAV6 in naïve canine sera (**Table 5.1**), and our findings differ from recent reports of high titers of anti-AAV6 NAb in canine sera (Rapti, Louis-Jeune et al. 2012, Shin, Yue et al. 2012). Pooled canine serum was previously reported to have high titers of NAb against AAV6 (1:1024) (Rapti, Louis-Jeune et al. 2012), however, in our study this was markedly lower (1:16). The discrepancy between the results may be due to different lot numbers of the pooled serum samples. In addition to low NAb titers based on inhibition assays, the positive myocardial transduction with rAAV6 in our study strongly suggests that pre-existing neutralizing antibodies or factors such as galectin-3 binding protein in canine sera were unlikely to inhibit the transduction of systemically delivered rAAV6 vectors in our canine models. The discrepancy between our study and others may be due to the source and breed of dogs from which sera were drawn. Prior studies tested sera from dogs that were generated in-house and included pure breeds (beagle, golden retriever, Labrador retriever and Welsh corgi) and a mixture of all four breeds (Denard, Beley et al. 2012, Rapti, Louis-Jeune et al. 2012, Shin, Yue et al. 2012), or used sera that was purchased commercially in lyophilized form (Rapti, Louis-Jeune et al. 2012). Furthermore, results from two of these studies were derived from the

same population of dogs, in which, curiously, newborn pups were born with higher titers of NAb against AAV6 than that of their dams (1:40 to 1:80), and titers further increased until age 8 months then diminished as the dogs aged (1:5 and 1:20) (Rapti, Louis-Jeune et al. 2012, Shin, Yue et al. 2012). Thus, observations that canine sera contain high titers of NAb against rAAV6 do not hold true for all canine colonies. In addition, canine studies using rAAV6 that sourced animals from other facilities did not report the presence of pre-existing NAb (Halbert, Madtes et al. 2010) or reported only low titers of NAb (Bish, Sleeper et al. 2011). The incidence of neutralizing activity against rAAV2, 5 and 6 in adult humans is low, and it has been suggested that sero-positivity against AAV6 was due to cross-reacting antibodies generated by previous exposure to rAAV2 (Halbert, Miller et al. 2006). Importantly, the same study showed that children under the age of 12 did not exhibit neutralizing antibodies to AAV2, thus suggesting a potentially large window of opportunity for treating young DMD patients with rAAV6 can be applied to many humans in the clinical setting without concerns of neutralization.

The absence of high titers of pre-existing neutralizing antibodies against rAAV6 and rAAV9 in canine serum may explain why the addition of empty capsids had the opposite effect on striated muscle transduction in the dog compared to mouse. It has previously been shown that empty capsids can act as decoys for anti-AAV antibodies, protecting AAV vectors from neutralization (Mingozzi, Anguela et al. 2013). While the required level of excess empty capsids increases with increasingly higher titers of NAb, in the presence of low anti-AAV titer, formulations with a 1000x excess of empty capsids actually resulted in a 60% loss of transgene expression, likely due to interference of empty capsids with vector receptor binding (Mingozzi, Anguela et al. 2013). The

presence of a 3-4 fold excess empty capsids in our study increased the transduction efficiency of rAAV6 and rAAV9 delivered intramuscularly and systemically to mice (**Figs. 5.1, 5.2**). It is unclear how empty capsids would aid transduction *via* intramuscular injection, but our results here are consistent with our prior studies in mice using rAAV6-RSV-hPLAP (Schultz et al., submitted).

In conclusion, we demonstrated that rAAV6 can transduce the heart of juvenile dogs similarly or better than rAAV9 following jugular vein administration, despite detection of higher vector genome levels in whole tissue extracts of the rAAV9 injected animals. However, while rAAV6 also had much greater transduction efficiency than rAAV9 in differentiated mouse muscle cultures, in mice, and following intramuscular injection in dogs, AAV9 appeared to provide higher transduction of canine limb muscles following jugular vein delivery. Employing a combination of techniques such as isolated limb perfusion or vector recirculation methods to target the hindlimb muscles, or pre-formulation with designed empty capsids could lead to more widespread transduction with rAAV (Gregorevic, Schultz et al. 2009, Chicoine, Montgomery et al. 2014). The inclusion of muscle-specific transcriptional regulatory cassettes may reduce undesired transgene expression in non-muscle tissues, and in non-muscle cells within cardiac and skeletal muscle. Such regulatory cassettes may also be critical for reducing T-cell responses against transgene product, thereby facilitating long-term transgene expression (Wang, Allen et al. 2007). The results of our study in young, immunosuppressed dogs, which are of comparable size to newborn human infants, may be used as a guide for further development of clinical applications for early intervention or treatment of Duchenne muscular dystrophy as well as other muscular dystrophies.

Materials and Methods

Animals

All animal experiments were approved by the Institutional Animal Care and Use Committee of the University of Washington. Recombinant AAV serotype comparisons were performed in C57BL6 wild-type male mice age 2.5-4 months. Wild-type beagles (8-12 weeks old for jugular vein infusion and 6 months for intramuscular injections) were purchased from Marshall Bioresources (North Rose, New York, USA). Beagles were acclimatized at UW animal facility for one week prior to immunosuppression with cyclosporine (Neoral, 15 mg/kg) and mycophenolate mofetil (MMF, 5 mg/kg). Immunosuppression was given orally twice daily. Blood was drawn twice a week to monitor the health of the beagles and to maintain serum trough levels of cyclosporine at 400-600 ng/ml throughout the experiment.

Vector production

Recombinant AAV6 vector was produced and prepared as previously described (Gregorevic et al., 2009). Briefly, genome-containing vectors were produced by $CaPO_4$ transfection of HEK 293D cells with plasmids containing rAAV-CMV-hPLAP-SV40pA or rAAV-CK8-hPLAP-SV40pA vector genomes and pDGM6, pDGM8 or pDGM9 packaging/helper genes. pDGM8 and pDGM9 capsid genes were synthesized by sub-cloning into pDGM6 (Guy Odom and Daniel Miller, respectively) using *SwaI* and *ClaI* restriction endonuclease sites and confirmed by DNA sequencing. Seventy-two hours after transfection, medium and cells were harvested and freeze/thawed or processed through a microfluidizer (Microfluidics, Newton, MA) prior to 0.22-μm filtration

(Millipore, Billerica, MA). For AAV6, vector particles were purified from the clarified lysate by affinity chromatography over a HiTrap heparin column (GE Healthcare, Chalfont St. Giles, UK), sedimented overnight at RCF 131,101 x g through a 40% sucrose cushion then resuspended in Hank's buffered salt solution (HBSS) (Invitrogen, Carlsbad, CA). For AAV8 and AAV9, vectors were purified using the optimized protocol as previously described (Ayuso, Mingozzi et al. 2010). Briefly, lysate from transfected cells and the culture medium were clarified by centrifugation at RCF 2000 x g for 30 min then vector particles were PEG precipitated, resuspended in buffer (50 mM HEPES, 150 mM NaCl, 20mM EDTA, 1% sarkosyl, pH 8) and layered on a 1.3 g/ml, 1.5 g/ml CsCl 'step' gradient. The region of the gradient containing vector genomes was collected and adjusted to 1.37g/ml CsCl. For all AAV vectors, empty capsids were removed from the preparation by isopycnic gradient ultracenrifugation (1.37 g/mL CsCl, RCF 148,463 x g for 72 h). Empty and full capsid bands were identified visually, collected separately, then dialyzed to HBSS and sterile filtered (0.22 μm Millex-GP; Millipore). Finally, empty or full capsids were sedimentated once again through a 40% Sucrose cushion as described above. Empty or full capsid pellets were each resuspended in HBSS and reconstituted in native ratios to generate full and full + empty vector preparations. Vector genome titer was determined by Southern blot with a DNA standard of known quantity (**Fig. 5.1**).

Capsid Quantitation

Vector/capsid dilutions were mixed with 2.5% β-mercaptoethanol, and 4x SDS-PAGE loading buffer (Invitrogen, Carlsbad, CA), and heated to 95°C for 2 minutes. Multiple dilutions of each sample were loaded on a 4-12% a NuPAGE Novex Bis-Tris

Mini Gel (Invitrogen, Carlsbad, CA). Gels were stained for protein with Bio-Safe Coomassie (Bio-Rad, Hercules, CA) according to manufacturer's instructions. Relative capsid concentrations were determined by densitometry using Image J (**Fig. 5.1**).

Neutralizing antibody assays

Dilutions of 36 canine serum samples (neat or 1:2, 1:20, 1:40, 1:80, 1:160, 1:320) were incubated with rAAV6-CMV-hPLAP at 37^{o}C for 1 hr then applied to HT1080 cells. Prior to incubation with rAAV6 vector, serum samples were first heat inactivated at 56^{o}C for complement inactivation. All serum samples were drawn from dogs bred and provided by Marshall Bioresources (North Rose, New York, USA). hPLAP stains were performed 3 days later. Cells were fixed in 3.7 % methanol-stabilized formaldehyde for 10 minutes at room temperature, then washed three times in 1xPBS and heat inactivated at 65^{o}C for 1 hour in PBS. Sigma *FAST* BCIP/NBT substrate solution (Sigma, St. Louis, MO) was applied to each well and incubated overnight at room temperature in the dark. Solution was removed the next day and replaced with 1xPBS, and AP-positive focus forming units were counted. The reciprocal of the highest dilution of serum that inhibited rAAV transduction by >50% compared with rAAV6 alone was defined as the neutralizing titer.

Cell culture

C2C12 cells were plated at ~80% confluence on gelatin-coated 6-well plates with standard growth media (DMEM, 20% FBS, 1% penicillin-streptomycin (P/S)) overnight then washed three times with 1x Saline G prior to infection with rAAV-CK8-hPLAP. Vectors were diluted to the desired concentrations in differentiation media (DMEM, 2%

HS, 1% P/S). Cells in each well were incubated with 0.5 ml of diluted virus at 37^{o}C for approximately 2 hours. Cultures were then brought to a final volume of 2 ml with differentiation media and incubated overnight (37^{o}C in 95% O_2 5 % CO_2 atmostphere). To determine the transduction efficiency of each serotype, AP staining was performed at day 3 post-differentiation using the protocol described above.

Protein and placental alkaline phosphatase tissue lysate assays

Placental alkaline phosphatase activity was detected using the Phospha-Light system (Applied Biosystems, Bedford, MA) according to manufacturer's instructions. Lysates were obtained by first grinding frozen tissue into a powder. Lysis buffer (0.5% NaDOC, 50 mM Tris pH 7.5, 150 mM NaCl, 1% Triton X-100, supplemented with complete protease inhibitor cocktail (cOmplete, Mini, Roche, Indianapolis, IN) was added to frozen tissue powder in a 5:1 volume ratio and homogenized with a pellet pestle and motor (Kimble-Kontes, Vineland, NJ) in a microcentrifuge tube, on ice. Tubes were spun at 10,000g for 10 minutes at 4°C. Supernatant was transferred to new tubes and stored at -80°C until used. Total protein concentration was measured using a Coomassie Plus kit according to manufacturer's instructions (Pierce, Rockford, IL). Alkaline phosphatase activity was measured using a Phospha-Light System (Applied Biosystems, Bedford, MA), according to manufacturer's instructions. Both measurements were performed with a Victor^{3}V multilabel counter (PerkinElmer, Shelton, CT) using microplates.

Vector administration in mice

Mice were anesthetized by isoflurane for all injections. rAAV vectors were diluted in HBSS to a volume of 30 µl to a dose of $1x10^{10}$ vg, $1x10^{11}$ vg and $1x10^{12}$ vg for direct intramuscular injection into the mouse tibialis anterior, using a 31-gauge 0.5-mL insulin syringe (BD, Franklin Lakes, NJ) driven longitudinally into the muscle from the distal end to approximately half the muscle length. Vector doses of $5x10^{12}$ vg, $1x10^{13}$ vg and $2x10^{13}$ vg were brought up to a volume of 200 µl for systemic injection via the retro-orbital sinus with a 27 $^{5}/_{8}$ gauge 1.0-mL insulin syringe (BD).

Vector administration in canines

Jugular vein infusion: Beagles were anesthetized intravenously with ketamine (5.5 mg/kg) and diazepam (0.27 mg/kg) prior to intubation and were maintained on 2% isoflurane throughout the procedure. A catheter was inserted through the left internal jugular vein being positioned ~6 cm distal to the entry position. Lines were flushed with saline and approximately 4-5 min prior to vector infusion, beagles were administered with diphenhydramine (4 mg/kg). Vector was diluted with sterile HBSS to a volume of 4ml, and was administered at a rate of 4ml/min. Lines were again flushed with saline after infusion. Beagles were closely monitored for adverse reactions during recovery from anesthesia.

Intramuscular injections: Beagles were anaesthetized (drugs and doses as described above) and maintained on isoflurane during the procedure. Incisions were made in the left medial thigh and the surrounding connective tissue of the gracilis muscle was removed.

Each dose (10^{10} vg, 10^{11} vg) was injected in triplicates in 250 µl volume per injection. Beagles were treated with fentanyl (25 µg/hr) and carprofen (4 mg/kg) post-operation.

Necropsy

Systemically injected beagles were euthanized 4 weeks after vector infusion. Heart, diaphragm, intercostals, limb muscles as well as spleen, liver, lung, kidney, brain, testes, tongue and duodenum were harvested and either embedded in OCT or snap frozen in liquid nitrogen for detection of AP activity and vector genome analyses.

Histochemical staining

For hPLAP staining, sections were fixed with ice cold 4% paraformaldehyde, washed three times in cold PBS, placed in 65°C PBS for 90 minutes, rinsed in room temperature PBS, and washed in AP Buffer (100 mM Tris-HCl pH 9.5, 100 mM NaCl, 10 mM MgCl2) for 10 minutes. Excess liquid was removed from the sections, and Sigma *FAST* BCIP/NBT substrate solution (Sigma, St. Louis, MO) was applied to each section for 20 minutes at room temperature in the dark. Slides were rinsed three times in room temperature PBS, dehydrated in an ascending series of ethanol (70-100%), cleared with xylene, then coverslipped with Permount mounting media (Fisher Scientific, Fair Lawn, NJ). For hematoxylin and eosin (H&E) staining, muscle sections were first fixed for 5 minutes in absolute methanol, stained according to a standard H&E protocol, and dehydrated and mounted as described above.

Quantitative PCR Analysis

DNA extracts were generated from selected tissues using DNAeasy Blood & Tissue Kit (Qiagen, Valencia, CA). All real time PCR reactions were performed on an Applied Biosystems 7500 Real Time PCR System using TaqMan Universal PCR Master Mix (Life Technologies), custom primers (IDT), and custom probes (Eurofins Genomics, Hunstville, AL). The following hPLAP/SV40 primer-probe set was used to quantify copies of vector genomes; (Forward 5'- CCCCGCGTTGCTTCCT -3', Reverse 5'-CAAGTTAGATCTCGACGGTATCGA -3', Probe 5'-6FAM-AGACGGCCACTGCTCCCTGAAGCT-BHQ1 -3'). The following primer-probe set was used to quantify copies of endogenous Pax7 gene; (Pax7 Primers: 5'-CCAAGGCCGGGTCAATCAG-3', 5'-AGATGACACAGGGCCGGA-3'; Pax7 probe: 5'-6FAM-CGACCCCTGCCTAACCACATCCG-BHQ1-3'). Samples were measured in triplicate and calculated as vector genome gene number per diploid genome.

Notes to Chapter 5

The work in this chapter is currently in preparation for publication:

Ramos JN*, Seto S*, Finn E, Mushtaq A, Nguyen Q, Hauschka SD, Odom GL and Chamberlain JS: Comparison of rAAV6 and rAAV9 transduction via jugular vein delivery to young canines

*These authors contributed equally to this work.

Contributions to the work as follows:

JNR*: Design and implementation of the canine jugular vein delivery experiments, including participation and presence in the administration and surgeries, daily immunosuppression, blood draws, necropsies, manipulation of blood and tissue as well as analysis. Design and implementation of rAAV vector experiments in mice, including vector delivery, tissue manipulation, and analysis. Contributed to writing of the manuscript, with feedback and suggestions from JT, SDH, GLO, and JSC.

JS*: Design and implementation of the canine jugular vein delivery experiments, including participation and presence in the administration and surgeries, daily immunosuppression, blood draws, necropsies, manipulation of blood and tissue as well as analysis. Designed and implemented neutralizing antibody experiments, including analysis. Composed the majority of the manuscript, with feedback and suggestions from JNR, SDH, GLO, and JSC.

EF: Vector production and input on experimental design.

AM: Assistance with canine tissue manipulation and analysis.

QN: Design and implementation of experiments, including creation of myogenic regulatory cassette and assistance with canine necropsies.

SDH: Input on experimental design and writing of the manuscript.

GLO: Design and implementation of the canine jugular vein delivery experiments, including participation and presence in the administration and surgeries, daily immunosuppression, blood draws, necropsies, manipulation of tissue as well as analysis. Contributed to writing of the manuscript, with feedback and suggestions from JNR, JT, SDH, and JSC.

JSC: Experimental design and writing of the manuscript.

Chapter 6

Perspectives and Future Directions

Duchenne muscular dystrophy (DMD) is the most common of the muscular dystrophies, afflicting approximately 1 in 3500 newborn males (Emery 2002). This recessive, X-linked disease is primarily characterized by the progressive loss of muscle mass, strength, and ambulation. The inability to halt the progression of DMD with available pharmacological agents and palliative treatments has spurred experimental methods to treat this devastating disease. One promising approach is to replace the mutated *dystrophin* gene with one that can halt or prevent the dystrophic pathophysiology. Recombinant adeno-associated virus (rAAV) vectors have shown great promise for gene therapy of DMD, since several serotypes have displayed a high tropism for striated muscle (Muir and Chamberlain 2009, Wang, Tapscott et al. 2011).

Previous studies revealed that rAAV vectors have a limiting packaging capacity of approximately 5.0 kb, which is almost a third the size of the *dystrophin* coding DNA (Dong, Nakai et al. 2010, Wu, Yang et al. 2010). Studies of patients afflicted by the milder allelic disease, Becker muscular dystrophy (BMD), revealed that in-frame deletions could result in the expression of a truncated, less functional dystrophin (Koenig, Beggs et al. 1989, England, Nicholson et al. 1990, Beggs, Hoffman et al. 1991). Further studies in mice identified regions that are crucial and those that are dispensable for a functional, truncated dystrophin protein (Abmayr S 2006). These miniaturized dystrophin constructs, or micro-dystrophins, were small enough to be encoded by rAAV vectors, thus resolving the packaging capacity issue. The rescue of DMD animal models with

rAAV/micro-dystrophin vectors has been repeatedly demonstrated (Seto, Ramos et al. 2012).

Micro-dystrophins tested to date protect muscles from contraction-induced injury and improve the specific force generation capacity when expressed in dystrophic models for DMD. However, micro-dystrophins don't perform as well as the full-length dystrophin expressed in normal striated muscle. The studies within this body of work (see Chapter 2) tested novel micro-dystrophin constructs in *mdx*^{4cv} mice and compared their functionality against a previously characterized construct (μDysH3). We identified novel micro-dystrophins that were able to provide increased protection from contraction-induced injury and specific force generation. However, no single novel construct was able to display improved functionality in both of these aspects. The exact reasons why certain novel constructs performed better than others remains unclear.

Despite being the largest domain of the dystrophin protein, no crystal structure has yet been resolved for the rod domain. *In vitro* biochemical studies and computer simulations of the rod domain suggest that this region exhibits various biochemical and structural properties (Le Rumeur, Winder et al. 2010, Legrand, Giudice et al. 2011). It is possible that the rod domain composition in certain constructs were more conducive to proper folding, stability, and assembling of DGC members without steric hindrance than others. To carry this study forward, future studies can examine the properties of our novel constructs μDys5 and μDys7, which yielded the most promising results from our assays. A set of studies including *in vitro* (e.g. circular dichroism and immunoprecipitation) and *in vivo* (e.g. morphology and physiological studies with different muscle groups) would expand our understanding of these constructs. Such studies could reveal structural and

folding properties and determine what other proteins bind to these micro-dystrophins. Also, the functionality of these novel micro-dystrophins need to be evaluated additional muscle groups, especially in the heart since cardiac complications attribute to approximately 20% of deaths in DMD patients (Bushby, Muntoni et al. 2003, Finsterer and Stollberger 2003). While it is important to follow up these studies in more detail, it must be recognized that even higher functioning micro-dystrophins could be discovered from future screenings. There are numerous rod domain compositions that can be rationally designed and tested, beyond what was done in this body of work. Further refinement of regulatory expression cassettes may contribute to further designs by becoming smaller and thus allowing more of the dystrophin protein to be encoded in rAAV vectors.

In our studies, we also evaluated the stability of one of our first-generation micro-dystrophin constructs (Harper, Hauser et al. 2002) with conditional ablation studies in transgenic mice (see Chapter 3). The stability of this protein was found to be dramatically lower than the full-length dystrophin in murine skeletal muscle (Ahmad, Brinson et al. 2000). In the context of treating dystrophic muscle, rAAV/micro-dystrophin vectors must express fast enough to allow the protein to halt ongoing degeneration and necrosis or risk being cleared out with the myofibers that they failed to transduce and rescue. Increased stability of micro-dystrophins may alleviate the pressure of needing a promoter that expresses at a physiologically higher level than the endogenous promoter driving the expression of the full-length dystrophin isoform. Although no toxicity has been observed from overexpressing dystrophin (Cox, Cole et al. 1993), the use of the cytomegalovirus (CMV) or Rous sarcoma virus (RSV) promoters in rAAV vectors prevents the use of

larger, more functional, micro-dystrophins. Smaller, myogenic-specific promoters may not exhibit the same expression kinetics as CMV or RSV promoters. Therefore, future experiments could focus on increasing the stability of micro-dystrophins. A possible approach is to investigate post-translational modification of micro-dystropins with small ubiquitin-related modifiers, which can increase the lifespan and stability of proteins (Hay 2005). In addition to ascertaining the stability of micro-dystrophin, we also determined that adult skeletal muscle could not sustain its ablated expression.

Dystrophic pathophysiological characteristics were observed within weeks after micro-dystrophin ablation. Rescuing dystrophic animal models with rAAV vectors has been repeatedly demonstrated, but it remains unclear how long micro-dystrophin expression will persist in treated muscle. While our studies did not evalute this exact scenario, they did reveal that losing micro-dystrophin expression is detrimental to skeletal muscle. The prospects of rAAV-mediated gene therapy for DMD should also address the possibility of losing therapeutic transgenes from muscle maintenance (e.g. exercise-induced or contusion injuries). The damaged muscle would be regenerated, in part, by the myogenic stem cells, or satellite cells, but rAAV vectors won't transduce most of these cells. We found that multiple rAAV serotypes cannot effectively transduce satellite cells even though these tested serotypes transduce myofibers within the same tissue (see Chapter 4). Therefore, significant loss of transduced myofibers would require repeat administration of rAAV/micro-dystrophin vectors.

As the number of studies of rAAV vectors for gene therapy grows, our understanding of immunological responses to these vectors improves (Rogers, Martino et al. 2011, Wang, Tapscott et al. 2011, Mingozzi and High 2013). In this body of work (see

Chapter 3), we aimed to validate a combination of cyclosporine (CsA) and a non-depleting CD4 (NDCD4) antibody for a transient immunosuppression regimen previously reported to attenuate a humoral response to rAAV (McIntosh, Cochrane et al. 2012). The use of this regimen prevented a cell-mediated response in our studies, but failed to prevent a humoral response to AAV serotypes 6 and 9, both of which have a tropism for striated muscle (Zincarelli, Soltys et al. 2008, Zincarelli, Soltys et al. 2010). Nevertheless, we show that two, and even three, systemic administrations of rAAV6 vectors was tolerated at doses of therapeutic relevance for DMD. To our knowledge, this is the first report of such findings in immunocompetent mice. Interestingly, repeat administration of rAAV9 vectors was unsuccessful. These results raise additional questions that may serve as the groundwork for additional studies. A set of experiments could further characterize AAV serotypes that exhibit a high tropism for striated muscle. Instead of focusing on tropism of myogenic cells, future studies could focus on tropism of antigen-presenting cells and lymphocytes. Such studies may explain the discrepancies observed in our repeat administration studies.

Another aim for future experiments would be achieving systemic readministration in dystrophic mice. Our studies only examined repeat administration by intramuscular injections. Future work will need to determine if the increased presence of immune cells within the *mdx*^{4cv} muscle and vasculature will be adequately suppressed to avoid a cell-mediated response or anaphylaxis. If the CsA and NDCD4 antibody regimen cannot tolerate repeat transduction, other immunosuppressive agents reported to attenuate a humoral immune response to rAAV vectors can be added to the regimen and tested. Finding an immunosuppressive regimen that achieves systemic readministration of rAAV

vectors in dystrophic mice would then require validation in larger dystrophic animal models. Previous studies have already shown that rAAV vectors can elicit a cell-mediated response from a single challenge in canines (Wang, Tapscott et al. 2011). This is just one aspect of rAAV studies that has been difficult to translate from murine to canine models. Another aspect is delivery of rAAV vectors to larger animal models.

Although direct intramuscular injections of rAAV vectors can provide valuable information of transduction efficiencies and local immune responses, intravascular administration is the more therapeutically relevant approach. Intramuscular injections to deep tissue or severely afflicted muscles may pose a greater risk than benefit. Infusing rAAV vectors into the vasculature is a less invasive approach for transducing striated muscle. Previous canine studies have demonstrated widespread transduction of muscle by intravascular administration, but to a greater degree in neonatal canines (Yue, Ghosh et al. 2008, Gregorevic, Schultz et al. 2009, Ohshima, Shin et al. 2009, Kornegay, Li et al. 2010, Pan, Yue et al. 2013). In a set of experiments, we focused on comparing transduction efficiencies of multiple rAAV serotypes and vector formulations in the canine model (Chapter 5). These studies examined the biodistribution of rAAV vectors after jugular vein infusion into canines that were 2-4 months of age. We found that jugular vein infusion did achieve transduction of the heart and aorta, but had dramatically less transduction of skeletal muscles. Non-muscle organs, such as the liver and duodenum, were found to uptake most of the vector genomes by this route of administration. Achieving saturating transduction levels with rAAV vectors in dogs requires a huge amount of vector production work. Exploring another method of vector administration may improve the transduction efficiency of striated muscle and the use of

limited resources dedicated to rAAV vector production. Such studies are already underway in our laboratory. A dialysis machine, traditionally used for patients with renal complications, has been adapted to create an extracorporeal circuit (ECC) that can recirculate a bolus of rAAV vector (Bieber, Halldorson et al. 2013). By maintaining physiological homeostasis, a target group of tissues that are "downstream" of the intravascular infusion sites can be repeatedly exposed to a passing bolus of rAAV vector. Thus far, our unpublished data suggests that this method of delivery results in higher transduction of hind limb skeletal muscles than a previously established method of infusion into the femoral artery (Gregorevic, Schultz et al. 2009). Additional studies can also be designed to target the heart and/or diaphragm using the ECC method, which would have great implications for DMD gene therapy, as most patients succumb to premature death due to cardio/respiratory complications (Emery 2002).

Gene therapy research for DMD has revealed encouraging results for scientists, clinicians, and patients alike. Despite the approximately 5.0 kb packing capacity of rAAV vectors, this issue has been resolved by miniaturizing dystrophin into highly functional, truncated proteins. Immunological responses to rAAV vectors are obstacles that face pre-clinical and clinical studies in large animals and humans, respectively. However, various combinations of immunosuppressing agents have effectively allowed repeat administration of rAAV vectors in mouse DMD models. This provides a starting point for further studies aimed to tolerate repeat administration of rAAV vectors in larger mammals. Previous studies, along with a set of studies presented here, demonstrate the ability to target striated muscles throughout the body of large animal models. The novel work presented in the preceding chapters focused on several aspects of rAAV-mediated

gene therapy for DMD. We propose that our findings augment the knowledge of several obstacles facing gene therapy for DMD and the experimental methodologies that may treat and eventually cure this disease.

References

Aartsma-Rus, A., A. A. Janson, W. E. Kaman, M. Bremmer-Bout, G. J. van Ommen, J. T. den Dunnen and J. C. van Deutekom (2004). "Antisense-induced multiexon skipping for Duchenne muscular dystrophy makes more sense." Am J Hum Genet **74**(1): 83-92.

Abmayr S, C. J. (2006). The structure and function of dystrophin. Molecular Mechanisms of Muscular Dystrophies. W. SJ. Georgetown, Landes Biosciences**:** 14-34.

Adams, M. E., N. Kramarcy, S. P. Krall, S. G. Rossi, R. L. Rotundo, R. Sealock and S. C. Froehner (2000). "Absence of alpha-syntrophin leads to structurally aberrant neuromuscular synapses deficient in utrophin." J Cell Biol **150**(6): 1385-1398.

Adams, M. E., Y. Tesch, J. M. Percival, D. E. Albrecht, J. I. Conhaim, K. Anderson and S. C. Froehner (2008). "Differential targeting of nNOS and AQP4 to dystrophin-deficient sarcolemma by membrane-directed alpha-dystrobrevin." J Cell Sci **121**(Pt 1): 48-54.

Ahmad, A., M. Brinson, B. L. Hodges, J. S. Chamberlain and A. Amalfitano (2000). "Mdx mice inducibly expressing dystrophin provide insights into the potential of gene therapy for duchenne muscular dystrophy." Hum Mol Genet **9**(17): 2507-2515.

Ai, H. W., N. C. Shaner, Z. Cheng, R. Y. Tsien and R. E. Campbell (2007). "Exploration of new chromophore structures leads to the identification of improved blue fluorescent proteins." Biochemistry **46**(20): 5904-5910.

Akache, B., D. Grimm, K. Pandey, S. R. Yant, H. Xu and M. A. Kay (2006). "The 37/67-kilodalton laminin receptor is a receptor for adeno-associated virus serotypes 8, 2, 3, and 9." J Virol **80**(19): 9831-9836.

Alexander, I. E., D. W. Russell and A. D. Miller (1994). "DNA-damaging agents greatly increase the transduction of nondividing cells by adeno-associated virus vectors." J Virol **68**(12): 8282-8287.

Alisky, J. M., S. M. Hughes, S. L. Sauter, D. Jolly, T. W. Dubensky, Jr., P. D. Staber, J. A. Chiorini and B. L. Davidson (2000). "Transduction of murine cerebellar neurons with recombinant FIV and AAV5 vectors." Neuroreport **11**(12): 2669-2673.

Allen, H. D., K. M. Flanigan, P. T. Thrush, I. Dvorchik, H. Yin, C. Canter, A. M. Connolly, M. Parrish, C. M. McDonald, E. Braunlin, S. D. Colan, J. Day, B. Darras and J. R. Mendell (2013). "A randomized, double-blind trial of lisinopril and losartan for the treatment of cardiomyopathy in duchenne muscular dystrophy." PLoS Curr **5**.

Allen, J. M., C. L. Halbert and A. D. Miller (2000). "Improved adeno-associated virus vector production with transfection of a single helper adenovirus gene, E4orf6." Mol Ther **1**(1): 88-95.

Ambrosio, C. E., M. C. Valadares, E. Zucconi, R. Cabral, P. L. Pearson, T. P. Gaiad, M. Canovas, M. Vainzof, M. A. Miglino and M. Zatz (2008). "Ringo, a Golden Retriever

Muscular Dystrophy (GRMD) dog with absent dystrophin but normal strength." Neuromuscul Disord **18**(11): 892-893.

Aoki, Y., T. Yokota, T. Nagata, A. Nakamura, J. Tanihata, T. Saito, S. M. Duguez, K. Nagaraju, E. P. Hoffman, T. Partridge and S. Takeda (2012). "Bodywide skipping of exons 45-55 in dystrophic mdx52 mice by systemic antisense delivery." Proc Natl Acad Sci U S A **109**(34): 13763-13768.

Araki, E., K. Nakamura, K. Nakao, S. Kameya, O. Kobayashi, I. Nonaka, T. Kobayashi and M. Katsuki (1997). "Targeted disruption of exon 52 in the mouse dystrophin gene induced muscle degeneration similar to that observed in Duchenne muscular dystrophy." Biochem Biophys Res Commun **238**(2): 492-497.

Arnett, A. L., L. R. Beutler, A. Quintana, J. Allen, E. Finn, R. D. Palmiter and J. S. Chamberlain (2013). "Heparin-binding correlates with increased efficiency of AAV1- and AAV6-mediated transduction of striated muscle, but negatively impacts CNS transduction." Gene Ther **20**(5): 497-503.

Asokan, A., D. V. Schaffer and R. J. Samulski (2012). "The AAV vector toolkit: poised at the clinical crossroads." Mol Ther **20**(4): 699-708.

Atchison, R. W., B. C. Casto and W. M. Hammon (1965). "Adenovirus-Associated Defective Virus Particles." Science **149**(3685): 754-756.

Ayuso, E., F. Mingozzi, J. Montane, X. Leon, X. M. Anguela, V. Haurigot, S. A. Edmonson, L. Africa, S. Zhou, K. A. High, F. Bosch and J. F. Wright (2010). "High AAV vector purity results in serotype- and tissue-independent enhancement of transduction efficiency." Gene Ther **17**(4): 503-510.

Baloh, R. and P. A. Cancilla (1972). "An appraisal of histochemical fiber types in Duchenne muscular dystrophy." Neurology **22**(12): 1243-1252.

Banks, G. B. and J. S. Chamberlain (2008). "The value of mammalian models for duchenne muscular dystrophy in developing therapeutic strategies." Curr Top Dev Biol **84**: 431-453.

Banks, G. B., A. C. Combs, J. R. Chamberlain and J. S. Chamberlain (2008). "Molecular and cellular adaptations to chronic myotendinous strain injury in mdx mice expressing a truncated dystrophin." Hum Mol Genet **17**(24): 3975-3986.

Banks, G. B., P. Gregorevic, J. M. Allen, E. E. Finn and J. S. Chamberlain (2007). "Functional capacity of dystrophins carrying deletions in the N-terminal actin-binding domain." Hum Mol Genet **16**(17): 2105-2113.

Banks, G. B., L. M. Judge, J. M. Allen and J. S. Chamberlain (2010). "The polyproline site in hinge 2 influences the functional capacity of truncated dystrophins." PLoS Genet **6**(5): e1000958.

Bantel-Schaal, U., I. Braspenning-Wesch and J. Kartenbeck (2009). "Adeno-associated virus type 5 exploits two different entry pathways in human embryo fibroblasts." J Gen Virol **90**(Pt 2): 317-322.

Bantel-Schaal, U., B. Hub and J. Kartenbeck (2002). "Endocytosis of adeno-associated virus type 5 leads to accumulation of virus particles in the Golgi compartment." J Virol **76**(5): 2340-2349.

Barton-Davis, E. R., L. Cordier, D. I. Shoturma, S. E. Leland and H. L. Sweeney (1999). "Aminoglycoside antibiotics restore dystrophin function to skeletal muscles of mdx mice." J Clin Invest **104**(4): 375-381.

Bauer, R., V. Straub, A. Blain, K. Bushby and G. A. MacGowan (2009). "Contrasting effects of steroids and angiotensin-converting-enzyme inhibitors in a mouse model of dystrophin-deficient cardiomyopathy." Eur J Heart Fail **11**(5): 463-471.

Beggs, A. H., E. P. Hoffman, J. R. Snyder, K. Arahata, L. Specht, F. Shapiro, C. Angelini, H. Sugita and L. M. Kunkel (1991). "Exploring the molecular basis for variability among patients with Becker muscular dystrophy: dystrophin gene and protein studies." Am J Hum Genet **49**(1): 54-67.

Belanto, J. J., T. L. Mader, M. D. Eckhoff, D. M. Strandjord, G. B. Banks, M. K. Gardner, D. A. Lowe and J. M. Ervasti (2014). "Microtubule binding distinguishes dystrophin from utrophin." Proc Natl Acad Sci U S A **111**(15): 5723-5728.

Benedetti, S., H. Hoshiya and F. S. Tedesco (2013). "Repair or replace? Exploiting novel gene and cell therapy strategies for muscular dystrophies." FEBS J **280**(17): 4263-4280.

Bennett, S. R., F. R. Carbone, F. Karamalis, R. A. Flavell, J. F. Miller and W. R. Heath (1998). "Help for cytotoxic-T-cell responses is mediated by CD40 signalling." Nature **393**(6684): 478-480.

Bhosle, R. C., D. E. Michele, K. P. Campbell, Z. Li and R. M. Robson (2006). "Interactions of intermediate filament protein synemin with dystrophin and utrophin." Biochem Biophys Res Commun **346**(3): 768-777.

Bieber, S., J. B. Halldorson, E. Finn, S. Ahmad, J. S. Chamberlain and G. L. Odom (2013). "Extracorporeal delivery of rAAV with metabolic exchange and oxygenation." Sci Rep **3**: 1538.

Biggar, W. D., V. A. Harris, L. Eliasoph and B. Alman (2006). "Long-term benefits of deflazacort treatment for boys with Duchenne muscular dystrophy in their second decade." Neuromuscul Disord **16**(4): 249-255.

Bish, L. T., M. M. Sleeper, B. Brainard, S. Cole, N. Russell, E. Withnall, J. Arndt, C. Reynolds, E. Davison, J. Sanmiguel, D. Wu, G. Gao, J. M. Wilson and H. L. Sweeney (2008). "Percutaneous transendocardial delivery of self-complementary adeno-associated virus 6 achieves global cardiac gene transfer in canines." Mol Ther **16**(12): 1953-1959.

Bish, L. T., M. M. Sleeper and H. L. Sweeney (2011). "Percutaneous transendocardial delivery of self-complementary adeno-associated virus 6 in the canine." Methods in Molecular Biology **709**: 369-378.

Blake, D. J., A. Weir, S. E. Newey and K. E. Davies (2002). "Function and genetics of dystrophin and dystrophin-related proteins in muscle." Physiol Rev **82**(2): 291-329.

Blankinship, M., P. Gregorevic and J. Chamberlain (2006). Gene Therapy of Muscular Dystrophy Using Adeno-Associated Viral Vectors: Promises and Limitations. Duchenne Muscular Dystrophy: Advances in Therapeutics. J. Chamberlain and T. Rando, Informa Healthcare**:** 413-438.

Blankinship, M. J., P. Gregorevic, J. M. Allen, S. Q. Harper, H. Harper, C. L. Halbert, A. D. Miller and J. S. Chamberlain (2004). "Efficient transduction of skeletal muscle using vectors based on adeno-associated virus serotype 6." Mol Ther **10**(4): 671-678.

Boutin, S., V. Monteilhet, P. Veron, C. Leborgne, O. Benveniste, M. F. Montus and C. Masurier (2010). "Prevalence of serum IgG and neutralizing factors against adeno-associated virus (AAV) types 1, 2, 5, 6, 8, and 9 in the healthy population: implications for gene therapy using AAV vectors." Hum Gene Ther **21**(6): 704-712.

Brack, A. S., I. M. Conboy, M. J. Conboy, J. Shen and T. A. Rando (2008). "A temporal switch from notch to Wnt signaling in muscle stem cells is necessary for normal adult myogenesis." Cell Stem Cell **2**(1): 50-59.

Brenman, J. E., D. S. Chao, H. Xia, K. Aldape and D. S. Bredt (1995). "Nitric oxide synthase complexed with dystrophin and absent from skeletal muscle sarcolemma in Duchenne muscular dystrophy." Cell **82**(5): 743-752.

Brooks, S. V. and J. A. Faulkner (1988). "Contractile properties of skeletal muscles from young, adult and aged mice." J Physiol **404**: 71-82.

Brunelli, S. and P. Rovere-Querini (2008). "The immune system and the repair of skeletal muscle." Pharmacol Res **58**(2): 117-121.

Buchlis, G., G. M. Podsakoff, A. Radu, S. M. Hawk, A. W. Flake, F. Mingozzi and K. A. High (2012). "Factor IX expression in skeletal muscle of a severe hemophilia B patient 10 years after AAV-mediated gene transfer." Blood **119**(13): 3038-3041.

Bulfield, G., W. G. Siller, P. A. Wight and K. J. Moore (1984). "X chromosome-linked muscular dystrophy (mdx) in the mouse." Proc Natl Acad Sci U S A **81**(4): 1189-1192.

Burger, C., O. S. Gorbatyuk, M. J. Velardo, C. S. Peden, P. Williams, S. Zolotukhin, P. J. Reier, R. J. Mandel and N. Muzyczka (2004). "Recombinant AAV viral vectors pseudotyped with viral capsids from serotypes 1, 2, and 5 display differential efficiency and cell tropism after delivery to different regions of the central nervous system." Mol Ther **10**(2): 302-317.

Burkholder, T. J., B. Fingado, S. Baron and R. L. Lieber (1994). "Relationship between muscle fiber types and sizes and muscle architectural properties in the mouse hindlimb." J Morphol **221**(2): 177-190.

Burkin, D. J. and S. J. Kaufman (1999). "The alpha7beta1 integrin in muscle development and disease." Cell Tissue Res **296**(1): 183-190.

Burzyn, D., W. Kuswanto, D. Kolodin, J. L. Shadrach, M. Cerletti, Y. Jang, E. Sefik, T. G. Tan, A. J. Wagers, C. Benoist and D. Mathis (2013). "A special population of regulatory T cells potentiates muscle repair." Cell **155**(6): 1282-1295.

Bushby, K., R. Finkel, D. J. Birnkrant, L. E. Case, P. R. Clemens, L. Cripe, A. Kaul, K. Kinnett, C. McDonald, S. Pandya, J. Poysky, F. Shapiro, J. Tomezsko, C. Constantin and D. M. D. C. C. W. Group (2010). "Diagnosis and management of Duchenne muscular dystrophy, part 2: implementation of multidisciplinary care." Lancet Neurol **9**(2): 177-189.

Bushby, K., F. Muntoni and J. P. Bourke (2003). "107th ENMC international workshop: the management of cardiac involvement in muscular dystrophy and myotonic dystrophy. 7th-9th June 2002, Naarden, the Netherlands." Neuromuscular disorders : NMD **13**(2): 166-172.

Calcedo, R., L. H. Vandenberghe, G. Gao, J. Lin and J. M. Wilson (2009). "Worldwide epidemiology of neutralizing antibodies to adeno-associated viruses." J Infect Dis **199**(3): 381-390.

Campbell, K. P. (1995). "Three muscular dystrophies: loss of cytoskeleton-extracellular matrix linkage." Cell **80**(5): 675-679.

Campbell, K. P. and S. D. Kahl (1989). "Association of dystrophin and an integral membrane glycoprotein." Nature **338**(6212): 259-262.

Carnwath, J. W. and D. M. Shotton (1987). "Muscular dystrophy in the mdx mouse: histopathology of the soleus and extensor digitorum longus muscles." J Neurol Sci **80**(1): 39-54.

Chamberlain, J. (2004). "PCR-mediated Mutagenesis."

Chamberlain, J. and T. Rando (2006). Duchenne Muscular Dystrophy: Advances in Therapeutics. New York, Taylor and Francis.

Chamberlain, J. R. and J. S. Chamberlain (2010). "Muscling in: Gene therapies for muscular dystrophy target RNA." Nat Med **16**(2): 170-171.

Chamberlain, J. R., U. Schwarze, P. R. Wang, R. K. Hirata, K. D. Hankenson, J. M. Pace, R. A. Underwood, K. M. Song, M. Sussman, P. H. Byers and D. W. Russell (2004). "Gene targeting in stem cells from individuals with osteogenesis imperfecta." Science **303**(5661): 1198-1201.

Chamberlain, J. S., J. B. Jaynes and S. D. Hauschka (1985). "Regulation of creatine kinase induction in differentiating mouse myoblasts." Mol Cell Biol **5**(3): 484-492.

Chamberlain, J. S., J. Metzger, M. Reyes, D. Townsend and J. A. Faulkner (2007). "Dystrophin-deficient mdx mice display a reduced life span and are susceptible to spontaneous rhabdomyosarcoma." FASEB J **21**(9): 2195-2204.

Chao, H., Y. Liu, J. Rabinowitz, C. Li, R. J. Samulski and C. E. Walsh (2000). "Several log increase in therapeutic transgene delivery by distinct adeno-associated viral serotype vectors." Mol Ther **2**(6): 619-623.

Chapman, V. M., D. R. Miller, D. Armstrong and C. T. Caskey (1989). "Recovery of induced mutations for X chromosome-linked muscular dystrophy in mice." Proc Natl Acad Sci U S A **86**(4): 1292-1296.

Chicoine, L. G., C. L. Montgomery, W. G. Bremer, K. M. Shontz, D. A. Griffin, K. N. Heller, S. Lewis, V. Malik, W. E. Grose, C. J. Shilling, K. J. Campbell, T. J. Preston, B. D. Coley, P. T. Martin, C. M. Walker, K. R. Clark, Z. Sahenk, J. R. Mendell and L. R. Rodino-Klapac (2014). "Plasmapheresis eliminates the negative impact of AAV antibodies on microdystrophin gene expression following vascular delivery." Mol Ther **22**(2): 338-347.

Childers, M. K., R. Joubert, K. Poulard, C. Moal, R. W. Grange, J. A. Doering, M. W. Lawlor, B. E. Rider, T. Jamet, N. Daniele, S. Martin, C. Riviere, T. Soker, C. Hammer, L. Van Wittenberghe, M. Lockard, X. Guan, M. Goddard, E. Mitchell, J. Barber, J. K. Williams, D. L. Mack, M. E. Furth, A. Vignaud, C. Masurier, F. Mavilio, P. Moullier, A. H. Beggs and A. Buj-Bello (2014). "Gene therapy prolongs survival and restores function in murine and canine models of myotubular myopathy." Sci Transl Med **6**(220): 220ra210.

Chirmule, N., K. Propert, S. Magosin, Y. Qian, R. Qian and J. Wilson (1999). "Immune responses to adenovirus and adeno-associated virus in humans." Gene Ther **6**(9): 1574-1583.

Chirmule, N., W. Xiao, A. Truneh, M. A. Schnell, J. V. Hughes, P. Zoltick and J. M. Wilson (2000). "Humoral Immunity to Adeno-Associated Virus Type 2 Vectors following Administration to Murine and Nonhuman Primate Muscle." Journal of Virology **74**(5): 2420-2425.

Clegg, C. H., T. A. Linkhart, B. B. Olwin and S. D. Hauschka (1987). "Growth factor control of skeletal muscle differentiation: commitment to terminal differentiation occurs in G1 phase and is repressed by fibroblast growth factor." J Cell Biol **105**(2): 949-956.

Coccia, E. M., M. Severa, E. Giacomini, D. Monneron, M. E. Remoli, I. Julkunen, M. Cella, R. Lande and G. Uze (2004). "Viral infection and Toll-like receptor agonists induce a differential expression of type I and lambda interferons in human plasmacytoid and monocyte-derived dendritic cells." Eur J Immunol **34**(3): 796-805.

Cohn, R. D., C. van Erp, J. P. Habashi, A. A. Soleimani, E. C. Klein, M. T. Lisi, M. Gamradt, C. M. ap Rhys, T. M. Holm, B. L. Loeys, F. Ramirez, D. P. Judge, C. W. Ward and H. C. Dietz (2007). "Angiotensin II type 1 receptor blockade attenuates TGF-beta-induced failure of muscle regeneration in multiple myopathic states." Nat Med **13**(2): 204-210.

Constantin, B. (2014). "Dystrophin complex functions as a scaffold for signalling proteins." Biochim Biophys Acta **1838**(2): 635-642.

Cooper, B. J., N. J. Winand, H. Stedman, B. A. Valentine, E. P. Hoffman, L. M. Kunkel, M. O. Scott, K. H. Fischbeck, J. N. Kornegay, R. J. Avery and et al. (1988). "The homologue of the Duchenne locus is defective in X-linked muscular dystrophy of dogs." Nature **334**(6178): 154-156.

Cordier, L., G. P. Gao, A. A. Hack, E. M. McNally, J. M. Wilson, N. Chirmule and H. L. Sweeney (2001). "Muscle-specific promoters may be necessary for adeno-associated virus-mediated gene transfer in the treatment of muscular dystrophies." Hum Gene Ther **12**(2): 205-215.

Corrado, K., J. A. Rafael, P. L. Mills, N. M. Cole, J. A. Faulkner, K. Wang and J. S. Chamberlain (1996). "Transgenic mdx mice expressing dystrophin with a deletion in the actin-binding domain display a "mild Becker" phenotype." J Cell Biol **134**(4): 873-884.

Coulton, G. R., N. A. Curtin, J. E. Morgan and T. A. Partridge (1988). "The mdx mouse skeletal muscle myopathy: II. Contractile properties." Neuropathol Appl Neurobiol **14**(4): 299-314.

Coulton, G. R., J. E. Morgan, T. A. Partridge and J. C. Sloper (1988). "The mdx mouse skeletal muscle myopathy: I. A histological, morphometric and biochemical investigation." Neuropathol Appl Neurobiol **14**(1): 53-70.

Cousens, L. P., R. Peterson, S. Hsu, A. Dorner, J. D. Altman, R. Ahmed and C. A. Biron (1999). "Two roads diverged: interferon alpha/beta- and interleukin 12-mediated pathways in promoting T cell interferon gamma responses during viral infection." J Exp Med **189**(8): 1315-1328.

Coutelier, J. P., J. T. van der Logt, F. W. Heessen, G. Warnier and J. Van Snick (1987). "IgG2a restriction of murine antibodies elicited by viral infections." J Exp Med **165**(1): 64-69.

Cox, G. A., N. M. Cole, K. Matsumura, S. F. Phelps, S. D. Hauschka, K. P. Campbell, J. A. Faulkner and J. S. Chamberlain (1993). "Overexpression of dystrophin in transgenic mdx mice eliminates dystrophic symptoms without toxicity." Nature **364**(6439): 725-729.

Cox, G. A., S. F. Phelps, V. M. Chapman and J. S. Chamberlain (1993). "New mdx mutation disrupts expression of muscle and nonmuscle isoforms of dystrophin." Nat Genet **4**(1): 87-93.

Cox, G. A., Y. Sunada, K. P. Campbell and J. S. Chamberlain (1994). "Dp71 can restore the dystrophin-associated glycoprotein complex in muscle but fails to prevent dystrophy." Nat Genet **8**(4): 333-339.

Crawford, G. E., J. A. Faulkner, R. H. Crosbie, K. P. Campbell, S. C. Froehner and J. S. Chamberlain (2000). "Assembly of the dystrophin-associated protein complex does not require the dystrophin COOH-terminal domain." J Cell Biol **150**(6): 1399-1410.

Crosbie, R. H., J. Heighway, D. P. Venzke, J. C. Lee and K. P. Campbell (1997). "Sarcospan, the 25-kDa transmembrane component of the dystrophin-glycoprotein complex." J Biol Chem **272**(50): 31221-31224.

Darras, B. T., P. Blattner, J. F. Harper, A. J. Spiro, S. Alter and U. Francke (1988). "Intragenic deletions in 21 Duchenne muscular dystrophy (DMD)/Becker muscular dystrophy (BMD) families studied with the dystrophin cDNA: location of breakpoints on HindIII and BglII exon-containing fragment maps, meiotic and mitotic origin of the mutations." Am J Hum Genet **43**(5): 620-629.

Darras, B. T. and H. R. Jones (2000). "Diagnosis of pediatric neuromuscular disorders in the era of DNA analysis." Pediatr Neurol **23**(4): 289-300.

Davidson, B. L., C. S. Stein, J. A. Heth, I. Martins, R. M. Kotin, T. A. Derksen, J. Zabner, A. Ghodsi and J. A. Chiorini (2000). "Recombinant adeno-associated virus type 2, 4, and 5 vectors: transduction of variant cell types and regions in the mammalian central nervous system." Proc Natl Acad Sci U S A **97**(7): 3428-3432.

Davie, A. M. and A. E. Emery (1978). "Estimation of proportion of new mutants among cases of Duchenne muscular dystrophy." J Med Genet **15**(5): 339-345.

Davies, K. E., P. L. Pearson, P. S. Harper, J. M. Murray, T. O'Brien, M. Sarfarazi and R. Williamson (1983). "Linkage analysis of two cloned DNA sequences flanking the Duchenne muscular dystrophy locus on the short arm of the human X chromosome." Nucleic Acids Res **11**(8): 2303-2312.

Day, K., G. Shefer, J. B. Richardson, G. Enikolopov and Z. Yablonka-Reuveni (2007). "Nestin-GFP reporter expression defines the quiescent state of skeletal muscle satellite cells." Dev Biol **304**(1): 246-259.

Deconinck, A. E., J. A. Rafael, J. A. Skinner, S. C. Brown, A. C. Potter, L. Metzinger, D. J. Watt, J. G. Dickson, J. M. Tinsley and K. E. Davies (1997). "Utrophin-dystrophin-deficient mice as a model for Duchenne muscular dystrophy." Cell **90**(4): 717-727.

DelloRusso, C., J. M. Scott, D. Hartigan-O'Connor, G. Salvatori, C. Barjot, A. S. Robinson, R. W. Crawford, S. V. Brooks and J. S. Chamberlain (2002). "Functional correction of adult mdx mouse muscle using gutted adenoviral vectors expressing full-length dystrophin." Proc Natl Acad Sci U S A **99**(20): 12979-12984.

Demaster, A., X. Luo, S. Curtis, K. D. Williams, D. J. Landau, E. J. Drake, D. M. Kozink, A. Bird, B. Crane, F. Sun, C. R. Pinto, T. T. Brown, A. R. Kemper and D. D. Koeberl (2012). "Long-term efficacy following readministration of an adeno-associated virus vector in dogs with glycogen storage disease type Ia." Hum Gene Ther **23**(4): 407-418.

Denard, J., C. Beley, R. Kotin, R. Lai-Kuen, S. Blot, H. Leh, A. Asokan, R. J. Samulski, P. Moullier, T. Voit, L. Garcia and F. Svinartchouk (2012). "Human galectin 3 binding protein interacts with recombinant adeno-associated virus type 6." Journal of Virology **86**(12): 6620-6631.

Dong, B., H. Nakai and W. Xiao (2010). "Characterization of genome integrity for oversized recombinant AAV vector." Mol Ther **18**(1): 87-92.

Donoviel, D. B., M. A. Shield, J. N. Buskin, H. S. Haugen, C. H. Clegg and S. D. Hauschka (1996). "Analysis of muscle creatine kinase gene regulatory elements in skeletal and cardiac muscles of transgenic mice." Mol Cell Biol **16**(4): 1649-1658.

Dorner, T. and A. Radbruch (2007). "Antibodies and B cell memory in viral immunity." Immunity **27**(3): 384-392.

Duan, D. (2011). "Duchenne muscular dystrophy gene therapy: Lost in translation?" Res Rep Biol **2011**(2): 31-42.

Duan, D., P. Sharma, J. Yang, Y. Yue, L. Dudus, Y. Zhang, K. J. Fisher and J. F. Engelhardt (1998). "Circular intermediates of recombinant adeno-associated virus have defined structural characteristics responsible for long-term episomal persistence in muscle tissue." J Virol **72**(11): 8568-8577.

Duboc, D., C. Meune, B. Pierre, K. Wahbi, B. Eymard, A. Toutain, C. Berard, G. Vaksmann, S. Weber and H. M. Becane (2007). "Perindopril preventive treatment on mortality in Duchenne muscular dystrophy: 10 years' follow-up." Am Heart J **154**(3): 596-602.

Dunant, P., M. C. Walter, G. Karpati and H. Lochmuller (2003). "Gentamicin fails to increase dystrophin expression in dystrophin-deficient muscle." Muscle Nerve **27**(5): 624-627.

Dunckley, M. G., D. R. Love, K. E. Davies, F. S. Walsh, G. E. Morris and G. Dickson (1992). "Retroviral-mediated transfer of a dystrophin minigene into mdx mouse myoblasts in vitro." FEBS Lett **296**(2): 128-134.

Emery, A. E. (2002). "The muscular dystrophies." Lancet **359**(9307): 687-695.

Emery, A. E. H. (2003). Duchenne muscular dystrophy. Oxford ; New York, Oxford University Press.

England, S. B., L. V. Nicholson, M. A. Johnson, S. M. Forrest, D. R. Love, E. E. Zubrzycka-Gaarn, D. E. Bulman, J. B. Harris and K. E. Davies (1990). "Very mild muscular dystrophy associated with the deletion of 46% of dystrophin." Nature **343**(6254): 180-182.

Ervasti, J. M. (2003). "Costameres: the Achilles' heel of Herculean muscle." J Biol Chem **278**(16): 13591-13594.

Fabbrizio, E., A. Bonet-Kerrache, J. J. Leger and D. Mornet (1993). "Actin-dystrophin interface." Biochemistry **32**(39): 10457-10463.

Faust, S. M., P. Bell, B. J. Cutler, S. N. Ashley, Y. Zhu, J. E. Rabinowitz and J. M. Wilson (2013). "CpG-depleted adeno-associated virus vectors evade immune detection." J Clin Invest **123**(7): 2994-3001.

Fedorov, Y. V., N. C. Jones and B. B. Olwin (1998). "Regulation of myogenesis by fibroblast growth factors requires beta-gamma subunits of pertussis toxin-sensitive G proteins." Mol Cell Biol **18**(10): 5780-5787.

Felsburg, P. J. (2002). "Overview of immune system development in the dog: comparison with humans." Human and Experimental Toxicology **21**(9-10): 487-492.

Finsterer, J. and C. Stollberger (2003). "The heart in human dystrophinopathies." Cardiology **99**(1): 1-19.

Flanigan, K. M., K. Campbell, L. Viollet, W. Wang, A. M. Gomez, C. M. Walker and J. R. Mendell (2013). "Anti-dystrophin T cell responses in Duchenne muscular dystrophy: prevalence and a glucocorticoid treatment effect." Human Gene Therapy **24**(9): 797-806.

Forrest, S. M., G. S. Cross, A. Speer, D. Gardner-Medwin, J. Burn and K. E. Davies (1987). "Preferential deletion of exons in Duchenne and Becker muscular dystrophies." Nature **329**(6140): 638-640.

Foster, H., P. S. Sharp, T. Athanasopoulos, C. Trollet, I. R. Graham, K. Foster, D. J. Wells and G. Dickson (2008). "Codon and mRNA sequence optimization of microdystrophin transgenes improves expression and physiological outcome in dystrophic mdx mice following AAV2/8 gene transfer." Mol Ther **16**(11): 1825-1832.

Fougerousse, F., M. Bartoli, J. Poupiot, L. Arandel, M. Durand, N. Guerchet, E. Gicquel, O. Danos and I. Richard (2007). "Phenotypic correction of alpha-sarcoglycan deficiency by intra-arterial injection of a muscle-specific serotype 1 rAAV vector." Molecular therapy : the journal of the American Society of Gene Therapy **15**(1): 53-61.

Gao, G., L. T. Bish, M. M. Sleeper, X. Mu, L. Sun, Y. Lou, J. Duan, C. Hu, L. Wang and H. L. Sweeney (2011). "Transendocardial delivery of AAV6 results in highly efficient and global cardiac gene transfer in rhesus macaques." Hum Gene Ther **22**(8): 979-984.

Gao, G. P., M. R. Alvira, L. Wang, R. Calcedo, J. Johnston and J. M. Wilson (2002). "Novel adeno-associated viruses from rhesus monkeys as vectors for human gene therapy." Proc Natl Acad Sci U S A **99**(18): 11854-11859.

Gardner, K. L., J. A. Kearney, J. D. Edwards and J. A. Rafael-Fortney (2006). "Restoration of all dystrophin protein interactions by functional domains in trans does not rescue dystrophy." Gene Ther **13**(9): 744-751.

Gaschen, F. P., E. P. Hoffman, J. R. Gorospe, E. W. Uhl, D. F. Senior, G. H. Cardinet, 3rd and L. K. Pearce (1992). "Dystrophin deficiency causes lethal muscle hypertrophy in cats." J Neurol Sci **110**(1-2): 149-159.

Gilbert, R., R. W. Dudley, A. B. Liu, B. J. Petrof, J. Nalbantoglu and G. Karpati (2003). "Prolonged dystrophin expression and functional correction of mdx mouse muscle following gene transfer with a helper-dependent (gutted) adenovirus-encoding murine dystrophin." Hum Mol Genet **12**(11): 1287-1299.

Gilchrist, S. C., M. P. Ontell, S. Kochanek and P. R. Clemens (2002). "Immune response to full-length dystrophin delivered to Dmd muscle by a high-capacity adenoviral vector." Mol Ther **6**(3): 359-368.

Goldberg, L. R., I. Hausmanowa-Petrusewicz, A. Fidzianska, D. J. Duggan, L. S. Steinberg and E. P. Hoffman (1998). "A dystrophin missense mutation showing persistence of dystrophin and dystrophin-associated proteins yet a severe phenotype." Ann Neurol **44**(6): 971-976.

Gomez-Merino, E. and J. R. Bach (2002). "Duchenne muscular dystrophy: prolongation of life by noninvasive ventilation and mechanically assisted coughing." American journal of physical medicine & rehabilitation / Association of Academic Physiatrists **81**(6): 411-415.

Goncalves, M. A., J. M. Janssen, Q. G. Nguyen, T. Athanasopoulos, S. D. Hauschka, G. Dickson and A. A. de Vries (2011). "Transcription factor rational design improves directed differentiation of human mesenchymal stem cells into skeletal myocytes." Mol Ther **19**(7): 1331-1341.

Graca, L., K. Honey, E. Adams, S. P. Cobbold and H. Waldmann (2000). "Cutting edge: anti-CD154 therapeutic antibodies induce infectious transplantation tolerance." J Immunol **165**(9): 4783-4786.

Grady, R. M., R. W. Grange, K. S. Lau, M. M. Maimone, M. C. Nichol, J. T. Stull and J. R. Sanes (1999). "Role for alpha-dystrobrevin in the pathogenesis of dystrophin-dependent muscular dystrophies." Nat Cell Biol **1**(4): 215-220.

Greenberg, D. S., Y. Sunada, K. P. Campbell, D. Yaffe and U. Nudel (1994). "Exogenous Dp71 restores the levels of dystrophin associated proteins but does not alleviate muscle damage in mdx mice." Nat Genet **8**(4): 340-344.

Greer, K. L., H. Lochmuller, K. Flanigan, S. Fletcher and S. D. Wilton (2014). "Targeted exon skipping to correct exon duplications in the dystrophin gene." Mol Ther Nucleic Acids **3**: e155.

Gregorevic, P., J. M. Allen, E. Minami, M. J. Blankinship, M. Haraguchi, L. Meuse, E. Finn, M. E. Adams, S. C. Froehner, C. E. Murry and J. S. Chamberlain (2006). "rAAV6-microdystrophin preserves muscle function and extends lifespan in severely dystrophic mice." Nat Med **12**(7): 787-789.

Gregorevic, P., M. J. Blankinship, J. M. Allen, R. W. Crawford, L. Meuse, D. G. Miller, D. W. Russell and J. S. Chamberlain (2004). "Systemic delivery of genes to striated muscles using adeno-associated viral vectors." Nat Med **10**(8): 828-834.

Gregorevic, P., D. R. Plant, K. S. Leeding, L. A. Bach and G. S. Lynch (2002). "Improved contractile function of the mdx dystrophic mouse diaphragm muscle after insulin-like growth factor-I administration." Am J Pathol **161**(6): 2263-2272.

Gregorevic, P., B. R. Schultz, J. M. Allen, J. B. Halldorson, M. J. Blankinship, N. A. Meznarich, C. S. Kuhr, C. Doremus, E. Finn, D. Liggitt and J. S. Chamberlain (2009). "Evaluation of vascular delivery methodologies to enhance rAAV6-mediated gene transfer to canine striated musculature." Mol Ther **17**(8): 1427-1433.

Hadri, L., R. Bobe, Y. Kawase, D. Ladage, K. Ishikawa, F. Atassi, D. Lebeche, E. G. Kranias, J. A. Leopold, A. M. Lompre, L. Lipskaia and R. J. Hajjar (2010). "SERCA2a gene transfer enhances eNOS expression and activity in endothelial cells." Mol Ther **18**(7): 1284-1292.

Halbert, C. L., D. K. Madtes, A. E. Vaughan, Z. Wang, R. Storb, S. J. Tapscott and A. D. Miller (2010). "Expression of human alpha1-antitrypsin in mice and dogs following AAV6 vector-mediated gene transfer to the lungs." Molecular therapy : the journal of the American Society of Gene Therapy **18**(6): 1165-1172.

Halbert, C. L., A. D. Miller, S. McNamara, J. Emerson, R. L. Gibson, B. Ramsey and M. L. Aitken (2006). "Prevalence of neutralizing antibodies against adeno-associated virus (AAV) types 2, 5, and 6 in cystic fibrosis and normal populations: Implications for gene therapy using AAV vectors." Human Gene Therapy **17**(4): 440-447.

Halbert, C. L., E. A. Rutledge, J. M. Allen, D. W. Russell and A. D. Miller (2000). "Repeat transduction in the mouse lung by using adeno-associated virus vectors with different serotypes." J Virol **74**(3): 1524-1532.

Halbert, C. L., T. A. Standaert, M. L. Aitken, I. E. Alexander, D. W. Russell and A. D. Miller (1997). "Transduction by adeno-associated virus vectors in the rabbit airway: efficiency, persistence, and readministration." J Virol **71**(8): 5932-5941.

Halbert, C. L., T. A. Standaert, C. B. Wilson and A. D. Miller (1998). "Successful readministration of adeno-associated virus vectors to the mouse lung requires transient immunosuppression during the initial exposure." J Virol **72**(12): 9795-9805.

Hannon, K., A. J. Kudla, M. J. McAvoy, K. L. Clase and B. B. Olwin (1996). "Differentially expressed fibroblast growth factors regulate skeletal muscle development through autocrine and paracrine mechanisms." J Cell Biol **132**(6): 1151-1159.

Harper, S. Q., M. A. Hauser, C. DelloRusso, D. Duan, R. W. Crawford, S. F. Phelps, H. A. Harper, A. S. Robinson, J. F. Engelhardt, S. V. Brooks and J. S. Chamberlain (2002). "Modular flexibility of dystrophin: implications for gene therapy of Duchenne muscular dystrophy." Nat Med **8**(3): 253-261.

Hartigan-O'Connor, D., C. J. Kirk, R. Crawford, J. J. Mule and J. S. Chamberlain (2001). "Immune evasion by muscle-specific gene expression in dystrophic muscle." Mol Ther **4**(6): 525-533.

Hauser, M. A., A. Robinson, D. Hartigan-O'Connor, D. A. Williams-Gregory, J. N. Buskin, S. Apone, C. J. Kirk, S. Hardy, S. D. Hauschka and J. S. Chamberlain (2000). "Analysis of muscle creatine kinase regulatory elements in recombinant adenoviral vectors." Mol Ther **2**(1): 16-25.

Hay, R. T. (2005). "SUMO: a history of modification." Mol Cell **18**(1): 1-12.

Hayashi, S. and A. P. McMahon (2002). "Efficient recombination in diverse tissues by a tamoxifen-inducible form of Cre: a tool for temporally regulated gene activation/inactivation in the mouse." Dev Biol **244**(2): 305-318.

Hemmings, L., P. A. Kuhlman and D. R. Critchley (1992). "Analysis of the actin-binding domain of alpha-actinin by mutagenesis and demonstration that dystrophin contains a functionally homologous domain." J Cell Biol **116**(6): 1369-1380.

Herson, S., F. Hentati, A. Rigolet, A. Behin, N. B. Romero, F. Leturcq, P. Laforet, T. Maisonobe, R. Amouri, H. Haddad, M. Audit, M. Montus, C. Masurier, B. Gjata, C. Georger, M. Cherai, P. Carlier, J. Y. Hogrel, A. Herson, Y. Allenbach, F. M. Lemoine, D. Klatzmann, H. L. Sweeney, R. C. Mulligan, B. Eymard, D. Caizergues, T. Voit and O. Benveniste (2012). "A phase I trial of adeno-associated virus serotype 1-gamma-sarcoglycan gene therapy for limb girdle muscular dystrophy type 2C." Brain **135**(Pt 2): 483-492.

Hoffman, E. P., R. H. Brown, Jr. and L. M. Kunkel (1987). "Dystrophin: the protein product of the Duchenne muscular dystrophy locus." Cell **51**(6): 919-928.

Honey, K., S. P. Cobbold and H. Waldmann (1999). "CD40 ligand blockade induces CD4+ T cell tolerance and linked suppression." J Immunol **163**(9): 4805-4810.

Horowitz, E. D., K. S. Rahman, B. D. Bower, D. J. Dismuke, M. R. Falvo, J. D. Griffith, S. C. Harvey and A. Asokan (2013). "Biophysical and ultrastructural characterization of adeno-associated virus capsid uncoating and genome release." J Virol **87**(6): 2994-3002.

Hsu, P. D., E. S. Lander and F. Zhang (2014). "Development and Applications of CRISPR-Cas9 for Genome Engineering." Cell **157**(6): 1262-1278.

Huard, J., W. G. Feero, S. C. Watkins, E. P. Hoffman, D. J. Rosenblatt and J. C. Glorioso (1996). "The basal lamina is a physical barrier to herpes simplex virus-mediated gene delivery to mature muscle fibers." J Virol **70**(11): 8117-8123.

Huard, J., R. Roy, J. P. Bouchard, F. Malouin, C. L. Richards and J. P. Tremblay (1992). "Human myoblast transplantation between immunohistocompatible donors and recipients produces immune reactions." Transplant Proc **24**(6): 3049-3051.

Hurlbut, G. D., R. J. Ziegler, J. B. Nietupski, J. W. Foley, L. A. Woodworth, E. Meyers, S. D. Bercury, N. N. Pande, D. W. Souza, M. P. Bree, M. J. Lukason, J. Marshall, S. H. Cheng and R. K. Scheule (2010). "Preexisting immunity and low expression in primates highlight translational challenges for liver-directed AAV8-mediated gene therapy." Mol Ther **18**(11): 1983-1994.

Ibraghimov-Beskrovnaya, O., J. M. Ervasti, C. J. Leveille, C. A. Slaughter, S. W. Sernett and K. P. Campbell (1992). "Primary structure of dystrophin-associated glycoproteins linking dystrophin to the extracellular matrix." Nature **355**(6362): 696-702.

Ilsley, J. L., M. Sudol and S. J. Winder (2002). "The WW domain: linking cell signalling to the membrane cytoskeleton." Cell Signal **14**(3): 183-189.

Im, W. B., S. F. Phelps, E. H. Copen, E. G. Adams, J. L. Slightom and J. S. Chamberlain (1996). "Differential expression of dystrophin isoforms in strains of mdx mice with different mutations." Hum Mol Genet **5**(8): 1149-1153.

Inagaki, K., S. Fuess, T. A. Storm, G. A. Gibson, C. F. McTiernan, M. A. Kay and H. Nakai (2006). "Robust systemic transduction with AAV9 vectors in mice: efficient global cardiac gene transfer superior to that of AAV8." Mol Ther **14**(1): 45-53.

Inagaki, K., S. M. Lewis, X. Wu, C. Ma, D. J. Munroe, S. Fuess, T. A. Storm, M. A. Kay and H. Nakai (2007). "DNA palindromes with a modest arm length of greater, similar 20 base pairs are a significant target for recombinant adeno-associated virus vector integration in the liver, muscles, and heart in mice." J Virol **81**(20): 11290-11303.

Inagaki, K., C. Piao, N. M. Kotchey, X. Wu and H. Nakai (2008). "Frequency and spectrum of genomic integration of recombinant adeno-associated virus serotype 8 vector in neonatal mouse liver." J Virol **82**(19): 9513-9524.

Ishikawa-Sakurai, M., M. Yoshida, M. Imamura, K. E. Davies and E. Ozawa (2004). "ZZ domain is essentially required for the physiological binding of dystrophin and utrophin to beta-dystroglycan." Hum Mol Genet **13**(7): 693-702.

Ivanovska, I., G. Wuite, B. Jonsson and A. Evilevitch (2007). "Internal DNA pressure modifies stability of WT phage." Proc Natl Acad Sci U S A **104**(23): 9603-9608.

Janssen, P. M., J. D. Murray, K. E. Schill, N. Rastogi, E. J. Schultz, T. Tran, S. V. Raman and J. A. Rafael-Fortney (2014). "Prednisolone attenuates improvement of cardiac and

skeletal contractile function and histopathology by lisinopril and spironolactone in the mdx mouse model of Duchenne muscular dystrophy." PLoS One **9**(2): e88360.

Jiao, S., P. Williams, R. K. Berg, B. A. Hodgeman, L. Liu, G. Repetto and J. A. Wolff (1992). "Direct gene transfer into nonhuman primate myofibers in vivo." Hum Gene Ther **3**(1): 21-33.

Jones, N. C., Y. V. Fedorov, R. S. Rosenthal and B. B. Olwin (2001). "ERK1/2 is required for myoblast proliferation but is dispensable for muscle gene expression and cell fusion." J Cell Physiol **186**(1): 104-115.

Judge, L. M., M. Haraguchiln and J. S. Chamberlain (2006). "Dissecting the signaling and mechanical functions of the dystrophin-glycoprotein complex." J Cell Sci **119**(Pt 8): 1537-1546.

Kameya, S., Y. Miyagoe, I. Nonaka, T. Ikemoto, M. Endo, K. Hanaoka, Y. Nabeshima and S. Takeda (1999). "alpha1-syntrophin gene disruption results in the absence of neuronal-type nitric-oxide synthase at the sarcolemma but does not induce muscle degeneration." J Biol Chem **274**(4): 2193-2200.

Kawabe, T., T. Naka, K. Yoshida, T. Tanaka, H. Fujiwara, S. Suematsu, N. Yoshida, T. Kishimoto and H. Kikutani (1994). "The immune responses in CD40-deficient mice: impaired immunoglobulin class switching and germinal center formation." Immunity **1**(3): 167-178.

Kenyon, N. S., M. Chatzipetrou, M. Masetti, A. Ranuncoli, M. Oliveira, J. L. Wagner, A. D. Kirk, D. M. Harlan, L. C. Burkly and C. Ricordi (1999). "Long-term survival and function of intrahepatic islet allografts in rhesus monkeys treated with humanized anti-CD154." Proc Natl Acad Sci U S A **96**(14): 8132-8137.

Kimura, E., J. J. Han, S. Li, B. Fall, J. Ra, M. Haraguchi, S. J. Tapscott and J. S. Chamberlain (2008). "Cell-lineage regulated myogenesis for dystrophin replacement: a novel therapeutic approach for treatment of muscular dystrophy." Hum Mol Genet **17**(16): 2507-2517.

Kirk, A. D., L. C. Burkly, D. S. Batty, R. E. Baumgartner, J. D. Berning, K. Buchanan, J. H. Fechner, Jr., R. L. Germond, R. L. Kampen, N. B. Patterson, S. J. Swanson, D. K. Tadaki, C. N. TenHoor, L. White, S. J. Knechtle and D. M. Harlan (1999). "Treatment with humanized monoclonal antibody against CD154 prevents acute renal allograft rejection in nonhuman primates." Nat Med **5**(6): 686-693.

Kobayashi, Y. M., E. P. Rader, R. W. Crawford, N. K. Iyengar, D. R. Thedens, J. A. Faulkner, S. V. Parikh, R. M. Weiss, J. S. Chamberlain, S. A. Moore and K. P. Campbell (2008). "Sarcolemma-localized nNOS is required to maintain activity after mild exercise." Nature **456**(7221): 511-515.

Koenig, M., A. H. Beggs, M. Moyer, S. Scherpf, K. Heindrich, T. Bettecken, G. Meng, C. R. Muller, M. Lindlof, H. Kaariainen and et al. (1989). "The molecular basis for

Duchenne versus Becker muscular dystrophy: correlation of severity with type of deletion." Am J Hum Genet **45**(4): 498-506.

Koenig, M., E. P. Hoffman, C. J. Bertelson, A. P. Monaco, C. Feener and L. M. Kunkel (1987). "Complete cloning of the Duchenne muscular dystrophy (DMD) cDNA and preliminary genomic organization of the DMD gene in normal and affected individuals." Cell **50**(3): 509-517.

Koenig, M., A. P. Monaco and L. M. Kunkel (1988). "The complete sequence of dystrophin predicts a rod-shaped cytoskeletal protein." Cell **53**(2): 219-228.

Koo, T., A. Malerba, T. Athanasopoulos, C. Trollet, L. Boldrin, A. Ferry, L. Popplewell, H. Foster, K. Foster and G. Dickson (2011). "Delivery of AAV2/9-microdystrophin genes incorporating helix 1 of the coiled-coil motif in the C-terminal domain of dystrophin improves muscle pathology and restores the level of alpha1-syntrophin and alpha-dystrobrevin in skeletal muscles of mdx mice." Hum Gene Ther **22**(11): 1379-1388.

Koo, T., T. Okada, T. Athanasopoulos, H. Foster, S. Takeda and G. Dickson (2011). "Long-term functional adeno-associated virus-microdystrophin expression in the dystrophic CXMDj dog." The journal of gene medicine **13**(9): 497-506.

Koo, T., L. Popplewell, T. Athanasopoulos and G. Dickson (2014). "Triple trans-splicing adeno-associated virus vectors capable of transferring the coding sequence for full-length dystrophin protein into dystrophic mice." Hum Gene Ther **25**(2): 98-108.

Koo, T. and M. J. Wood (2013). "Clinical trials using antisense oligonucleotides in duchenne muscular dystrophy." Hum Gene Ther **24**(5): 479-488.

Kornegay, J. N., J. R. Bogan, D. J. Bogan, M. K. Childers, J. Li, P. Nghiem, D. A. Detwiler, C. A. Larsen, R. W. Grange, R. K. Bhavaraju-Sanka, S. Tou, B. P. Keene, J. F. Howard, Jr., J. Wang, Z. Fan, S. J. Schatzberg, M. A. Styner, K. M. Flanigan, X. Xiao and E. P. Hoffman (2012). "Canine models of Duchenne muscular dystrophy and their use in therapeutic strategies." Mamm Genome **23**(1-2): 85-108.

Kornegay, J. N., J. Li, J. R. Bogan, D. J. Bogan, C. Chen, H. Zheng, B. Wang, C. Qiao, J. F. Howard, Jr. and X. Xiao (2010). "Widespread muscle expression of an AAV9 human mini-dystrophin vector after intravenous injection in neonatal dystrophin-deficient dogs." Mol Ther **18**(8): 1501-1508.

Kotchey, N. M., K. Adachi, M. Zahid, K. Inagaki, R. Charan, R. S. Parker and H. Nakai (2011). "A potential role of distinctively delayed blood clearance of recombinant adeno-associated virus serotype 9 in robust cardiac transduction." Mol Ther **19**(6): 1079-1089.

Kuang, S., M. A. Gillespie and M. A. Rudnicki (2008). "Niche regulation of muscle satellite cell self-renewal and differentiation." Cell Stem Cell **2**(1): 22-31.

Kunkel, L. M., J. F. Hejtmancik, C. T. Caskey, A. Speer, A. P. Monaco, W. Middlesworth, C. A. Colletti, C. Bertelson, U. Muller, M. Bresnan, F. Shapiro, U. Tantravahi, J. Speer, S. A. Latt, R. Bartlett, M. A. Pericak-Vance, A. D. Roses, M. W. Thompson, P. N. Ray, R. G. Worton, K. H. Fischbeck, P. Gallano, M. Coulon, C. Duros, J. Boue, C. Junien, J. Chelly, G. Hamard, M. Jeanpierre, M. Lambert, J. C. Kaplan, A. Emery, H. Dorkins, S. McGlade, K. E. Davies, C. Boehm, B. Arveiler, C. Lemaire, G. J. Morgan, M. J. Denton, J. Amos, M. Bobrow, F. Benham, E. Boswinkel, C. Cole, V. Dubowitz, K. Hart, S. Hodgson, L. Johnson, A. Walker, L. Roncuzzi, A. Ferlini, C. Nobile, G. Romeo, D. E. Wilcox, N. A. Affara, M. A. Ferguson-Smith, M. Lindolf, H. Kaariainen, A. de la Chapelle, V. Ionasescu, C. Searby, R. Ionasescu, E. Bakker, G. J. van Ommen, P. L. Pearson, C. R. Greenberg, J. L. Hamerton, K. Wrogemann, R. A. Doherty, R. Polakowska, C. Hyser, S. Quirk, N. Thomas, J. F. Harper, B. T. Darras and U. Francke (1986). "Analysis of deletions in DNA from patients with Becker and Duchenne muscular dystrophy." Nature **322**(6074): 73-77.

Kunkel, L. M., A. P. Monaco, W. Middlesworth, H. D. Ochs and S. A. Latt (1985). "Specific cloning of DNA fragments absent from the DNA of a male patient with an X chromosome deletion." Proc Natl Acad Sci U S A **82**(14): 4778-4782.

Lai, Y., G. D. Thomas, Y. Yue, H. T. Yang, D. Li, C. Long, L. Judge, B. Bostick, J. S. Chamberlain, R. L. Terjung and D. Duan (2009). "Dystrophins carrying spectrin-like repeats 16 and 17 anchor nNOS to the sarcolemma and enhance exercise performance in a mouse model of muscular dystrophy." J Clin Invest **119**(3): 624-635.

Lai, Y., J. Zhao, Y. Yue and D. Duan (2013). "alpha2 and alpha3 helices of dystrophin R16 and R17 frame a microdomain in the alpha1 helix of dystrophin R17 for neuronal NOS binding." Proc Natl Acad Sci U S A **110**(2): 525-530.

Lannergren, J., J. D. Bruton and H. Westerblad (2000). "Vacuole formation in fatigued skeletal muscle fibres from frog and mouse: effects of extracellular lactate." J Physiol **526 Pt 3**: 597-611.

Le Bon, A., N. Etchart, C. Rossmann, M. Ashton, S. Hou, D. Gewert, P. Borrow and D. F. Tough (2003). "Cross-priming of CD8+ T cells stimulated by virus-induced type I interferon." Nat Immunol **4**(10): 1009-1015.

Le Rumeur, E., S. J. Winder and J. F. Hubert (2010). "Dystrophin: more than just the sum of its parts." Biochim Biophys Acta **1804**(9): 1713-1722.

Lefaucheur, J. P. and A. Sebille (1995). "The cellular events of injured muscle regeneration depend on the nature of the injury." Neuromuscul Disord **5**(6): 501-509.

Legrand, B., E. Giudice, A. Nicolas, O. Delalande and E. Le Rumeur (2011). "Computational study of the human dystrophin repeats: interaction properties and molecular dynamics." PLoS One **6**(8): e23819.

Li, C., K. Goudy, M. Hirsch, A. Asokan, Y. Fan, J. Alexander, J. Sun, P. Monahan, D. Seiber, J. Sidney, A. Sette, R. Tisch, J. Frelinger and R. J. Samulski (2009). "Cellular

immune response to cryptic epitopes during therapeutic gene transfer." Proc Natl Acad Sci U S A **106**(26): 10770-10774.

Li, H., M. O. Lasaro, B. Jia, S. W. Lin, L. H. Haut, K. A. High and H. C. Ertl (2011). "Capsid-specific T-cell responses to natural infections with adeno-associated viruses in humans differ from those of nonhuman primates." Mol Ther **19**(11): 2021-2030.

Li, H., S. Tuyishime, T. L. Wu, W. Giles-Davis, D. Zhou, W. Xiao, K. A. High and H. C. Ertl (2011). "Adeno-associated virus vectors serotype 2 induce prolonged proliferation of capsid-specific CD8+ T cells in mice." Mol Ther **19**(3): 536-546.

Li, S., E. Kimura, R. Ng, B. M. Fall, L. Meuse, M. Reyes, J. A. Faulkner and J. S. Chamberlain (2006). "A highly functional mini-dystrophin/GFP fusion gene for cell and gene therapy studies of Duchenne muscular dystrophy." Hum Mol Genet **15**(10): 1610-1622.

Lieber, R. L. and S. R. Ward (2013). "Cellular mechanisms of tissue fibrosis. 4. Structural and functional consequences of skeletal muscle fibrosis." Am J Physiol Cell Physiol **305**(3): C241-252.

Lim, R. W. and S. D. Hauschka (1984). "EGF responsiveness and receptor regulation in normal and differentiation-defective mouse myoblasts." Dev Biol **105**(1): 48-58.

Liu, Y., A. D. Santin, M. Mane, M. Chiriva-Internati, G. P. Parham, A. Ravaggi and P. L. Hermonat (2000). "Transduction and utility of the granulocyte-macrophage colony-stimulating factor gene into monocytes and dendritic cells by adeno-associated virus." Journal of interferon & cytokine research : the official journal of the International Society for Interferon and Cytokine Research **20**(1): 21-30.

Liu, Y. L., F. Mingozzi, S. M. Rodriguez-Colon, S. Joseph, E. Dobrzynski, T. Suzuki, K. A. High and R. W. Herzog (2004). "Therapeutic levels of factor IX expression using a muscle-specific promoter and adeno-associated virus serotype 1 vector." Hum Gene Ther **15**(8): 783-792.

Lompre, A. M., L. Hadri, E. Merlet, Z. Keuylian, N. Mougenot, I. Karakikes, J. Chen, F. Atassi, A. Marchand, R. Blaise, I. Limon, S. W. McPhee, R. J. Samulski, R. J. Hajjar and L. Lipskaia (2013). "Efficient transduction of vascular smooth muscle cells with a translational AAV2.5 vector: a new perspective for in-stent restenosis gene therapy." Gene Therapy **20**(9): 901-912.

Lorain, S., D. A. Gross, A. Goyenvalle, O. Danos, J. Davoust and L. Garcia (2008). "Transient immunomodulation allows repeated injections of AAV1 and correction of muscular dystrophy in multiple muscles." Mol Ther **16**(3): 541-547.

Lostal, W., K. Kodippili, Y. Yue and D. Duan (2014). "Full-length dystrophin reconstitution with adeno-associated viral vectors." Hum Gene Ther.

Lund, F. E. and T. D. Randall (2010). "Effector and regulatory B cells: modulators of CD4+ T cell immunity." Nat Rev Immunol **10**(4): 236-247.

Maguire, K. K., L. Lim, S. Speedy and T. A. Rando (2013). "Assessment of disease activity in muscular dystrophies by noninvasive imaging." J Clin Invest **123**(5): 2298-2305.

Malhotra, S. B., K. A. Hart, H. J. Klamut, N. S. Thomas, S. E. Bodrug, A. H. Burghes, M. Bobrow, P. S. Harper, M. W. Thompson, P. N. Ray and et al. (1988). "Frame-shift deletions in patients with Duchenne and Becker muscular dystrophy." Science **242**(4879): 755-759.

Mann, C. J., E. Perdiguero, Y. Kharraz, S. Aguilar, P. Pessina, A. L. Serrano and P. Munoz-Canoves (2011). "Aberrant repair and fibrosis development in skeletal muscle." Skelet Muscle **1**(1): 21.

Manning, W. C., S. Zhou, M. P. Bland, J. A. Escobedo and V. Dwarki (1998). "Transient immunosuppression allows transgene expression following readministration of adeno-associated viral vectors." Hum Gene Ther **9**(4): 477-485.

Manzur, A. Y., T. Kuntzer, M. Pike and A. Swan (2008). "Glucocorticoid corticosteroids for Duchenne muscular dystrophy." Cochrane Database Syst Rev(1): CD003725.

Marshall, J. L., E. Chou, J. Oh, A. Kwok, D. J. Burkin and R. H. Crosbie-Watson (2012). "Dystrophin and utrophin expression require sarcospan: loss of alpha7 integrin exacerbates a newly discovered muscle phenotype in sarcospan-null mice." Hum Mol Genet **21**(20): 4378-4393.

Marshall, J. L. and R. H. Crosbie-Watson (2013). "Sarcospan: a small protein with large potential for Duchenne muscular dystrophy." Skelet Muscle **3**(1): 1.

Martari, M., A. Sagazio, A. Mohamadi, Q. Nguyen, S. D. Hauschka, E. Kim and R. Salvatori (2009). "Partial rescue of growth failure in growth hormone (GH)-deficient mice by a single injection of a double-stranded adeno-associated viral vector expressing the GH gene driven by a muscle-specific regulatory cassette." Hum Gene Ther **20**(7): 759-766.

Martino, A. T., M. Suzuki, D. M. Markusic, I. Zolotukhin, R. C. Ryals, B. Moghimi, H. C. Ertl, D. A. Muruve, B. Lee and R. W. Herzog (2011). "The genome of self-complementary adeno-associated viral vectors increases Toll-like receptor 9-dependent innate immune responses in the liver." Blood **117**(24): 6459-6468.

Matsushita, T., S. Elliger, C. Elliger, G. Podsakoff, L. Villarreal, G. J. Kurtzman, Y. Iwaki and P. Colosi (1998). "Adeno-associated virus vectors can be efficiently produced without helper virus." Gene Ther **5**(7): 938-945.

Mays, L. E., L. H. Vandenberghe, R. Xiao, P. Bell, H. J. Nam, M. Agbandje-McKenna and J. M. Wilson (2009). "Adeno-associated virus capsid structure drives CD4-dependent CD8+ T cell response to vector encoded proteins." J Immunol **182**(10): 6051-6060.

Mays, L. E. and J. M. Wilson (2011). "The complex and evolving story of T cell activation to AAV vector-encoded transgene products." Mol Ther **19**(1): 16-27.

McCabe, E. R., J. Towbin, J. Chamberlain, L. Baumbach, J. Witkowski, G. J. van Ommen, M. Koenig, L. M. Kunkel and W. K. Seltzer (1989). "Complementary DNA probes for the Duchenne muscular dystrophy locus demonstrate a previously undetectable deletion in a patient with dystrophic myopathy, glycerol kinase deficiency, and congenital adrenal hypoplasia." J Clin Invest **83**(1): 95-99.

McCarty, D. M., S. M. Young, Jr. and R. J. Samulski (2004). "Integration of adeno-associated virus (AAV) and recombinant AAV vectors." Annu Rev Genet **38**: 819-845.

McHeyzer-Williams, M., S. Okitsu, N. Wang and L. McHeyzer-Williams (2012). "Molecular programming of B cell memory." Nat Rev Immunol **12**(1): 24-34.

McIntosh, J. H., M. Cochrane, S. Cobbold, H. Waldmann, S. A. Nathwani, A. M. Davidoff and A. C. Nathwani (2012). "Successful attenuation of humoral immunity to viral capsid and transgenic protein following AAV-mediated gene transfer with a non-depleting CD4 antibody and cyclosporine." Gene Ther **19**(1): 78-85.

McLaughlin, S. K., P. Collis, P. L. Hermonat and N. Muzyczka (1988). "Adeno-associated virus general transduction vectors: analysis of proviral structures." J Virol **62**(6): 1963-1973.

Mendell, J. R., K. Campbell, L. Rodino-Klapac, Z. Sahenk, C. Shilling, S. Lewis, D. Bowles, S. Gray, C. Li, G. Galloway, V. Malik, B. Coley, K. R. Clark, J. Li, X. Xiao, J. Samulski, S. W. McPhee, R. J. Samulski and C. M. Walker (2010). "Dystrophin immunity in Duchenne's muscular dystrophy." N Engl J Med **363**(15): 1429-1437.

Mendell, J. R., L. R. Rodino-Klapac, X. Q. Rosales, B. D. Coley, G. Galloway, S. Lewis, V. Malik, C. Shilling, B. J. Byrne, T. Conlon, K. J. Campbell, W. G. Bremer, L. E. Taylor, K. M. Flanigan, J. M. Gastier-Foster, C. Astbury, J. Kota, Z. Sahenk, C. M. Walker and K. R. Clark (2010). "Sustained alpha-sarcoglycan gene expression after gene transfer in limb-girdle muscular dystrophy, type 2D." Ann Neurol **68**(5): 629-638.

Metzinger, L., D. J. Blake, M. V. Squier, L. V. Anderson, A. E. Deconinck, R. Nawrotzki, D. Hilton-Jones and K. E. Davies (1997). "Dystrobrevin deficiency at the sarcolemma of patients with muscular dystrophy." Hum Mol Genet **6**(7): 1185-1191.

Mingozzi, F., X. M. Anguela, G. Pavani, Y. Chen, R. J. Davidson, D. J. Hui, M. Yazicioglu, L. Elkouby, C. J. Hinderer, A. Faella, C. Howard, A. Tai, G. M. Podsakoff, S. Zhou, E. Basner-Tschakarjan, J. F. Wright and K. A. High (2013). "Overcoming preexisting humoral immunity to AAV using capsid decoys." Sci Transl Med **5**(194): 194ra192.

Mingozzi, F. and K. A. High (2013). "Immune responses to AAV vectors: overcoming barriers to successful gene therapy." Blood **122**(1): 23-36.

Mingozzi, F., M. V. Maus, D. J. Hui, D. E. Sabatino, S. L. Murphy, J. E. Rasko, M. V. Ragni, C. S. Manno, J. Sommer, H. Jiang, G. F. Pierce, H. C. Ertl and K. A. High (2007). "CD8(+) T-cell responses to adeno-associated virus capsid in humans." Nat Med **13**(4): 419-422.

Mingozzi, F., J. J. Meulenberg, D. J. Hui, E. Basner-Tschakarjan, N. C. Hasbrouck, S. A. Edmonson, N. A. Hutnick, M. R. Betts, J. J. Kastelein, E. S. Stroes and K. A. High (2009). "AAV-1-mediated gene transfer to skeletal muscle in humans results in dose-dependent activation of capsid-specific T cells." Blood **114**(10): 2077-2086.

Miura, P. and B. J. Jasmin (2006). "Utrophin upregulation for treating Duchenne or Becker muscular dystrophy: how close are we?" Trends Mol Med **12**(3): 122-129.

Monaco, A. P., C. J. Bertelson, S. Liechti-Gallati, H. Moser and L. M. Kunkel (1988). "An explanation for the phenotypic differences between patients bearing partial deletions of the DMD locus." Genomics **2**(1): 90-95.

Monteilhet, V., S. Saheb, S. Boutin, C. Leborgne, P. Veron, M. F. Montus, P. Moullier, O. Benveniste and C. Masurier (2011). "A 10 patient case report on the impact of plasmapheresis upon neutralizing factors against adeno-associated virus (AAV) types 1, 2, 6, and 8." Mol Ther **19**(11): 2084-2091.

Moser, H. (1984). "Duchenne muscular dystrophy: pathogenetic aspects and genetic prevention." Hum Genet **66**(1): 17-40.

Mosmann, T. R., H. Cherwinski, M. W. Bond, M. A. Giedlin and R. L. Coffman (1986). "Two types of murine helper T cell clone. I. Definition according to profiles of lymphokine activities and secreted proteins." J Immunol **136**(7): 2348-2357.

Motamed, K., D. J. Blake, J. C. Angello, B. L. Allen, A. C. Rapraeger, S. D. Hauschka and E. H. Sage (2003). "Fibroblast growth factor receptor-1 mediates the inhibition of endothelial cell proliferation and the promotion of skeletal myoblast differentiation by SPARC: a role for protein kinase A." J Cell Biochem **90**(2): 408-423.

Moxley, R. T., 3rd, S. Ashwal, S. Pandya, A. Connolly, J. Florence, K. Mathews, L. Baumbach, C. McDonald, M. Sussman, C. Wade, N. Quality Standards Subcommittee of the American Academy of and S. Practice Committee of the Child Neurology (2005). "Practice parameter: corticosteroid treatment of Duchenne dystrophy: report of the Quality Standards Subcommittee of the American Academy of Neurology and the Practice Committee of the Child Neurology Society." Neurology **64**(1): 13-20.

Muir, L. A. and J. S. Chamberlain (2009). "Emerging strategies for cell and gene therapy of the muscular dystrophies." Expert Rev Mol Med **11**: e18.

Murphy, S. L., H. Li, F. Mingozzi, D. E. Sabatino, D. J. Hui, S. A. Edmonson and K. A. High (2009). "Diverse IgG subclass responses to adeno-associated virus infection and vector administration." J Med Virol **81**(1): 65-74.

Nakai, H., S. Fuess, T. A. Storm, S. Muramatsu, Y. Nara and M. A. Kay (2005). "Unrestricted hepatocyte transduction with adeno-associated virus serotype 8 vectors in mice." J Virol **79**(1): 214-224.

Nakai, H., E. Montini, S. Fuess, T. A. Storm, M. Grompe and M. A. Kay (2003). "AAV serotype 2 vectors preferentially integrate into active genes in mice." Nat Genet **34**(3): 297-302.

Nakai, H., S. R. Yant, T. A. Storm, S. Fuess, L. Meuse and M. A. Kay (2001). "Extrachromosomal recombinant adeno-associated virus vector genomes are primarily responsible for stable liver transduction in vivo." J Virol **75**(15): 6969-6976.

Nam, H. J., M. D. Lane, E. Padron, B. Gurda, R. McKenna, E. Kohlbrenner, G. Aslanidi, B. Byrne, N. Muzyczka, S. Zolotukhin and M. Agbandje-McKenna (2007). "Structure of adeno-associated virus serotype 8, a gene therapy vector." J Virol **81**(22): 12260-12271.

Ng, R., G. B. Banks, J. K. Hall, L. A. Muir, J. N. Ramos, J. Wicki, G. L. Odom, P. Konieczny, J. Seto, J. R. Chamberlain and J. S. Chamberlain (2012). "Animal models of muscular dystrophy." Prog Mol Biol Transl Sci **105**: 83-111.

Ng, R., L. Govindasamy, B. L. Gurda, R. McKenna, O. G. Kozyreva, R. J. Samulski, K. N. Parent, T. S. Baker and M. Agbandje-McKenna (2010). "Structural characterization of the dual glycan binding adeno-associated virus serotype 6." J Virol **84**(24): 12945-12957.

Noguchi, S., E. Wakabayashi, M. Imamura, M. Yoshida and E. Ozawa (1999). "Developmental expression of sarcoglycan gene products in cultured myocytes." Biochem Biophys Res Commun **262**(1): 88-93.

Odom, G. L., P. Gregorevic, J. M. Allen and J. S. Chamberlain (2011). "Gene therapy of mdx mice with large truncated dystrophins generated by recombination using rAAV6." Mol Ther **19**(1): 36-45.

Ohshima, S., J. H. Shin, K. Yuasa, A. Nishiyama, J. Kira, T. Okada and S. Takeda (2009). "Transduction efficiency and immune response associated with the administration of AAV8 vector into dog skeletal muscle." Molecular therapy : the journal of the American Society of Gene Therapy **17**(1): 73-80.

Ohtsuka, Y., K. Udaka, Y. Yamashiro, H. Yagita and K. Okumura (1998). "Dystrophin acts as a transplantation rejection antigen in dystrophin-deficient mice: implication for gene therapy." J Immunol **160**(9): 4635-4640.

Olwin, B. B. and S. D. Hauschka (1988). "Cell surface fibroblast growth factor and epidermal growth factor receptors are permanently lost during skeletal muscle terminal differentiation in culture." J Cell Biol **107**(2): 761-769.

Olwin, B. B. and A. Rapraeger (1992). "Repression of myogenic differentiation by aFGF, bFGF, and K-FGF is dependent on cellular heparan sulfate." J Cell Biol **118**(3): 631-639.

Ozawa, E. (2004). The muscle fiber cytoskeleton: The dystrophin system. Myology. F.-A. C. Engel A. New York, McGraw-Hill**:** 455-470.

Ozawa, E., I. Nishino and I. Nonaka (2001). "Sarcolemmopathy: muscular dystrophies with cell membrane defects." Brain Pathol **11**(2): 218-230.

Pacak, C. A., C. S. Mah, B. D. Thattaliyath, T. J. Conlon, M. A. Lewis, D. E. Cloutier, I. Zolotukhin, A. F. Tarantal and B. J. Byrne (2006). "Recombinant adeno-associated virus serotype 9 leads to preferential cardiac transduction in vivo." Circ Res **99**(4): e3-9.

Pan, X., Y. Yue, K. Zhang, W. Lostal, J. H. Shin and D. Duan (2013). "Long-term robust myocardial transduction of the dog heart from a peripheral vein by adeno-associated virus serotype-8." Hum Gene Ther **24**(6): 584-594.

Pankajakshan, D., T. O. Makinde, R. Gaurav, M. Del Core, G. Hatzoudis, I. Pipinos and D. K. Agrawal (2012). "Successful transfection of genes using AAV-2/9 vector in swine coronary and peripheral arteries." The Journal of surgical research **175**(1): 169-175.

Pavalko, F. M. and C. A. Otey (1994). "Role of adhesion molecule cytoplasmic domains in mediating interactions with the cytoskeleton." Proc Soc Exp Biol Med **205**(4): 282-293.

Peter, A. K., J. L. Marshall and R. H. Crosbie (2008). "Sarcospan reduces dystrophic pathology: stabilization of the utrophin-glycoprotein complex." J Cell Biol **183**(3): 419-427.

Petrof, B. J., J. B. Shrager, H. H. Stedman, A. M. Kelly and H. L. Sweeney (1993). "Dystrophin protects the sarcolemma from stresses developed during muscle contraction." Proc Natl Acad Sci U S A **90**(8): 3710-3714.

Petry, H., A. Brooks, A. Orme, P. Wang, P. Liu, J. Xie, P. Kretschmer, H. S. Qian, T. W. Hermiston and R. N. Harkins (2008). "Effect of viral dose on neutralizing antibody response and transgene expression after AAV1 vector re-administration in mice." Gene Ther **15**(1): 54-60.

Pien, G. C., E. Basner-Tschakarjan, D. J. Hui, A. N. Mentlik, J. D. Finn, N. C. Hasbrouck, S. Zhou, S. L. Murphy, M. V. Maus, F. Mingozzi, J. S. Orange and K. A. High (2009). "Capsid antigen presentation flags human hepatocytes for destruction after transduction by adeno-associated viral vectors." J Clin Invest **119**(6): 1688-1695.

Plant, D. R., F. E. Colarossi and G. S. Lynch (2006). "Notexin causes greater myotoxic damage and slower functional repair in mouse skeletal muscles than bupivacaine." Muscle Nerve **34**(5): 577-585.

Politano, L., G. Nigro, V. Nigro, G. Piluso, S. Papparella, O. Paciello and L. I. Comi (2003). "Gentamicin administration in Duchenne patients with premature stop codon. Preliminary results." Acta Myol **22**(1): 15-21.

Prins, K. W., J. L. Humston, A. Mehta, V. Tate, E. Ralston and J. M. Ervasti (2009). "Dystrophin is a microtubule-associated protein." J Cell Biol **186**(3): 363-369.

Qin, S., S. P. Cobbold, H. Pope, J. Elliott, D. Kioussis, J. Davies and H. Waldmann (1993). ""Infectious" transplantation tolerance." Science **259**(5097): 974-977.

Qin, S. X., S. Cobbold, R. Benjamin and H. Waldmann (1989). "Induction of classical transplantation tolerance in the adult." J Exp Med **169**(3): 779-794.

Qin, S. X., M. Wise, S. P. Cobbold, L. Leong, Y. C. Kong, J. R. Parnes and H. Waldmann (1990). "Induction of tolerance in peripheral T cells with monoclonal antibodies." Eur J Immunol **20**(12): 2737-2745.

Rafael, J. A., G. A. Cox, K. Corrado, D. Jung, K. P. Campbell and J. S. Chamberlain (1996). "Forced expression of dystrophin deletion constructs reveals structure-function correlations." J Cell Biol **134**(1): 93-102.

Rafael-Fortney, J. A., N. S. Chimanji, K. E. Schill, C. D. Martin, J. D. Murray, R. Ganguly, J. E. Stangland, T. Tran, Y. Xu, B. D. Canan, T. A. Mays, D. A. Delfin, P. M. Janssen and S. V. Raman (2011). "Early treatment with lisinopril and spironolactone preserves cardiac and skeletal muscle in Duchenne muscular dystrophy mice." Circulation **124**(5): 582-588.

Rahimov, F. and L. M. Kunkel (2013). "The cell biology of disease: cellular and molecular mechanisms underlying muscular dystrophy." J Cell Biol **201**(4): 499-510.

Rapti, K., V. Louis-Jeune, E. Kohlbrenner, K. Ishikawa, D. Ladage, S. Zolotukhin, R. J. Hajjar and T. Weber (2012). "Neutralizing antibodies against AAV serotypes 1, 2, 6, and 9 in sera of commonly used animal models." Molecular therapy : the journal of the American Society of Gene Therapy **20**(1): 73-83.

Rath, A., A. R. Davidson and C. M. Deber (2005). "The structure of "unstructured" regions in peptides and proteins: role of the polyproline II helix in protein folding and recognition." Biopolymers **80**(2-3): 179-185.

Ray, P. N., B. Belfall, C. Duff, C. Logan, V. Kean, M. W. Thompson, J. E. Sylvester, J. L. Gorski, R. D. Schmickel and R. G. Worton (1985). "Cloning of the breakpoint of an X;21 translocation associated with Duchenne muscular dystrophy." Nature **318**(6047): 672-675.

Rezniczek, G. A., P. Konieczny, B. Nikolic, S. Reipert, D. Schneller, C. Abrahamsberg, K. E. Davies, S. J. Winder and G. Wiche (2007). "Plectin 1f scaffolding at the sarcolemma of dystrophic (mdx) muscle fibers through multiple interactions with beta-dystroglycan." J Cell Biol **176**(7): 965-977.

Richard, E., G. Douillard-Guilloux, L. Batista and C. Caillaud (2008). "Correction of glycogenosis type 2 by muscle-specific lentiviral vector." In Vitro Cell Dev Biol Anim **44**(10): 397-406.

Richter, M., A. Iwata, J. Nyhuis, Y. Nitta, A. D. Miller, C. L. Halbert and M. D. Allen (2000). "Adeno-associated virus vector transduction of vascular smooth muscle cells in vivo." Physiological Genomics **2**(3): 117-127.

Ridge, J. P., F. Di Rosa and P. Matzinger (1998). "A conditioned dendritic cell can be a temporal bridge between a CD4+ T-helper and a T-killer cell." Nature **393**(6684): 474-478.

Rivera, V. M., G. P. Gao, R. L. Grant, M. A. Schnell, P. W. Zoltick, L. W. Rozamus, T. Clackson and J. M. Wilson (2005). "Long-term pharmacologically regulated expression of erythropoietin in primates following AAV-mediated gene transfer." Blood **105**(4): 1424-1430.

Riviere, C., O. Danos and A. M. Douar (2006). "Long-term expression and repeated administration of AAV type 1, 2 and 5 vectors in skeletal muscle of immunocompetent adult mice." Gene Ther **13**(17): 1300-1308.

Rodino-Klapac, L. R., C. L. Montgomery, W. G. Bremer, K. M. Shontz, V. Malik, N. Davis, S. Sprinkle, K. J. Campbell, Z. Sahenk, K. R. Clark, C. M. Walker, J. R. Mendell and L. G. Chicoine (2010). "Persistent expression of FLAG-tagged micro dystrophin in nonhuman primates following intramuscular and vascular delivery." Mol Ther **18**(1): 109-117.

Rogers, G. L., A. T. Martino, G. V. Aslanidi, G. R. Jayandharan, A. Srivastava and R. W. Herzog (2011). "Innate Immune Responses to AAV Vectors." Front Microbiol **2**: 194.

Roma, J., F. Munell, A. Fargas and M. Roig (2004). "Evolution of pathological changes in the gastrocnemius of the mdx mice correlate with utrophin and beta-dystroglycan expression." Acta Neuropathol **108**(5): 443-452.

Rosenblatt, J. D., A. I. Lunt, D. J. Parry and T. A. Partridge (1995). "Culturing satellite cells from living single muscle fiber explants." In Vitro Cell Dev Biol Anim **31**(10): 773-779.

Rybakova, I. N., K. J. Amann and J. M. Ervasti (1996). "A new model for the interaction of dystrophin with F-actin." J Cell Biol **135**(3): 661-672.

Sacco, A., F. Mourkioti, R. Tran, J. Choi, M. Llewellyn, P. Kraft, M. Shkreli, S. Delp, J. H. Pomerantz, S. E. Artandi and H. M. Blau (2010). "Short telomeres and stem cell exhaustion model Duchenne muscular dystrophy in mdx/mTR mice." Cell **143**(7): 1059-1071.

Sack, B. K., S. Merchant, D. M. Markusic, A. C. Nathwani, A. M. Davidoff, B. J. Byrne and R. W. Herzog (2012). "Transient B cell depletion or improved transgene expression

by codon optimization promote tolerance to factor VIII in gene therapy." PLoS One **7**(5): e37671.

Sakamoto, A., K. Ono, M. Abe, G. Jasmin, T. Eki, Y. Murakami, T. Masaki, T. Toyo-oka and F. Hanaoka (1997). "Both hypertrophic and dilated cardiomyopathies are caused by mutation of the same gene, delta-sarcoglycan, in hamster: an animal model of disrupted dystrophin-associated glycoprotein complex." Proc Natl Acad Sci U S A **94**(25): 13873-13878.

Sakamoto, M., K. Yuasa, M. Yoshimura, T. Yokota, T. Ikemoto, M. Suzuki, G. Dickson, Y. Miyagoe-Suzuki and S. Takeda (2002). "Micro-dystrophin cDNA ameliorates dystrophic phenotypes when introduced into mdx mice as a transgene." Biochem Biophys Res Commun **293**(4): 1265-1272.

Salio, M., M. J. Palmowski, A. Atzberger, I. F. Hermans and V. Cerundolo (2004). "CpG-matured murine plasmacytoid dendritic cells are capable of in vivo priming of functional CD8 T cell responses to endogenous but not exogenous antigens." J Exp Med **199**(4): 567-579.

Salva, M. Z., C. L. Himeda, P. W. Tai, E. Nishiuchi, P. Gregorevic, J. M. Allen, E. E. Finn, Q. G. Nguyen, M. J. Blankinship, L. Meuse, J. S. Chamberlain and S. D. Hauschka (2007). "Design of tissue-specific regulatory cassettes for high-level rAAV-mediated expression in skeletal and cardiac muscle." Mol Ther **15**(2): 320-329.

Sander, M., B. Chavoshan, S. A. Harris, S. T. Iannaccone, J. T. Stull, G. D. Thomas and R. G. Victor (2000). "Functional muscle ischemia in neuronal nitric oxide synthase-deficient skeletal muscle of children with Duchenne muscular dystrophy." Proceedings of the National Academy of Sciences of the United States of America **97**(25): 13818-13823.

Sandona, D. and R. Betto (2009). "Sarcoglycanopathies: molecular pathogenesis and therapeutic prospects." Expert Rev Mol Med **11**: e28.

Schmidt, M., L. Govindasamy, S. Afione, N. Kaludov, M. Agbandje-McKenna and J. A. Chiorini (2008). "Molecular characterization of the heparin-dependent transduction domain on the capsid of a novel adeno-associated virus isolate, AAV(VR-942)." J Virol **82**(17): 8911-8916.

Schnepp, B. C., R. L. Jensen, C. L. Chen, P. R. Johnson and K. R. Clark (2005). "Characterization of adeno-associated virus genomes isolated from human tissues." J Virol **79**(23): 14793-14803.

Schoenberger, S. P., R. E. Toes, E. I. van der Voort, R. Offringa and C. J. Melief (1998). "T-cell help for cytotoxic T lymphocytes is mediated by CD40-CD40L interactions." Nature **393**(6684): 480-483.

Schultz, B. R. and J. S. Chamberlain (2008). "Recombinant adeno-associated virus transduction and integration." Mol Ther **16**(7): 1189-1199.

Scott, W., J. Stevens and S. A. Binder-Macleod (2001). "Human skeletal muscle fiber type classifications." Phys Ther **81**(11): 1810-1816.

Seto, J. T., J. N. Ramos, L. Muir, J. S. Chamberlain and G. L. Odom (2012). "Gene replacement therapies for duchenne muscular dystrophy using adeno-associated viral vectors." Curr Gene Ther **12**(3): 139-151.

Sharp, N. J., J. N. Kornegay, R. J. Bartlett, W. Y. Hung and M. J. Dykstra (1993). "Notexin-induced muscle injury in the dog." J Neurol Sci **116**(1): 73-81.

Shefer, G. and Z. Yablonka-Reuveni (2005). "Isolation and culture of skeletal muscle myofibers as a means to analyze satellite cells." Methods Mol Biol **290**: 281-304.

Shen, S., K. D. Bryant, S. M. Brown, S. H. Randell and A. Asokan (2011). "Terminal N-linked galactose is the primary receptor for adeno-associated virus 9." J Biol Chem **286**(15): 13532-13540.

Shin, J. H., Y. Yue, B. Smith and D. Duan (2012). "Humoral immunity to AAV-6, 8, and 9 in normal and dystrophic dogs." Hum Gene Ther **23**(3): 287-294.

Sicinski, P., Y. Geng, A. S. Ryder-Cook, E. A. Barnard, M. G. Darlison and P. J. Barnard (1989). "The molecular basis of muscular dystrophy in the mdx mouse: a point mutation." Science **244**(4912): 1578-1580.

Siegal, F. P. (1999). "The Nature of the Principal Type 1 Interferon-Producing Cells in Human Blood." Science **284**(5421): 1835-1837.

Smith, R. H. (2008). "Adeno-associated virus integration: virus versus vector." Gene Ther **15**(11): 817-822.

Souders, C. A., S. L. Bowers and T. A. Baudino (2009). "Cardiac fibroblast: the renaissance cell." Circ Res **105**(12): 1164-1176.

Stamler, J. S. and G. Meissner (2001). "Physiology of nitric oxide in skeletal muscle." Physiol Rev **81**(1): 209-237.

Stedman, H. H., H. L. Sweeney, J. B. Shrager, H. C. Maguire, R. A. Panettieri, B. Petrof, M. Narusawa, J. M. Leferovich, J. T. Sladky and A. M. Kelly (1991). "The mdx mouse diaphragm reproduces the degenerative changes of Duchenne muscular dystrophy." Nature **352**(6335): 536-539.

Stone, M. R., A. O'Neill, D. Catino and R. J. Bloch (2005). "Specific interaction of the actin-binding domain of dystrophin with intermediate filaments containing keratin 19." Mol Biol Cell **16**(9): 4280-4293.

Sudres, M., S. Cire, V. Vasseur, L. Brault, S. Da Rocha, F. Boisgerault, C. Le Bec, D. A. Gross, V. Blouin, B. Ryffel and A. Galy (2012). "MyD88 signaling in B cells regulates the production of Th1-dependent antibodies to AAV." Mol Ther **20**(8): 1571-1581.

Sun, B., S. P. Young, P. Li, C. Di, T. Brown, M. Z. Salva, S. Li, A. Bird, Z. Yan, R. Auten, S. D. Hauschka and D. D. Koeberl (2008). "Correction of multiple striated muscles in murine Pompe disease through adeno-associated virus-mediated gene therapy." Mol Ther **16**(8): 1366-1371.

Swain, S. L., K. K. McKinstry and T. M. Strutt (2012). "Expanding roles for CD4(+) T cells in immunity to viruses." Nat Rev Immunol **12**(2): 136-148.

Tai, P. W., C. L. Smith, J. C. Angello and S. D. Hauschka (2012). "Analysis of fiber-type differences in reporter gene expression of beta-gal transgenic muscle." Methods Mol Biol **798**: 445-459.

Takeshima, Y., H. Nishio, H. Sakamoto, H. Nakamura and M. Matsuo (1995). "Modulation of in vitro splicing of the upstream intron by modifying an intra-exon sequence which is deleted from the dystrophin gene in dystrophin Kobe." J Clin Invest **95**(2): 515-520.

Takeshima, Y., H. Wada, M. Yagi, Y. Ishikawa, Y. Ishikawa, R. Minami, H. Nakamura and M. Matsuo (2001). "Oligonucleotides against a splicing enhancer sequence led to dystrophin production in muscle cells from a Duchenne muscular dystrophy patient." Brain Dev **23**(8): 788-790.

Tangye, S. G., C. S. Ma, R. Brink and E. K. Deenick (2013). "The good, the bad and the ugly - TFH cells in human health and disease." Nat Rev Immunol **13**(6): 412-426.

Tarantal, A. F. and C. C. Lee (2010). "Long-term luciferase expression monitored by bioluminescence imaging after adeno-associated virus-mediated fetal gene delivery in rhesus monkeys (Macaca mulatta)." Hum Gene Ther **21**(2): 143-148.

Templeton, T. J. and S. D. Hauschka (1992). "FGF-mediated aspects of skeletal muscle growth and differentiation are controlled by a high affinity receptor, FGFR1." Dev Biol **154**(1): 169-181.

Ten Broek, R. W., S. Grefte and J. W. Von den Hoff (2010). "Regulatory factors and cell populations involved in skeletal muscle regeneration." J Cell Physiol **224**(1): 7-16.

Thomas, G. D., M. Sander, K. S. Lau, P. L. Huang, J. T. Stull and R. G. Victor (1998). "Impaired metabolic modulation of alpha-adrenergic vasoconstriction in dystrophin-deficient skeletal muscle." Proc Natl Acad Sci U S A **95**(25): 15090-15095.

Thomas, G. D., P. W. Shaul, I. S. Yuhanna, S. C. Froehner and M. E. Adams (2003). "Vasomodulation by skeletal muscle-derived nitric oxide requires alpha-syntrophin-mediated sarcolemmal localization of neuronal Nitric oxide synthase." Circulation Research **92**(5): 554-560.

Tidball, J. G. and S. A. Villalta (2010). "Regulatory interactions between muscle and the immune system during muscle regeneration." Am J Physiol Regul Integr Comp Physiol **298**(5): R1173-1187.

Torelli, S., S. C. Brown, C. Jimenez-Mallebrera, L. Feng, F. Muntoni and C. A. Sewry (2004). "Absence of neuronal nitric oxide synthase (nNOS) as a pathological marker for the diagnosis of Becker muscular dystrophy with rod domain deletions." Neuropathol Appl Neurobiol **30**(5): 540-545.

Toromanoff, A., O. Adjali, T. Larcher, M. Hill, L. Guigand, P. Chenuaud, J. Y. Deschamps, O. Gauthier, G. Blancho, B. Vanhove, F. Rolling, Y. Cherel, P. Moullier, I. Anegon and C. Le Guiner (2010). "Lack of immunotoxicity after regional intravenous (RI) delivery of rAAV to nonhuman primate skeletal muscle." Mol Ther **18**(1): 151-160.

Townsend, M. J., J. G. Monroe and A. C. Chan (2010). "B-cell targeted therapies in human autoimmune diseases: an updated perspective." Immunol Rev **237**(1): 264-283.

Unzu, C., S. Hervas-Stubbs, A. Sampedro, I. Mauleon, U. Mancheno, C. Alfaro, R. E. de Salamanca, A. Benito, S. G. Beattie, H. Petry, J. Prieto, I. Melero and A. Fontanellas (2012). "Transient and intensive pharmacological immunosuppression fails to improve AAV-based liver gene transfer in non-human primates." J Transl Med **10**: 122.

van Deutekom, J. C., M. Bremmer-Bout, A. A. Janson, I. B. Ginjaar, F. Baas, J. T. den Dunnen and G. J. van Ommen (2001). "Antisense-induced exon skipping restores dystrophin expression in DMD patient derived muscle cells." Hum Mol Genet **10**(15): 1547-1554.

Vandenberghe, L. H., E. Breous, H. J. Nam, G. Gao, R. Xiao, A. Sandhu, J. Johnston, Z. Debyser, M. Agbandje-McKenna and J. M. Wilson (2009). "Naturally occurring singleton residues in AAV capsid impact vector performance and illustrate structural constraints." Gene Ther **16**(12): 1416-1428.

Vandenberghe, L. H., L. Wang, S. Somanathan, Y. Zhi, J. Figueredo, R. Calcedo, J. Sanmiguel, R. A. Desai, C. S. Chen, J. Johnston, R. L. Grant, G. Gao and J. M. Wilson (2006). "Heparin binding directs activation of T cells against adeno-associated virus serotype 2 capsid." Nat Med **12**(8): 967-971.

Verhaart, I. E., L. van Vliet-van den Dool, J. A. Sipkens, S. J. de Kimpe, I. G. Kolfschoten, J. C. van Deutekom, L. Liefaard, J. E. Ridings, S. R. Hood and A. Aartsma-Rus (2014). "The Dynamics of Compound, Transcript, and Protein Effects After Treatment With 2OMePS Antisense Oligonucleotides in mdx Mice." Mol Ther Nucleic Acids **3**: e148.

Vignali, D. A. and K. M. Vignali (1999). "Profound enhancement of T cell activation mediated by the interaction between the TCR and the D3 domain of CD4." J Immunol **162**(3): 1431-1439.

Villalta, S. A., H. X. Nguyen, B. Deng, T. Gotoh and J. G. Tidball (2009). "Shifts in macrophage phenotypes and macrophage competition for arginine metabolism affect the severity of muscle pathology in muscular dystrophy." Hum Mol Genet **18**(3): 482-496.

Wagner, K. R., S. Hamed, D. W. Hadley, A. L. Gropman, A. H. Burstein, D. M. Escolar, E. P. Hoffman and K. H. Fischbeck (2001). "Gentamicin treatment of Duchenne and Becker muscular dystrophy due to nonsense mutations." Ann Neurol **49**(6): 706-711.

Wallace, G. Q. and E. M. McNally (2009). "Mechanisms of muscle degeneration, regeneration, and repair in the muscular dystrophies." Annu Rev Physiol **71**: 37-57.

Wallace, L. M., A. Moreo, K. R. Clark and S. Q. Harper (2013). "Dose-dependent Toxicity of Humanized Renilla reniformis GFP (hrGFP) Limits Its Utility as a Reporter Gene in Mouse Muscle." Mol Ther Nucleic Acids **2**: e86.

Wang, B., J. Li and X. Xiao (2000). "Adeno-associated virus vector carrying human minidystrophin genes effectively ameliorates muscular dystrophy in mdx mouse model." Proc Natl Acad Sci U S A **97**(25): 13714-13719.

Wang, C., C. M. Wang, K. R. Clark and T. J. Sferra (2003). "Recombinant AAV serotype 1 transduction efficiency and tropism in the murine brain." Gene Ther **10**(17): 1528-1534.

Wang, Z., J. M. Allen, S. R. Riddell, P. Gregorevic, R. Storb, S. J. Tapscott, J. S. Chamberlain and C. S. Kuhr (2007). "Immunity to adeno-associated virus-mediated gene transfer in a random-bred canine model of Duchenne muscular dystrophy." Hum Gene Ther **18**(1): 18-26.

Wang, Z., C. S. Kuhr, J. M. Allen, M. Blankinship, P. Gregorevic, J. S. Chamberlain, S. J. Tapscott and R. Storb (2007). "Sustained AAV-mediated dystrophin expression in a canine model of Duchenne muscular dystrophy with a brief course of immunosuppression." Mol Ther **15**(6): 1160-1166.

Wang, Z., R. Storb, D. Lee, M. J. Kushmerick, B. Chu, C. Berger, A. Arnett, J. Allen, J. S. Chamberlain, S. R. Riddell and S. J. Tapscott (2010). "Immune responses to AAV in canine muscle monitored by cellular assays and noninvasive imaging." Mol Ther **18**(3): 617-624.

Wang, Z., S. J. Tapscott, J. S. Chamberlain and R. Storb (2011). "Immunity and AAV-Mediated Gene Therapy for Muscular Dystrophies in Large Animal Models and Human Trials." Front Microbiol **2**: 201.

Wang, Z., T. Zhu, C. Qiao, L. Zhou, B. Wang, J. Zhang, C. Chen, J. Li and X. Xiao (2005). "Adeno-associated virus serotype 8 efficiently delivers genes to muscle and heart." Nat Biotechnol **23**(3): 321-328.

Warner, L. E., C. DelloRusso, R. W. Crawford, I. N. Rybakova, J. R. Patel, J. M. Ervasti and J. S. Chamberlain (2002). "Expression of Dp260 in muscle tethers the actin cytoskeleton to the dystrophin-glycoprotein complex and partially prevents dystrophy." Hum Mol Genet **11**(9): 1095-1105.

Way, M., B. Pope, R. A. Cross, J. Kendrick-Jones and A. G. Weeds (1992). "Expression of the N-terminal domain of dystrophin in E. coli and demonstration of binding to F-actin." FEBS Lett **301**(3): 243-245.

Welch, E. M., E. R. Barton, J. Zhuo, Y. Tomizawa, W. J. Friesen, P. Trifillis, S. Paushkin, M. Patel, C. R. Trotta, S. Hwang, R. G. Wilde, G. Karp, J. Takasugi, G. Chen, S. Jones, H. Ren, Y. C. Moon, D. Corson, A. A. Turpoff, J. A. Campbell, M. M. Conn, A. Khan, N. G. Almstead, J. Hedrick, A. Mollin, N. Risher, M. Weetall, S. Yeh, A. A. Branstrom, J. M. Colacino, J. Babiak, W. D. Ju, S. Hirawat, V. J. Northcutt, L. L. Miller, P. Spatrick, F. He, M. Kawana, H. Feng, A. Jacobson, S. W. Peltz and H. L. Sweeney (2007). "PTC124 targets genetic disorders caused by nonsense mutations." Nature **447**(7140): 87-91.

Weller, M. L., P. Amornphimoltham, M. Schmidt, P. A. Wilson, J. S. Gutkind and J. A. Chiorini (2010). "Epidermal growth factor receptor is a co-receptor for adeno-associated virus serotype 6." Nat Med **16**(6): 662-664.

Winbanks, C. E., C. Beyer, H. Qian and P. Gregorevic (2012). "Transduction of skeletal muscles with common reporter genes can promote muscle fiber degeneration and inflammation." PLoS One **7**(12): e51627.

Winder, S. J. (1997). "The membrane-cytoskeleton interface: the role of dystrophin and utrophin." J Muscle Res Cell Motil **18**(6): 617-629.

Winder, S. J., T. J. Gibson and J. Kendrick-Jones (1995). "Dystrophin and utrophin: the missing links!" FEBS Lett **369**(1): 27-33.

Wolff, J. A., R. W. Malone, P. Williams, W. Chong, G. Acsadi, A. Jani and P. L. Felgner (1990). "Direct gene transfer into mouse muscle in vivo." Science **247**(4949 Pt 1): 1465-1468.

Wright, J. F., J. Wellman and K. A. High (2010). "Manufacturing and regulatory strategies for clinical AAV2-hRPE65." Curr Gene Ther **10**(5): 341-349.

Wu, B., P. Lu, C. Cloer, M. Shaban, S. Grewal, S. Milazi, S. N. Shah, H. M. Moulton and Q. L. Lu (2012). "Long-term rescue of dystrophin expression and improvement in muscle pathology and function in dystrophic mdx mice by peptide-conjugated morpholino." Am J Pathol **181**(2): 392-400.

Wu, Z., A. Asokan and R. J. Samulski (2006). "Adeno-associated virus serotypes: vector toolkit for human gene therapy." Mol Ther **14**(3): 316-327.

Wu, Z., E. Miller, M. Agbandje-McKenna and R. J. Samulski (2006). "Alpha2,3 and alpha2,6 N-linked sialic acids facilitate efficient binding and transduction by adeno-associated virus types 1 and 6." J Virol **80**(18): 9093-9103.

Wu, Z., H. Yang and P. Colosi (2010). "Effect of genome size on AAV vector packaging." Mol Ther **18**(1): 80-86.

Xiao, W., N. Chirmule, M. A. Schnell, J. Tazelaar, J. V. Hughes and J. M. Wilson (2000). "Route of administration determines induction of T-cell-independent humoral responses to adeno-associated virus vectors." Molecular therapy : the journal of the American Society of Gene Therapy **1**(4): 323-329.

Xiao, X., J. Li and R. J. Samulski (1998). "Production of high-titer recombinant adeno-associated virus vectors in the absence of helper adenovirus." J Virol **72**(3): 2224-2232.

Xu, J., T. M. Foy, J. D. Laman, E. A. Elliott, J. J. Dunn, T. J. Waldschmidt, J. Elsemore, R. J. Noelle and R. A. Flavell (1994). "Mice deficient for the CD40 ligand." Immunity **1**(5): 423-431.

Yablonka-Reuveni, Z., K. Day, A. Vine and G. Shefer (2008). "Defining the transcriptional signature of skeletal muscle stem cells." J Anim Sci **86**(14 Suppl): E207-216.

Yaffe, D. and O. Saxel (1977). "Serial passaging and differentiation of myogenic cells isolated from dystrophic mouse muscle." Nature **270**(5639): 725-727.

Yin, H., F. Price and M. A. Rudnicki (2013). "Satellite cells and the muscle stem cell niche." Physiol Rev **93**(1): 23-67.

Yuasa, K., M. Yoshimura, N. Urasawa, S. Ohshima, J. M. Howell, A. Nakamura, T. Hijikata, Y. Miyagoe-Suzuki and S. Takeda (2007). "Injection of a recombinant AAV serotype 2 into canine skeletal muscles evokes strong immune responses against transgene products." Gene Ther **14**(17): 1249-1260.

Yue, Y., A. Ghosh, C. Long, B. Bostick, B. F. Smith, J. N. Kornegay and D. Duan (2008). "A single intravenous injection of adeno-associated virus serotype-9 leads to whole body skeletal muscle transduction in dogs." Mol Ther **16**(12): 1944-1952.

Zaiss, A. K., M. J. Cotter, L. R. White, S. A. Clark, N. C. Wong, V. M. Holers, J. S. Bartlett and D. A. Muruve (2008). "Complement is an essential component of the immune response to adeno-associated virus vectors." J Virol **82**(6): 2727-2740.

Zaiss, A. K., Q. Liu, G. P. Bowen, N. C. Wong, J. S. Bartlett and D. A. Muruve (2002). "Differential activation of innate immune responses by adenovirus and adeno-associated virus vectors." J Virol **76**(9): 4580-4590.

Zhang, G., J. J. Ludtke, C. Thioudellet, P. Kleinpeter, M. Antoniou, H. Herweijer, S. Braun and J. A. Wolff (2004). "Intraarterial delivery of naked plasmid DNA expressing full-length mouse dystrophin in the mdx mouse model of duchenne muscular dystrophy." Hum Gene Ther **15**(8): 770-782.

Zhang, Y., N. Chirmule, G. p. Gao and J. Wilson (2000). "CD40 Ligand-Dependent Activation of Cytotoxic T Lymphocytes by Adeno-Associated Virus Vectors In Vivo: Role of Immature Dendritic Cells." Journal of Virology **74**(17): 8003-8010.

Zhu, J., X. Huang and Y. Yang (2009). "The TLR9-MyD88 pathway is critical for adaptive immune responses to adeno-associated virus gene therapy vectors in mice." J Clin Invest **119**(8): 2388-2398.

Zincarelli, C., S. Soltys, G. Rengo, W. J. Koch and J. E. Rabinowitz (2010). "Comparative cardiac gene delivery of adeno-associated virus serotypes 1-9 reveals that AAV6 mediates the most efficient transduction in mouse heart." Clin Transl Sci **3**(3): 81-89.

Zincarelli, C., S. Soltys, G. Rengo and J. E. Rabinowitz (2008). "Analysis of AAV serotypes 1-9 mediated gene expression and tropism in mice after systemic injection." Mol Ther **16**(6): 1073-1080.